Proceedings of the International Conference:

Georisks in the Mediterranean and their mitigation

UNIVERSITY OF MALTA - VALLETTA CAMPUS
20 - 21 July 2015

Volume edited by: Galea P., Borg R.P., Farrugia D.,
Agius M.R., D'Amico S., Torpiano A., Bonello M.

Proceedings of the International Conference:

GEORISKS IN THE MEDITERRANEAN AND THEIR MITIGATION

University of Malta - Valletta Campus
20-21 July 2015

Organizing Committee
Dr. Pauline Galea
Dr. Sebastiano D'Amico
Dr. Ruben P. Borg
Dr. Matthew R. Agius
Ms. Daniela Farrugia
Prof. Alex Torpiano
Dr. Marc Bonello
Ms Ann-Marie Ellul
Ms Alison Darmanin
Ms. Lucienne Bugeja

Volume Edited by: **Galea P., Borg R.P., Farrugia D., Agius M.R., D'Amico S., Torpiano A., Bonello M..**

An international scientific conference organised by the
Seismic Monitoring and Research Unit, Department of Geoscience, Faculty of Science,
Department of Civil and Structural Engineering and
Department of Construction and Property Management, Faculty of the Built Environment,
University of Malta.

Part of the SIMIT project:
Integrated civil protection system for the Italo-Maltese cross-border area.

Italia-Malta Programme – Cohesion Policy 2007-2013

A sea of opportunities for the future
Tender part-financed by the European Union
European Regional Development Fund (ERDF)
Co-financing rate: 85% EU Funds; 15% National Funds.
Investing in your future.

Proceedings of the International Conference: GEORISKS IN THE MEDITERRANEAN AND THEIR MITIGATION
Edited by: Galea P., Borg R.P., Farrugia D., Agius M.R., D'Amico S., Torpiano A., Bonello M.

Important Notice
The publisher does not assume any responsibility for any damage or injury to property or persons arising out of the use of any materials, instructions, methods or ideas contained in this book. Opinions and statements expressed in this book are those of the authors and not those of the publisher. Furthermore, the publisher does not take any responsibility for the accuracy of information contained in the present volume.
For interpretation of the references to colour, the reader is referred to the web version of the book.
A free online copy of this book is available at www.mistralservice.it

Table of contents

Foreword

This conference is one of the activities organised within the SIMIT strategic project (Integrated Cross-Border Italo-Maltese System of Civil Protection), Italia-Malta Operational Programme 2007 – 2013. SIMIT aims to establish a system of collaboration in Civil Protection procedures and data management between Sicilian and Maltese partners, so as to guarantee the safety and protection of the citizens and infrastructure of the cross-border area. It is led by the Department of Civil Protection of the Sicilian region, and has as other partners the Department of Civil Protection of Malta and the Universities of Palermo, Catania and Malta. SIMIT was launched in March 2013, and will come to a close in October 2015.

Ever since the initial formulation of the project, it has been recognised that a state of national preparedness and correct strategies in the face of natural hazards cannot be truly effective without a sound scientific knowledge of the hazards and related risks. The University of Malta, together with colleagues from other Universities in the project, has been contributing mostly to the gathering and application of scientific knowledge, both in earthquake hazard as well as in building vulnerability. The issue of seismic hazard in the cross-border region has been identified as deserving foremost importance. South-East Sicily in particular has suffered on more than one occasion the effects of large devastating earthquakes. Malta, although fortunately more removed from the sources of such large earthquakes, has not been completely spared of their damaging effects. The drastic increase in the building density over recent decades has raised the level of awareness and concern of citizens and authorities about our vulnerability. These considerations have spurred scientists from the cross-border region to work together towards a deeper understanding of the underlying causes and nature of seismic and associated hazards, such as landslide and tsunami. The SIMIT project has provided us with the means of improving earthquake surveillance and analysis in the Sicily Channel and further afield in the Mediterranean, as well as with facilities to study the behaviour of our rocks and buildings during earthquake shaking. The role of the civil engineering community in this endeavour cannot be overstated, and this is reflected in the incorporation, from the beginning, of the civil engineering component in the SIMIT project. Constructing safer buildings is now accepted to be the major option towards human loss mitigation during strong earthquakes, and this project has provided us with a welcome opportunity for interaction between the two disciplines. Finally the role of the Civil Protection authorities must occupy a central position, as we recognize the importance of their prevention, coordination and intervention efforts, aided by the input of the scientific community.

This conference brings together a diversity of geoscientists and engineers whose collaboration is the only way forward to tackling issues and strategies for risk mitigation. Moreover we welcome the contribution of participants from farther afield than the Central Mediterranean, so that their varied experience may enhance our efforts. We are proud to host the conference in the historic city of Valletta, in the heart of the Mediterranean, which also serves as a constant reminder of the responsibility of all regions to protect and conserve our collective heritage.

Dr. Pauline Galea
Chair, Local Organising Committee
20 -21 July 2015

Keynote Lectures

A NEW EARTHQUAKE MONITORING STRATEGY IN A CROSS-BORDER SEISMIC ZONE

Mucciarelli, M.[1]

[1]*Centro Ricerche Sismologiche – Istituto Nazionale di Oceanografia e di Geofisica Sperimentale, Trieste, Italy, mmucciarelli@inogs.it*

Introduction

The CRS-OGS was founded soon after the Friuli earthquake in 1976. That seismic sequence was localised using only the historical Trieste seismographic station (TRI, at that time in the WWSSN network), with analogical recording on photographic paper. Since then, the digital evolution of seismological instrumentation has brought many improvement and refinements, but the central paradigm is still the same: record the earthquake at some stations, solve the inverse problem to determine the hypocentre and then try to provide to Civil Protection authorities a more or less refined estimate of the affected area. In the last years, the CRS has moved toward a new, integrated monitoring strategy that can be summarised as: from monitoring for the sake of seismology to monitoring for the benefit of stakeholders.

Seismologist are of course interested in more precise epicentre determination, focal parameters and so on, but we should not forget the role of earthquake monitoring for the mitigation of seismic risk, providing useful information to Civil Protection, to public and private companies and to the population in general.

The main lines of the new monitoring development are:

1. a true trans-frontier network, integrated with an early warning system;
2. diffusion of cost-effective accelerometers for measurements on free-field and inside buildings;
3. involvements of Civil Protection volunteers for rapid assessment of earthquake effects;
4. development of specialised monitoring (GNSS, Borehole, Induced Seismicity).

All the above lines must comply with a sustainability strategy to ensure long term maintenance of the integrated monitoring system.

Trans-frontier network and EEW

Since 2012, the networks operating in Friuli Venezia Giulia region (Italy), Austria and Slovenia signed a cooperation agreement for an initiative named CE3RN (Central Eastern Europe Earthquake Research Network, www.ce3rn.eu). In 2014 also Croatia joined the initiative. The agreement formalised an already existing data exchange between partners, but included also the decision to share ideas about network maintenance and good practices, the installation of new station to improve the network geometry, and the the set-up of a joint earthquake early warning system (EEW) with the cooperation of the University of Naples (Picozzi *et*

al., 2015). The lead time of the EEW in the area is probably too short to allow for a full implementation of automatic switches or alarms that are the typical application of EEW, but it is nevertheless very important to have a rapid, back-up alert system that can provide preliminary data to the Civil Protection Agencies in the area that can be used in the case that a large earthquake could cause a massive failure of communication systems, avoiding possible "blind areas" of the traditional location and alert system.
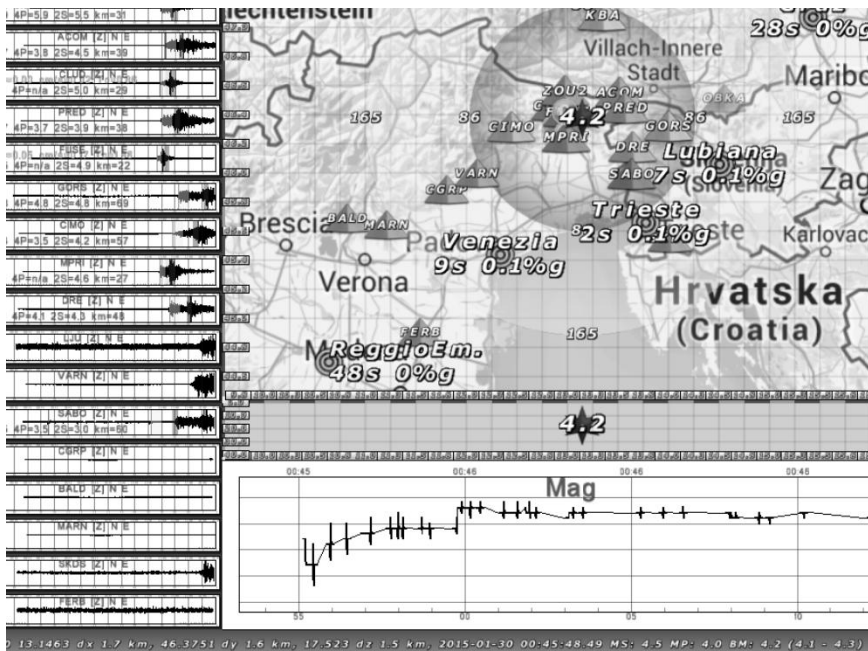
Figure 1. Snapshot of the playback of the PRESTo EEW system during the 30 January 2015 ML 4.1 earthquake.

The system is now undergoing a training phase to tweak the parameters needed for earthquake location and magnitude estimate. During the period May–December 2014, the EEW system PRESTo detected real time 23 earthquakes in the magnitude range 1.7 to 4.1, of which 14 were correctly detected, while 4 and 3 events resulted in missed and false alerts, respectively.

Cost-effective instrumentation

The second aim that OGS-CRS is pursuing is a strategy for a diffuse accelerometric monitoring in free-field and on structures. It is obvious that in the aftermath of an earthquake, a very large number of direct measurement of acceleration would improve the shaking map and also could provide a first glance of damage distribution, enhancing the Civil Protection ability to respond. The problem is that high-end professional instrumentation is now costing to much to be sustainable for a local administration, while low-end, low-cost instrumentation

could be not precise enough. OGS-CRS is actively engaged in research projects with electronic manufactures to try to fill the hole on the shelf (Fig. 2) designing a cost-effective accelerometer with a target price in the range of hundreds Euro, with a sensitivity below 1/1000 g . The first prototypes will undergo testing in the lab and in the field at the end of summer 2015. The first installations will be performed in a project involving the cities of Ferrara, Matera and Enna, funded by the Italian Ministry of Education, University and Research in the framework of the Smart Cities initiative.
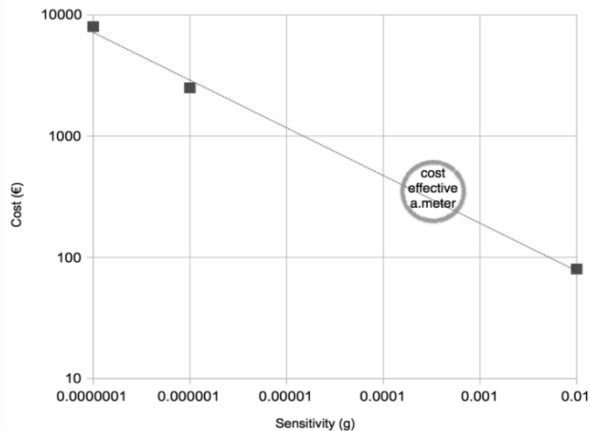
Figure 2. The missing product that is needed to promote diffuse monitoring of structures.

The use of trained volunteers

To complement the future availability of diffuse accelerometric data, OGS-CRS is already taking advantage of a characteristic of Civil Protection in Italy: the widespread presence of trained volunteers. The mainstream of the rapid reconnaissance of earthquake effects is nowadays based on the so called DYFI maps (Did You Feel It). The DYFI maps are compiled thanks to the contribution of citizens that fill forms on web site of seismological organisations, at national or international level.

The two main problems with DYFI maps is that they are intended to provide a result expressed in term of a macroseismic scale so the citizen answers must be somehow processed to have an uniform and comparable results, and in this treatment it is difficult to avoid the bias due to difference in population density. Together with the Civil Protection of the Friuli Venezia Giulia Region, OGS-CRS has started the training of a limited group of volunteers for each of the municipality of the region. They are asked to answer to few simple questions, communicating with the situation room of Civil Protection with the quickest mean available (dedicated web page, sms, radio message). The data does not need any processing and returns a simple rank of effects: not felt, felt, felt with panic, minor damage, serious damage. An event of magnitude 4.1 last January provided the first test of

the method. The rank of effects correlated well with the instrumental shake map, highlighting a lobe of higher effects corresponding to the area with the highest PGA and PGV, while the DYFI maps returned a more isotropic pattern, centred on the most populated city instead than on the epicentre.

Development of specialised monitoring

The scientific part of earthquake monitoring needs the implementation of some specialised instrumentation. OGS-CRS maintains a GNSS network named FREDNET that has the peculiarity of being the only one in Italy providing free RTK service to practitioners using geodetic quality monumentation, antennas and receivers (http://www.crs.inogs.it/frednet/EnglishSite/XFReDNetHomeENG.htm). Each station is now undergoing an update to be able to provide GNSS data sampled at 10 Hz. The implementation of high-frequency sampling is done using low-cost mini-computers (Raspberry PI) and local data storage. Each station will also be complemented with a cost-effective accelerometers so to have the possibility, in case of a strong earthquake, to have unsaturated and unbiased ground motion recording form 0 to 100 Hz. In Italy, and in Europe in general, there is a lack of borehole-surface earthquake recordings that are much widespread in USA or Japan. To provide the best possible estimate of site effects, OGS-CRS and other partners have just started a collaboration to install this kind of instrumentation and provide site characterisation and data dissemination. The cooperation is called NISBAS and the data are available at the web site www.nisbas.it.

Finally, OCS-CRS is tackling the problem of induced seismicity, that is causing concern to the population after the Emilia, 2012 earthquake that was at first considered as a possible case of triggered seismicity. This kind of monitoring requires a very sensitive seismic network, a fair cooperation with industrial operations manager, and a full-disclosure policy toward citizens. OGS-CNR runs the monitoring network at Collalto, Italy, around a gas storage plant. More information, including the examples of communication to population are available at the site http://rete-collalto.crs.inogs.it/en, while the scientific outcomes of the network are described in Priolo *et al.* (2015)

References
Picozzi M., L. Elia, D. Pesaresi, A. Zollo, M. Mucciarelli, A. Gosar, W. Lenhardt, and M. Živcic (2015) Trans-national earthquake early warning (EEW)
in north-eastern Italy, Slovenia and Austria: first
experience with PRESTo at the CE3RN network, Adv. Geosci., 40, 51–61, doi:10.5194/adgeo-40-51-2015
Priolo E., M. Romanelli, M. P. Plasencia Linares, M. Garbin, L. Peruzza, M. A. Romano, P. Marotta, P. Bernardi, L. Moratto, D. Zuliani, and P. Fabris (2015) Seismic Monitoring of an Underground Natural Gas Storage Facility: The Collalto Seismic Network; Seismological Research Letters, 86, 109-123, doi:10.1785/0220140087

DERIVATION OF SEISMIC FRAGILITY CURVES FOR MASONRY BUILDINGS WITH THE AID OF ADVANCED ANALYSIS TOOLS

Kappos, A.J.[1]

[1]*Department of Civil Engineering,City University London, Director of Centre for Civil Engineering Structures,Northampton Sq., London EC1V 0HB, Andreas.Kappos.1@city.ac.uk*

Background and scope

A large part of the building stock in seismic-prone areas worldwide areunreinforced masonry (URM) structures that have been designed without seismic design considerations. Proper seismic assessment of such structures is quite a challenge, particularly so if their response well into the inelastic range, up to local or global failure, has to be predicted, as typically required in fragility analysis. A critical issue in this respect is the absence of rigid diaphragm action (due to the presence of relatively flexible floors), which renders particularly cumbersome the application of popular and convenient nonlinear analysis methods like the static pushover analysis. This keynote lecture addresses masonry buildings representative of Southern European practice, which are analysed in both their pristine condition and after applying retrofitting schemes typical of those implemented in pre-earthquake strengthening programmes. Non-linear behaviour is evaluated using dynamic response-history analysis, which is found to be more effective and even easier to apply in this building type wherein critical modes are of a local nature, due to the absence of diaphragm action. Fragility curves are then derived for both the initial and the strengthened buildings, exploring alternative definitions of seismic damage states. The derived fragility curves are used to carry out a feasibility study, including both benefit-cost and life-cycle analysis, and evaluate the effectiveness of the strengthening programme that was recently implemented in the school buildings of Cyprus.

Nonlinear analysis of structures without a predominant mode in the direction of the analysis can, in principle, be carried out using the modal pushover approach(Chopra& Goel 2002); this means that the number of independent pushover analyses to be carried out in each direction is dictated by the number of modes that contribute up to a substantial fraction of the total mass (around 80%). Unfortunately, unlike what happens in reinforced concrete buildings and bridges wherein 2-3 modes are typically sufficient for capturing the horizontal response, in 3D URM buildings without rigid diaphragms even 20 or 30 modes might not be enough for activating a substantial part of the building mass, since the modes are of a local nature. Moreover, the location of critical deformations is generally different in each mode, which means that resistance curves (commonly referred to as pushover curves) have not only to be drawn with respect to different monitoring points (this is also the case with bridges, see Paraskeva et al. 2006) but also, if they are plotted in terms of the total base shear (as commonly done), they might not

even have a physically sound shape (i.e. one without snapbacks). Finally, results from all these separate analyses have to be statistically combined (e.g. SRSS), which gives rise to a number of problems and inconsistencies, especially in the case of member forces (e.g. pier shears). On top of the theoretical problems, implementation of such a procedure is as yet not 'automatised', hence results from different nonlinear analyses have to be combined 'manually' (i.e. using a spreadsheet). These problems can be overcome if dynamic response history analysis, which captures the effect of all modes, is used

A methodology for nonlinear dynamic analysis of masonry buildings has been recently proposed by Kappos & Papanikolaou (2015). An equivalent frame model (Kappos et al. 2002) is used for unreinforced masonry buildings (Fig. 1-left). The envelope moment (M) vs. rotation (θ) curves for pier 'plastic hinges' are multi-linear, including both pre- and post-peak response and are calculated using the method suggested by Penelis (2006), which accounts for both flexure and shear deformations. The hysteresis rules are simple elastoplastic, resulting in the behaviour shown in Fig. 1-right. For spandrel 'hinges', the analytical procedure suggested by Cattari& Lagomarsino (2008)is followed. Finally, the ground is modelled by a system of springs at the bottom of each pier. The input for the response-history analysis consists of an appropriately defined set of accelerograms, scaled to increasingly higher values of peak ground acceleration (PGA), until 'failure' is reached, the most convenient (but not the most rigorous) option being artificial, spectrum-compatible motions; tools for rigorously selecting natural records are also available (Katsanos&Sextos, 2013).
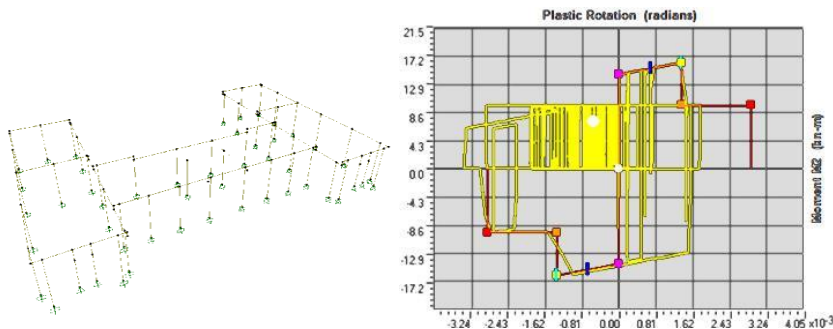
Figure 1.Equivalent frame model of a single-storey URM building (left) and hysteretic M-θ relationship for a pier subjected to seismic action inducing substantial damage.

Fragility curves for unreinforced masonry buildings

Results from incremental nonlinear dynamic analysis of masonry buildings following the aforementioned method are used to derive fragility curves for URM buildings. Critical in this respect is the definition of damage states, which entails a number of problems, mainly arising from the fact that damage is concentrated in only some parts of the building. A synthesis of damage state definitions from the recent international literature is provided in Table 1 (Kappos & Papanikolaou,

2015); the choice of the proper damage descriptor is a major issue in fragility analysis.

Table 1.Damage state definitions for masonry buildings.

Damage state	Description	Associated performance level	Drift	Displacement (from pushover curve)	Shear resistance criteria
DS1	Negligible structural damage; low non-structural damage	Immediate occupancy		$0.7\Delta_y$	first pier attaining its maximum shear
DS2	Minor structural damage and/or moderate non-structural damage	Damage limitation	1‰	$0.7\Delta_y+5(\Delta_u- 0.7\Delta_y)/100$	weighted story drift equals value at the attainment ofmaximum base shear
DS3	Significant structural damage and extensive non-structural damage.	Life safety	3‰	$0.7\Delta_y+20(\Delta_u-0.7\Delta_y)/100$	20% degradation in maximum base shear capacity
DS4	Collapse; repairing the building is not feasible.	Collapse prevention	5‰	Δ_u	-

Kappos & Papanikolaou(2015) define damage states (DS) on the basis of two criteria: (i) Local criterion (member level) based on specific points of the M-θ backbone curve (Fig. 1) e.g. DS3 starts at the point of strength drop; (ii) Global criterion (building level), wherein due to the inherent uncertainty in existing heuristic criteria (last column of Table 1), upper and lower bounds have to be explored, essentially at an ad-hoc basis. It is noted that if the strength degradation part of member response is modelled, the global criterion does not have to define a building damage state as that corresponding to a single masonry pier reaching this state; recommended percentages of failed members (URM piers) vary from 10 to 20%.

Seismic fragility curves are then derived using the commonly adopted assumption of lognormal distribution. Fig. 2 shows different sets of fragility curves for a typical single-storey URM building model (Kappos & Papanikolaou 2015) modelled as shown in Fig. 1; lower/middle/upper limits correspond to different assumptions made regarding the definition of global damage state (i.e. single pier reaches DS, 10% and 20% of piers reach DS). It is clear that the 'series

connection assumption' ('failure' of a single member) is not a realistic one, whereas, at least in this case, the 10% limit seems to be the most appropriate.
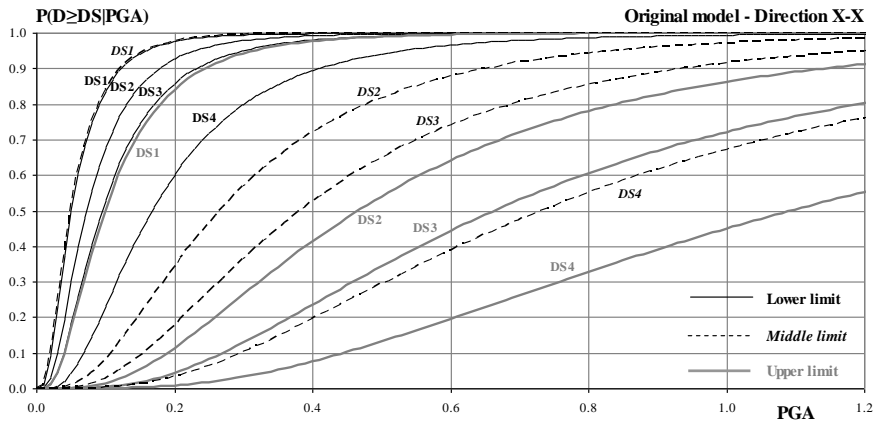
Figure 2.Fragility curves for a typical single-storey URM building model in its original condition.

Evaluation of strengthening programme of school buildings

In Cyprus, after a series of earthquakes that occurred between 1995 and 1999, it was decided to carry out an unprecedented internationally seismic retrofitting of most of the school buildings, taking into account the sensitivity of the society towards these structures. Applying the methodology summarised in the previous two sections, representative school buildings were analysed in both their pristine condition and after applying retrofitting schemes typical of those implemented in the aforementioned large-scale strengthening programme. Fragility curves such as those of Fig. 2 were derived for URM buildings, while corresponding curves for reinforced concrete buildings were also derived (Chrysostomou et al. 2015).These curves were used to carry out a feasibility study, including both benefit-cost and life-cycle analysis, with a viewto evaluating the effectiveness of the strengthening programme.

Typical results of life-cycle analysis of URM school buildings are shown in Fig. 3 ('w' and 'wo' mean with and without considering fatalities in the economic loss assessment). The analysis was found to be very sensitive to the definition of damage states; for the conservative definition of damage thresholds, i.e. the "series system", Fig. 3 suggests that the recommended retrofit level is 100% (full strengthening, e.g. with a rigid but light diaphragm), whereas for the least conservative definition, the recommended retrofit level is 0 (i.e. no strengthening).
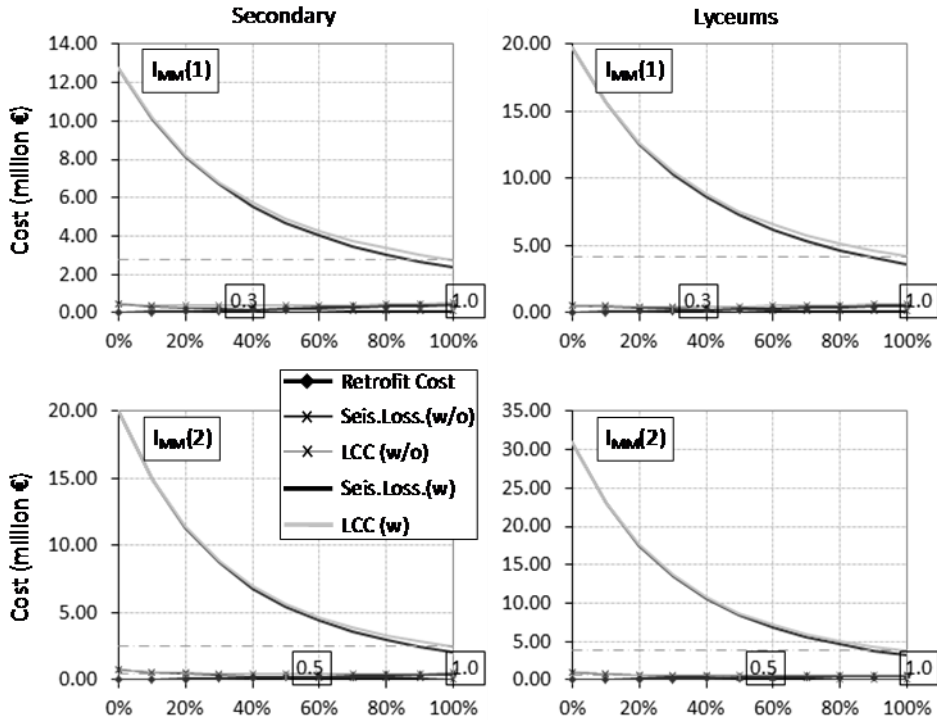
Figure 3.Life-cycle cost analysis for unreinforced masonry school buildings (secondary, lyceums) for two different seismic hazard relationships.

The main conclusions of the feasibility study reported in detail in Chrysostomou et al. (2015) can be summarised as follows:

- Decisions regarding the seismic rehabilitation of existing buildings require both engineering and economic studies and consideration of social priorities.
- Valuable insight regarding retrofit benefits, as assessed from benefit-cost analysis, can be gained from such studies, for instance that the feasibility of a retrofit scheme is determined more by its ability to reduce structural damage for moderate rather than strong earthquakes, at least in the common case of areas of moderate seismic hazard, as Cyprus that was studied herein.
- Casualties influence benefit/cost ratios more when collapse probability is drastically reduced due to retrofit. Problems arise in adequately quantifying the statistical value of human life; the reference value used (€500,000) is an upper bound by the Greek standards, but is a rather conservative value for other western countries (e.g. the US). Nevertheless it amplified, in some cases up to 8 times, the benefit/cost ratios, thus shifting the outcome of the analysis towards the feasibility of retrofit. In any case, protection of life is undoubtedly the primary criterion for pre-earthquake strengthening, especially in high-occupancy buildingslike schools.

Acknowledgements

References

Cattari, S. and Lagomarsino, S. (2008) A strength criterion for the flexural behaviour of spandrels in un-reinforced masonry walls, 14th World Conference on Earthquake Engineering, Beijing, China, paper No. 05-04-0041.

Chopra, AK and Goel, RK (2002).A modal pushover analysis procedure for estimating seismic demands for buildings, Earthquake Engineering & Structural Dynamics, 31(3), 561–582.

Chrysostomou, C.Z., Kyriakides, N., Papanikolaou, V., Kappos, A.J., Dimitrakopoulos. E., Giouvanidis A. (2015). Vulnerability assessment and feasibility analysis of seismic strengthening of school buildings" Bull. of Earthquake Engineering *(accepted subject to minor revision)*.

Kappos A.J. and Papanikolaou, V.K. (2015). Nonlinear dynamic analysis of masonry buildings and definition of seismic damage states, The Open Construction and Building Technology Journal, (*in press*)

Kappos A.J., Penelis, G.G., and Drakopoulos, C. (2002) Evaluation of simplified models for the analysis of unreinforced masonry (URM) buildings, Journal of Structural Engineering, ASCE, 128(7), 890-897.

Katsanos, E.I. and Sextos, A.G. (2013).ISSARS: An integrated software environment for structure-specific earthquake ground motion selection, Advances in Engineering Software, 58(1), 70–85.

Paraskeva, Th., Kappos, A.J., and Sextos, A.G. (2006).Extension of modal pushover analysis to seismic assessment of bridges, Earthquake Engineering & Structural Dynamics, 35(10), 1269-1293.

Penelis, G. G. (2006). An Efficient Approach for Pushover Analysis of Unreinforced Masonry (URM) Structures, Journal of Earthquake Engineering, 10(3), 359–379.

Geohazards, Geology and Geophysics

RE-EVALUATION OF THE SEISMICITY AND SEISMIC HAZARD ASSESSMENT OF LIBYA

Abdunnur Ben-Suleman[1], Abdalmonam A.Swissi[1]
[1]*Geophysics Department /University of Tripoli, Libya,*
a.bensuleman@gp.uot.edu.ly babdunnur@yahoo.com

Libya, located at the central Mediterranean margin of the African shield, underwent many episodes of orogenic activity that shaped its geological setting. The present day deformation of Libya is the result of the Eurasia-Africa continental collision. The tectonic evolution of Libya has yielded a complex crustal structure that is composed of a series of basins and uplifts. This study aims to explain in detail the seismicity and seismic hazard assessment of Libya using new data recorded by theLibyan National Seismograph Network (LNSN) incorporating other available geophysical and geological information.

Detailed investigations of the Libyan seismicity indicate that Libya has experienced earthquakes of varying magnitudes.The seismic activity of Libya shows dominant trends of seismicity with most of the seismic activity concentrated along the northern coastal areas. Four major clusters of seismicity were quite noticeable.

Fault plane solution was estimated for earthquakes recorded by the Libyan National Seismograph Network in northwestern and northeastern Libya. Results of fault plane solution suggest that normal faulting was dominant in the westernmost part of Libya; strike slip faulting was dominant in northern-central part of Libya. The north-eastern part of the country suggests that dip-dip faulting were more prevalent.

STRATIGRAPHIC FEATURES OF THE MALTESE ARCHIPELAGO: A SYNTHESIS

Baldassini, N.[1], Di Stefano, A.[1]

[1]Dipartimento di Scienze Biologiche, Geologiche e Ambientali, Università di Catania, Corso Italia 57, 95129 Catania, nbaldas@unict.it, distefan@unict.it

Structural and geomorphologic framework of the Maltese archipelago

The Maltese archipelago lies in the central Mediterranean area (90 km south of Sicily and 350 km north of Libya), and consists of three main islands (Malta, Gozo and Comino) and numerous smaller islands. The ca. N-S convergent tectonic context between the African and Eurasian plates is considered as the main force shaping the Mediterranean starting from the Late Mesozoic. The geodynamic evolution of the Mediterranean area during the Cenozoic has been driven by the subduction of the tethyan oceanic crust below the neighbouring continental plates (Gueguen et al., 1998; Carminati and Doglioni, 2005). Between the Neogene and Quaternary periods, the Maltese archipelago has been involved in these tectonic modifications (Finetti et al., 1984; Dart, 1993; Catalano et al., 2009; De Guidi et al., 2013).

The Maltese Graben System lies within the African Plate in the foreland of the Appennine-Maghrebides fold-and-thrust belt and represents the north-easternmost part of the Pantelleria Rift. Its geodynamic evolution has been driven by the onset of two different fault systems recognized throughout the whole Sicily Channel Rift Zone (Central-Western Mediterranean): one with ENE-WSW trend, and the other with NW-SE direction. Different interpretations have been provided with reference to the phases of activation of these two fault systems. According to Dart et al. (1993), the Maltese Graben System is the result of the coeval development of the two main rift trends (the NW-SE and the ENE-WSW trending normal faults), which have occurred during the Pliocene Epoch. These authors recognized a pre-rift phase (older than 21 Ma) and an early syn-rift phase (21-6 Ma) characterized by the development of neptunian dykes (Illies, 1980; Pedley, 1990; Gardiner et al., 1995). The acme of the tectonic activity is represented by a late syn-rift phase (older than 5 Ma), and a post-rift phase (<1.5 Ma). According to Corti et al. (2006) and Catalano et al. (2009), the two systems of faults were reactivated in the late Quaternary by dextral strike-slip motions.

The most important structural element characterizing the Maltese archipelago is represented by the Victoria Line Fault (VLF in Fig. 1), a ENE-WSW trending fault crossing the northern part of Malta island from Fommir-Rih Bay, (on the west) to Madliena Tower (on the northeast). North of the VLF, the tectonic processes gave rise to a sequence of horsts and grabens, recognizable on field as a well evident alternation of ridges and valleys (Fig. 1A, B). To the same family of faults belongs also the South Gozo Fault (SGF in Fig. 1), which crosses the island from Mgarr ix-Xini (on the southeast) to Rasil-Qala (on the east). The southern

block of the island of Malta is conversely dominated by the less pronounced NW-SE faulting, mostly represented by the Maghlaq Fault (Fig. 1).

Tectonic activity played a key role in shaping the landscape of the Maltese archipelago. Due to the NE-ward tilting, the highest elevations are located in the northwestern part of Malta island (Figs. 1, 2) and along the western coast of Gozo island (Fig. 1), in correspondence of the major fault lines. These latter parts of the coasts are characterized by sub-vertical cliffs increasing in thickness northward. Similarly, the surface waters are distributed in a direction aligned along or parallel to the SW-NE trending faults, triggering the formation of numerous valleys well evident in figure 1 (Paskoff, 1985).Low-lying coasts are widely distributed in the eastern and north-eastern part of the Malta island and in the northern of Gozoisland, where there are frequent boulders accumulations linked both to storm and tsunami waves (Mottershead et al., 2014).
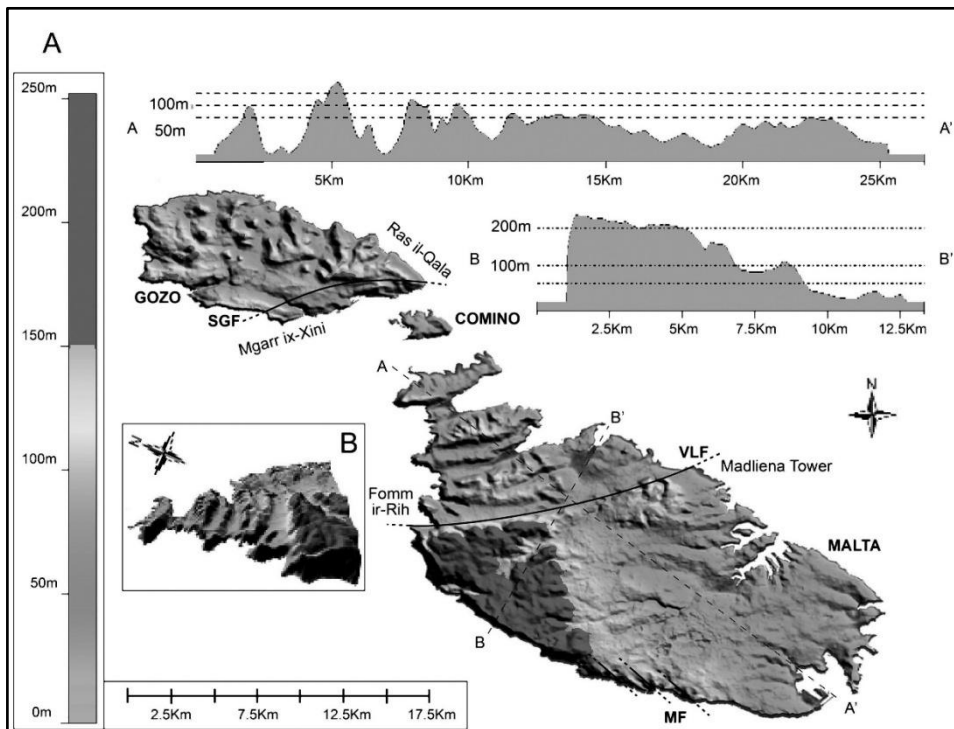
Figure 1. Digital Terrain Model (DTM) of the Maltese archipelago showing the main morphological evidences. VLF=Victoria Line Fault; MF=Maghlaq Fault; SGF=South Gozo Fault. B) Perspective view from west of the DTM highlighting the horst and graben structure of the northern part of the island of Malta.

Furthermore, the occurrence in these areas of more easily erodible lithologies facilitated the development of deep inlets, which have formed in response to the Quaternary marine ingression (Magri, 2001). This is well evident in

the il-Wiedtal-Kalkara and of il-Wied ta' Rinella fluvial valleys, which flow into the Grand Harbour and Marsamxett Harbour, respectively.

The coasts of the Maltese archipelago are characterized by numerous coves of semi-circular shape, produced by solution of carbonates by the percolation water and consequent collapse of the structure. On the island of Gozo these structures can be recognized along the west coast(Qawraand DweiraBay), while on the island of Malta are more widely distributed. Examples are the structures of BlueGrotto along the southern coast and Paradise Bay, along the northwestern coast.

Lithostratigraphy of the Maltese succession

The Maltese sedimentary succession highlights shallow water carbonate deposits in its older and younger terms and of marly-carbonate to marly-clayey in the intermediates. The succession consists of five formations ranging between the late Oligocene (Chattian) to the pre-evaporitic Messinian (Giannelli and Salvatorini, 1972, 1975; Pedley, 1976; Oil Exploration Directorate, 1993; Mazzei, 1986; Jacobs et al., 1996; Foresi et al., 2008, 2011; Mourik et al., 2011; Baldassini et al., 2013) and is composed, in stratigraphic order by the Lower Coralline Limestone Fm, consisting of late Oligocene (Chattian) (Giannelli and Salvatorini, 1972; Felix, 1973; Pedley, 1976; Brandano et al., 2009) bioclastic limestones showing a maximum thickness of 140 min outcrop (Oil Exploration Directorate, 1993), the Globigerina Limestone Fm, late Oligocene (late Chattian) to middle Miocene (Langhian) in age (Giannelli and Salvatorini, 1972; Foresi et al., 2007; Baldassini et al., 2013; Baldassini and Di Stefano, 2015) and widelydistributed throughout the archipelago, highlighting maximum thickness exceeding 200 m (Foresi et al., 2011, 2014). This formation consists of pelagic marly limestones and is subdivided, based on the occurrence of phosphoritic conglomerate beds (Pedley, 1976; Rose et al., 1992;Baldassini and Di Stefano, 2015), into the Lower (massive bedded biomicrites and biomicrosparites, wackestones and packstones), Middle (marlybiomicrites, mudstones and marly mudstones) and Upper (hard limestones, wackestones and subordinate calcareous marls and mudstones) Globigerina Limestone members. This formation is followed by the middle (Serravallian) to late (Tortonian) Miocene in age (Giannelli and Salvatorini, 1975; Sprovieri et al., 2002; Hilgen et al., 2009) Blue Clay Fm, which shows maximum thickness of 75 m (Oil Exploration Directorate, 1993) and consists of alternating dark-grey and pale-grey marly clays.The Greensand Fm, late Miocene (Tortonian) in age (Giannelli andSalvatorini, 1975; Mazzei, 1986; Kienel et al., 1995), consists of greenish marly/clayey glauconite sands and arenites. It poorly crops out in the archipelago and shows maximum thickness of about 11 m (Oil Exploration Directorate, 1993). The Maltese succession is closed by the shallow-water bioclasticlimestones of the Upper Coralline Limestone Fm, late Miocene (pre-evaporitic Messinian) in age (Giannelli and Salvatorini, 1975; Russo andBossio, 1975; Mazzei, 1986) and showing a maximum thickness of 170 m (Oil Exploration Directorate, 1993). Within the SIMIT project numerous geological and stratigraphic surveys were carried out both in Malta and in Gozo paying particular attention to those areas

where the lithological features are associated to greater vulnerability and, consequently, where the risk was more pronounced. The study areas were selected based on the presence of more or less powerful thicknesses of the marly/clayey lithotypes referred to the intermediate unit of the Globigerina Limestone Fm(Middle Globigerina Limestone Mb) orto the Blue Clay Fm. In fact, this lithotype, due to its plastic feature, isusually responsible for the fracturing of overlying formations(more evident in the Upper Coralline Limestone).Detailed analyses were mostly carried close to the Victoria Line Fault and in the northwestern part of Malta, where the outcrops of Il-Blata,Gnejna Bay and Qammieh have been measured, sampled and analyzed. The lithological log and bio-chrono stratigraphic results obtained here allowed us to perform correlations with other well-known sequences such as Dingli and that of Rasil-Pellegrin (respectively south and just north of the Victoria Line Fault), highlighting differences in the thicknesses of the formations along the coast (Fig. 2). The lithostratigraphic approach highlighted a sharp decrease in thickness of the Lower Coralline Limestone Fm northward. The formation reaches its maximum thicknesses south of the Victoria Line Fault where it exceeds 50 m both at Dingli and Il-Blata (Fig. 2) and forms vertical cliffs (Fig. 1A). North of the fault, the formation poorly crops out only in the Qammieh section, while at Rasil-Pellegrin and Gnejna Bay it lies below the sea level. A similar behavior is recognizable also for the Lower Globigerina Limestone Mb, which does not crop out from the sea in the two sections immediately north of the fault (see the sections of Rasil-Pellegrin and Gnejna Bay in Fig. 2).The Middle Globigerina Limestone Mbcovers different depositional intervals between the outcrops located south and north of the Victoria Line Fault. In fact, through a litho- and bio-stratigraphic approach we documented the presence in the sections of Dingli and Il-Blata of an interval of deposition, early Aquitanian in age and represented by massive whitish limestones (Baldassini and Di Stefano, 2015), which is totally missed or not deposited in the northern outcrops (Fig. 2).These dissimilarities between the two areas can be explained supposing different locations within the depositional basin, being more distal for the southern outcrops, and more marginal for northern, probably in a context of local synsedimentary tectonic activity.The Burdigalian calcareous marls, typical of the member both in Malta and Gozo, are instead present in the Dingli and Il Blata outcrops as well as at Qammieh. As highlighted for the Lower Coralline Fm and for the Lower Globigerina Limestone Mb, also the Middle Globigerina Limestone Mb does not crop out in the sections of Rasil-Pellegrin and Gnejna Bay due to the post-depositional activity of the fault (Fig. 2). The three lithotypes of the Upper Globigerina Limestone Mb crops out, pointing to similar thicknesses, in all the considered outcrops (Fig. 2). However, in the section of Il-Blata, a late Burdigalian deposition was recognized which is absent in others area along the western and northwestern coast. Also in this case, this depositional uniqueness can be linked to different position within the basin as well as to synsedimentary tectonic activity. The Blue Clay Fmdisplays thicknesses of about 30-35 m at Dingli and Il-Blata and reaches 70 m immediately north of the fault in the Rasil-Pellegrin outcrop (Fig. 2).

The thickness of the formation reduces northward to values comparable to those recognized south of the fault both in the Gnejna Bay and Qammieh outcrops. It is conceivable that during the deposition a wider accommodation space developed in the Rasil-Pellegrin area probably due to local synsedimetary tectonic activity. All the considered outcrops are involved in landslide phenomena and is responsible for the collapsed boulders from the overlying Upper Coralline LimestoneFm. The Greensand Fm occurs with thicknesses never exceeding 1 m along the entire coast. The Upper Coralline Limestone Fmshows thicknesses between 30 and 50 m in the considered outcrops (Fig. 2), realizing south of the Victoria Line Fault a wide plateau, which is reported in figure 1A, characterized by the higher elevations. In all the considered areas, collapses (mainly due to the percolation waters), fracturing and differential settlements of the Upper Coralline Limestone Fm are frequent and linked to the presence of several meters of the underlying marl deposits of the Blue Clay Fm (Fig. 2).
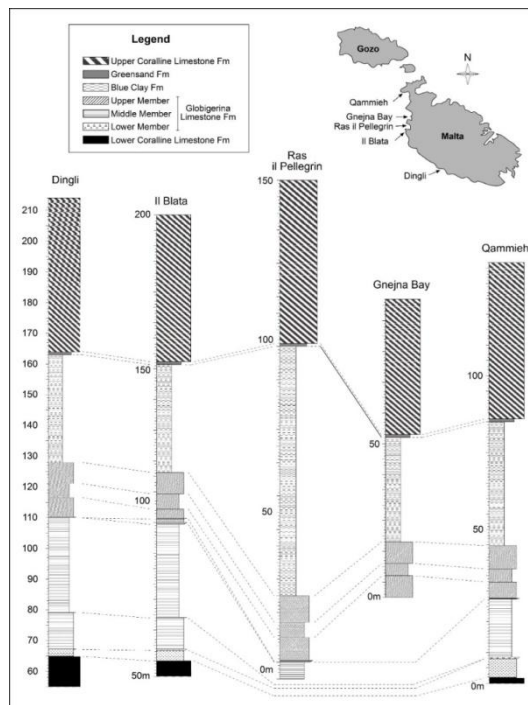
Figure 2. Lithostratigraphic logs and correlations of the considered outcrops.

References

Baldassini N. and A. Di Stefano (2015). New insights on the Oligo-Miocene succession bearing phosphatic layers of the Maltese Archipelago, Italian Journal of Geosciences, doi: 10.3301/IJG.2014.52

Baldassini, N., Mazzei, R., Foresi, L.M., Riforgiato F. and G. Salvatorini (2013). Calcareous plankton bio-chronostratigraphy of the Maltese Globigerina Limestone member, Acta Geologica Polonica 63 (1) 105-135.

Brandano, M., Frezza, V., Tomassetti, L. and M. Cuffaro (2009). Heterozoan carbonates in oligotrophic tropical waters: the Attard member of the lower coralline limestone formation (Upper Oligocene, Malta),Palaeogeography, Palaeoclimatology, Palaeoecology, 274(1) 54-63.

Carminati, E., and C. Doglioni (2005). Mediterranean tectonics,in Encyclopedia of Geology, Volume 2, R.C. Selley, Cocks, L.M.R. and Plimer, I.R. (Editor), Elsevier/Academic Press, Amsterdam, 135-146.

Catalano, S., De Guidi, G., Lanzafame, G., Monaco, C. and L. Tortorici (2009). Late Quaternary deformation on the island on Pantelleria: New constraints for the recent tectonic evolution of the Sicily Channel Rift (southern Italy), Journal of Geodynamics 48 75–82.

Corti, G., Cuffaro, M., Doglioni, C., Innocenti, F. and P. Manetti (2006). Coexisting geodynamic processes in the Sicily Channel,Geological Society of America Special Papers409 83-96.

Dart, C.J., Bosence, D.W.J. andK.R. McClay (1993). Stratigraphy and structure of the Maltese graben system, Journal of the Geological Society 150 (6) 1153-1166.

De Guidi, G., Lanzafame, G., Palano, M., Puglisi, G., Scaltrito, A. andL. Scarfì (2013). Multidisciplinary study of the Tindari Fault (Sicily, Italy) separating ongoing contractional and extensional compartments along the active Africa–Eurasia convergent boundary, Tectonophysics 588 1–17.

Felix, R. (1973). Oligo-Miocene stratigraphy of Malta and Gozo, MededelingenLandbouwhogeschoolWageningen 73 1-104.

Finetti, I.R. (1984). Struttura e evoluzione della microplacca adriatica,Bollettino di Oceanografia Teorica e Applicata 2 115-123.

Foresi, L.M., Baldassini, N., Sagnotti, L., Lirer, F., Di Stefano, A., Caricchi, C., Verducci, M., Salvatorini, G. and R. Mazzei (2014). Integrated stratigraphy of the St. Thomas section (Malta Island): a reference section for the lower Burdigalian of the Mediterranean Region,Marine Micropaleontology 111 66-89.

Foresi, L.M., Mazzei, R., Salvatorini, G. andF. Donia (2008). Biostratigraphy and chronostratigraphy of the Maltese Lower Globigerina Limestone Member (Globigerina Limestone Formation): new preliminary data based on calcareous plankton, Bollettino della Società Paleontologica Italiana 46 (2-3) 175-181.

Foresi, L.M., Verducci, M., Baldassini, N., Lirer, F., Mazzei, R., Salvatorini, G., Ferraro, G. and S. Da Prato (2011). Integrated stratigraphy of St. Peter's Pool section (Malta): new age for the Upper Globigerina Limestone Member and progress towards the Langhian GSSP,Stratigraphy 8, 125-143.

Gardiner, W., Grasso, M. andD. Sedgeley (1995). Plio-Pleistocene fault movement as evidence for megablock kinematics within the Hyblean-Malta Plateau, central Mediterranean, Journal of Geodynamics 19 35–51.

Giannelli, L. and G. Salvatorini (1972). I Foraminiferi planctonici dei sedimenti terziari dell'Arcipelago Maltese. Biostratigrafia del "Globigerina Limestone" I, Atti della Società Toscana di Scienze Naturali, Memorie Serie A 79 49-74.

Giannelli, L. and G. Salvatorini (1975). I Foraminiferi planctonici dei sedimenti terziari dell'Arcipelago Maltese. Biostratigrafia di "Blue Clay", "Greensand" and "Upper Coralline Limestone" II, Atti della Società Toscana di Scienze Naturali, Memorie, Serie A 82 1-24.

Gueguen, E., Doglioni, C. andM. Fernandez (1998). On the post 25 Ma geodynamic evolution of the western Mediterranean, Tectonophysics 298 259-269.

Hilgen, F.J., Abels, H.A., Iaccarino, S.M., Krijgsman, W., Raffi, I., Sprovieri, R., Turco, E. and W.J. Zachariasse (2009). The Global Stratotype Section and Point (GSSP) of the Serravallian Stage (Middle MJiocene), Episodes 32 152-166.

Illies, J.H. (1980). Mechanism of graben formation, Tectonophysics 73 249-266.

Jacobs, E., Weissert, H., Shield, G. and P.Stille(1996). The Monterey event in the Mediterranean: A record from shelf sediments of Malta,Palaeogeography, Palaeoclimatology, Palaeoecology 11 (6) 717-728.

Kienel, U., Rehfeld, U. and S.M.Bellas(1995). The Miocene Blue Clay formation of the Maltese Islands: Sequence stratigraphic and paleoceanographic implications based on calcareous nannofossil stratigraphy, Berliner GeowissenschaftlicheAbhandlungen 16 533–557.

Magri, O. (2001). Slope instability along the north-west coast in Malta, Ph.D. Thesis, University of Durham, UK.

Mazzei, R.(1986). The Miocene sequence of the Maltese Islands: biostratigraphic and chronostratigraphic references based on nannofossils,AttidellaSocietà Toscana di ScienzeNaturali, MemorieSerie A 92 165-197.

Mottershead, D., Bray, M., Soar, P. and P.J.Farrer(2014). Extreme wave events in the central Mediterranean: Geomorphic evidence of tsunami on the Maltese Islands,Zeitschrifyt fur Geomorphologie 58 (3) 385-411.

Mourik, A.A., Abels, H.A., Hilgen, F.J., Di Stefano, A. and W.J.Zachariasse(2011). Improved astronomical age constrains for the Middle Miocene climate transition based on high-resolution stable isotopes records from the central Mediterranean Maltese Islands, Paleoceanography 26 PA1210.

Oil Exploration Directorate (1993). Geological Map of the Maltese Island: Sheets 1, Malta island; Sheet 2, Gozo Island, British Geological Survey, Publication of the Oil Exploration Directorate, Office of the Prime Minister, Malta.

Paskoff, R. (1985). Malta, in The world's coastlines, Bird, E.C. and Schwartz, M.L. (Editor), Van Nosstrand Reinhold, New York, 431-437.

Pedley, H.M.(1976). A paleoecological study of the Upper coralline Limestone Terebratula-Aphelesia Bed (Miocene, Malta) based on bryozoan growth-forms and brachiopod distribution,Palaeogeography, Palaeoclimatology, Palaeoecology 20 209-234.

Pedley, H.M.(1990). Syndepositional tectonics affecting Cenozoic and Mesozoic deposition in the Malta and SE Sicily areas (Central Mediterranean) and their bearing on Mesozoic reservoir development in the N Malta offshore region, Marine and Petroleum Geology 7 171-180.

Rose, E.P.F., Pratt, S.K. and S.M. Bennett (1992). Evidence for Sea-Level Changes in the Globigerina Limestone Formation (Miocene) of the Maltese Islands, Paleontologia y Evoluciò 24-25 265-276.

Russo, A. and A. Bossio (1975). Prima caratterizzazione degli ostracodi per la biostratigrafia e la paleoecologia del Miocene dell'arcipelago Maltese, Bollettino della Società Paleontologica Italiana 15 215-227.

Sprovieri, M., Caruso, A., Foresi, L.M., Bellanca, A., Neri, R., Mazzola, S. and R. Sprovieri (2002). Astronomical calibration of the upper Langhian/lower Serravallian record of Ras Il-Pellegrin section (Malta Island, central Mediterranean), Rivista Italiana di Paleontologia e Stratigrafia 108 (2) 183–193

HUNTING FOR PAST EARTHQUAKES IN THE CENTRAL MEDITERRANEAN; SOME EMBLEMATIC CASES FROM THE SICILIAN COLLISION ZONE

Barreca, G.[1], Guzzetta, L. [2] Ferranti, L.,[3]Monaco, C[1]

[1]*Dipartimento di Scienze Biologiche, Geologiche ed Ambientali, Sezione di Scienze della Terra, Università di Catania, cmonaco@unict.it, g.barreca@unict.it*
[2]*INAF, Osservatorio Astronomico di Capodimonte, Napoli, lauraguzzetta@hotmail.com*
[3]*Dipartimento di Scienze della Terra, dell'Ambiente e delle Risorse (DiSTAR), Università di Napoli "Federico II", luigi.ferranti@unina.it*

Introduction

Archaeological evidence for an earthquake is not always clear or unambiguous (Ambraseys, 2006). Where they are verified by geological and archaeological studies, faulted architectural relics represent valuable data in understanding active tectonics and seismic hazard of a region. In many cases, they represent the missing tiles of a seismic puzzle dataset, providing useful information and filling gaps in historical seismicity. From this perspective, countries rich in ancient ruins, such as those bordering the Mediterranean Sea, can offer a natural laboratory for this discipline. In this area, ancient buildings damaged by earthquakes have been described since the beginning of the last century (e.g., Lanciani, 1918; Evans, 1928), even though modern and interdisciplinary methodologies have been applied only recently (e.g., Karcz and Kafri, 1978; Stiros, 2001;Noller and Lightfoot, 1997; Hancock and Altunel, 1997; Galadini and Galli, 2004).Among many other countries, Sicily represents a suitable place in investigating past earthquakes as it exhibits a large amount of archaeological information, the majority of these concentrated in the period between the fourth century B.C. and the fourth–fifth century A.D. Archaeological rests consist of buildings, fortified walls, streets, canals and other kinds of artefacts which can provide useful chronological markers for constraining possible earthquakes in the past. In this contribution we present field evidence for past earthquakes by means emblematic cases of faulted archaeological relics along the Sicilian Collision Zone. Examples come from two different archaeological sites located in central and western Sicily respectively where faulting involves man-made structures of old Greek and Roman age. Findings provide useful constraints on the seismic history/hazard of the analysed regions

Background

The Sicilian Collision Zone in the Central Mediterranean, originated since the Neogene from the deformation of several paleogeographic domains originally located between the African and the European plates (Dewey et al., 1989). The

Neogene-Quaternary subduction/collision dynamics have mainly involved Meso-Cenozoiccarbonate (platform and basin) successions of the Africa continental palaeo-margin and oceanic series of the Neotethys. Tectonic shortening and thrust piling gave rise to a foreland–verging fold and thrust belt to date largely exposed on continental Sicily. Thrust migration was also accompanied by sedimentation in piggy-back basins (Grasso and Butler, 1991; Barreca, 2014), most of them well preserved in the central-western portion of the collision zone. The long-living convergence that affect the central Mediterranean and Sicily, has been occasionally perturbed by the recent Ionian slab dynamic and back-arc opening northwards (Faccenna et al., 2001) resulting into a complicate geodynamic scenario with reorganization at plate boundaries (Goes et al., 2004) and the shaping of a series of crustal blocks with independent kinematics. The modern seismotectonic configuration is depicted by GPS velocity fields (Palano et al., 2012) and supported by available focal solutions (Neri et al., 2005), the latter indicating that strike–slip, normal and reverse-oblique kinematics can occur simultaneously. In particular, a significant change in the kinematics behaviour seems to occur in central-eastern Sicily along a large NW-SE trending kinematic boundary that appear to separate an extensional domain in the NE (the Peloritani block) from a contraction alone in the SW (Barreca et al., 2014). Both domains are prone to produce big earthquakes as testified by the occurrence of several destructive events, among these the December 28, 1908 Messina event (M=7.1) in the north eastern sector and the January 15, 1968 Belice earthquake (M=6) in western Sicily.

Previous archaeo-seismological studies and historical catalogues (Boschi et al., 2000; Working Group CPTI, 2004) suggest that large earthquakes have struck Sicily in the past even though their seismogenic sources, hypo central locations and dimension have remained enigmatic for a long time. Major ancient seismic events have been held accountable for severe damages all over Sicily, such as the A.D. 361 event (Guidoboni et al., 1994), whose epicentral location is vaguely reported in central Sicily, and the 370-300 B.C. earthquake, considered responsible for the collapse of the Greek temples of Selinunte (Guidoboni et al., 2002) in the western portion of the Sicilian Collision Zone.

Evidence for faulted archaeological remains
Central Sicily

Evidence for Roman-age faulting has been found in central Sicily (Fig. 1A)along the archaeological site of Mount Alburchia, which is located ~3 km southwest of Gangi village. The ancient site was built on the northern slope of the ridge and it is characterized by a number of Roman cult manufactures consisting of religious shrines ("edicole votive") dated to fourth century A.D. (Naselli, 1956; Tusa, 1958; Manganaro, 1965).They have been excavated on Middle–Upper Miocene conglomerates and sands (Jones and Grasso,1995; Barreca, 2014). Structurally, the ridge is a gentle NE-SW trending syncline but it is also transversally sliced by a more recent strike and dip-slip fault association (Fig.1B).As evidenced by displaced sandy layers within the conglomeratic

bedrock, dip-slip structures consist of high-angle faults with extensional motion. Interestingly, faults cross cut also the archaeological site (Fig. 1C) and one of these propagated through a votive niche (Fig 1D), clearly offsetting its plastered roof of about 15 cm (Fig. 1E). Since fault breaks the hard cobbles of the bedrock, this type of deformation has been associated to a very rapid (impulsive) stress propagation (see Moretti, 1990). This suggests that the fault displacement of the Roman architectural relic was probably related to a coseismic slip.

According to empirical relationship of Wells and Coppersmith (1994) for normal faults and considering the displacement of 15 cm, the observed deformation can be related to an earthquake of magnitude ~6. Previous archaeological studies in the nearby (Beck et al., 1975)evidenced that ceramics and coins production drastically reduced at the end of the fourth century A.D. Further, recent excavations (Storey, 2002) have brought to light a fourth century A.D. grave where remains of women and children are mixed, an unusual common burials for the Roman culture. All these clues strongly support the hypothesis that a strong earthquake probably occurred in this area during the Late Roman period.

Western Sicily

The Greek city of Selinunte, today one of the largest archaeological site in the Mediterranean, is located along the coastline of SW Sicily facing the Sicily Channel (Fig. 2A). The city was built on a hill of middle-upper Pleistocene marine sediments and it extends for about 270 hectares. Archeological studies, based on the dynamics of the collapse of some temples and fortification walls (Guidoboni et al., 2002, Bottari et al., 2009) supported the hypothesis that the city was struck by large earthquakes in the past. In particular, two strong earthquakes have been identified; 370-300 B.C and 300-600 A.D. on the basis of some pottery pieces founded below the collapsed blocks and of chronological considerations (Guidoboni et al.,2002). Further, the overturning toward the North of the majority of the columns give useful information about the dynamic of the seismic event, suggesting a ground motion toward the South. According to the tectonic setting of the area (Monaco et al., 1996), this direction is compatible with a seismic slip on a roughly E-W trending thrust fault.

Field surveys have been recently undertaken along the Belice Valley in order to detect possible evidences of active tectonics, since the area was shaken by the January 15, 1968 earthquake (M=6). Just south of the Castelvetrano modern town, an archaeological site lies on the crest of a NE-SW trending anticline which deforms lower-middle Pleistocene terraced calcarenites (Fig. 2B). The site has an age ranging from Bronze to ancient Greek age (De Miro, personal communication) and includes an ancient street excavated on the calcarenites (Fig. 2C). Detailed structural measurements revealed that a SE-dipping, N30E striking reverse fault dislocates the street (Fig. 2D) with an offset of about 5 cm. Using empirical fault-displacement relationships (Wells and Coppersmith, 1994) for reverse faults, this displacement can be related to an M ~ 6 earthquake.
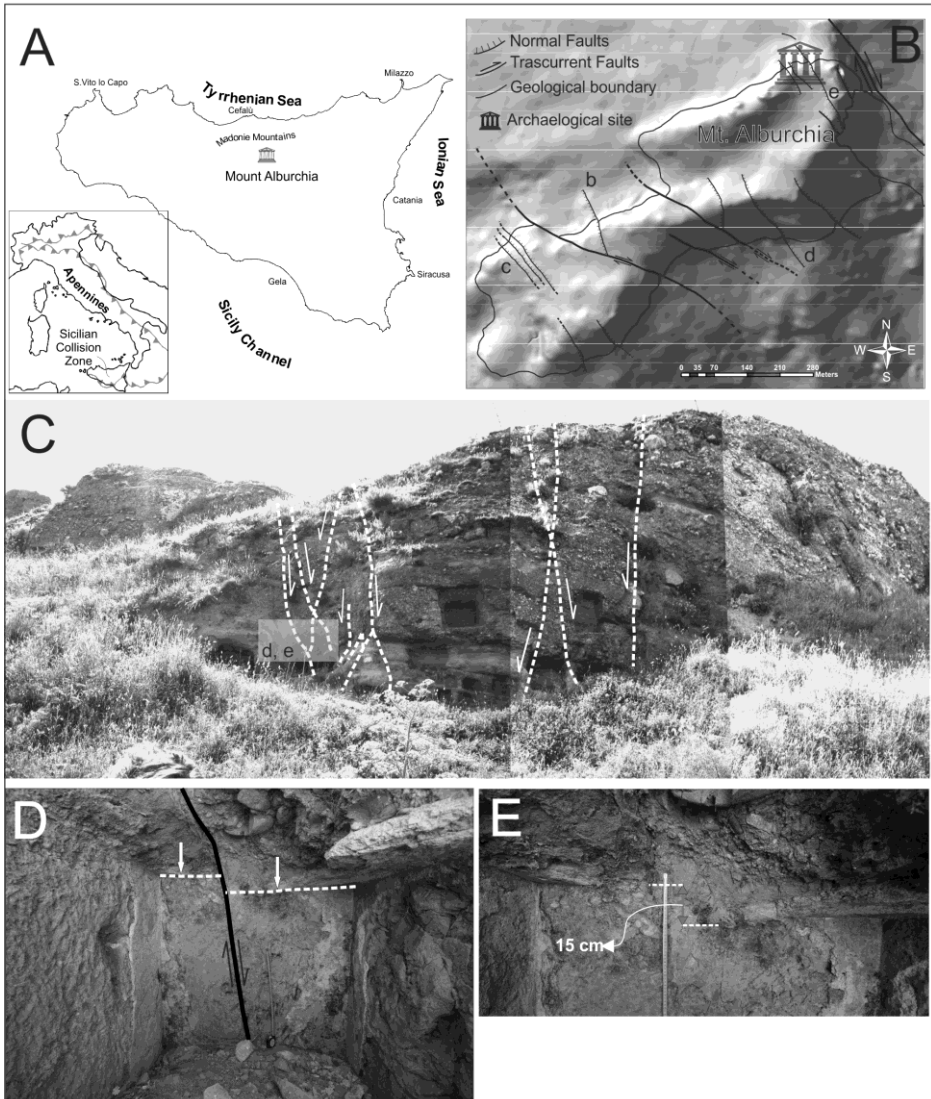
Fig. 1 –a) Location of the archaeological site of Mt. Alburchia in the frame of the Sicilian Collision Zone. B) Structural setting of Mt. Alburchia characterized by a gentle NE-SW trending syncline sliced by younger strike-slip and dip-slip faults association. C) Picture from the northern slope of Mt. Alburchia which displays the faulted votive niche. One of these faults D) cross-cut a votive niche displacing its plastered roof (E) of about 15 cm.
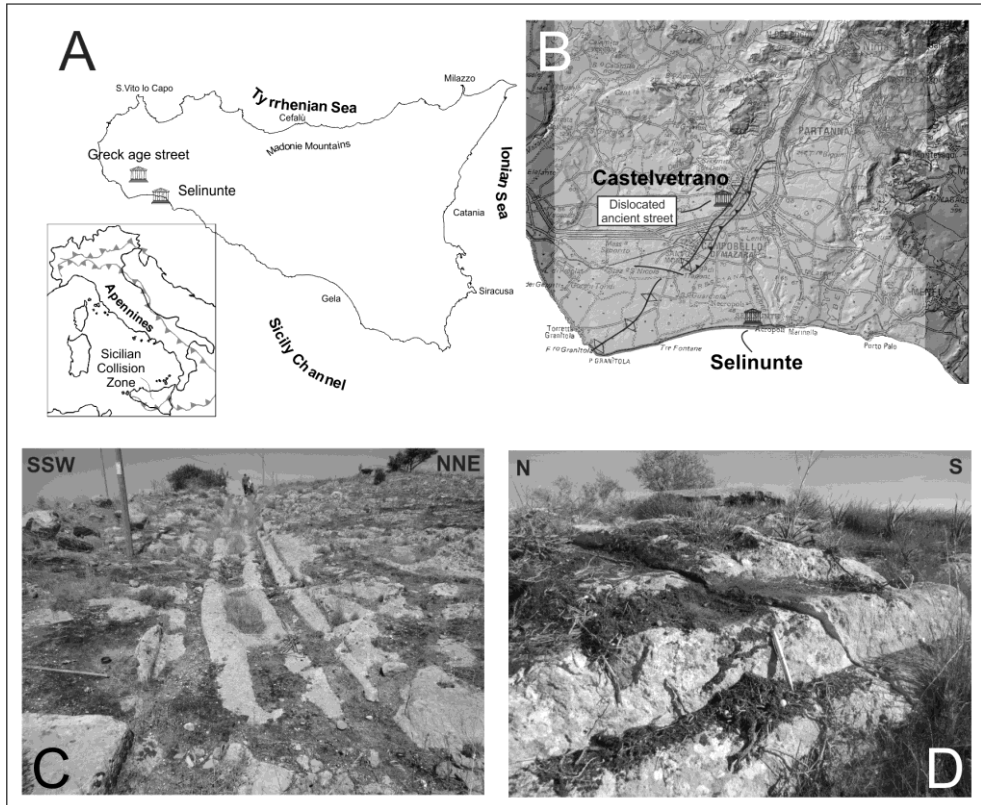
Fig. 2 –a) Location of the study area in the western portion of the Sicilian Collision Zone with indicated the position of the archaeological site of Selinunte. B) Structural setting of the area between Selinunte and Castelvetrano given by NE-SW trending folds and thrusts deforming a Middle-late Pleistocene sequence. D) particular of the ancient street (Greck age) dislocated by a N30E oriented back-thrust (D).

Discussion and conclusions

Detailed field surveys from the central-western portion of the Sicilian Collision Zone provide evidences for two emblematic cases of faulted archaeological relics. The first case comes from the central portion of the collision zone and it concerns the findings of a faulted, IV Century A.D, man-made structures along the Mount Alburchia, located about 3Km SW of the Gangi village. Faulting displacement and previous archaeological investigations clearly suggest that the area experienced a strong earthquake in the past. The analysis of historical seismicity from available earthquake catalogues (Boschi et al., 2000; Working Group CPTI, 2004) revealed that the A.D. 361 earthquake (I = VIII MCS; Mw = 6.3) is the only strong seismic event able to produce superficial effects with ground displacements, and thus magnitude (~6),comparable to that observed/calculated atMount Alburchia. Faulted archaeological remains in the SW sector of the collision zone indicate that another strong earthquake occurred in this area after the

construction of the ancient street (from Bronze to ancient Greek age). Findings fall within the seismogenic zone where the 1968 Belice seismic sequence occurred and the calculated magnitude (~6) is capable of destroying the nearby temples of Selinunte, located just about 7 km toward the SE.

Geo-archeological studies here presented provided powerful constraints on the seismic history of the two investigated sectors and revealed that seismogenic faulting in the Sicilian Collision zone can occur by distinct kinematic, as clearly evidenced by the observed ground ruptures.These confirm that the central-western portion of this zone undergoes active thrusting and shearingin response to aregional ~5–6 mm/yrNW-SEAfrica- Europe convergence (Palano et al., 2012).

References

Ambraseys, N.N., (2006). Earthquakes and archaeology: Journal of Archaeological Science, v. 33, p. 1008–1016, doi: 10.1016/j.jas.2005.11.006.

Barreca, G. (2014). Geological-structural outlines of the southern Madonie Mts. (Central Northern Sicily). Journal of Maps, http://dx.doi.org/10.1080/17445647.2014.977972.

Barreca, G., Scarfì, L., Cannavò.F., Koulakov, I., Monaco,C. (2014).Structural and seismological clues for a lithospheric scale tear fault system in central-eastern Sicily (Italy).GNGTS 2014, Bologna Italy, 85

Beck, P., Maccari, B., and Poisson, M.J.(1975). Prospezione archeologica a Gangi Vecchio: Archeologia Medievale, v. II, p. 382–386.

Boschi, E., Guidoboni, E., Ferrari, G., Gasperini, P., Mariotti, D., and Valensise, G. (2000). Catalogue of strong Italian earthquakes from 461 a.C. to 1997: Annali di Geofisica, v. 43, no. 4, p. 843–868 and CD-ROM.

Bottari, C., Stiros, S.C., Teramo, A. (2009). Archaeological evidence for destructive earthquakes in Sicily between 400 B.C. and A.D. 600.Geoarchaeology 24 (2),147–175, http://dx.doi.org/10.1002/gea.20260.

Dewey, J.F., Helman, M.L., Turco, E., Hutton, D.H.W., and Knott, S.D. (1989).Kinematicsof the Western Mediterranean. In: Coward, M.P., Dietrich, D., Park, R.G. (Eds.),Alpine Tectonics, vol. 45. Geological Society of London Special Publication, pp.265–283.

Evans, A.J. (1928). The Palace of Minos at Knossos II: London, Macmillan, 547 p.

Faccenna, C., Becker, T.W., Lucente, F. P., Jolivet, L., Rossetti, F. (2001). History of subduction and back-arc extension in the central Mediterranean, Geophys. J. Int., 145, 809–820,doi:10.1046/j.0956-540x.2001.01435.x

Galadini, F., and Galli, P. (2004). The 346 A.D. earthquake (central-southern Italy): An archaeoseismological approach: Annali di Geofisica, v. 43, no. 2–3, p. 885–905.

Goes, S., D. Giardini, S. Jenny, C. Hollenstein, Kahle, H.-G., Geiger, A. (2004).A recent reorganization in the south-central Mediterranean, Earth Planet.Sci. Lett., 226, 335–345, doi:10.1016/j.epsl.2004.07.038

Guidoboni, E., Comastri, A., and Traina, G. (1994). Catalogue of Ancient Earthquakes in the Mediterranean Area up to the 10th Century: Bologna, ING,504 p.

Guidoboni, E., Muggia, A., Marconi, C., Boschi, E. (2002). A case study in archaeo-seismology. The collapses of the Selinunte Temples (Southwestern Sicily): two earthquakes identified. Bull. Seismol.Soc. Am. 92, 2961–2982.

Hancock, P.L., and Altunel, E. (1997). Faulted archaeological relics at Hierapolis (Pamukkale), Turkey: Journal of Geodynamics, v. 24, p. 21–36, doi: 10.1016/S0264-3707(97)00003-3.

Jones, R.E., and Grasso, M. (1995).Paleotectonics and sediment dispersal pathways in north-central Sicily during the late Tortonian: StudiGeologiciCamerti, Volume Speciale 1995/2, p. 279–291.

Karcz, I., and Kafri, U. (1978). Evaluation of supposed archaeoseismic damage in Israel: Journal of Archaeological Science, v. 5, p. 237–253, doi:10.1016/0305-4403(78)90042-0.

Lanciani, R. (1918). Segni di terremoti negli antichi edifizi di Roma antica: Roma, Bollettino della Archeologia Comunale, p. 1–30.

Monaco, C., Mazzoli, S., Tortorici, L. (1996). Active thrust tectonics in western Sicily (southern Italy): the 1968 Belice earthquakes sequence. Terra Nova 8,372–381.

Moretti, A. (1990). Fratture di origine tettonica nei ciottoli dei conglomerati: Elementi strutturali probabilmente connessi a grandi terremoti: Rendiconti Società Geologica Italiana, v. 13, p. 77–84.

Neri, G., Barberi, G., Oliva, G., Orecchio, B., 2005. Spatial variations of seismogenic stress orientations in Sicily, south Italy. Phys. of the Earth and Planet. Int., 148, 175–191.

Noller, J.S., and Lightfoot, K. (1997). An archaeoseismic approach and method for the study of active strike slip faults: Geoarchaeology, v. 12, p. 117–135, doi: 10.1002/(SICI)1520-6548(199703)12:2<117::AID-GEA2>3.0.CO;2-7.

Palano, M., Ferranti, L., Monaco, C., Mattia, M., Aloisi, M., Bruno, V., Cannavò, F., Siligato, G. (2012). GPS velocity and strain fields in Sicily and southern Calabria, Italy: updated geodetic constraints on tectonic block interaction in the central Mediterranean. J. Geophys. Res., 117, B07401.

Stiros, S.C. (2001). The A.D. 365 Crete earthquake and possible clustering during the fourth to sixth centuries in the Eastern Mediterranean: A review of historical and archaeological data: Journal of Structural Geology, v. 23, p. 545–562, doi: 10.1016/S0191-8141(00)00118-8.

Storey, G. (2002).Preliminary investigations at the site of GangiVecchio, Gangi, Province of Palermo, Sicily, Italy. July 22 to August 6, 2000: Report to Dr. Francesca Spatafora, Soprintendenza BB.CC.AA., Palermo, Italy, p. 1–8.

Wells, D.L., and Coppersmith, K.J. (1994). New empirical relationship among magnitude, rupture length, rupture width, rupture area, and surface displacement: Bulletin of the Seismological Society of America, v. 84, no. 4, p. 974–1002.

SEISMOLOGICAL AND SEISMIC REFLECTION EVIDENCE FOR ACTIVE TECTONICS IN THE EASTERN ALBORAN BASIN

Bouskri, G.[1], Elabbassi, M.[2], El Ouai, D.[1], Ammar, A.[2], Harnafi, M.[1]

[1]*Department of Geology, Scientific Institute of Rabat, Mohamed V University, Ibn Battota Avenue, P.B. 703,Agdal 10106, MOROCCO, ghizlane.bouskri@gmail.com, elouai@israbat.ac.ma, harnafi@israbat.ac.ma*

[2]*Department of Geology & Faculty of Sciences, Mohamed V University, 4 Ibn Battouta Avenue P.B. 1014 RP, MOROCCO, elabbassi@hotmail.com, siadammar@fsr.ac.ma*

Being one of the most seismic active areas in the western Mediterranean Sea, the northern region of Morocco shows a complex tectonic behaviour. We used dense seismological data acquired from 2008 to 2014 within international collaboration between Scientific Institute, Mohammed V University of Rabat, Morocco and European and American partners. Indeed, many projects were carried out (e.g. topo-Iberia project by ICTJA CSIC (Spain) and Picasso project by IRIS – Oregon University, USA). Thus, 59 broadband stations were deployed in total. PICASSO stations were equipped with Guralp CMG 3T sensors and Quanterra 330 digitizers, however Topo-Iberia stations have Nanometrics Trilium 120P sensors and Taurus digitizers, with records with a sample rate of 100 sample/sec. This data helped us to discriminate evidence of dense seismic activity, with moderate magnitudes (maximal magnitude was 6.4) in north of Morocco.
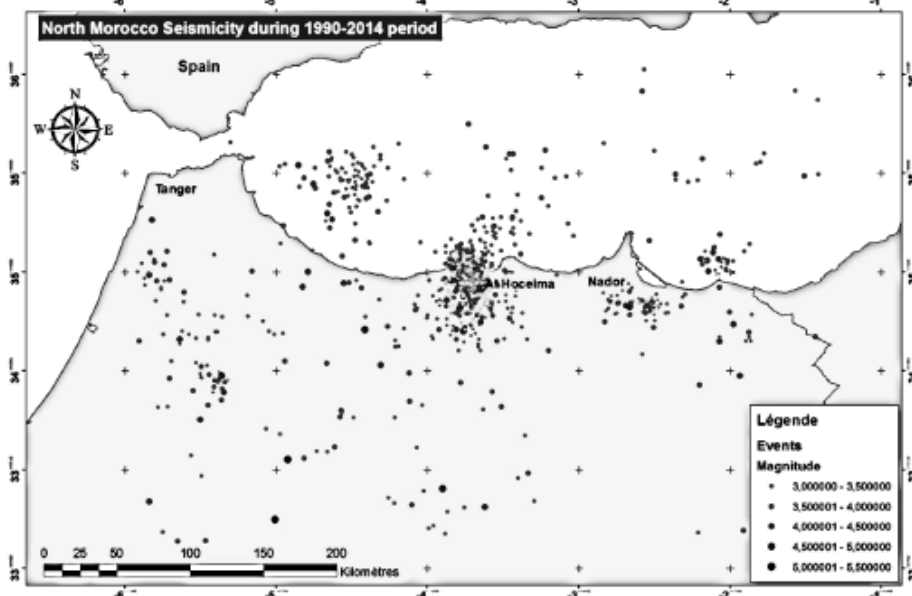
Fihure 1: Figure 1. Seismicity in the North of Morocco during 1990-2014 period
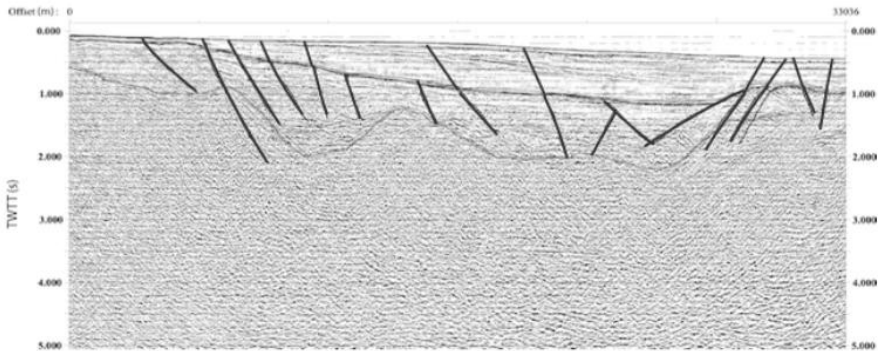
Figure 2: Seismic reflection line showing active faults through actual sediments

These events, with their locations and source parameters, show clear alignments. Moreover, a dense seismic reflection survey has been carried out on the offshore of northern Morocco. Analysis of this grid profiles allowed us to elaborate a structural and tectonic model of the northern Moroccan margin, between 'Cap des Trois Fourches' and 'Cap de l'Eau'. These seismic lines of about 1000 km long each, correlated with ODP drilling data, reveal the influence of recent tectonic activity in relationship with some normal faults, trending N030°, reverse faults trending N-S and N140°, and a major strike slip fault (Nekor fault) that suddenly changes direction from N40° to N80°. These faults have been probably active since the Miocene, and affect obliquely the actual geological structures.

Acknowledgements

References

Chumakov, I. S. (1973). Geological history of the Mediterranean at the end of the Miocene-the beginning of the Pliocene according to new data. Initial Reports of the Deep Sea Drilling Project, 13(2), 1241-1242.

Stich, D., Serpelloni, E., de Lis Mancilla, F., & Morales, J. (2006). Kinematics of the Iberia–Maghreb plate contact from seismic moment tensors and GPS observations. Tectonophysics, 426(3), 295-317.

van der Woerd, J., Dorbath, C., Ousadou, F., Dorbath, L., Delouis, B., Jacques, E., Haessler, H. (2014). The Al Hoceima Mw 6.4 earthquake of 24 February 2004 and its aftershocks sequence. Journal of Geodynamics, 77, 89-109.

COMBINING GEOLOGICAL AND GEOPHYSICAL DATA: NEW INSIGHTS ABOUT WESTERN CATANZARO TROUGH (CALABRIA, SE TYRRHENIAN SEA)

Brutto, F.[1], Muto, F.[1], Loreto, M.F.[2], CritelliS.[1], Tripodi V.[1]

[1]*Department Biology, Ecology and Earth Science, University of Calabria, 87036, Arcavacata di Rende (CS), Italy. e-mail: fabrizio.brutto@gmail.com*

[1]*Department Biology, Ecology and Earth Science, University of Calabria, 87036, Arcavacata di Rende (CS), Italy. e-mail: francesco.muto@unical.it*

[2]*Science Marine Institute – National Research Council, U.O.S. Bologna, Via Gobetti 101, 40129 Bologna, Italy. e-mail: filomena.loreto@bo.ismar.cnr.it*

[1]*Department Biology, Ecology and Earth Science, University of Calabria, 87036, Arcavacata di Rende (CS), Italy. e-mail: salvatore.critelli@unical.it*

[1]*Department Biology, Ecology and Earth Science, University of Calabria, 87036, Arcavacata di Rende (CS), Italy. e-mail: vinstripodi@libero.it*

Introduction and geological framework

The western Catanzaro Trough represents a Neogene- Quaternary sedimentary basin, belonging to a well-developed *arc-shaped* structure located in the central Calabrian Arc (Southern Apennines; Van Dijk et al., 2000), extended from off-shore, Sant'Eufemia Gulf basin (SE Tyrrhenian Sea) to the on-shore area, Catanzaro Basin, and confined on land from north to south by Sila and Serre Massif, respectively. The convergence between the African and European platescaused rapid southeast-ward migration of the Calabrian block above Ionian slab, driven by opposite vertical axis rotation along the WNW-ESE oriented northern and southern edges (Mattei et al., 2007), Pollino Fault Zone and Taormina Line, respectively (Langone et al., 2006). The result of the rapid trench migration is the opening of the Tyrrhenian back-arc basin during Upper Miocene -Pleistocene age, and the fragmentation of Calabrian Arc into structural highs and transversal marine sedimentary basins (Tripodi et al., 2013, Tansi et al., 2007), Catanzaro Trough is one of these. The study area is influenced by different NW-SE major transcurrent faults and their antithetic lineaments that show alternating episodes of transtensional and transpressional activity. These structures belong to the larger fault system, named Lamezia-Catanzaro Fault, which partly corresponds to the sinuous NW-SE trending transcurrent fault previously recognized by Van Dijk et al. (2000). These faults, arranged in a right-hand *en´echelon*pattern, dissected the Oligocene-Early Miocene orogenic belt made of Alpine nappes overthrusted the Apennine Chain (Tansi et al., 2007).

After this time, the detachment of Ionian slab changes the geodynamic scenario in the central Mediterranean region: Tyrrhenian back-basin shows no more extension and the Calabrian Arc undergoes a tectonic rebound (Mattei et al., 2007 and reference therein). The most evident consequence of the widespread

Quaternary uplift is the formation of marine terraces and ca. N-S elongated basins formation, bordered by several NE-SW and N-S -trending faults, mainly developed along the Tyrrhenian coastline of Calabria (Tortorici et al., 2003). The Calabria Arc presents the highest probability of occurrence of major earthquakes, in particular, the Catanzaro Trough and the neighbouring areas was affected by the most destructive historical earthquakes of whole Italy (1638, 1659 and 1905 earthquakes and, 1783 earthquakes sequence) tentatively related to different trending normal faults. Some of these earthquakes have been associated with tsunamis which caused further damages, especially, along the Tyrrhenian coast (Platanesi and Tinti 2002, Jacques et al., 2001).

Combining on land geo-structural with marine geophysical data, we performed a detailed study of processes which have controlled the late Quaternary evolution of the Catanzaro Trough, providing further constraints about the seismogenetic sources in the area.

Results
Structural data

In order to better understand the geological evolution of this area new structural data, related to the main faults system, have been acquired during the fieldwork study carried out in the Catanzaro Basin. The analysis, applied to brittle elements and classified on the base of kinematics and fault directions, shows a significant preponderance of the NE-SW and subordinately N-S normal faults which offset diffusely Middle – Upper Pleistocene deposits (Figure 1).

The fieldwork data display more than one direction of striations on the NE-SW andN-S fault planes, defining the events chronology that have characterized the western termination of Catanzaro Trough during the Quaternary age. These data have been processed by software DAISY (Salvini, 2002). As shown by superposition of slickenside and scattering of rotational axes (rotaxes), oriented mainly along a NE-SW direction, the NE–SW and N–S faults systems (stereographic projection of fault poles in Figure 1) are reactivated as normal faultson pre-existing structures (Brutto et al., 2015). These concentrations correspond to a WNW-ESE extensional direction (σ_3).

Geophysical data

Furthermore we have interpreted some on-shore and off-shore geophysical data (Multichannel, and Chirp) with different resolution and penetration. Chirp profiles and high resolution morpho-bathymetric map have been acquired in the northeastern portion of the SE Tyrrhenian Sea, aboard the R/V OGS-Explora, in the frame of the ISTEGE project (Loreto et al., 2012) whereas the multichannel profiles come fromEnis.p.a. in the frame of ViDEPI project. Although the low quality of ViDEPI lines, the E-W oriented CZ-329-78 multichannel seismic profile (Figure 2b) shows thickness increase and small dislocations of layers, amongst shot points 160 – 190, revealing the activity of a not before identified W-dipping normal fault, which crosses the Upper Miocene up to the Pleistocene (*S. Pietro Lametino Fault* in Figure 2a and 2b).
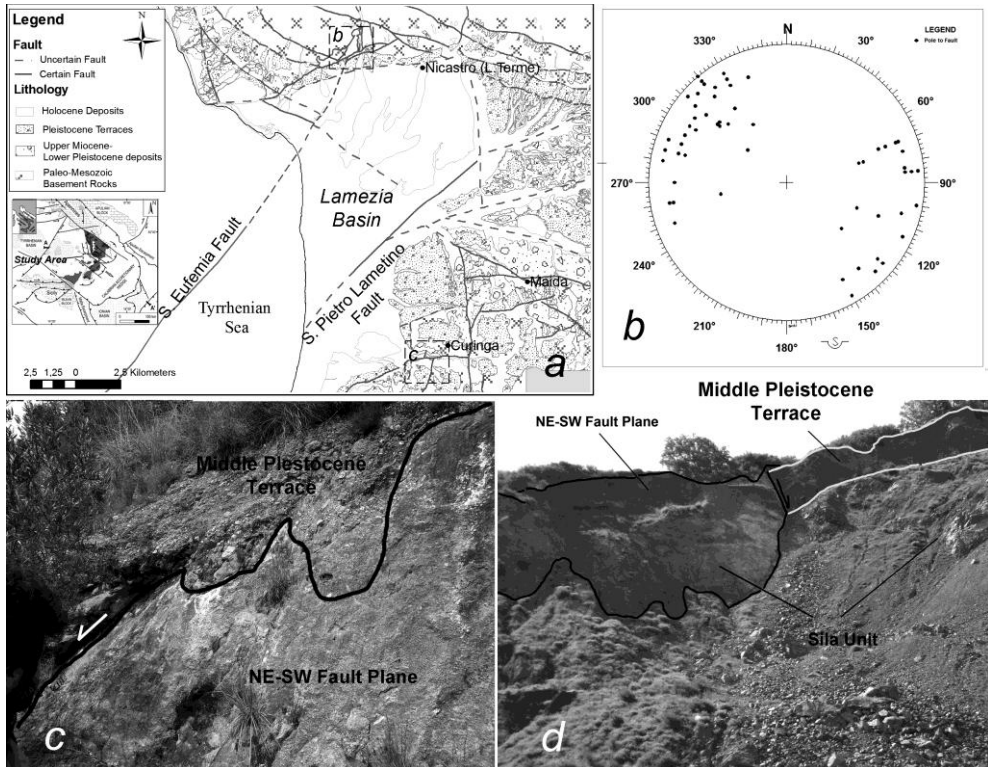
Figure 1. a) Geo-structural sketch map of western Catanzaro Trough;b) stereographic projection of fault poles (Schmidt's net, lower hemisphere); c) and d) NE- SW normal faults with opposite fault dipping: SW and NE respectively, showing recent activity (evidence of the Pleistocene deposits fault offset).

This study, combined with the morphotectonic analysis carried out in the western portion of Catanzaro Trough allowed us to extent northward this fault, thus showing a NE-SW strike. In the same way, ER-77-502 ViDEPI multichannel seismic line (Figure 2c) images a gentle fold, NNE-SSW oriented and nearly perpendicular to the coastline (visible well on morpho-bathymetric map; Figure 2a), bordered to the south by a normal fault which cuts the entire UpperMiocene - Quaternary sedimentary succession, contributing to the partial eastward deepening of the Sant'Eufemia Gulf.

The recent activity of this fault can be observed in the Ch_59 Chirp profile (Figure 2d), it offsets the uppermost layer (less than 100 m depth), this seismic line, related to the previous one, displays clearly a NE-SW orientation and normal kinematics. Based on the previous works (Loreto et al., 2013) we state that this structure is part of the NE-trending Sant'Eufemia normal Fault which was considered the best candidate as seismogenic source of the 1905 Calabrian earthquake.
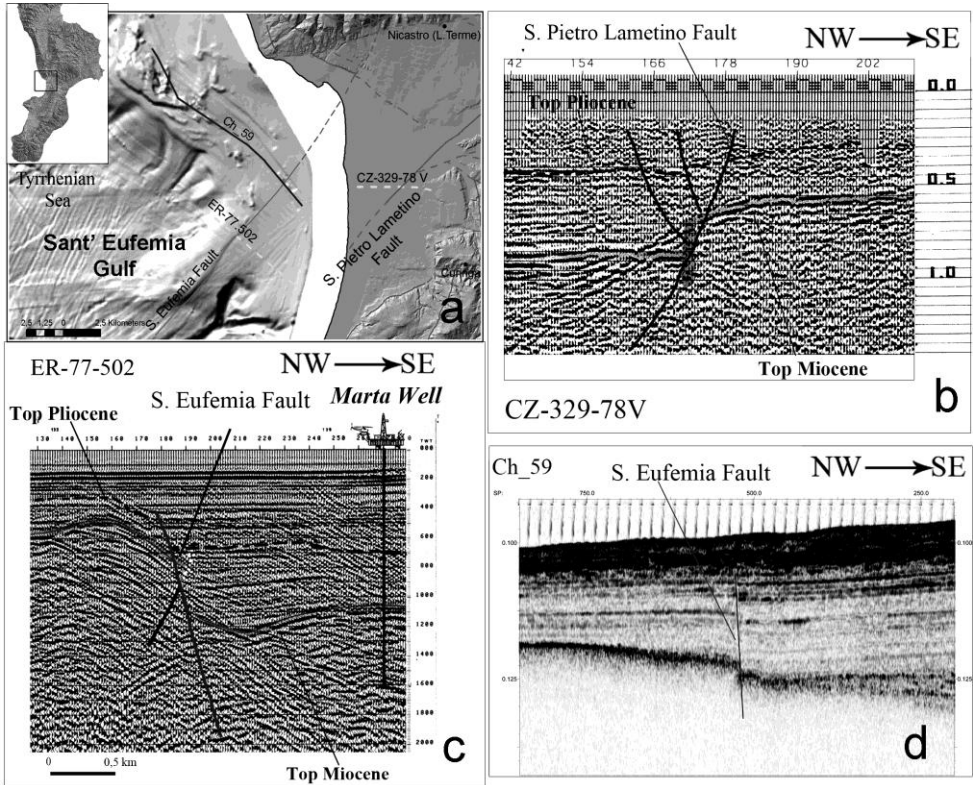
Figure 2. Geophysical data: a) high resolution morpho-bathymetry and digital elevation model (DEM, cell size: 10 m) of western Catanzaro Trough; b) multi-channel seismic CZ-329-77 (from ViDEPI project), c) multi-channel seismic ER-77-502 (ViDEPI project); d) sub-bottom profiles Ch_59 (ISTEGE project).

Discussion

The combination of geological and geophysical data, acquired along the SE Tyrrhenian Sea facing the Central Calabrian Arc, allowed us to recognize two main faults systems that influenced the Quaternary evolution of the western Catanzaro Trough: the NE-SW and the, secondary, N-S oriented normal faults systems. The two sets of faults, causing locally the Pleistocene split of the off-shore and on-shore portion of Catanzaro Trough, produce the development of NE-SW elongated Quaternary basin depocentre, Lamezia Basin, arranged as a Graben System (Figure 1a). The fieldwork data, combined with on-shore geophysical (Figure 2b) and morphotectonicanalysis, show the presence of the above mentioned fault patterns that displace locally Middle- Upper Pleistocene Terraces, corresponding to a not before identified W-dipping normal fault, S. Pietro Lametino Fault, which borders the eastern termination of Lamezia Basin.

Similarly, the off-shore geophysical data, ER-77-502 (Figure 2c) and Chirp seismic profile (Figure 2d), show clearly the NE- trending Sant'Eufemia Fault cutting the shallow sedimentary units representing the western barrier of the

Quaternary basin. Integrating seismic lines analysis with fieldwork structural data, we suggest within this tectonic framework that the Sant'Eufemia Fault, extended through the whole Sant'Eufemia Gulf, could continue also on-land reaching the morphological northern edge of the Catanzaro Trough, increasing the fault length, previously proposed by Loreto et al. (2013) and, as a result, the seismogenic potential of this source, in relation to the 8 September 1905 earthquake.

In agreement with Jacques et al., 2001, who state that the main destructive earthquake sources bound NNE-SSW trending steep range front (Coastal and Serre Range, Aspromonte and Messina Strait), the NE-SW and N-S trend normal faults play a relevant role as part of recent seismo-tectonic processes controlling the Late Quaternary geodynamic of the central Calabrian Arc.

Considering these features, the improvement of geological and structural knowledge of western Catanzaro Trough could provide new insights about the evaluation of the seismic and tsunami hazard in the frame of a new urban development planning and the existing infrastructures safeguarding.

Acknowledgements

References
Brutto F., F.Muto, M.F. Loreto, V. Tripodi, and S. Critelli (2015).Plio-Quaternary structural evolution of the western Catanzaro Trough (Calabria, South Italy), Conferences abstract EGU General Assembly 2015, Vienna, Austria, 12-17 April.
Jacques E., C. Monaco, P. Tapponnier, L. Tortorici, and T. Winter (2001).Faulting and earthquake triggering during the 1783 Calabria seismic sequence, Geophys. J. Int., 147, 499–516.
Langone A., E. Gueguen, G. Prosser, A. Caggianelli, and A. Rottura (2006). The Curinga-Girifalco fault zone (northern Serre, Calabria) and its significance within the Alpine tectonic evolution of the western Mediterranean, Journal of Geodynamics, 42, 140–158.
Loreto, M.F., F. Zgur, L. Facchin, U. Fracassi, F. Pettenati, I. Tomini, M. Burca, P. Diviacco, C. Sauli, G. Cossarini, C. De Vittor, D. Sandron, and the Explora technicians team (2012). In Search of New Imaging For Historical Earthquakes: A New Geophysical Survey Offshore Western Calabria (Southern Tyrrhenian Sea, Italy), Boll. Geof.Teor.App., v. 53. http://dx.doi.org/10.4430/bgta0046.
Loreto M.F., U. Fracassi, A. Franzo, P. Del Negro, F. Zgur, and L. Facchin (2013). Approaching the seismogenic source of the Calabria 8 September 1905 earthquake: New geophysical, geological and biochemical data from the S. Eufemia Gulf (S Italy), Marine Geology, 343, 62–75.
Mattei M., F. Cifelli, and N. D'Agostino (2007). The evolution of the Calabrian arc: Evidence from paleomagnetic and GPS observations, Earth Planet. Sci. Lett., 263, 259-274.
Piatanesi, A., and S. Tinti (2002).Numerical modelling of the September 8, 1905 Calabrian (southern Italy) tsunami. Geophysical Journal International, 150, 271–284.

Salvini F. (2002): http://host.uniroma3.it/progetti/fralab/Downloads.

Tansi, C., F. Muto, S. Critelli, and G. Iovine (2007).Neogene–Quaternary strike-slip tectonics in the central Calabria Arc (southern Italy), J. Geodyn., 43, 397–414.

Tortorici G., M. Bianca, G. De Guidi, C. Monaco, and L. Tortorici (2003). Fault activity and marine terracing in the Capo Vaticano area (southern Calabria) during the Middle-Late Quaternary, Quaternary International, 101–102, 269–278.

Tripodi V., F. Muto, and S. Critelli (2013). Structural style and tectono - stratigraphic evolution of the Neogene - Quaternary Siderno Basin, southern Calabrian Arc, Italy, International Geology Review, 55, 468 – 481.

Van Dijk J.P., M. Bello, G.P. Brancaleoni, G. Cantarella, V. Costa, A. Frixa, F. Golfetto, S. Merlini, M. Riva, S. Torricelli, C. Toscano, and A. Zerilli (2000). A regional structural model for the northern sector of the Calabrian Arc (southern Italy), Tectonophysics, 324, 267-320.

THE LITHOSPHERIC STRUCTURE OF THE GIBRALTAR ARC AND POSSIBLE IMPLICATIONS FOR SEISMIC HAZARD IN THE WESTERN MEDITERRANEAN

Carbonell, R[1], J. Díaz[1], J. Gallart[1] and PICASSO working group

[1]CSIC-ICTJ. Inst. Earth Sciences JaumeAlmera, LluísSolé I Sabrís s/n, 08028 Barcelona, Spain ramon.carbonell@csic.es, jdiaz@ictja.csic.es, jgallart@ictja.csic.es

The Gibraltar arc and associated broad seismogenic zone that includes the southern Iberian Peninsula and northern part of the Morocco, hosts the convergent boundary between the European and African Plates. The area is characterized by low to moderate magnitude shallow earthquakes, although large historical events have also occurred. The crustal deformation is reflected by the topographic features. Characteristic topographic features are the Beticorogen in Iberia and in Morocco the Atlas Mountains and the Rif Cordillera. The latter two orogenic belts are the response of different geodynamic processes acting at lithospheric scale caused by the complex plate interaction. The zone delineates an arcuate arc system known as the Gibraltar arc limiting to the west Alboran basin. The area is characterized by a relatively large amount of earthquake activity at various depths and with broad spectra of focal mechanisms. Within the last decade a large international effort has been devoted to the area. Key multi-seismic projects have been developed that aim to constrain the structure, composition and tectonic scenario from south of the Atlas to the Betics, across the Rif Cordillera and the Alboran basin. The multidisciplinary research program included: natural source (earthquakes) recording with temporal deployments of broad band (BB) instrumentation and, controlled source seismic acquisition experiments where spatially dense recording of wide-angle seismic reflection shot gathers were acquired. The natural source experiments consisted ofa transect from Merzouga across the Gibraltar Arc and into the Iberian Peninsula (until south of Toledo) and, a nearly regular grid of BB instruments. The controlled source data-sets were able to constrain the crustal structure and provide seismic P-wave propagation velocity models from the coast across the Rif and the Atlas. From south to north the crust features a relatively moderate crustal root beneath the Middle Atlas which can reach 40 km clearly differing from the 35 km thickness value observed at both sides of this root. Travel time inversion results position the crustal root just south of the High Atlas defining a thrusted mantle wedge and, also a limited crustal imbrication is suggested in the Middle Atlas. The most surprising feature is a prominent and unexpected crustal root (over 50 km) located beneath the external Rif and identified by both the wide-angle data and receiver function studies. To the east of this feature the crust thins rapidly by 20 km across the Nekkor fault zone, suggested to be related to the sharp change in crustal thickness. The

constrained crustal structure in the study area is interpreted to be driven by the sub-crustal dynamic processes associated with the oblique collision and long history of subduction of the Neotethys ocean lithosphere. The detailed knowledge on the crustal structure achieved by this high resolution imaging geophysical techniques is an asset to evaluate the earthquake and potential tsunami hazard for the coasts of North Africa and western Europe

NEOGENE TECTONIC REACTIVATION IN THE NORTH-CENTRAL SECTOR OF THE SICILY CHANNEL IN THE FRAME OF THE SOUTHWARD ADVANCING OF THE GELA NAPPE

Cavallaro, D.[1], Monaco, C.[1], Polonia, A.[2], Sulli, A.[3], Di Stefano, A.[1]

[1]*Dipartimento di Scienze Biologiche, Geologiche ed Ambientali, University of Catania, Italy, danilocav@tiscali.it; distefan@unict.it; cmonaco@unict.it*
[2]*Istituto di Scienze Marine (ISMAR-CNR), Bologna, Italy, alina.polonia@ismar.cnr.it*
[3]Dipartimento della Terra e del Mare, University of Palermo, Italy, attilio.sulli@unipa.it

Introduction

In this paper we present a review of seismic data collected in the Sicily Channel to better understand the tectonic evolution of its north-central sector. The study area (fig. 1) is bounded by the southern coast of Sicily to the north, the Malta Plateau to the east, the Malta Graben to the south and the Nameless Banks to the west. The analysed seismic dataset is composed of two single-channel 30-KJ sparker seismic profiles acquired by ISMAR-CNR (Bologna, Italy) during the 70's, together with 26 multi-channel seismic reflection profiles and well log data (belonging to the Italian Commercial Zone "G" and collected during the 80's by few oil companies), available within the ViDEPI (Visibility of Petroleum Exploration Data in Italy) project by the Italian Ministry of the Economic Development (http://unmig.sviluppoeconomico.gov.it/videpi/videpi.asp).

The resolution and the quality of the seismic data vary remarkably because of the different acquisition and processing parameters and energy systems used during the surveys.
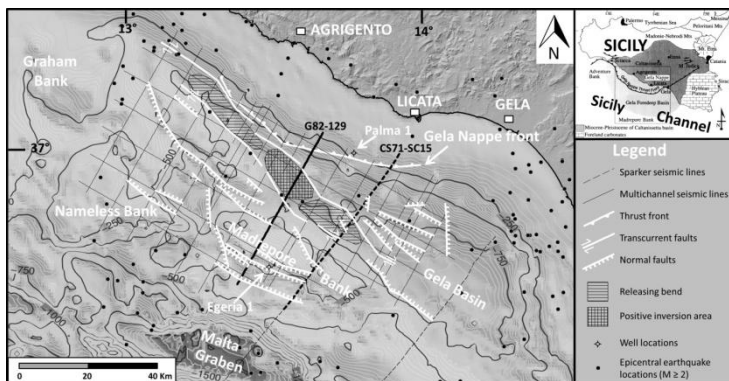
Fig. 1 Structural and batymetric map of the study area (batimetry from SRTM, Shuttle Radar Topography Mission) with the analysed seismic dataset and well locations; inset modified from Lickorish et al. (1999).

The seismic profiles (available in raster format) were converted to SEG-Y format files, using the SegY Transformer application of Geo-Suite and the SeisPhro software and interpreted through the same Geo-Suite software.

Geological setting of the north-central sector of the Sicily Channel

Within the geodynamic framework of the central Mediterranean area, the Sicily Channel belongs to the central portion of the northern margin of the African continental plate, called Pelagian Block (Burollet et al., 1978; Boccaletti et al., 1984), representing the foreland area of the Sicilian sector of the Neogene Apenninian-Maghrebian fold-and-thrust belt. The Pelagian Block is characterized by a 25–35 km thick continental crust (Scarascia et al., 2000), except in correspondence of the Sicily Channel rift zone, where the crustal thinning is evident since the Moho is less than 20 km deep (Finetti, 1984).

The continental upper crust of the Sicily Channel consists of a 6–7 km thick Mesozoic–Cenozoic shallow to deep water carbonate sedimentary successions, with repeated intercalations of volcanics (Torelli et al., 1995), covered by Upper Tortonian-Lower Messinian siliciclastic deposits. This sedimentary cover crops out in the Sciacca area and in the Hyblean Plateau, located in southwestern and southeastern Sicily respectively, and in the Lampedusa and Malta islands. The overlying deposits are represented by Plio-Quaternary clastic sequences that are widespread all over the channel.

The morpho-structural setting of the Sicily Channel is a composite array of shallow continental shelves (Adventure, Malta and Tunisia Plateaux), several banks reflecting a sedimentary (e.g. Bannock Seamount, Madrepore Bank) or volcanic (e.g. Graham, Nameless, Terribile Banks) origin, fault-controlled rift basins (Pantelleria, Linosa and Malta Grabens) and foredeeps (Gela and Adventure basins). As a consequence the area is characterized by a very irregular bathymetry with a pretty shallow seafloor interrupted by a succession of depressions and topographic highs.

This tectonic framework is the product of the Neogene continental collision between the African and European plates associated with the Neogene-Quaternary NW-SE rifting (Jongsma et al., 1985; Boccaletti et al., 1987; Reuther et al., 1993). The rifting has been interpreted in different ways, because of its complexity. The Sicily Channel is considered a dextral shear zone located in front of the Africa–Europe collisional belt where the tectonic depressions of the rift represent large pull-apart basins involving deep crustal levels (Finetti 1984; Jongsma et al., 1985; Reuther and Eisbacher 1985; Ben-Avraham et al., 1987; Boccaletti et al., 1987; Cello 1987; Finetti and Del Ben, 2005). A mechanism of intraplate rift, related to NE-SW directed displacement of Sicily away from Africa, has been also proposed (Illies, 1981). The rifting was interpreted by Argnani, (1990), as due to mantle convections developed during the roll-back of the African lithosphere slab beneath the Tyrrhenian basin. Corti et al. (2006) suggested that the formation of the extensional structures are related to the occurrence of two independent tectonic processes, the Apenninian-Maghrebian accretion and the

Sicily Channel passive rifting, that acted simultaneously and overlapped each other. The rifting process was accompanied by widespread Pliocene–Pleistocene to recent alkali-basalt volcanism mainly concentrated on the islands of Pantelleria and Linosa and in correspondence of the Graham, Terribile and Nameless Banks. In the northern sector of the Sicily Channel, local crustal thickness variations of the northern African plate margin influenced the geometry and the segmentation of the Afro-European convergence zone, driving the formation or reactivation of N-S trending transfer zones. The Adventure Plateau offshore western Sicily and the Hyblean Plateau to the east represent two structural carbonate highs, bounded, respectively, along their western and eastern margins, by two strike-slip fault zones (Reuther et al., 1993).

The area in between is occupied by the Caltanissetta basin and shows a local crustal thinning; this feature, together with the relative low basal friction of the Caltanissetta basin lithologies, favored a major southward advancing of the chain compared to the adjacent platform areas, producing an irregular thrust front (Lickorish et al., 1999).

Seismic stratigraphy

We analyzed a tight grid of seismic profiles orthogonal and parallel to the trend of major fault systems. A great part of the NE-SW trending seismic profiles (including those shown in fig. 2) cross orthogonally, from north to south, the frontal sector of the Gela Nappe, the Gela Basin and the Madrepore Bank. Fig. 2 represents two key seismic profiles selected among the entire dataset: the multi-channel seismic profiles have a good penetration until some 5 sec TWT (fig. 2b), while the sparker profiles (fig. 2a) have less penetration (about 2.5 sec TWT) but higher resolution, allowing a better understanding of the upper part of the sedimentary section.

The profiles were calibrated through the available litho-cronostratigraphic well data relative to the Egeria 1 and Palma 1 wells, located on top of the Madrepore Bank and inside the Gela Basin, respectively. The well log Egeria 1 highlighted the lack of Plio-Quaternary sediments on top of the Madrepore Bank, while Palma 1 crosses the Gela Nappe lying on top of the lowest Gela Basin sequence. The Gela Basin is a WNW-ESE trending narrow, weakly deformed Plio-Quaternary foredeep basin, located at the front of the Apenninian-Maghrebian fold and thrust belt of Sicily. It extends from land (Hyblean Plateau) to southern Sicily offshore, showing a maximum depth of about 900 m. The basin formed from late Pliocene is related to the flexure of the carbonate substrate due to loading of the frontal nappe (Catalano et al., 1996). It is filled with about 2000 m of shallowing-upward marine Plio-Quaternary sediments (Colantoni 1975, Argnani et al., 1986). The depositional fill consists of pelagic marly limestones (Trubi Formation), silty pelites and sandy clays, lying unconformably above the Messinian evaporites. Seismic analysis of the basin succession allow to identify a thin package (350-400 m) of Pliocene deposits (characterized by low-amplitude reflections), overlain by a thick (1500-1800 m) Pleistocene sequence, exhibiting high-amplitude reflections

with a good lateral continuity in the lowest part and more recent chaotic reflections upward.

The Gela basin is affected by multiple slope failures originated during the late-Quaternary. Basin sequences show, in fact, evidence of several acoustically chaotic and/or transparent units, characterized by irregular upper surfaces, interpreted as large mass-transport deposits. The sedimentary sequence involved in the landslide deposits is at least 700 m thick, as confirmed by Trincardi and Argnani (1990). The seafloor morphology shows also evidence of old (partially buried) and recent landslide deposits (Minisini et al., 2007), as highlighted by the Sparker seismic profile (fig. 2a).

The Gela Basin is partially occupied by the allochthonous units of the front of the chain forming the Gela Nappe (Ogniben, 1969), that represents the outermost and youngest thrust sheet of the Apenninian-Maghrebian fold-and-thrust belt in Sicily. It is mainly developed onshore in the Caltanissetta Basin (Antonelli et al., 1988) and extends 20-25 km offshore the coast between Sciacca and Gela, where it forms a large south-facing NW-SE trending arc. On seismic profiles the Gela Nappe rests on lower Pleistocene sediments of the Gela Basin and appears as a wedge-shaped body, up to 2.5 km thick, with a chaotic internal geometry, characterized by discontinuous reflections of variable amplitude. It is formed by a series of imbricated thrusts containing packages of folded and faulted deposits, resulted from a process of tectonic accretion.

The seismic profile of fig. 2b shows the Gela Nappe emplacement occurred into three different stages (Lower Pliocene, Upper Pliocene and Lower Pleistocene). The basal thrust displays an overall displacement of more than 5 km. The bulk of the body is made up by Neogene deposits. High-amplitude discontinuous reflections (assigned to the Messinian evaporites) marks the top of upper Miocene shales and is draped by a thin (250-350 ms TWT) relatively undisturbed Pliocene cover characterized by low-amplitude and low-continuity reflections. The Pliocene strata have been folded on top of the nappe suggesting that during this time span the accretionary wedge was still moving and also subject to internal shortening as confirmed by Lickorish et al. (1999). The propagation of the thrust front stopped in Lower Pleistocene. The Madrepore Bank is a NW-SE trending, 50 km long and 18 km large monocline dipping toward NE, with a tilt angle ranging from 4° to 6° and characterized by a depth ranging from 175 to 750 m. Its top is pretty flat highlighting evidences of diffuse erosion. On seismic profiles the southernmost portion of the Madrepore Bank is characterized by a sequence of high-to-medium amplitude and high-continuity reflections belonging to the Jurassic-Miocene carbonate succession without Plio-Quaternary sediments.
 Southwards, along the deeper portion of the Madrepore Bank, this sequence is covered by the Upper Miocene marls, overlain by the Messinian evaporites and by a thin cover of Pliocene sediments showing low-amplitude reflections. The northern boundary of the Madrepore Bank is characterized by a steep SW dipping normal fault system showing distinct normal drags as result of fault motion, with a cumulative vertical downthrown of 1.5 km.
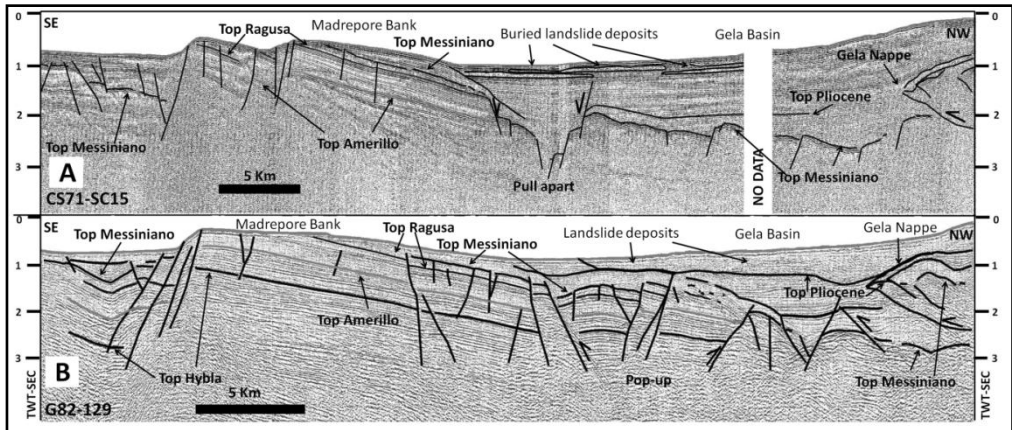
Fig. 2 CS71-SC15 single-channel Sparker (a) and G82-129 multi-channel (b) seismic profiles; for location see fig. 1.

Tectonic setting of the area

The seismo-stratigraphic analysis allows to identify a set of NW-SE trending normal faults (fig. 1), characterizing large part of the foreland area. This extensional deformation was active contemporaneously with Miocene and Plio-Pleistocene convergence as already proposed by Argnani (1990) and may be the result of flexure of the foreland plate due to loading of the advancing Apenninian-Maghrebian fold-and-thrust belt (Cogan et al., 1989).

In the northernmost part of the study area (in correspondence of the northern boundary of the Madrepore Bank), an about 8 km large and more than 50 km long strike-slip belt has been identified. It is formed by two WNW-ESE to NW-SE trending faults, interpreted as Miocene normal faults affecting the African foreland, which were reactivated during early-middle Pliocene by dextral strike-slip motion, as consequence of the Africa-Europe convergence. The strike-slip belt shows a releasing bend geometry, being characterized by a pull-apart basin; this last is bounded by systems of steep normal faults, with an overall step arrangement and a cumulative vertical downthrown of some 900 m (fig. 2a). No evidences of volcanism were identified by seismic profiles within the releasing bend. In the central sector of the belt, just in correspondence of the maximum southern advancing and thickness of the Gela Nappe, this extensional structure shows a late Pliocene local (15-20 km large) contractional reactivation, being affected by a well-defined "pop-up" structure.

The contractional process is also highlighted by the tectonic inversion of a N-dipping extensional fault located below the outermost sector of the Gela Nappe (fig. 2b), associated with an anticline growth in the hanging wall of the fault. Supplementary evidences of the compressive tectonic affecting this area are represented by the increase of the tilting of the Madrepore Bank in correspondence of the "pop-up" structure in comparison with the adjacent sectors and by the clear

arching of the seismic reflectors located inside the basin on the back of the Madrepore Bank (fig. 2b). Moreover, the tectonic map displays few N-S and NNE-SSW trending faults (fig. 1), that, according to Ghisetti et al. (2009) could be inherited from the Mesozoic carbonate substratum and reactivated by compression during middle Pliocene to early Pleistocene, causing an E-W shortening of the Gela Nappe. The reconstructed tectonic framework suggests the occurrence of a Pliocene poli-phase fault zone south of the Gela Nappe, characterized by a strike-slip reactivation of Miocene NW-SE trending normal faults and a subsequent local positive tectonic inversion as a consequence of the southernmost advancing of the front of the Apenninian-Maghrebian fold-and-thrust belt (the Gela Nappe). This geodynamic evolution testifies the local superposition of contractional structures on extensional ones, all related to the general NW-SE oriented Africa-Europe convergence. As regards active tectonics, published GPS data (Palano et al., 2012) indicate that NE-SW extension is still active between Lampedusa and Malta, at a rate of 1.4 mm/yr and interlaces with the convergence. However only a few low energy seismic events (fig. 1) have been recorded along the analyzed belt during the last 30 years (data from ISIDe, Italian Seismic Instrumental and parametric Data-basE"). A more detailed analysis of seismicity could provide information on the ongoing tectonic processes.

References

Antonelli, M., R. Franciosi, G. Pezzi, A. Querci, G.P. Ronco, and F. Vezzani (1988). Paleogeographic evolution and structural setting of the northern side of the Sicily Channel, Mem. Soc. Geol. Ital. 41 141-157.

Argnani, A., S. Cornini, L. Torelli, and N. Zitellini (1986). Neogene-Quaternary foredeep system in the Strait of Sicily, Mem. Soc. Geol. Ital. 36 123-130.

Argnani, A. (1990). The Strait of Sicily rift zone: foreland deformation related to the evolution of a back-arc basin, J. Geodyn. 12 311-331.

Ben-Avraham, Z., A. Nur, and G. Cello (1987). Active transcurrent fault system along the north African passive margin, Tectonophysics 141 249-260.

Boccaletti, M., G. Cello, and L. Tortorici (1987). Transtensional tectonics in the Sicily Channel. J. Struct, Geol. 9 869–876.

Boccaletti, M., R. Nicolich, and L. Tortorici (1984). The Calabrian Arc and the Ionian Sea in the dynamic evolution of the Central Mediterranean, Mar. Geol. 55 219–245.

Burollet, P.F., J. M. Mugniot, and P. Sweeney (1978). The geology of the Pelagian block: the margins and basins of southern Tunisia and Tripolitania, in The Ocean Basins and Margins. The Western Mediterranean, A.E.M. Nairn, W.H. Kanes, and F.G. Stelhi (Editors), Plenum, New York, 4b 331–359.

Catalano, R., P. Di Stefano, A. Sulli and F.P. Vitale (1996). Paleogeography and structure of the central Mediterranean: Sicily and its offshore area. Tectonophysics 260 291–323.

Cello G. (1987). Structure and deformation processes in the Strait of Sicily ''rift zone'', Tectonophysics 141 237–247.

Cogan, J., L. Rigo, M. Grasso, and I. Lerche (1989). Flexural tectonics of SE Sicily, J. Geodyn. 11, 189 – 241.

Colantoni P. (1975). Note di Geologia Marina sul Canale di Sicilia, Giornale di Geologia 2 40 1 181-207.

Corti, G., M. Cuffaro, C. Doglioni, F. Innocenti, and P. Manetti (2006). Coexisting geodynamic processes in the Sicily Channel, in Postcollisional tectonics and magmatism in the Mediterranean region and Asia, Y. Dilek, and S. Pavlides (Editors), Geol. Soc. Am. Spec. paper 409 83–96.

Finetti, I.R., (1984). Geophysical study of the Sicily Channel rift zone, Boll. di Geof. Teorica e Appl. 12 263–341.

Finetti I.R., and A. Del Ben (2005). Crustal tectono-stratigraphic setting of the Pelagian foreland from new CROP seismic data, in CROP project: deep seismic exploration of the central Mediterranean and Italy, I. R. Finetti (Editor), Atlases in Geoscience 1, Elsevier, 581–595.

Ghisetti, F.C., A.R. Gorman, M. Grasso, and L. Vezzani (2009). Imprint of foreland structure on the deformation of a thrust sheet. The Plio-Pleistocene Gela Nappe (southern Sicily, Italy), Tectonics 28, TC4015, doi:10.1029/2008TC002385.

Illies, J.H. (1981). Graben formation – the Maltese Islands – a case history, Tectonophysics 73 151–168.

Jongsma, D., J.E. Van Hinte, J.M. Woodside (1985). Geologic structure and neotectonics of the North African continental margin south of Sicily, Mar. Pet. Geol. 2 156–179.

Lickorish, W.H., M. Grasso, R.W.H. Butler, A. Argnani, and R. Maniscalco (1999). Structural styles and regional tectonic setting of the ''Gela Nappe'' and frontal part of the Maghrebian thrust belt in Sicily, Tectonics 18 655 – 668.

Minisini, D., F. Trincardi, A. Asioli, M. Canu, and F. Foglini (2007). Morphologic variability of exposed mass-transport deposits on the eastern slope of Gela Basin (Sicily Channel), Basin Res. 19 217-240.

Ogniben, L. (1969). Schema introduttivo alla geologia del confine calabrolucano. Mem, Soc. Geol. Ital. 8 435–763.

Palano M., L. Ferranti, C. Monaco, M. Mattia, M. Aloisi, V. Bruno, F. Cannavò, and G. Siligato (2012). GPS velocity and strain fields in Sicily and southern Calabria, Italy: Updated geodetic constraints on tectonic block interaction in the central Mediterranean, Journ. of Geophys. Research 117, b07401, doi:10.1029/2012jb009254.

Reuther, C.D., and G.H. Eisbacher (1985). Pantelleria rift-crustal extension in a convergent intraplate setting, Geol. Rundsch. 74 585–597.

Reuther C.D, Z. Ben-Avraham, and M. Grasso (1993). Origin and role of major strike-slip transfers during plate collision in the central Mediterranean. Terra Nova 5 3 249–257.

Scarascia, S., R. Cassinis, A. Lozej, and A. Nebuloni (2000). A seismic and gravimetric model of crustal structures across the Sicily Channel Rift Zone, Boll. Soc. Geol. Ital. 19 213–222.

Torelli, L., M. Grasso, G. Mazzoldi, D. Peis, and D. Gori (1995). Cretaceous to Neogene structural evolution of the Lampedusa shelf (Pelagian Sea, Central Mediterranean), Terra Nova 7, 200–212.

Trincardi, F., and A. Argnani (1990). Gela submarine slide: A major basin-wide event in the Plio-Quaternary foredeep of Sicily, Geo Mar. Lett. 10 1 13–21.

GEOLOGY AND SEISMIC ACTIVITY AND THEIR INDUCED EFFECTS IN THE NORTH-WEST OF ALGERIA

Louni Chahira[1], Belhai Djelloul[2]

[1]CGS Centre National de rechercheappliquéeenGénieparasismique. Rue Kaddour Rahim prolongée Hussein-Dey ALGER, louni.chahira@gmail.com
[2]DUSTHB, FSTGAT, Departement de Geologie, Bab Ezzouar-El Alia, ALGER, Belhai2001@yahoo.fr

The North-West of Algeria is crossed by several reverse and normal active faults. All these faults are the cause of the seismicity for a very long time. Without going back to the historic periods, we can cite the most recent and devastating earthquakes that affected this region, such as Blida (2013, 2014), BeniHaoua (2012), Ain Benian(1994), Larhat-Gouraya (1891), Tipaza(1990), Chenoua(1989), and Chlef (1980). This seismic activity causes damage and presents a major risk for the inhabited environment of this region.

It is certain that this seismic activity will continue in the future because it is a result of a convergent plate environment (Africa and Europe). The rough nature of the seismic activity is the origin of instabilities in the ground (landslides), rocks of stones and liquefaction. These landslides are favoured by morphological factors (slopes and reliefs), physical factors (the persistent rain falls and snow), factors associated to the anthropological activity and geological factors (lithological nature, weak grounds), and the material types.

In these littoral regions exist few resistant grounds of sedimentary nature (marls, clays, alternations stoneware pelites of flysches type etc.) and alluvial deposits, but also resistant grounds such as schists and quartzites of the base, the limestones and volcanic rocks. These grounds, although resistant they are weakened by recurrences of earthquakes, damaging roads and the infrastructures which threaten the population. These instabilities are observed in several places that are not shielded from seismic disasters.

GEOLOGICAL AND SEISMOLOGICAL CONSTRAINS FOR FAULT REACTIVATION IN THE HYBLEAN FORELAND (SE SICILY, ITALY)

Cultrera, F. [1], Barreca, G. [1] Scarfì, L. [2] , Monaco, C. [1]

1Department of Biol., Geol. and Env. Sciences, University of Catania, C.so Italia 57, Italy, fcultrera@unict.it

1Department of Biol., Geol. and Env. Sciences, University of Catania, C.so Italia 57, Italy, g.barreca@unict.it

1Department of Biol., Geol. and Env. Sciences, University of Catania, C.so Italia 57, Italy, cmonaco@unict.it

2National Institute of Geophysics and Volcanology, Piazza Roma 2, Catania, Italy, luciano.scarfi@ingv.it

Introduction

Inherited structural discontinuities play a key role on the strain distribution in a newly-settled tectonic regime affecting a given area (Bonini et al., 2012). Pre-existing faults are surfaces along which the cohesive strength and the friction coefficient are lower than surrounding intact rocks (Etheridge, 1986) and they may constitute preferential ways to accommodate the re-oriented stress since formation of new faults is mechanically unfavourable. Conditions for faults reactivation (and relative earthquakes nucleation) are governed by the friction laws (Sibson, 1985; Scholz, 1998) and their resulting kinematic strictly depends on their orientation with respect to the superimposed stress field. Particularly, when the trend of the pre-existing faults is nearly perpendicular or oblique to the orientations of maximum horizontal stress, high angle dip-slip faults are inclined to be reactivated as strike-slip mode rather than reverse one (Letouzey et al., 1990).

Between the October 2011 and the July 2012, many hundreds of low-magnitude earthquakes occurred in a small area of the Hyblean Plateau (HP, SE Sicily, Italy), one of the most seismically active region of Italian Peninsula. Most events clustered along the Cavagrande Canyon, an impressive fluvial incision of Sicily and the deepest of the HP. Multiplet events within the seismic sequences allowed us to perform a 3D modelling of the accountable fault plane by using common GIS interpolations. Results have been tested by a detailed morpho-structural analysis at the topographic projection of the modelled plane. The comparison between seismological and field data have allowed us to infer a recent stress pattern reorganization along this sector of the HP and to identify a new seismogenic structure (capable of generating M~6 earthquakes) resulting from tectonic reactivation.

Geological outlines

The HP (Fig.1A) consists of ~10 km thick shallow to deep-water Mesozoic to Quaternary carbonate sequences with repeated intercalations of volcanic products (Grasso et al,. 2004). It represents the northernmost emerged portion of a larger foreland domain, the Pelagian Block (Burollet et al., 1978). This is a ~25-30

km thick continental crust portion of the north-Africa margin extending from the Sahel region of Tunisia eastward to the Malta escarpment, a ~NNW-SSE striking active normal to oblique fault system, which separates the Pelagian Block from the Ionian oceanic basin (Nicolich et al., 2000). The current tectonic setting of the HP must be framed in the geodynamics of Mediterranean basin which are dominated by the complex NNW-SSE Neogene-Quaternary convergence processes between Nubia and Eurasia plates (Faccenna et al., 2001). In this context the HP represents a crustal indenter forming a forebulge structure due to the underthrusting of the foreland lithosphere beneath the advancing Appenninic-Maghrebian Chain (AMC, Billi et al., 2006). Bulging have produced bending in the HP with the development of a gentle NE-SW trending hinge zone (roughly parallel with the trend of the AMC) accompanied by extensional tectonics along coaxial outer-arc fault systems. Bulging-related fault systems are represented by NE-SW oriented extensional dip-slip faults that generally occur at the edges of the HP whereas other systems, mainly NW-SE trending, affect its internal portion. Apart from the well-known extensional tectonics, oblique deformation has also been documented in the HP and particularly at its western sector (the Scicli Line, Ghisetti and Vezzani, 1980).

Seismotectonics

The HP is one of the most seismically hazardous region of Italy since it has been shaken by large earthquakes in historical times such as the February 4, 1169 and the January 11, 1693 events (Fig.1B). The latter is commonly reported as the strongest seismic event of the Italian Peninsula (with estimated magnitudes of about 7.4) causing more than 54.000 casualties and extensive damages in the whole Eastern Sicily (Bianca et al., 1999; Visini et al., 2009). The current seismotectonic setting of the HP is well depicted by an intense seismic activity (Fig. 1B), characterized by low-moderate magnitude ($1.0 \leq ML \leq 4.6$) and hypocentral depths in the range of 15-25 km (Musumeci et al., 2014). Nevertheless, in the last 20 yrs (1994-2013, "Catalogo dei Terremoti della Sicilia Orientale–Calabria Meridionale", http://www.ct.ingv.it/ufs/analisti/catalogolist.php) the highest density of earthquakes has occurred in the southeastern sector of the HP. Here, the epicentral distribution seems mainly to follow the NW-SE fault systems and less the NE-SW oriented ones. Available focal solutions (Musumeci et al., 2014) indicate that seismic faulting in the HP mostly occurs by strike-slip, subordinately normal and rarely reverse kinematics.

The 2011-2012 Cavagrande Canyon seismic swarms

Between the October 2011 and the July 2012, several low-magnitude seismic swarms occurred along the Cavagrande Canyon, one of the most impressive fluvial gorge of Sicily and the deepest of HP (Fig.1C). Each swarm was characterized by many hundreds of small magnitude earthquakes for a total of about 500 events. Despite their low magnitude ($1.0 \leq ML \leq 3.7$), the sequences represent the biggest strain release in the Hyblean area in the last ten years (D'Amico et al., 2014). Earthquakes locations indicate the activation of a

seismogenic volume, depicting a WNW-ESE to NW-SE trend, similarly to other seismic clusters located in the surrounding areas of the HP (see Musumeci et al., 2014). Accordingly, computed focal solutions (Fig.1C) indicate right-lateral movements on the same direction. Hypocentral depth ranges from 5 to 10 km b.s.l., whereas typical seismogenic depths of the HP are between 15 and 25 km. The strongest event (ML=3.7, 8 Km depth), occurred on 27 June 2012, was widely felt in the Hyblean area up to about 60 km from the epicenter and caused slight damages in the surrounding towns. Historical dataset (CPT11 by Rovida et al., 2011) reveals that the same area was shaken by a M=4.5 event in 1696 (Fig.1C), the epicentral location of which is reported very close to the seismic swarms here analyzed.
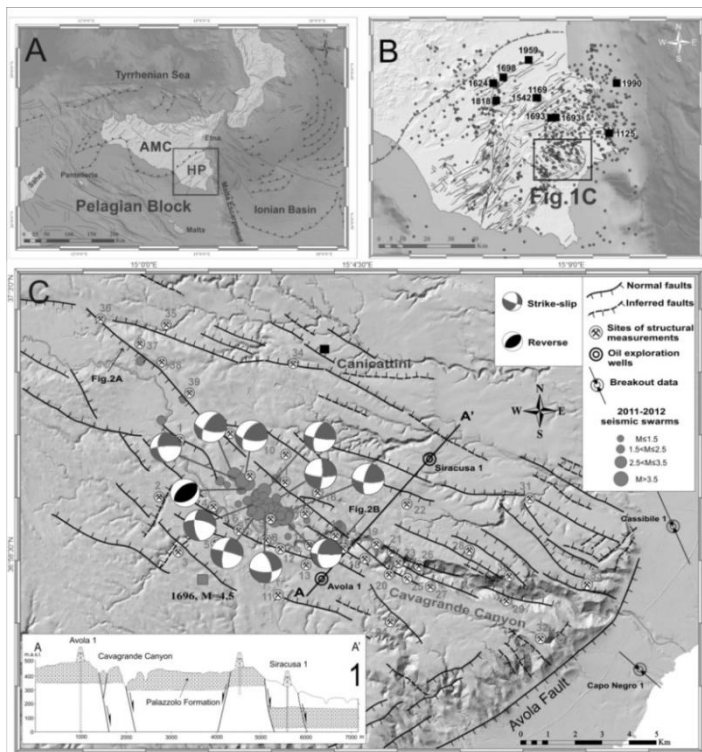
Fig. 1 –A) Tectonic sketch map of the Central Mediterranean area showing the major structural domains with draped the main tectonic boundaries. The Hyblean Plateau (HP) is a portion of the Pelagian Block, a larger continental crustal sector of the Africa margin. Dashed black line with teeth represents the NE-SW oriented front of the Appenninic-Maghrebian Chain (AMC). B) Location of the instrumental (1994-2013; from "Catalogo dei Terremoti della Sicilia Orientale–Calabria Meridionale", http://www.ct.ingv.it/ufs/analisti/catalogolist.php) and historical earthquakes (M>5, from Rovida et al., 2011) in the studied area, shown by circles and squares, respectively. C) Structural map of the area shacked by the 2011-2012 seismic swarms and collected focal plane solutions. The M=4.5 April 20 1696 earthquake is also reported (Rovida et al., 2011).

Fault plane GIS modelling

A careful analysis of the events located in the investigated area has revealed that most of the Cavagrande earthquakes form a family of events with similar waveform signatures, called "multiplets", which have been interpreted as due to repeated slip on the same fault plane (Tsujiura, 1983 among others). Their location can be defined with high precision, in the order of few meters enabling to investigate small tectonic features. Following the method proposed by Fremont and Malone (1987) (see Scarfì et al., 2005 for further details about the procedures), we were able to relocate with great accuracy a dataset of 42 well-recorded multiplet events. Assuming that the 3D spatial distribution of a clustered earthquakes sequence may mimic the geometry of the active fault from which the events nucleated, we try to model the tectonic structure responsible for the Cavagrande Canyon earthquakes by managing the relocated multiplets into a GIS software as point features. Geographic coordinates and hypocentral depth (x, y and z attributes) were used as point cloud for surface generation that has been produced by applying a common interpolation method (i.e. "Natural Neighbor", Sibson, 1981) which produces a manifold surface that follows the real spatial position of the input data point. From the modelled surface we have derived the relative aspect (the dip-direction) and slope (the dip-degree) representation, hence the attitude of the fault plane/asperity where rupture nucleated. This method provides a WNW-ESE (N99E) oriented plane plunging in average at 77° towards the SSW (Fig.2A). The obtained strike is the average value of the attitude calculated for all the minor cells forming the whole manifold surface.

Field data

To test the work flow used for reconstructing the 3D fault plane/asperity geometry, we have performed a detailed field analysis of the area and in particular along the topographic projection of the modelled fault plane (Fig. 2B) and in the nearby. The study area is characterized by outcrops of Middle-Upper Miocene carbonate sediments, a largely-exposed rocky series with near-horizontal strata attitude. As a whole, the area is mainly deformed by a Neogene to Quaternary WNW-ESE to NW-SE oriented fault systems which form horst and graben associations (see Fig.1C). NW-SE striking segments affect the NW portion of the Cavagrande river basin, giving rise to a narrow (~2 km wide) structural depression near the epicentral area. The NE side of the graben, roughly the zone at the topographic projection of the modelled fault plane (Fig. 2B), is controlled by a ~10 km long, N130E trending fault, dipping towards the SW of ~75°. At a more detailed scale, the tectonic structure consists of three fault segments with bell-shaped scarps connected by a series of variously oriented joints and calcite filled fractures. Faults kinematic has been inferred by slickenlines which suggest a pure extensional motion (pitch 90-100°) for these structures. Fault scarps reach the maximum height of about 80 m (Fig. 2C) that progressively reduces at their tips (e.g. ~0.3 m, Fig. 2D).
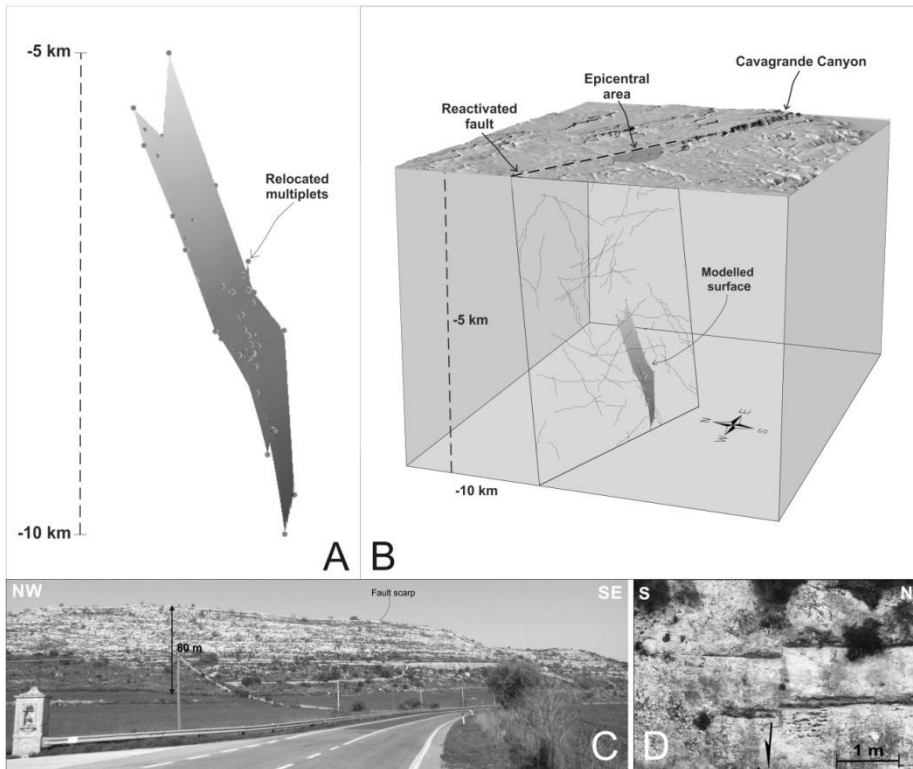
Fig. 2 –A) Fault plane attitude as modelled from the multiplet hypocentral parameters (x, y and z, the spheres) identified within the Cavagrande Canyon seismic swarms. The interpolation algorithms used into the GIS platform is the "Natural Neighbor" (Sibson, 1981) which provide a ~77° dipping, WNW-ESE oriented surfaces whose projection at surface matches well with an observed fault segment B). C) 80 m high fault scarp of the fault segment mapped at the topographic projection of the modelled rupture surface which exhibits a normal motion at its SE tip with a displacement of 0.3 m (D).

Even though most of exposed fault segments do not exhibit clear kinematic indicators, the vertical displacement and the dipping towards the respective hanging-walls of the fault planes suggest that they can be interpreted as pure extensional structures. This is also confirmed by a geological cross section (see inset 1 in Fig. 1C) constructed by using available commercial boreholes (e.g. the Avola1 and Siracusa1 wells; see Fig. 1C for locations) and others wells available from water research.

Discussion and conclusion

The occurrence of several destructive earthquakes in historical time and the intense current day seismic activity scattered all over the Hyblean area (Fig. 1B), unequivocally suggest that faulting is still active even though several aspects concerning the characteristics (type, geometry and location) of seismogenic sources have still not been satisfactorily explored. In spite of the field evidences which

point out prevailing extensional tectonic features, an intriguing aspect is that: i) most of focal solutions computed for the current day Hyblean seismicity reveal a contrasting faulting mechanism in which the strike-slip one (and rarely reverse), generated under a NNW-SSE sub-horizontal max stress axes, is the more widespread (Musumeci et al., 2014); ii) geodetic data highlight contraction along the northern edge of the HP (Palano et al., 2012); iii) bore-hole break-out data (Ragg et al., 1999) suggest that the whole Hyblean area is currently deformed by a NNW oriented sub-horizontal max stress axis. Multiplets detected within the October 2011-July 2012 Cavagrande Canyon seismic sequences have allowed us to perform a 3D modelling of the accountable fault plane (Fig. 2A and B). The latter consists of a WNW-ESE oriented surface plunging at 77° towards the SSW, a trend similar to that of several normal fault segments outcropping in the investigated area (Fig. 1C). In particular, at the topographic projection of the modelled surface we detected a ~10 km long NW-SE trending tectonic structure, dipping towards the SW of ~75°. It consists of three discrete fault segments with bell-shaped scarps connected by variously oriented joints and calcite filled fractures. Within a reasonable uncertainty and considering that at the epicentral area there are no other main outcropping fault segments with comparable attitude (i.e. with SSW dipping), we can assess that the modelled fault plane might represent a reactivated portion of this larger structural discontinuity. The discrepancy between the focal mechanisms-derived and field-observed fault kinematic can be explained as a dextral strike-slip reworking along an WNW-ESE to NW-SE pre-existing normal fault segment which could be capable of generating M~6 earthquakes (Wells and Coppersmith, 1994). The occurrence of a single generation of slickenlines along the outcropping fault planes, indicating normal faulting, could be due to lacking of rupture propagation at surface. As suggested by available focal solutions for this sector of HP (Musumeci et al., 2014), the re-utilization in dextral strike-slip mode of older structural discontinuities could have involved a larger WNW-ESE to NW-SE normal fault configuration and could be explained as the result of a change in the trajectory of the prevailing max stress axis (from vertical to horizontal) due to an ongoing stress pattern reorganization along this sector of the HP. The progressive SE migration of deep-seated thrusts in the AMC (see Lavecchia et al., 2007), according to a sub-horizontal NNW oriented σ1, probably have transferred a rate of the tectonic pushing to the HP, with consequent reactivation from normal to reverse along the NE-SW faults system (see Catalano et al., 2006) and from normal to right-lateral along the NW-SE oriented ones. Since the Hyblean area is one of the most seismically hazardous region of Italian Peninsula, the occurrence of the 2011-2012 seismic swarms should be considered in the context of seismic risk mitigation.

References

Bianca, M., Monaco, C., Tortorici, L., and L. Cernobori (1999). Quaternary normal faulting in southeastern Sicily (Italy): a seismic source for the 1693 large earthquake. Geophys. J. Int., 139, 370-394.

Billi, A., Porreca, M., Faccenna, C., and M. Mattei (2006). Magnetic and structural constraints for the non-cylindrical evolution of a continental forebulge (Hyblea, Italy). Tectonics 25, TC3011. http://dx.doi.org/10.1029/2005TC001800.

Bonini, M., Sani, F., and B. Antonielli (2012). Basin inversion and contractional reactivation of inherited normal faults: A review based on previous and new experimental models. Tectonophysics 522–523, 55–88.

Burollet, P.F., Mugniot, G.M., and P. Sweeney (1978). The geology of the Pelagian Block: the margins and basins of Southern Tunisia and Tripolitania. In: Nairn, A., Kanes, W., Stelhi, F.G., (Eds.). The Ocean Basins and Margins. Plenum Press, 4 B, pp. 331–339.

Catalano, S., De Guidi, G., Lanzafame, G., Monaco, C., Torrisi, S., Tortorici, G., and L. Tortorici (2006). Inversione tettonica positiva tardo-quaternaria nel Plateau Ibleo (Sicilia SE). Rend. Soc. Geol. It., 2, Nuova Serie, pp. 118–120.

D'Amico, S., Ferrari, F., Maiolino, V., Messina, A., and A. Ursino (2014). Studio preliminare di due sequenze di microterremoti accadute nel 2011 e nel 2012 nell'area dei Monti Iblei Orientali (Sicilia Sud-orientale, Italia). Atti 33° Convegno GNGTS, Bologna, 1: 61-66.

Etheridge, M.A. (1986). On the reactivation of extensional fault systems. Philos. Trans. R. Soc. Lond., Ser. A317, 179–194.

Faccenna, C., Becker, T.W., Lucente, F.P., Jolivet, L., and F. Rossetti (2001). History of subduction and back-arc extension in the central Mediterranean. Geophys. J. Int. 145, 809–820. http://dx.doi.org/10.1046/j.0956-540X.2001.01435.x.

Fremont, M.J., and S. D. Malone (1987). High precision relative locations of earthquakes at Mount St. Helens, Washington, J. Geophys. Res. 92, 10, 223-10, 236

Ghisetti, F., and L. Vezzani (1980). The structural features of the Hyblean Plateau and the Mount Judica area (South-Eastern Sicily): a microtectonic contribution to the deformational history of the Calabrian arc. Boll. Soc. Geol. It. 99, 55–102.

Lavecchia, G., Ferrarini, F., de Nardis, R., Visini, F., and M.S. Barbano (2007a). Active thrusting as a possible seismogenic source in Sicily (southern Italy): Some insights from integrated structural-kinematic and seismological data. Tectonophysics 445, 145–167, doi:10.1016/j.tecto.2007.07.007.

Letouzey, J., Werner, P., and A. Marty (1990). Fault reactivation and structural inversion. Backarc and intraplate compressive deformations. Example of the eastern Sunsa shelf (Indonesia). Tectonophysics, 183, 341-362. http://dx.doi.org/10.1016/0040-1951(90)90425-8.

Musumeci, C., Scarfì, L., Palano, M., and D. Patanè (2014). Foreland segmentation along an active convergent margin: New constraints in southeastern Sicily (Italy) from seismic and geodetic observations, Tectonophysics, http://dx.doi.org/10.1016/j.tecto.2014.05.017.

Nicolich, R., Laigle, M., Hirn, A., Cernobori, L., and J. Gallard (2000). Crustal structure of the Ionian margin of Sicily: Etna volcano in the frame of regional evolution, Tectonophysics, 329, 121–139, doi:10.1016/S0040-1951(00)00192-X.

Palano, M., Ferranti, L., Monaco, C., Mattia, M., Aloisi, M., Bruno, V., Cannavò, F., and G. Siligato (2012). GPS velocity and strain fields in Sicily and southern Calabria, Italy: updated geodetic constraints on tectonic block interaction in the central Mediterranean. J. Geophys. Res. 117. http://dx.doi.org/10.1029/2012JB009254B07401.

Ragg, S., Grasso, M., B. Müller (1999). Patterns of tectonic stress in Sicily from borehole breakout observations and finite element modeling. Tectonics 18 (4), 669–685. http://dx.doi.org/10.1029/1999TC900010.

Rovida, A., Camassi, R., Gasperini, P., and M. Stucchi (2011): CPTI11, the 2011 version of the Parametric Catalogue of Italian Earthquakes. INGV, Milano, Bologna, http://emidius.mi.ingv.it/CPTI, DOI:10.6092/INGV. IT-CPTI11.

Scarfì, L., Langer, H., and A. Scaltrito (2005). Relocation of microearthquake swarms in the Peloritani mountains—implications on the interpretation of seismotectonic patterns in NE Sicily, Italy. Geophys. J. Int. 163, 225–237, doi:10.1111/j.1365-246X.2005.02720.x.

Scholz, C.H. (1998). Earthquakes and friction laws. Nature 391, 37–42.

Sibson, R. (1981). "A Brief Description of Natural Neighbor Interpolation," chapter 2 in Interpolating Multivariate Data. New York: John Wiley & Sons, 21–36.

Sibson, R.H. (1985). A note on fault reactivation. J. Struct. Geol.7 (6), 751–754.

Tsujiura M. (1983). Waveform and spectral features of earthquake swarms and foreshocks: in special reference to earthquake prediction. Bull. Earth. Res. Inst. Tokyo Univ. 58, 65–133.

Visini, F., De Nardis, R., Barbano, M.S., and G. Lavecchia (2009). Testing the seismogenic sources of the January 11th, 1693 Sicilian earthquake (Io X/XI): insights from macroseismic field simulations. Ital. J. Geosci. 128 (1), 147–156.

Wells, D.L., and K.J. Coppersmith (1994). New empirical relationships among magnitude, rupture length, rupture width, rupture area, and surface displacement. Bull. Seismol. Soc. Am., 84, 974-1002

NEW INSIGHTS ON THE TECTONIC EVOLUTION OF THE LAMPEDUSA SHELF FROM INTERPRETATION OF SEISMIC REFLECTION PROFILES AND FIELD DATA

Meccariello, M.[1], Ferranti, L.[1], Barreca, G.[2], Di Stefano, A.[2], Monaco, C.[2]

[1]*Dipartimento di Scienze della Terra, dell'Ambiente e delle Risorse (DiSTAR), Università di Napoli "Federico II", melania.meccariello@unina.it; luigi.ferranti@unina.it*

[2]*Dipartimento di Scienze biologiche, geologiche e ambientali,Sezione di Scienze della Terra, Università di Catania,gbarreca@unict.it ; distefan@unict.it ;cmonaco@unict.it*

The Lampedusa shelf

The Lampedusa shelf is part of the Pelagian Block, which served as the foreland of the Sicilian-Maghrebian chain developed during Tertiary collision between Europe and the North African continental margin (Ben Avraham et al., 1990; Lentini et al., 1994; Barreca et al., 2014). The shelf does not present bathymetric evidence of tectonics, because of the relatively low deformation rates, the age of the main tectonic stages, and the masking from the recent depositional cover. Nevertheless, analysis of multichannel seismic (MCS) reflection profiles, corroborated by field observations on Lampedusa, reveals a structural setting characterized by a series of ~WNW-ESE elongated topographic highs separated by relatively smaller parallel basins. This framework arises from two tectonic stages that acted in different times.

Shortening stage

During the Late Cretaceous-Early Tertiary, the shelf was affected by compressive events producing uplift, folding and reverse displacement along ~WNW-ESE trending faults, which partly reactivated Lower Cretaceous extensional structures (Torelli et al., 1995). Contraction mainly acted within the offshore SW of Lampedusa Island, which emerged through one of these compressive movements. MCS profile analysis integrated with field observations on the Cala Creta fault in the eastern part of the island allows to interpret Lampedusa as a transpressive push-up structure.

Although this deformation stage was already known and attributed to the Paleogene (Torelli et al., 1995; Grasso et al., 1999), our 3D interpretation of seismic lines highlights activity of the transpressive structures also in more recent times than previously believed. As a matter of fact, the reverse faults cut the unconformity which is interpreted as the Messinian horizon.

On-land, between Cala Creta and Cala Pisano, in the eastern portion of the island, a carbonate succession pertaining to the Capo Grecale member (Lampedusa Form., Tortonian; Grasso and Pedley, 1985), is deformed by a series of fault

segments and by a set of fractures that developed within a wide deformation zone along the cliff. Analyzed fault segments are generally NW-SE oriented and dip to the south-west with angles ranging from 45° to sub-vertical. Fault planes often exhibit striated surfaces with pitch angles between 30° and 60° that, according to the dipping of the fault planes, indicate an oblique left-lateral transpressive motion for these structures.

Extensional stage

Starting from Late Miocene, the area was affected by NE-SW oriented stretching. The extensional structures were limited to the NE part of the shelf adjoining the Linosa Graben, and have a WNW-ESE trend parallel to faults flanking the main grabens in the central part of the Sicily Channel (Torelli et al., 1995). Thus, the connection between the faults in the shelf and the rift zone of the Channel in term of structural style and activity is significant of the same tectonic process. The extensional deformation was vigorous during the Early Pliocene and strongly diminished after then. However, published GPS data (Palano et al., 2012) indicate extension is still active NE of Lampedusa, and interlaces with NW-SE compression west of the island, suggesting that part of the transpressive faults studied here could became reactivated on occasion.

References

Barreca, G., Bruno, V., Cocorullo, C., Cultrera, F., Ferranti, L., Guglielmino, F., Guzzetta, L., Mattia, M., Monaco, C., Pepe, F. (2014). Geodetic and geological evidence of active tectonics in south-western Sicily (Italy). Special Issue "Geodynamics of the Mediterranean", Journal of Geodynamics, 82, 138-149

Ben-Avraham, Z., Boccaletti, M., Cello, G., Grasso, M., Lentini, F., Torelli, L., Tortorici, L. (1990). Principali domini strutturali originatisi dalla collisione neogenico-quaternaria nel Mediterraneo centrale. Memorie della Società Geologica Italiana 45, 453-462.

Grasso, M., Pedley, H. Martyn (1985). The Pelagian islands: a new geological interpretation from sedimentological and tectonic studies and its bearing on the evolution of the central Mediterranean sea (Pelagian Block). Geologica Rom., 24, 13-34.

Grasso, M., Torelli, L., Mazzoldi, G.(1999). Cretaceous-Palaeogene sedimentation patterns and structural evolution of the Tunisian shelf, offshore the Pelagian Islands (Central Mediterranean). Tectonophysics, 315, 235-250.

Lentini, F., Carbone, S., Catalano, S.(1994). Main structural domains of the central Mediterranean region and their Neogene tectonic evolution. Bollettino di Geofisica Teorica e Applicata, v. 36 p. 103-125.

Palano, M., Ferranti, L., Monaco, C., Mattia, M., Aloisi, M., Bruno, V., Cannavò, F., Siligato, G. (2012). GPS velocity and strain fields in Sicily and southern Calabria, Italy: Updated geodetic constraints on tectonic block interaction in the central Mediterranean. Journal of Geophysical Research, vol. 117, b07401, doi:10.1029/2012jb009254, 2012.

Torelli, L., Grasso, M., Mazzoldi, G., Peis, D., Gori, D., 1995. Cretaceous to Neogene structural evolution of the Lampedusa Shelf (Pelagian Sea, Central Mediterranean). Terra Nova, 7, 200-212.

CURRENT TECTONIC ACTIVITY IN THE NWSECTOR OF THE SICILY CHANNEL BASED ON SEISMIC PROFILE ANALYSIS

Meccariello, M.[1], Ferranti, L.[1], Pepe, F.[2]

[1]Dipartimento di Scienze della Terra, dell'Ambiente e delle Risorse (DiSTAR), Università di Napoli "Federico II", melania.meccariello@unina.it; luigi.ferranti@unina.it
[2]Dipartimento di Scienze della Terra e del Mare, Università di Palermo, fabrizio.pepe@unipa.it

Introduction

The joint interpretation of multichannel (from VIDEPI database) and unpublished high-resolution Sparker seismic reflection profiles, recorded offshore Punta Granitola in August 2013, integrated with well log data, has been used to reconstruct the upper crustal architecture of active structures in the NW sector of the Sicily Channel (central Mediterranean).

This sector forms a broad epicontinental platform, which extends from the Egadi Islands to the Sciacca offshore, and is bounded to the south by the continental rift-related depression of Pantelleria along the Channel axis. The area belongs to the northern African continental margin, and experienced the Neogene-Quaternary Africa-Europe collision that generated the Sicilian – Maghrebian chain (Dewey et al., 1989; Ben-Avraham et al., 1990).

Seismo-stratigraphy

Isopach maps of five seismic units whose age is bracketed between Cretaceous and Quaternary, outline the space-time migration of contractional fronts, which become progressively younger towards the SE. Where as emplacement of the western front of the chain occurred during the Middle-Upper Miocene, the eastern front formed during the Pliocene-Pleistocene. Within this tectonic framework, two basins characterised by different trend, age and tectonic evolution were recognized. The older Adventure foredeepto the NW shows its depocentre in correspondence of the Adventure Plateau. It is limited in the NW by the Maghrebian Thrust Front, and in the SE by the Adventure Thrust Front (Argnani et al., 1986). The younger Plio-Pleistocene foredeep is recognised ahead of the Adventure Thrust Front. The latter forms the offshore prolongation of the Campobello di Mazara-Castelvetrano alignment (Barreca et al., 2014).

Discussion

In the NW sector of the Sicily Channel, data and interpretation we present show that shortening was active till recently. Compressional tectonics is responsible for positive inversion of pre-existing structures, separating the Trapanese and Saccense domains. At places, small-scale reverse faults offset lower-middle Pleistocene calcarenites as well as the seafloor. Activity of the offshore structures corresponding to that recognised on land (Barreca et al., 2014),

suggest that oblique thrusting and folding occurs in response to NW–SE oriented contraction. Shortening is accommodated by high angle, NNW-dipping, upper crustal thrust ramps akin to the structure proposed as a possible source for the 1968 Belice earthquake sequence (Monaco et al., 1996).

References

Argnani, A., Cornini, S., Torelli, L., Zitellini, N. (1986). Neogene-Quaternary foredeep system in the Strait of Sicily.Mem. Soc. Geol. It., 36, 123-130.

Barreca, G., Bruno V., Cocorullo, C., Cultrera, F., Ferranti, L., Guglielmino, F., Guzzetta, L., Mattia, M., Monaco, C., Pepe, F. (2014). Geodetic and geological evidence of active tectonics in south-western Sicily (Italy). Special Issue "Geodynamics of the Mediterranean", Journal of Geodynamics.

Ben-Avraham, Z., Boccaletti, M., Cello, G., Grasso, M., Lentini, F., Torelli, L., Tortorici, L. (1990).Principali domini strutturali originatisi dalla collisione neogenico-quaternaria nel Mediterraneo centrale. Memorie della Società Geologica Italiana45, 453–462.

Dewey, J.F., Helman, M.L., Turco, E., Hutton, D.H.W., Knott, S.D. (1989). Kinematicsof the Western Mediterranean. In: Coward, M.P., Dietrich, D., Park, R.G. (Eds.),Alpine Tectonics, vol. 45. Geological Society of London Special Publication, pp.265–283.

Monaco, C., Mazzoli, S., Tortorici, L. (1996).Active thrust tectonics in westernSicily (southern Italy): the 1968 Belice earthquakes sequence. Terra Nova 8,372–381.

NEOTECTONIC DEFORMATION MODEL FOR THE NORTHERN ALGERIA: PALEOMAGNETIC AND STRUCTURAL CONSTRAINTS.

M.E.M. Derder[1], S. Maouche[1], B. Henry[2], B. Bayou[1], M. Amenna[1], M. Ayache[1].

[1] *C.R.A.A.G. B.P. 63 Bouzareah Alger ALGERIA*

[2] *Paléomagnétisme, Institut de Physique du Globe de Paris, Sorbonne Paris Cité, Univ. Paris Diderot and UMR 7154 CNRS, 4 avenue de Neptune, 94107 Saint-Maur cedex, Fra*

The present-day crustal deformation in North Africa is mainly driven by the NNW–SSE convergence between the African and Eurasian plates (Nocquet & Calais, 2004; Serpelloni *et al*., 2007). This convergence is accommodated over a wide deformation zone (the Tellian Atlas) implying existence of significant seismic activity. This domain represents the southern part of the Alpine ranges at the boundary between the African and Eurasian plates.The seismic activity is mainly characterized by moderate to destructive magnitude events as was shown by the 21 May 2003 Zemmouri earthquake (Mw=6.8) (Meghraoui *et al*., 2004) and the 10 October 1980 El Asnam (presently Chlef) earthquake (Mw=7.3) (Ouyed *et al*.,1981). These two earthquakes are the strongest recent ones that occurred in this part of Western Mediterranean area. According to the Algerian earthquake catalogue (Benouar, 1994) the earthquake activity is mainly concentrated in the intramountainousseismogenic basins which belong to the Tellian Atlas.

Related to the counterclockwise rotation of Africa with respect to Eurasia since the Late Cretaceous (Mckenzie, 1972), the movement between these two plates involves an oblique convergence forming a tectonic transpression system along the western part of North Africa. This NNW-SSE transpression, initiates faulting activity along "en echelon" NE-SW trending folds and associated reverse faults. Meghraoui et al. (1996) assumed that this "en echelon" system is related to the presence of deep major E–W strike-slip faults, evidenced by Boukerbout*et al*., (2015); Mauffret,(2007), Mauffret *et al*., (1987). The different "en echelon" structures define several NE-SW oriented tectonic blocks. For Meghraoui *et al*., (1996) and Meghraoui & Pondrelli, (2012), the active deformation in North Africa could be explained by a simple kinematic model of block rotation related to the transpression with NNW-SSE direction of plate convergence. We present in this study, the results obtained from four different structural and paleomagnetic studies carried out in Northern Algeria. These new data reveal existence of numerous clockwise block rotations and confirm thus the validity of this kinematic model at regional scale. The Tellian Atlas domain is then constituted of tectonic blocks delimited by strike-slip faults, as in a "bookshelf" model (Biggs et al., 2006). The results inferred from this work represent a starting point for more detailed studies in seismogenic zones. This constitutes a significant advancement for an assessment of seismic hazard in regions where large earthquakes are expected.

References

Benouar, D. (1994). Materials for the investigation of The seismicity of Algeria and Adjacent Regions During the Twentieth Century. *Annali di Geofisica*, volume XXXVII, N, 4.

Biggs, J., Bergman, E., Emmerson, B., Funning, G.J., Jackson, J., Parsons, B. & Wright, T.J. (2006). Fault identification for buried strike-slip earthquakes using InSAR: The 1994and 2004 Al Hoceima, Morocco earthquakes. *Geophysical Journal International*, 166, 3,1347–1362.

Boukerbout H., A. Abtout, D. Gibert, B. Henry, B. Bouyahiaoui and M.E.M Derder. "Aeromagnetic study of the Chlef region (Algeria): 2-D and 3-D imaging derived from the wavelet and ridgelet transforms and identification of deep magnetized structures." Submitted to Pure and Applied Geophysics.

Mauffret, A., 2007. The Northwestern (Maghreb) boundary of the Nubia (Africa) plate. Tectonophysics 429 (1–2), 21–44.

Mauffret, A., El Robrini, M., Gennesseaux, M., 1987. Indice de la compression récente en mer Méditerranée: un bassin losangique sur la marge algérienne. Bulletin de la Société Géologique de France III (8), 1195–1206 (6).

McKenzie, D.P. (1972). Active tectonics of the Mediterranean region.*Geophysical Journal of the Royal Astronomical Society, 30*, 109-185.

Meghraoui et al. (1996) Meghraoui, M., Morel J.L., Andrieux J. & M. Dahmani., 1996.Tectonique plio-quaternaire de la chaîne tello-rifaine et de la mer d'Alboran. Une zone complexe de convergence continent-continent. *Bulletin de la Société Géologique de France*, 167, 1, 141-157.

Meghraoui, M., Pondrelli, S., 2012. Active faulting and transpression tectonics alongthe plate boundary in north Africa. Annals of Geophysics 55 (5), 2012.http://dx.doi.org/10.4401/ag-4970.

Meghraoui, M., Maouche, S., Chemaa, B., Cakir, Z., Aoudia, A., Harbi, A., Alasset, P.J., Ayadi, A., Bouhadad, Y. &Benhamouda, F. (2004). Coastal uplift and thrustfaulting associated with the Mw = 6.8 Zemmouri (Algeria) earthquake of 21 May,2003. *Geophysical Research Letters*, 31, L19605, doi:10.1029/2004GL020466.

Nocquet & Calais, 2004; Nocquet, J. M. & Calais, E. (2004).Geodetic measurements of crustal deformation in theWestern Mediterranean and Europe.*Pure and Applied Geophysics*, 161, 661–681.

Ouyed, M., Meghraoui, M., Cisternas, A., Deschamp, A., Dorel, J., Frechet, F., Gaulon, R., Hatzfeld, D., Philip, H., 1981. Seismotectonics of the El Asnam earthquake.Nature ,292 (5818), 26–31.

Serpelloni, E., Vannucci, G., Pondrelli, S., Argnani, A., Casula, G., Anzidei, M., Baldi, P.,Gasperini, P., 2007.Kinematics of theWestern Africa–Eurasia plate boundaryfrom focal mechanisms and GPS data.Geophysical Journal International 169,1180–1200.

MEDITERRANEAN SEISMICITY IN A FRAME OF GLOBAL SEISMIC ACTIVITY

Sandu Ilie

*Moldavian Academy of Sciences, Institute of Geology and Seismology,
Republic of Moldova*

The paper presents an estimative study of global and regional seismicity (Mediterranean area). The 1965-2013 instrumental seismic data (provided by ISC) have been used to select the M4.5+ seismic events for complex statistical analysis. Using the recurrence relations between different magnitude scales, the seismic energy size were calibrated, the seismic energy release has been estimated. The main focus of the investigation is the accuracy of energy estimation.

Numerical computation algorithm has been performed by author using the Mathematica 4.1v software package.

TESTING THE MOMENT RATIO METHOD IN FORECASTING WORLDWIDE SEISMICITY

Talbi, A.[1], Mobarki, M.[1]

[1]*Departement étude et surveillance sismique, CRAAG BP 63 Bouzaréah 16340 Algérie, a.talbi@craag.dz, mourad.mobarki@gmail.com*

Introduction

The mean ratio (MR) alarm-based earthquake forecasting model is tested worldwide in several countries prone to earthquakes. This model defines a precursory alarm function to forecast future earthquakes in a given region, namely the alarm in each grid cell is linked to the ratio of the mean inter-event time over the variance. So far, this model was successfully tested in forecasting large earthquakes with magnitude $M \geq 7$, occurred in Japan. In this study, the MR model is tested on target earthquakes with different magnitude thresholds which occurred worldwide, taking into accounts the completeness of magnitudes.

Different local and global earthquake cataloguedata files were compiled and used in a series of retrospective tests applied at short, intermediate and long-term to evaluate the performance of the MR model. For example, Papazachoscatalogue covering the period -550–2010 was used to test seismicity in Greece, whereas USGS global catalogue has been considered in testing global seismicity. When taking into account completeness of magnitude,training time periods should start from the first yearensuring completeness of data for each threshold magnitude.

This choice leads to an optimal choice that guarantees larger and accurate working data base. Molchan error diagrams are used to evaluate the forecasting performance of the MR method. MR forecasting maps are optimal in a sense that ensure a minimum miss and alarm rates are constructed to check hits and failures scores in practice. Preliminary results show that MR model forecasts outscore random guessing and show good performance comparing to the relative intensity (RI) method.

Finally, implication of the MR forecasts in seismic hazard is discussed. Earthquakes occur as a result of abrupt change in stress along faults. Physical process behind nucleation remains largely unknown and physical parameters of faults and information on their location are challenging. Incomplete information available nowadays about some faults does not allow us to guess or appreciate long return time behaviour of strong events. In this context, earthquake forecasting appears complicated.

Nevertheless, valuable information is embedded in present seismicity catalogue database that tells part of the story of earthquake occurrences. In this study, we focus on testing worldwide seismicity using the mean ratio method (Talbi et al. 2013). Results show good performance of the MR method compared to both random guessing and the relative intensity RI method.

Methodology and results

First, the study region is covered using a regular grid. Then, the moment ratio score *MR* is calculated for each grid cell *C*, using the following relation (Talbi et al. 2013),

$$MR(C) = \frac{\bar{\bar{\xi}}}{\sigma_\xi^2} \qquad (1),$$

where $\bar{\bar{\xi}}$ and σ_ξ^2 are the arithmetic mean and the variance of the inter-event time series $\{\xi_i\}_{i=1}^n$, respectively. Inter-event time series is calculated for all events occurring inside a disk centered on the grid cell center. When suitable, the disk and/or the grid cell size *l* are enlarged to allow a minimum covering of the study region.

The set of grid cells that contains at least one observed MR score value defines the testing region *G*, with the MR alarm function P_{MR} for a given cell *C* defined as follows (Talbi et al. 2013),

$$P_{MR}(C) = \frac{1}{P_{MR}^{max}} MR(C) \qquad (2).$$

Division by the maximum observed score $P_{MR}^{max} = \max_{C \in G}(MR(C))$ is a normalizing factor to shift all $P_{MR}(C)$ values to the interval [0, 1].

Molchan diagram (Molchan 1997) plotting the miss rate ν against the space–time alarm rate τ obtained for different alarm thresholds are used to evaluate the forecasting performance of the MR method. In a Molchan diagram, the diagonal indicates a trivial random guess strategy, with any points significantly below this diagonal outscoring the random guessing strategy.

Figures 1 and 2 below show an example of an MR forecasting map for Greece and the corresponding Molchan diagram. Training and testing periods were set to 1890-1960 and 1960-2010 using $M \geq 5$ and $M \geq 6$ events, respectively. From Figure 2 it appears clearly that the MR method outscore random guessing strategy at 1%.
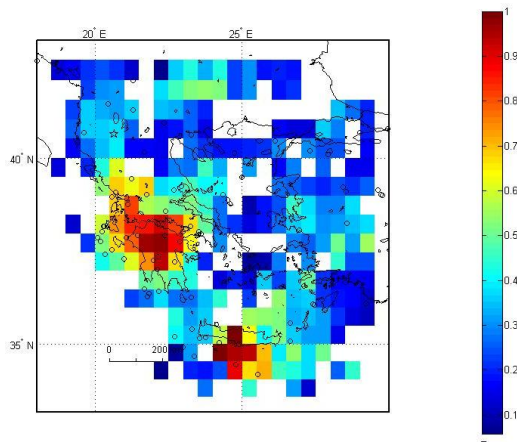
Figure 1.MR forecasting map obtained using M≥ 5.0 and M≥ 6.0 events that occurred during the training and testing periods 1890−1960 and 1960−2010, respectively.
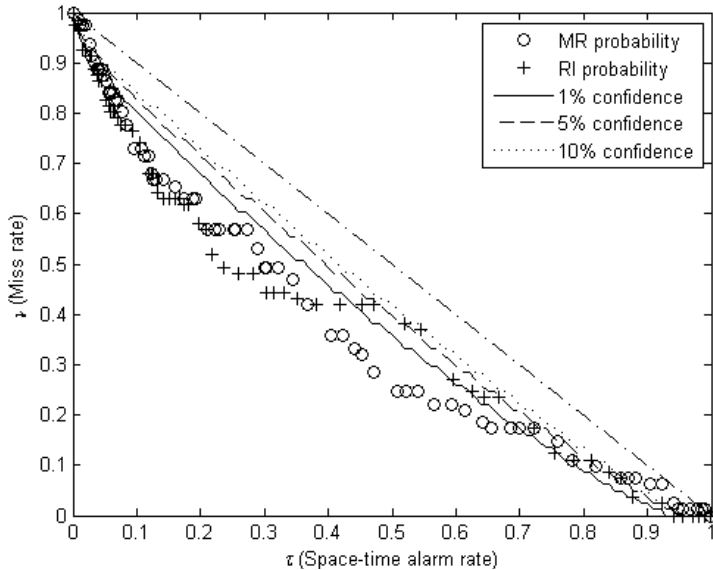
Figure 2.Molchan diagram for MR and RI methods both compared to the diagonal random guessing strategy.

Conclusions

The mean ratio (MR) method,when tested worldwide, shows good performance compared to both random and relative intensity RI strategies. Furthermore, the use of local and global catalogues allows us to discuss typical cases and get feedback.

References

Molchan, G., (1997). Earthquake prediction as a decision making problem, *Pure Appl. Geophys.,* **149**, 233–247.

Papazachos, B.C., Comninakis, P.E., Karakaisis, G.F., Karakostas, B.G., Papaioannou, Ch.A.,Papazachos, C.B. and E.M. Scordilis (2000). A catalogue of earthquakes in Greece andsurrounding area for the period 550BC-1999, Publ. Geophys.Laboratory, University ofThessaloniki, 1, 333pp.

Papazachos, B.C., Comninakis, P.E., Scordilis, E.M., Karakaisis, G.F. and C.B. Papazachos(2010).A catalogue of earthquakes in the Mediterranean and surrounding area for theperiod 1901 - 2010, Publ. Geophys.Laboratory, University of Thessaloniki.

Talbi A., Nanjo K., Satake K., Zhuang J. and M. Hamdache (2013). Inter-event times in a new alarm−based earthquake forecasting model. Geophysical Journal International, doi:10.1093/gji/ggt194.

GROUND MOTION SCALING IN THE SICILY CHANNEL: IMPLICATIONS FOR SEISMIC HAZARD ASSESSMENT

Akinci A.,[1] S., D'Amico[2], M.,Pischuitta[1]

[1] *Istituto Nazionale di Geofisica e Vulcanologia, Via di Vigna Murata 605, 00143 Rome, Italy, aybige.akinci@ingv.it,*

[2] *Department of Geosciences, University of Malta, Msida MSD 2080, Malta, sebastiano.damico@um.edu.mt*

Predictive ground motion relations are developed for the area around the Sicily Channel spanning the magnitude range $2.5 \leq M_w \leq 7.4$ and distances $10 \leq r \leq 300$ km. The parameters, Pseudo Spectral Velocities and Pseudo Spectral Accelerations at 0.33, 1 and 3.33Hz are derived from an empirically based stochastic ground motion model. To assess the spectral characteristics of attenuation, excitation and duration we use horizontal component recordings of local and regional earthquakes. The data set contains 1968 events ranging between $2.0 \leq M L \leq 5.2$. These 15955 broadband waveforms were recorded in the Sicily Channel from 2006 to 2012. We derive empirical excitation, site, and attenuation terms from peak ground velocities by applying an iterative damped least square regression. The results are then used to calibrate effective theoretical attenuation and excitation models. A grid search through the parameter space is applied to obtain the best fitting quality factor, $Q(f)$, and to constrain $G(r)$, the piece-wise linear geometrical spreading-function. The best fit is obtained for $Q(f) = 250 f^{0.40}$, $G(r) = r^{-1.0}$ (0 to 100 km), and $r^{-1.5}$ (>100 km). Modelling of the excitation terms based on the Brune's source spectrum and the optimum attenuation results in stress drops ranging between 20 and 250 bars and a $k = 0.05s$.

The main goal of this study is to improve the assessment of seismic hazard in Sicily Channel and surrounding region by providing improved site specific, predictive spectral ground motion estimates and their related uncertainties. To predict ground motions also at larger magnitudes than observed, a combination of measuring and modelling techniques (stochastic simulation method) is chosen. A second advantage of the stochastic simulation method is that all parameters of engineering interest, such as pseudo spectral accelerations, can be computed.

SEISMIC SOURCES MAPPING CASES OF STUDY: CONSTANTINE REGION (NORTH-EASTERN ALGERIA)

Aourari, S.

Seismic Hazard Department, National Centre of Research Applied for Earthquake Engineering CGS, 01 Kaddour Rahim Street, BO 252 Hussein Dey Algiers-Algeria, sahourari@hotmail.com

Introduction

The aim of study is to provide for the seismic hazard assessment, the static geometrical parameters (namely directions, lengths, types and dip) of active and suspected active faults surrounding Constantine region. The parameters of these faults are integrated later for the seismic hazard assessment, in a probabilistic approach to estimate the maximal magnitudes of probable earthquakes.

Constantine region belongs to Tell Atlas referred to as Maghrebides chain. This domain is the main seismically active region of North Algeria however the Eastern domain which include Constantine seems less active than the central and western domains. As a reminder, the Maghrebides are extending from North Africa to the Far East regrouping the peri- Mediterrannean orogens. They are a result of the opening and subsequent closure of the Tethys ocean basins system. Currently, a number of Miocene network faults or reactivated older alpine faults are potentially active. The study covers the region defined by [36.80° - 35.90° N], [6.12° - 7.24° E]. The region is characterized by a moderate seismicity and reveals neotectonic activity.

Historical seismicity

Several destructive historical earthquakes have occurred in the Tell Atlas, principally in Ech Cheliff, Oran, Algiers and Jijel areas. However, the seismicity is diffuse in the greater part of the country. In Constantine area, a number of historical earthquakes have induced maximum intensities VI MSK (Figure 1). Constantine city was shaken during the instrumental period by 3 earthquakes. The earthquake of August 4 1908 magnitude [Ms 5.2], the earthquake of August 6 1947 magnitude [Ms 5.0] and the October 27 1985 earthquake [Ms 6.0]. This event is the strongest and it was recorded by 474 international seismic stations. The quake was felt over 120 km from the epicenter and caused loss of life and extensive damage. Its macroseismic epicenter is located in El Aria locality where I_0 was assessed VIII MSK [Bounif (1987), Bounif et al., (1990), Bounif and Dorbath (1998)].

The seismicity recorded in NE Algeria is low to moderate. Figure 1 summarizes the events which have affected Constantine. In fact, during the 18th century, the area was marked by 07 small (Io ≤ V MSK) events. Since the 19 th century to the present: 03 events with magnitudes more than 5 have been recorded. The historical seismicity map reveals mainly 03 seismic zones, attesting the existence of seismic sources: Jijel area in coastal zone, Constantine- Mila areas

with a slight N-S and Guelma area located in the external domain of the Tell, and offshore where seismicity is mostly of undetermined magnitudes.
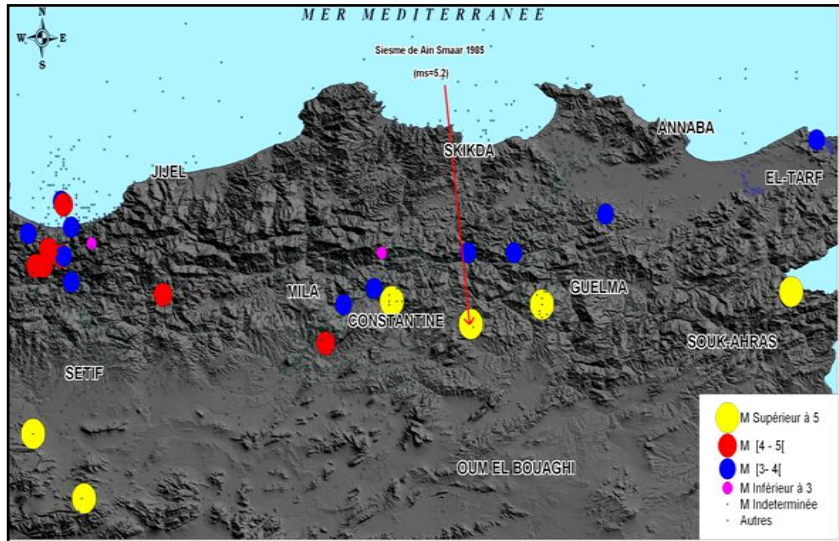
Figure 1: historical seismicity map of Eastern Algeria.Using M≥3.0. Events taken from Harbi, 2010 (for 1860 to January2008) and NEIC catalogue (data from 2008 to January 2012)

Tectonic setting

The Algerian Maghrebides are composed of sedimentary and metamorphic units of Meso- Cenozoic scales. Tectonic phases since the Mesozoïc- Cenozoïcare characterised by Tertiary compression phases whose paroxsymal phase took place in lower Miocene, extension phases of collision and magmatism related to the relative sliding and the convergence between the African and Eurasian plates.
A North-South section shows internal zones and external zones. The tectonics of Constantine Tell is due to the late Cretaceous and Miocene phases effects [Laffite 1939; Vault, 1967; Vila, 1980; Aris, 1998]. The Miocene paroxysmal phase produced significant folds distinguished in two principal directions NE- SW and E-W. Vila [1980] specifies that the alpine tectonics took place in several phases: Priabonian phase generated the "front thrust" episode in which is expressed epizonal metamorphism, the flysch overthrust nappe, Tellian nappes and the folding of parautochthon domain. The Burdigalian phase generated olistostromes, Numidian flysch and plicatives structures in internal zone. The Tortonian phase is expressed by decametric thrusting. The neotectonic phases were prelude from the middle Miocene by distension creating major post nappes basins. Then, since Pliocene a compression phase involving the reactivation of some faults which are mostly inherited of alpine periods. These faults are associated to an active network

of NE, E-W strike slip faults and E-W thrust faults affecting the Eastern Tell (Meghraoui et al., 1988).
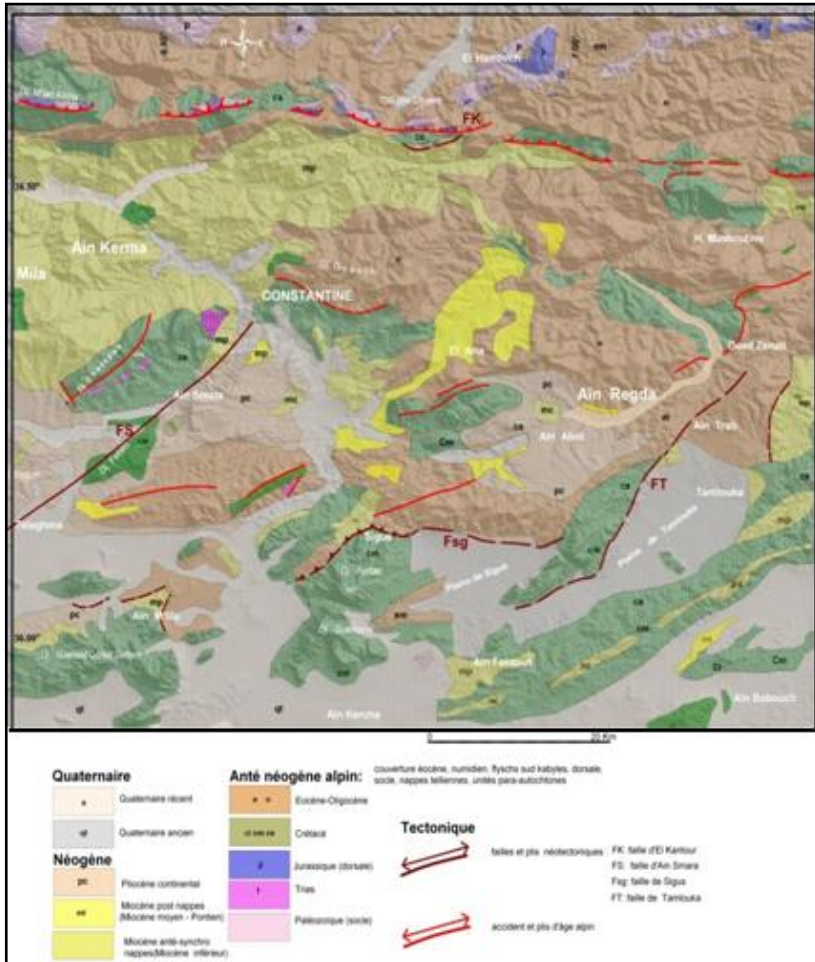
Figure 2: Neotectonic map of Constantine region. Legend of different units: - Socle kabyle (Paleozoïc terrains), Dorsale kabyle (Jurassic Eocene deposits) in Skikda area, Flyschs units and tellian nappes (Jurassic–Cretaceous–Tertiary deposits in Guelma Constantine), Post nappes basins (Plio Quaternary deposits in Tamlouka, Sigus), High Plateaus (Oum El Bouaghi area). Topography is from SRTM Digital Elevation Model with 90m resolution.

The study region presents geological indications concerning the recent activity. The neotectonic map shows scarps.

Seismic sources mapping

The seismic sources mapping is prerequisite for any regional seismic hazard analysis. Better understanding about tectonic structures help to better

characterize the geological seismic sources in terms of location, magnitude and recurrence. In fact, the geometrical parameters of active and supposed active faults are integrated later in the empirical formulas to estimate the maximal magnitudes of probable earthquakes designated MCE. Table 1 summarized geometrical parameters of active faults and supposed active faults listed below in order of potential to produce earthquakes in Constantine area

Table 1: Seismic sources lines

Source line	TYPE	Direction	Lengh (Km)	Dip	Depth
Ain Smara	sinistral strike slip	N060	> 50	sub -vertical	superficial
South Skikda	reverse	N090	≤10	< 40° to North	earth quak
Sigus	reverse	N080	30	/	es
Tamlouka	sinistral strike slip	N050	25	sub- vertical	[10- 18 [Km

The delineation of seismic sources consists of delimiting the seismic region into active geological provinces on basis of the post Neogene deformation and seismicity*: Zone I* corresponds to the geological province which reveals a Plio-Quaternary tectonic phase; consequently, the zone includes all active faults identified (observable hidden) to date. *Zone II* corresponds to the province that reveals a little Neogene deformation and low seismicity. *Zone III* corresponds to the geological province which reveals an uplift of ante Neogene terrain and very low seismicity. The North Eastern including Constantine region can be divided in (03) seismic sources (Fig.3):

Table 3:seismotectonic provinces of Eastern Algerian

ZONES			Limits
South Constantine Zone(ZI)		Zone oriented E-W, Superficial: 500 Km², Events magnitude Ms ≥ 4.5. Includes the 04 faults	North : front de nappes (regional accident system of reverses E-W faults) South : geomorphological limit of Plio-Quaternary basins (Tamlouka, Sigus)
North Constantine Zone(ZII)		E-W zone includes the Eastern marge and the littoral Events Ms [2 – 4].	North : offshore fault (Kharoubi, 2009) South : front de nappes fault
High Plateaus Zone (ZIII)		Low seismicity	North : l'avant-fosse miocène South: North Atlasic Accident (ANA)?

1- South Constantine Zone (ZI) superficial: 500 Km² and oriented globally E-W. The zone corresponds to the geological domain limited in the north by the front thrust accident and the southern boundary coincides with the geomorphological limit with Miocene "post nappes". The area encloses Ain Smara, El Kantour, Sigus, Tamlouka faults. Also, the zone concerns North and South Guelma faults, Hammam N'Baïl Bouchegouf which are not the subject of this study. The area has recorded maximum historical seismicity with earthquakes of magnitude Ms ≥ 4.5.

2- North Constantine Zone (ZII) is limited on the north by the offshore fault zone (Kharoubi, 2009) and the front thrust accident in the south. The source area (ZII) generally oriented E-W, includes the eastern offshore basin. The zone includes Skikda area characterized by seismicity with magnitudes Ms [2-4]. Western, Jijel area affected by destructor earthquake in 1856 with intensity evaluated X (MSK).

3- High Plateaus Zone (ZIII) includes the high plains of Oum El Bouaghi and Souk Ahras is characterized by the uplift of the ante Neogene terrains and low seismicity. The zone is limited on the north by the geomorphological boundary of "Avant-fosse miocène" and in the south by the north Atlas accident (ANA).
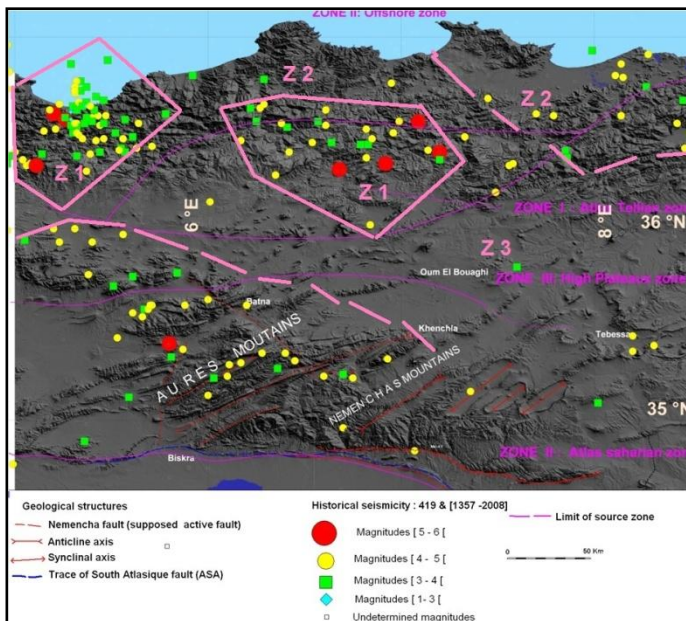
Figure 3: Source zones zonation of Eastern Algeria (Tell and Atlas domains)

References

Aoudia, A., Vaccari, F., Suhadolc, P. et Meghraoui, M., 2000. Seismogenic potential and earthquake hazard assessment in the Tell Atlas of Algeria. *Journal of Seismology*, 4, 79-88.

Auzende J.M (1978). Histoire tertiaire de la méditerranée occidentale. Thèse de Doctorat d'Etat à l'Université de Paris- VII, 130 pages.

Benouar.D. (1993). The seismicity of Algeria and adjacent regions during the twentieth century, PhD- Thesis, Imperial College of Science, Technology and Medecine, Univ. London, 712 pp.

Boudiaf, A., 1996. Etude sismotectonique de la région d'Alger et de la Kabylie (Algérie). Utilisation des Modèles Numériques de Terrain (MNT) et de télédétection pour la reconnaissance des structures tectoniques. *Thèse de Doctorat, Université de Montpellier II*, France, 274 p.

Bounif, A., H. Haessler & M. Meghraoui (1987) The Constantine (Northeast Algeria) earthquake of October 27, 1985: surface ruptures and aftershock study, Earth Planet Sc. Lett., 85, 451-460.

Bounif, M. A., (1990). Etude Sismotectonique en Algérie du Nord : Contribution à l'Etude d'un Tronçon de la Chaîne Tellienne à partir des Répliques du Séisme du 27 octobre 1985. Thèse de magister, USTHB-Alger, pp 155.

C.R.A.A.G. (1994). Les séismes en Algérie de 1365 à 1992. Publication du Centre de Recherche en Astronomie, Astrophysique et Géophysique.

Domzig A. (2006). Déformation active et récente, et structuration tectono-sédimentaire de la marge sous-marine algérienne. Thèse de Doctorat de l'Université de Bretagne Occidentale, 333pp.

Durand- Delga M. et Fontbote J. M. (1980). Le cadre structural de la Méditerranée occidentale. Mémoire B.R.G.M., 115, Orléans, pp. 57-85.

Groupe de Recherche Néotectonique de l'Arc de Gibraltar (1977). L'histoire tectonique récente (Tortonien à Quaternaire) de l'Arc de Gibraltar et des bordures de la mer d'Alboran. Bull. Soc. Géol. France, (7) 19,575-614.

Harbi, A., Maouche, S. and Ayadi, A. (1999). Neotectonics and associate seismicity in the Eastern Tellian Atlas of Algeria, J.Seismol. 3, 95–104.

Harbi, Assia (2001). Analyse de la sismicité et mise en évidence d'accidents actifs dans le Nord-Est Algérien, Thèse de Magistère, USTHB, Alger, 195 pp.

Harbi, A., S. Maouche and H. Benhallou, (2003b), «Re-appraisal of seismicity and seismotectonics in the north-eastern Algeria Part II: 20th century seismicity and seismotectonic analysis», Journal of Seismology, April, 2, volume 7: 221-234

Harbi, A. (2006). Evaluation de l'Aléa Sismique en Algérie du Nord par la Modélisation de l'Input Sismique dans les Zones Urbaines et l'Etablissement d'un Catalogue, Thèse Doctorat d'Etat en Sciences de la Terre, Spécialité : Géophysique, USTHB, Alger.

International Seismological Centre (ISC). 2010, On-Line Bulletin, http// www.isc.ac.uk,

Mc Kenzie D., (1972). Active tectonics of the Mediterranean region, Geophy. J.R. Astr. Soc. 30, 109-185.

Meghraoui M., Cisternas A. & Philip H. (1986). Seismotectonics of the lower Chelif basin: structural background of the El Asnam (Algeria) earthquake, Tectonics 5, 809-839.

Meghraoui M., (1988). Géologie des zones sismiques du nord de l'Algérie, tectonique active, paléosismologie, et synthèse sismotectonique, Phd- Thesis, Univ. Paris- sud Orsay, 356 pp.

Oussadou Farida(2012) : Etude du champ de contrainte au nord de l'Algérie dans le contexte ibéro-maghrébin par inversion des solutions focales. Th7se de doctorat. Faculté pp375

WCC (1984). Microzonation sismique de la region d'Ech Chéllif –Algérie. Etude d'aléa sismique Volume I. Woodward-Clyde Consultants

EXTREME WAVES IMPACT ON MALTA (MEDITERRANEAN SEA)

Biolchi, S.[1], Furlani, S.[1], Antonioli, F.[2], Baldassini N.[3], Cucchi, F.[1], Deguara J.[4],Devoto S.[1], Di Stefano A.[3], Evans J.[5],Gambin T.[6], Gauci R.[4], Mastronuzzi G.A.[7], Monaco C.[3], Scicchitano G.[8]

[1] *Department of Mathematics and Geosciences, University of Trieste, Italy, sbiolchi@units.it*
[2] *ENEA, Roma, Italy*
[3] *Departmentof Biological, Geological and Environmental Sciences, University of Catania, Italy,*
[4] *Department of Geography, University of Malta*
[5] *Department of Biology, University of Malta,*
[6] *Department of Classics and Archaeology, University of Malta*
[7] *Department of Earth and Geoenvironmental Sciences, University of Bari, Italy*
[8] *Studio geologi associati T.S.T, Messina, Italy*

Introduction

The accumulation of large boulders related to waves generated by tsunami and extreme storm events have been observed in different areas of the Mediterranean. Along the NE and E low-lying rocky coasts of Malta tens of large boulder deposits have been recognised and mapped (Furlani et al., 2011; Mottershead et al., 2014). These boulders are detached and moved by the seafloor by the action of sea waves. Reconstructing the history of these blocks and distinguishing events, such as storm waves or tsunami, play a crucial role in assessing the coastal vulnerability and risk. The Maltese coasts are seasonally affected by extreme storm waves: heavy seas are in fact frequent and are originated by the NE and NW winds. Moreover in the past some important tsunami events which occurred in the Mediterranean Sea, such as the 1693 and the 1908, have been reported on the historical chronicles of Malta (Galea, 2007). The seismicity is related mainly to the Malta Escarpment, the Sicily Channel Rift Zone and the Hellenic Arc. In this study we present a multidisplinary approach, which aim to characterize the boulder accumulations in order to assess the natural hazard for the coasts of Malta Island, where extreme waves have been and are able to detach and move large rocky blocks on the coast.

Study area

The Island of Malta lies in the Sicily Channel, which has been affected during Neogene-Quaternary age (Finetti, 1984; Dart et al., K.R., 1993) by continental rifting. It produced extensive structures, such as the Pantelleria, Malta and Linosa tectonic depressions, which are controlled by NW-SE normal faults.
The tectonic setting of Malta is characterized by two graben systems. The most ancient one, ENE-WSW oriented, has been active since early Miocene and caused the development of a horst and graben system, which is characterized by

alternating highlands and lowlands (Alexander, 1988). This system is crossed by faults belonging to the Pantelleria Rift, NW-SE oriented, which developed during the late Miocene and early Pliocene (Reuther &Eisbacher, 1985). The uplift caused by the Pantelleria Rift is responsible for the emergence of the island above sea level during Neogene-Quaternary and it also brought the island to a tilting position towards NNE (Alexander, 1988), with a resulting downlift of its eastern flanks. This tectonic development - with relatively higher topography and steep coasts along the western side of Malta and low-lying coasts along the eastern side - conditioned also the hydrological catchment of the islands during the pluvial Quaternary period, with fluvial channels draining heavily from WSW to a NNE direction. This caused a more intense fluvio-coastal erosion in the eastern part and the removal of a large part of the stratigraphic sequence in the lower topographic regions. These are the reasons why the eastern rocky coast is suitable, from a geomorphological viewpoint, for the accumulation of large boulders, from decimetric to metric in size, which are detached from the sea bottom by the waves and are deposited on the coast, also some tens of meters away from the coastline (Figure 1). Malta is formed by sedimentary rocks, deposited in shallow marine conditions between late Oligocene and Miocene (Pedley et al. 1976). The bedding is mainly horizontal or sub-horizontal.

The stratigraphic sequence starts with the Lower Coralline Limestone Formation (Upper Oligocene: Chattian, thickness: 140 m), which is characterized by bioclastic, bedded, grey limestones. It is followed by the soft and yellowish Globigerina Limestone Formation (late Oligocene – middle Miocene: late Chattian - Langhian, thickness: 20-207 m, Giannelli&Salvatorini, 1972; Baldassini et al., 2013) which is composed by massive fine-grained biomicrites. The sequence continues with the Blue Clay Formation (middle Miocene: late Langhian - early Tortonian, thickness: 20-75 m), mostly formed by alternating layers of dark-grey and pale-grey marls. The upper part of the sequence is made up of the Upper Coralline Limestone Formation (Upper Miocene: late Tortonian – early Messinian, thickness: 10-170 m), which is very similar to the oldest carbonate unit (Pedley et al., 1976).

Matherials and methods

The eastern low-lying coasts of Malta have been surveyed in order to identify and map all the boulder accumulations. Some of the them have already been described by Furlani et al. (2011) and Biolchi et al. (2014) at Armier Bay, and by Mottershead et al. (2014), at Ahrax Point, Water Park, Xghajra and Zonqor. The most representative boulders, in term of size, shape and distance to the coastline, were chosen for further analysis. The candidate boulders include the largest observed blocks, slab-like, roughly cubic and rectangular, as well as assembled andisolated ones.

In order to verify if the boulders are compatible with the storm wave regime of the area or if tsunami waves were responsible for their detachment, transport and deposition, we applied a hydrodynamic approach. In particular, the

Pignatelli et al. (2009), Nandasena et al. (2011) and Engel and May (2012) equations were applied in order to calculate the minimum tsunami and storm wave heights required to detach a boulder from the cliff-edge. Direct observations on each boulder were carried out, regarding size, direction and distance from the shoreline, whereas the unit weight was determined by means of the Schmidt Hammer (SH).
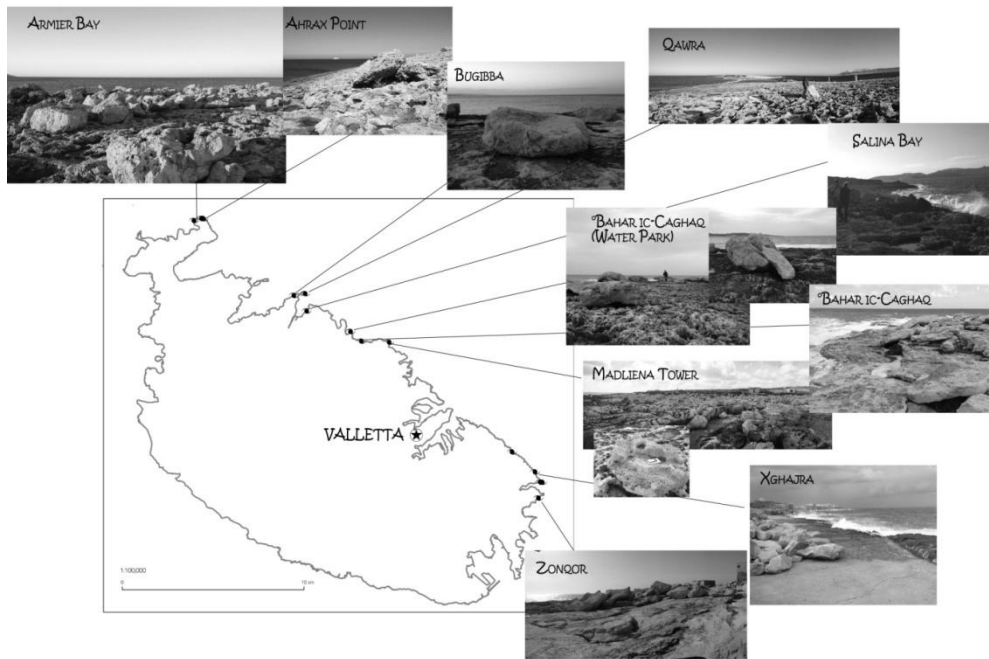
Figure 1.Location of the coastal boulder deposits and relative pictures.

As this approach also depends on the pre-transport environment, the most probable setting (submerged, sub-aerial, etc) prior to transportation has been determined. Moreover, detailed submerged profiles of the four coastal sites have been carried out by direct scuba surveying. The onshore megaboulders at each site were inspected to check for the presence of any biological structures, which can serve as a definite indicator of a marine (submerged) origin of the boulders since died just after their removal from underwater environment.

Finally, collected data have been compared to the Maltese wave data (Malta Maritime Authority, 2003; Malta Environment and Planning Authority, 2007;http://www.capemalta.net/maria/pages/waveforecast.html).

Results and conclusions

The three axes of the most representative boulders, together with their volume and their density are listed in Table 1. Density has been evaluated by means of the Katz

et al. (2000) formula, which relates the rebound values of a rock to the uniaxial compressive strength and its density. Moreover, the height of tsunami and storm waves required for detaching and moving a boulder from the coast edge, calculated with Nandasena et al. (2011), Pignatelli et al. (2009) and Engel and May (2012) approaches, are reported.

Table 1.Physical parameters of the boulders (axis a, b and c, volume and density) and results of the application of the hydrodynamic equations provided by Nandasena et al., 2011; Pignatelli et al., 2009 and Engel and May, 2012 respectively for Tsunami wave (T) and Storm wave (S)

SITE	BOULDER	a (m)	b (m)	c (m)	V (m³)	δ (g/cm³)	N_T (m)	N_S (m)	P_T (m)	P_S (m)	E_T (m)	E_S (m)
A H R A X	AA1	4.1	2.4	1.1	10.82	1.39	1.18	4.71	1.11	4.46	0.80	3.21
	AA2	2.8	1.2	1.1	3.70	1.70	2.18	8.71	2.06	8.24	0.49	1.97
	AA3	1.8	0.8	0.8	1.15	1.70	1.58	6.34	1.50	5.99	0.33	1.31
	AA4	3	2.2	0.65	4.29	1.70	1.29	5.15	1.22	4.87	0.90	3.61
P O I N T	AA5	2.25	1.9	0.3	1.28	1.70	0.59	2.38	0.56	2.25	0.78	3.11
	AA7	1.7	1	0.8	1.36	1.70	1.58	6.34	1.50	5.99	0.41	1.64
	AA8	2	1	0.5	1.00	1.70	0.99	3.96	0.94	3.75	0.41	1.64
	AA9	2	1.2	0.45	1.08	1.62	0.78	3.13	0.74	2.96	0.47	1.87
A R M I E R	AB1	4.2	2.8	0.5	5.88	1.78	1.10	4.41	1.04	4.17	1.20	4.80
	AB2	3.5	1.6	0.55	3.08	1.85	1.33	5.32	1.26	5.03	0.71	2.85
	AB3	2	1.6	0.8	2.56	1.62	1.39	5.57	1.32	5.27	0.62	2.50
	AB4	1.9	1.4	1.4	3.72	1.81	3.24	12.95	3.06	12.24	0.61	2.45
	AB6	1.6	1.2	0.5	0.96	1.70	0.99	3.96	0.94	3.75	0.49	1.97
	AB7	3.4	1.6	1.15	6.26	1.70	2.28	9.11	2.15	8.61	0.66	2.62
B A Y	C16	0.9	0.8	0.25	0.18	1.80	0.57	2.27	0.54	2.15	0.35	1.39
	AB5	2.56	1.06	0.92	2.50	1.70	1.82	7.29	1.72	6.89	0.43	1.74
	new	2.39	1.69	0.82	3.31	1.58	1.33	5.31	1.26	5.02	0.64	2.57
	Q2	0.75	0.55	0.5	0.21	1.70	0.99	3.96	0.94	3.75	0.23	0.90
B A H A R I C	B1	2.3	0.6	0.36	2.55	1.70	1.14	4.55	1.12	4.49	0.76	3.03
	B10	3.1	1.6	0.6	2.98	1.39	0.66	2.62	0.61	2.43	0.54	2.14
	B11	3.3	1.8	0.69	4.10	1.39	0.75	3.01	0.70	2.80	0.60	2.41
	B12	3.1	2.35	0.5	3.64	1.39	0.55	2.18	0.51	2.03	0.79	3.15
	B13	4.3	3.4	0.7	10.2	1.39	0.76	3.06	0.71	2.84	1.14	4.55

C A G H A Q	B14	3.2	2.1	1.1	7.39	1.39	1.20	4.81	1.11	4.46	0.70	2.81
	B2	4.35	3.65	0.4	6.35	1.80	0.87	3.48	0.86	3.44	1.58	6.33
	B3	2.4	1.8	0.55	2.38	1.80	1.20	4.78	1.18	4.73	0.78	3.12
	B4	2.6	1.7	0.7	3.09	1.80	1.52	6.09	1.50	6.01	0.74	2.95
	B5	2.15	1.93	0.7	2.90	1.80	1.52	6.09	1.50	6.01	0.84	3.35
	B6	2	1.5	0.55	1.65	1.80	1.20	4.78	1.18	4.73	0.65	2.60
	B7	2.3	1.6	0.36	1.32	1.80	0.78	3.13	0.77	3.09	0.69	2.78
	B8	3	2.4	1	7.20	1.80	2.17	8.70	2.15	8.59	1.04	4.17
	B9	3.3	1.65	0.6	3.27	1.39	0.66	2.62	0.61	2.43	0.55	2.21
B U G I B B A	LB1	4	2	1.2	9.60	1.70	2.44	9.78	2.25	8.99	0.82	3.28
	LB10	2.4	2.3	0.5	2.76	2.05	1.50	5.98	1.41	5.66	1.13	4.54
	LB2	2.9	1.65	1.05	5.02	1.98	3.03	12.13	2.79	11.15	0.79	3.16
	LB3	2.6	1.8	1.1	5.15	2.08	3.54	14.17	3.20	12.81	0.90	3.60
	LB4	3.3	2.8	0.6	5.54	1.62	1.09	4.37	0.99	3.95	1.09	4.37
	LB6	2.02	1.12	0.35	0.79	1.85	0.89	3.54	0.80	3.20	0.50	2.00
	LB7	1.98	1.8	1.1	3.93	2.02	3.34	13.35	3.02	12.07	0.87	3.50
	LB8	1.74	1.6	0.85	2.37	1.74	1.86	7.45	1.68	6.73	0.67	2.68
	LB9	2.5	2.15	0.8	4.30	1.70	1.63	6.52	1.50	5.99	0.88	3.52
Q A W R A	Qa1	1.8	1.4	1.3	3.28	1.80	2.95	11.81	2.79	11.17	0.61	2.43
	Qa2	2.2	1.2	0.65	1.72	1.80	1.54	6.18	1.40	5.58	0.52	2.08
	Qa3	1.5	1.5	0.7	1.58	1.85	1.77	7.08	1.60	6.40	0.67	2.68
	qawra_2	2	1.05	0.6	1.26	1.74	1.24	4.97	1.19	4.75	0.44	1.76
	qawra_3	2.3	1.5	1.1	3.80	1.88	2.74	10.95	2.62	10.47	0.68	2.72
P E M B R O K E	P1	2.55	1.2	0.6	1.84	2.24	2.18	8.72	2.02	8.09	0.65	2.60
	P10	2.55	1.5	0.35	1.34	2.08	1.07	4.26	1.02	4.08	0.75	3.00
	P16	2	1.3	0.4	1.04	1.80	0.90	3.60	0.86	3.44	0.56	2.26
	P2	2	1.5	0.65	1.95	2.20	2.28	9.11	2.11	8.45	0.80	3.18
	P3	2.85	2.7	0.8	6.16	2.19	2.78	11.11	2.58	10.31	1.43	5.70
	P4	2.5	1.8	0.7	3.15	2.08	2.20	8.79	2.04	8.15	0.90	3.60
	P5	2.8	1.5	0.7	2.94	2.08	2.20	8.79	2.04	8.15	0.75	3.00
	P6	2.4	2.1	0.7	3.53	2.08	2.20	8.79	2.04	8.15	1.05	4.21
	P7	2.55	1.4	0.5	1.79	2.08	1.52	6.09	1.46	5.82	0.70	2.80
	P9	2.55	1.5	0.6	2.30	2.08	1.83	7.31	1.75	6.99	0.75	3.00
Z	Z1	2.8	2.2	0.8	4.93	1.53	1.17	4.66	1.13	4.50	0.81	3.25

O N Q O R	Z10	4.1	2.2	0.7	6.31	1.74	1.47	5.86	1.39	5.54	0.92	3.69
	Z11	5.3	2.6	1.5	20.7	1.74	3.20	12.81	2.97	11.88	1.09	4.36
	Z12	2.3	1.2	0.7	1.93	1.49	0.97	3.86	0.90	3.59	0.43	1.72
	Z13	2.4	0.86	0.7	1.44	1.85	1.72	6.90	1.60	6.40	0.38	1.53
	Z14	5.1	1.55	1	7.91	1.78	2.25	8.99	2.08	8.34	0.66	2.66
	Z15	2.8	1.1	1	3.08	1.75	2.17	8.69	2.02	8.06	0.46	1.86
	Z2	2.7	1.8	0.5	2.43	1.70	0.97	3.88	0.94	3.75	0.74	2.95
	Z3	3.3	2.8	0.9	8.32	1.70	1.83	7.33	1.69	6.74	1.15	4.59
	Z4	4.35	3	0.7	9.14	1.74	1.51	6.03	1.39	5.54	1.26	5.03
	Z5	2.6	1.5	0.7	2.73	1.74	1.51	6.03	1.39	5.54	0.63	2.52
	Z6	8.5	4	1.2	40.8	1.74	2.46	9.84	2.38	9.50	1.68	6.71
	Z7	3.45	1.45	0.7	3.50	1.70	1.36	5.43	1.31	5.24	0.59	2.38
	Z8	3.3	2.2	0.7	5.08	1.88	1.76	7.04	1.67	6.66	1.00	4.00
	Z9	3.1	1.45	1	4.50	1.74	2.09	8.37	1.98	7.92	0.61	2.43

Concerning the pre-dislodgement setting of the boulders, a joint-bounded, submerged scenariois the most frequent, while for some blocks at Zonqor, Bugibba and Baharic-Caghaq, a subaerial joint bounded scenario is suggested.

Underwater surveying highlighted at Zonqor and Armier Bay a submerged scenario characterized by isolated boulders, both with fresh contours and coveredby algae and populated by marine organisms, niches and fresh detachment scarps. The sea bottom is similar to the subaerial geomorphological setting, being characterized by a gentle sloping platform, interrupted by small scarps which correspond to the bed planes.

The application of the hydrodynamic equations (Table 1) has highlighted that there are no correlation between density and volume values and the obtained results. As a consequence, the larger boulders do not necessarily require high waves to be detached from the cliff edge. Results from Nandasena et al. (2011) and Pignatelli et al. (2009) are very similar: the highest values are up to reach 14 and 13.35 m using Nandasena et al. (2011) and up to 12.8 and 12.7 m (Pignatelli et al. (2009), thus differing between them of less than 1 m. For all other values, the decrease of the storm wave height, decreases also the difference between the obtained results. Among the 77 selected boulders, the storm wave heights of 21 of them exceed 8 m. Conversely, the calculated tsunami wave heights are very low and range between 3.5 m (3.2 m for Pignatelli) and 0.55 m (0.51 m for Pignatelli). Engel and May (2012) equations provided very much lower values, suggesting storm wave heights ranging between 1 and 6 m. Most of storm wave heights are congruent with those measured on the Maltese Arcipelago (Malta Maritime Authority, 2003; Malta Environment and Planning Authority, 2007;

http://www.capemalta.net/maria/pages/waveforecast.html).During the stormiest months, the maximum wave values range between 5 and 5.5 m. However we can suppose that in correspondence to the coast, the run-up height can exceed 10 m, as testified by the cliff top storm deposits (CTSD) observed at significant elevations at Ahrax Point.

Biolchi et al. (2014) provided three Radiocarbon datings, performed on three marine organisms sampled from three boulders (AB5, C82 and Q2 of this study): 1083-1205 BP, 558-639 BP and post 1950 AD. These results suggested the possible occurrence of ancient extreme events, somehow correlated to historical tsunami events but also a very recent storm event.

Additional proof of recent extreme waves is provided by the tracks of freshly damaged karst surface, which were generated by rolling/saltation boulder transport, leading directly from the fresh scarp at the terrace edge to the boulder's current position.

While new radiocarbon dating are in progress, this preliminary study suggests the frequent occurrence of extreme storm waves on the island of Malta. This occurred especially along the north-eastern and eastern coasts, where the geomorphology of the coast, the sub-horizontal attitude of the strata and the low geomechanical properties of the rocks favoured the detachment of large boulders from the coast edge, both in submerged and subaerial conditions.

However, the possibility that also one or more tsunami events have affected these coasts is not excluded.

References

Alexander, D. (1988). A review of the physical geography of Malta and its significance for tectonic geomorphology,Quaternary Science Review, 7, 41-53.

Baldassini N., Mazzei R., Foresi L.M., Riforgiato F., and Salvatorini G. (2013). Calcareous plankton biochronostratigraphy of the Maltese Globigerina Limestone member, Acta Geol. Pol., 63(1), 105-135.

Biolchi, S., Furlani, S., Devoto, S., Gauci, R., Castaldini, D., and Soldati, M. (2014, in press). Geomorphological recognition, classification and spatial distribution of coastal landforms of Malta (Mediterranean Sea), Journal of Maps, DOI: 10.1080/17445647.2014.984001.

Dart, C.J., Bosence, D.W.J., and Mcclay, K.R. (1993).Stratigraphy and structure of the Maltese Graben system, Journal of the Geological Society, 150, 1153-1166.

Finetti, I.R. (1984). Geophysical study of the Sicily Channel Rift Zone, Bollettino di Geofisica Teorica ed Applicata, 26, 3-28.

Furlani, S., Biolchi, S., Devoto, S., Saliba, D., and Scicchitano, G. (2011).Large boulder along the NE Maltese coast: tsunami or storm wave deposits?, Jour. of Coast. Res., 61, pp. 470.

Galea, P.(2007). Seismic history of the Maltese Islands and considerations on seismic risk, Annals of Geophysics, 50 (6), 725-740.

Giannelli, L., and Salvatorini, G. (1972). I Foraminiferi planctonici dei sedimenti terziari dell'Arcipelago Maltese. Biostratigrafia del "Globigerina Limestone", I. Atti della Società Toscana di Scienze Naturali, Memorie Serie A, 79, 49-74.

Katz, O., Reches, Z., and Roegiers, J.C. (2000). Evaluation of mechanical rock properties using a Schmidt Hammer, Int. J. Rock Mech. Min., 37, 723-728.

Malta Environment and Planning Authority (2007). Detailed investigations and feasibility studies on land reclamation at two indicated search areas, Malta, Technical Report 1, volume 1.

Malta Maritime Authority (2003).Malta significant wave height study, Main Report.

Mottershead, D., Bray, M., Soar, P., and Farres, P.J.(2014). Extreme waves events in the central Mediterranean: Geomorphic evidence of tsunami on the Maltese Islands,Zeitschrift fur Geomorphologie, 58(3), 385-411.

Nandasena, N. A. K., Paris, R., and Tanaka, N.(2011). Reassessment of hydrodynamic equations: Minimum flow velocity to initiate boulder transport by high energy events (storms, tsunamis), Mar. Geol., 281, 70-84.

Pedley, H.M., House, M. R., and Waugh, B. (1976).The geology of Malta and Gozo, Proc. Geol. Ass., 87, 325-341.

Pignatelli, C., Sansò, P., and Mastronuzzi, G. (2009).Evaluation of tsunami flooding using geomorphologic evidence, Mar. Geol., 260, 6-18.

Reuther, C.D., andEisbacher, G.H. (1985).Pantelleria Rift crustal extension in a convergent intraplate setting. Int. J. Earth Sci., 74 (3), pp. 585-597.

THE BLIND FAULT MOSTAGANEM BOUKHEDIMI (PLATEAU OF MOSTAGANEM) NORTHWESTERN OF ALGERIA

Boukhedimi M Amine., Benhamouche, A., Machane, D.
National Centre of Applied Research in Earthquake Engineering CGS),), 01 Kaddour Rahim Street, BP 252 Hussein

On May 22, 2014 an earthquake of magnitude 5.2 ML (CRRAG) occurred at Bouguirat (Northwest Algeria) and its surroundings. This moderate seismic event was located in a region characterized by low seismic activity where few historical events have been observed.

This earthquake showed a maximum intensity of VIII on the MSK scale and caused serious damage located 2km south of the town of Bouguirat. In the epicentral region, 1 987 homes and eight public buildings were damaged in urban as well as 2,300 homes in rural areas. Several surface ruptures were observed in the field, all have been linked to shifts in gravity fields along slopes.

Table 1 : Hypocentral parameters of main shock

Ref.	Lat.	Long.	Z Km	Magnitude	Focal Mechanism
CGS (this study(BOUKHEDIMI2014))	35.772°N	0.309°E	4.00	-	
CSEM	35.730°N	0.170°E	10.00	Mw 4.8	-
USGS	35.785°N	0.241°E	10.00	Mw 4.8	-
GCMT	35.770°N	0.360°E	12.00	Mw 4.8	
GFZ	35.610°N	0.19°E	10.00	Mw 4.8	

The focal Mechanisms revealed by international institutions GFZ and ING immediately after the earthquake show solutions reverse fault trending NE-SW, which is consistent with the focal mechanisms of nearby earthquakes and the regional tectonic setting of African-Europe collision. The tectonic structure responsible of this earthquake would be a blind fault dipping SE associated with an anticline located 4km north-west of the city of Bouguirat. It would be a continuation of the faults that surround the chain of Dahra (chain of Algerian NW). Chain folds where the plateau of Mostaganem (including the folding of NW Bouguirat) can be considered as its western extremity
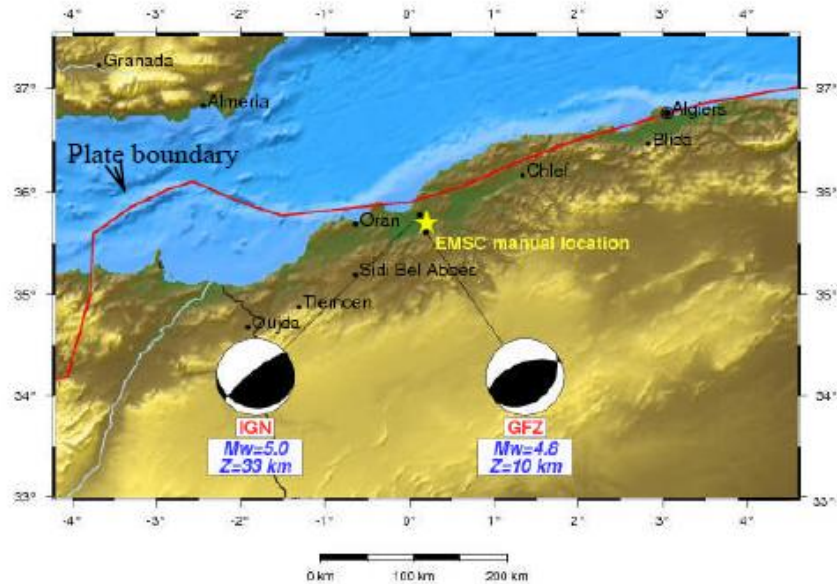
Fig 1: Focal mechanisms by IGN and GFZ institutions (EMSC manual location)
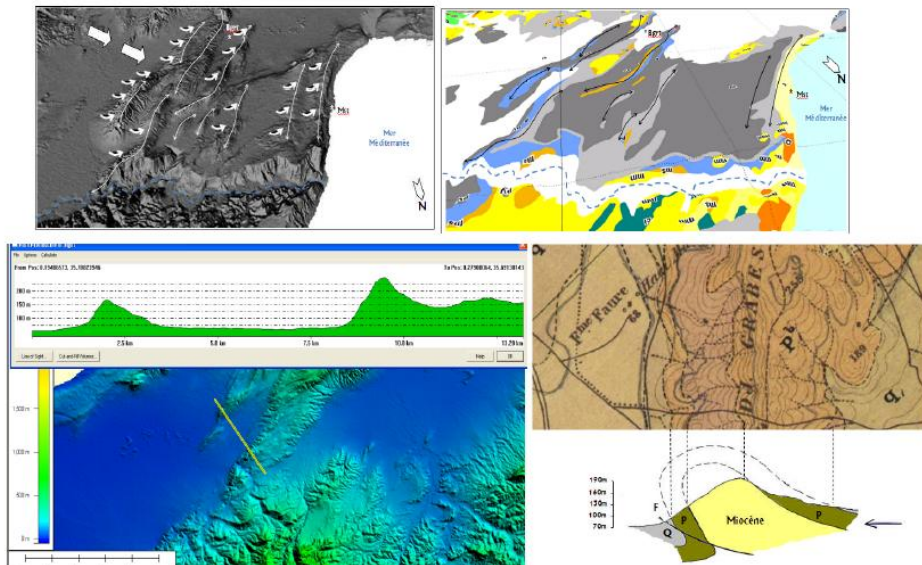
Fig. 2: Illustration of the originally structure of the earthquake (the blind fault) The straightened topography of folding and geological section indicates a blind fault dipping SE associated with an anticline.

92

References

Benouar, D., Aoudia, A., Maouche, S., and Meghraoui, M. (1994), The 18 August 1994 Mascara (Algeria)

earthquake – a quick-look report, Terra Nova, 6, 634-637.

Buforn, E., Bezzeghoud, M., Udias, A., and Pro, C. (2004), Seismic Sources on the Iberia-African Plate

Boundary and their Tectonic Implications, Pure appl. geophys., 161, doi 10.1007/s00024-003-2466-1.

Meghraoui, M. (1988), Géologie des zones sismiques du nord de l'Algérie: Paléosismologie, tectonique

active et synthèse sismotectonique, Thèse de doctorat, 356 pp., Université Paris XI.

Meghraoui, M., Morel, J.-L., Andrieux, J., and Dahmani, M. (1996), Tectonique plio-quaternaire de la

chaîne tello-rifaine et de la mer d'Alboran. Une zone complexe de convergence continent–continent, Bull.

Soc. Géol. Fr., 167(1), 141–157.

Yelles-Chaouche, A.K., Djellit, H., Beldjoudi, H., Bezzeghoud, M., and Buforn, E. (2004), The Ain

Temouchent (Algeria) Earthquake of December 22nd, 1999, Pure appl. geophys., 161, 607–621.

EVIDENCE OF EXTREME WAVE EVENTS FROM BOULDER DEPOSITS ON THE SOUTH-EAST COAST OF MALTA: STORM OR TSUNAMI?

Causon Deguara, J.[1], Gauci, R.[2]

[1]*Departmentof Geography University of Malta, joanna.causon-deguara.10@um.edu.mt*

[2]*Departmentof Geography University of Malta, ritienne.gauci@um.edu.mt*

Introduction

This study investigates the presence of a considerable quantity of boulders observed along a 3.5km stretch of coast situated between Xghajra and Zonqor on the SE coast of the Maltese Islands. The occurrence of such boulders has been associated with extreme wave events such as powerful storms or tsunamis. Studies on boulder deposits have been carried out on coasts that are exposed to varying wave and climatic regimes in different parts of the globe. Some of the studies carried out within the Mediterranean region include the coasts of France, Southern Italy, Greece, Egypt, Algeria and Malta. Conclusions from these studies vary with boulder movement being attributed to both storms and tsunamis. Distinguishing boulder deposits according to the type of extreme events debated and not always straightforward, especially on coasts with a history of tsunami occurrences. However, such studies shed light on the quality and magnitude of wave phenomena which impact on such coasts. The importance of understanding the magnitude and frequency of such phenomena lies in the potential risk that these may pose not just to coastal communities but also to local economies, considering the ever increasing coastal urbanisation and the use of coastal zone by various industries such as recreation, tourism, power generation, trade and port facilities.

Site Description and Methods

The study area is situated on a rocky coast where the lithology consists of a number of sedimentary limestone beds of variable thickness that exhibit a gentle dip towards the NE. These are dissected by discontinuities that run either in a perpendicular direction to the coast or subparallel to it. The point of contact between land and water at the shoreline varies from low ramps to shore platforms and low cliffs. The coastline is generally linear, trending NW-SE and facing the NE direction. The prevailing wave directions are primarily from the NW and E. The mean significant wave height is 1.22m over a 1 year period and 1.92m in winter. (Drago et al., 2013)

Storms in the region generally occur in the autumn and winter seasons. These are generated by the encounter of warm moist air of the Mediterranean with low pressure air systems moving from the Atlantic or the Eurasian and African land masses.

The central position of the Maltese Islands in the Mediterranean renders it exposed to the threats of potential tsunami waves generated by tectonic activity

from active seismic areas such as the Malta Escarpment, and the Calabrian and Hellenic Arcs. Such waves would propagate from a NE to E direction coinciding with the low lying and highly urbanized NE facing coast. At least two tsunamis are known to have reached the Maltese coastline, both following earthquakes, one in 1693 associated with the Malta Escarpment and the other in 1908 in Messina Straits (Camilleri 2005 and references therein).

Methods

Methods employed included field mapping of site characteristics (morphology, lithology and structure), the measurement of boulder dimensions, density and weight, distance from the shoreline, orientation, imbrication direction, general shape and position of boulders and possible type of movement. Numerical models were applied to estimate the wave height parameters needed to initiate boulder movement according to boulder position and type of movement. Results were then compared to local wave data to identify those boulders that require wave heights that exceed the regular storm wave height to initiate movement. Furthermore, a temporal analysis was carried out on some of these boulders by comparing aerial images.

Results

Observed boulders varied in size and lithology; their weight ranges from less than 1 tonne to more than 90 tonnes. They are located up to 83m from the shoreline and 12m above sea level. From the analysis of boulder shapes and geological structure, it may be deduced that the vast majority of the boulders originated from a joint bounded scenario. Numerical model results indicate that 16% of the boulders analysed could not have been dislodged by storm waves from such a joint bounded position, as wave height required to initiate movement exceeded the local registered maximum. However aerial imagery comparison also showed that some of these boulders had effectively changed position since 1967. Such movement could only have been carried out by storm waves, given that no tsunamigenic event is known to have occurred in recent times. Considering these observations and the distance from the shoreline at which they occurred, a storm wave origin may be considered as more plausible. However the possibility of tsunami impact such as the 1908 and 1693 events cannot be excluded.

The results indicate that boulder geomorphology research should not be based solely on numerical models but must also incorporate continuous in situ geomorphological observations to monitor active morphodynamic and geomorphic processes which may determine the rate of boulder movement prior to and following successive events. The mapping of boulder movement behaviour by storm waves demonstrated the site's exposure to such extreme storm waves and sheds light on the potential hazard they may represent on coastal land use.

Figure 1. Boulder clusters and boulder berm on a shore platform area at Xghajra, Malta.

Figure 2. Large boulder moved by storm waves at Zonqor.

Acknowledgements

References

Barbano, M.S. Gerardi, F. & Pirrotta C., 2011. Differentiation between boulders deposited by tsunamis and storm waves along the south-eastern Ionian coast of Sicily (Italy). Bollettino di Geofisica Teorica ed Applicata Vol.52, n.4, pp.707-728; December 2011 DOI 10.4430/bgta0022

Biolchi, S. et al., (2013). Large boulders accumulation along the NE Maltese coast: stormwaves or tsunami event? In: 8th International Conference (IAG) on Geomorphology, Geomorphology and Sustainability.Paris, France 27-31 August, 2013. p.259. Abstract only.

Camilleri, D.H., (2006). Tsunami construction risks in the Mediterranean – outlining Malta's scenario. Disaster Prevention and Management Vol. 15 No. 1, pp. 146-162. Emerald Group Publishing Limited

Drago, A. et al., (2013), Assessing the Offshore Wave Energy Potential for the Maltese Islands. In: Institute of Sustainable Energy, Sustainable Energy 2013: The ISE Annual Conference. Qawra, Malta 21March 2013. University of Malta.

Maouche, S. Morhange, C. & Meghraoui, M., (2009). Large boulder accumulation on the Algerian coast evidence tsunami events in the western Mediterranean. Marine Geology, 262(1–4), pp. 96-104.

Mastronuzzi, G. & Pignatelli, C., (2012). The boulder berm of Punta Saguerra (Taranto, Italy): a morphological imprint of the Rossano Calabro tsunami of April 24, 1836? Earth Planets Space, 64, pp 829–842.

Mottershead, D. Bray, M. Soar P. & Farres P.J., (2014). Extreme wave events in the central Mediterranean: Geomorphic evidence of tsunami on the Maltese Islands. Zeitschrift für Geomorphologie published online January 2014

Nandasena, N.A.K. Paris, R. & Tanaka, N., (2011). Reassessment of hydrodynamic equations: Minimum flow velocity to initiate boulder transport by high energy events (storms, tsunamis). Marine Geology, 281(1–4), pp. 70-84.

Scicchitano, G. Monaco, C. & Tortorici, L., 2007. Large boulder deposits by tsunami waves along the Ionian coast of south-eastern Sicily (Italy). Marine Geology, 238(1–4), pp. 75-91.

Shah-Hosseini, M. et al., 2013. Coastal boulders in Martigues, French Mediterranean: evidence for extreme storm waves during the Little Ice Age. Zeitschrift für Geomorphologie Supplementary Issues 01/2013; DOI:http://dx.doi.org/10.1127/0372-8854/2013/00132

FORECASTING MODERATE EARTHQUAKES A STEP TOWARDS SEISMIC RISK REDUCTION IN NORTHERN ALGERIA AND MOROCCO

M. Hamdache[1] and J.A. Peláez[2]

[1] *Departement Études et Surveillance Sismique, CRAAG, Algiers, Algeria.*
m_hamdache@hotmail.com
[2] *Department of Physics, University of Jaén, Jaén, Spain. japelaez@ujaen.es*

We study the correlation between locations of $MW \geq 5.0$ earthquakes and locations of $5.0 > MW \geq 4.0$ events for Northern Algeria and Morocco. To do it, a new an updated catalog including main events in the region has been used, considering earthquakes until June 2011. A preliminary study shows that it can be observed a relatively good agreement between locations for these two data sets, that is, minor to light earthquake locations could be used to forecast future places where will happen moderate to strong earthquakes. This is the basis of the so called cellular seismology, a method that assumes that seismicity delineates regions where future large earthquake will occur.

Then, we propose a time-independent forecasting model based on the spatially smoothed seismicity rate of $MW \geq 4.0$ earthquakes in this region from both historical and instrumental data. Neither geological nor tectonic data are included in the model. Initially, the area under study was divided into square cells (10 km x 10 km). The number of earthquakes with magnitude in the range MW 4.0-5.0 that have taken place at a given cell is counted and smoothed using a two-dimensional Gaussian filter. The used catalog is a declustered catalog for magnitudes above MW 4.0 compiled specifically for this work. Its completeness is a crucial factor in the suitability, reliability and credibility of the forecast.

The time-independent forecasting model is proposed from the computation of $MW \geq 5.0$ earthquake probabilities for each considered cell for different exposure times. Probabilities are computed considering that seismicity follows a Poisson process and the Gutenberg-Richter magnitude-frequency relationship. Thereby, forecasting earthquakes studies, like presented in this work, are key studies in order to delineate the areas in which it is more valuable to provide a certain level of protection for buildings and other facilities. This and other previous studies on seismic hazard carried out in this region, demonstrate the need for to make some changes in order to improve the seismic input in current Moroccan and Algerian building codes. Conducted studies on earthquake engineering research, reported in the scientific literature and defended in international meeting, must be serious reasons to update seismic provisions.

SEISMIC HAZARD PARAMETERS OF MAIN SEISMOGENIC SOURCE ZONE MODEL IN THE ALGERIA-MOROCCO REGION

Hamdache ,M[1], J. A. Pelaez[2]., A. Kijko[3], A.Smit[3]and R. Sawires[2]

[1]*Departement Études et Surveillance Sismique, CRAAG, Algiers, Algeria.*
m_hamdache@hotmail.com
[2]*Department of Physics, University of Jaén, Jaén, Spain. japelaez@ujaen.es*
[3]*University of Pretoria, Natural Hazard Centre, Africa, Pretoria, South Africa*

In this study, a seismogenic source zone model for the Algeria-Morocco region is proposed for seismic forecasting and seismic hazard studies. The delineation includes five zones based on available seismic and geological data. The zone model shown in figure 1, includes the Moroccan Meseta, the Rif, the Tell zone, the High Plateaux and the Atlas zone.
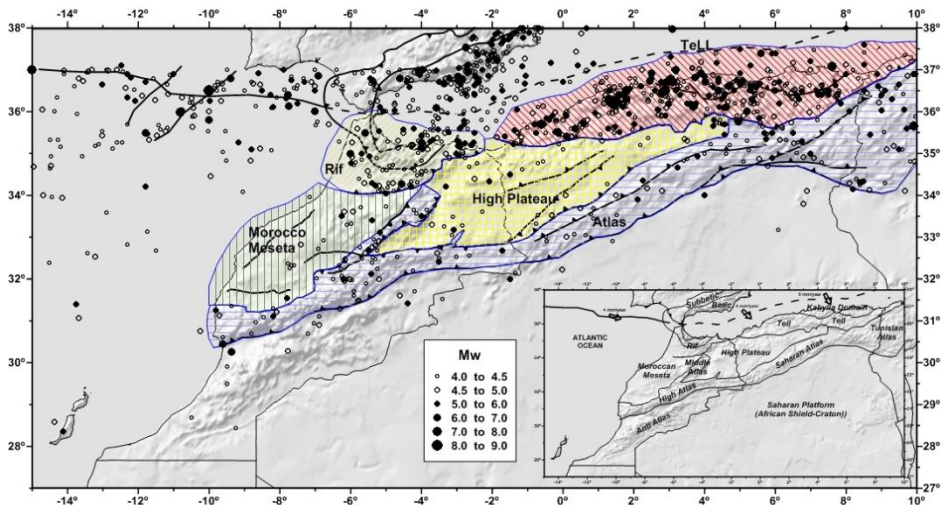
Figure 1. Map showing the five seismogenic zones included in the proposed model

Earthquake occurrence process in this region is modeled and analyzed using recent earthquake catalogs for northern Morocco and northern Algeria compiled in former studies (Peláez et al., 2007; Hamdache et al., 2010). For these catalogs, dependent events were identified and removed by adapting Gardner and Knopoff declustering procedure to the study region. Magnitudes of completeness were estimated using different methods, then the Poissonian character of the obtained sub-catalogs was analyzed.

The b-value of the Gutenberg-Richter recurrence relationship, considered as an area-specific seismic hazard parameter, was initially computed using the Weichert (1980) approach.

In order to characterize each seismogenic zone we have introduced a new parameter named seismic activity, defined as the number of earthquakes with magnitude above MW 4.0 in each seismogenic zone since 1925 by each 10 years and 10000 km2. It can be derived that in the Tell seismogenic zone happens of the order of 2.6 events with magnitude above MW 4.0 from 1925, by each decade and by each square cell of 100 km side.

The b-value estimation has been improved by using an extension of the Aki-Utsu b-value estimator for incomplete earthquake catalogs (Kijko and Smit, 2012). Taking into account that the maximum possible magnitude is an important parameter required by earthquake engineering community, disaster management agencies and insurance industry, a detailed analysis has been performed using different statistical methods related to the quality of the earthquake data file. As introduced by Kijko (2004) and Kijko and Singh (2011), these procedures are free from subjective assumptions and only depend on seismic data. From a statistical point of view, the estimation methods are divided into three classes: a) parametric procedures, b) non-parametric procedures, and c) based on the fit of the cumulative distribution function of earthquake magnitudes. Thus, the maximum possible magnitude is analyzed at each seismogenic zone and its probability distribution function is derived. In figure 2, some results are presented.
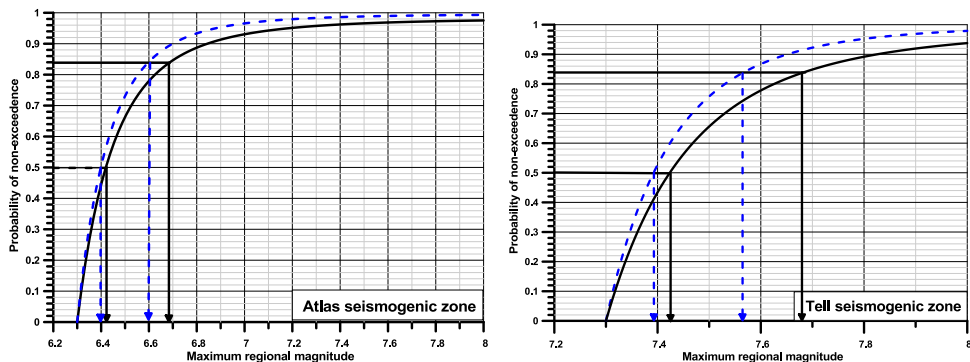
Figure 2: Estimation of the maximum regional magnitude using the Kijko-Sellevol estimator (K-S) and its probability distribution. The dashed line shows the Bayesian version of the K-S estimator. The plot shows the 84% and 50% confidence limits

Then, we derive the activity rate λ(m) for events above the magnitude m, and the return period for different magnitudes. The analysis has been performed at each seismogenic zone of the proposed model.

References

Gardner JK and Knopoff L (1974).Is the sequence of earthquakes in Southern California, with aftershocks removed, Poissonian?, Bulletin of the Seismological Society of America, 64: 1363-1367.

Hamdache M, Peláez JA, Talbi A and López Casado C (2010).A unified catalog of main earthquakes for northern Algeria from A.D 856 to 2008, Seismological Research Letters, 81: 732-739.

Kijko A (2004).Estimation of the maximum earthquake magnitude, mmax, Pure and Applied Geophysics, 161: 1-27.

Kijko A and Smit A (2012).Extension of the Aki-Utsu b-value estimator for incomplete catalogs, Bulletin of the Seismological Society of America, 102: 1283-1287.

Kijko A and Singh M (2011). Statistical tools for maximum possible earthquake magnitude estimation, Acta Geophysica, 59: 674-700.

Peláez JA, Chourak M, Tadili BA, Aït Brahim L, Hamdache M, López Casado C and Martínez Solares JM (2007). A catalog of main Moroccan earthquakes from 1045 to 2005, Seismological Research Letters, 78: 614-621.

Weichert DH (1980).Estimation of the earthquake recurrence parameters for unequal observation periods for dhoma, 15-66.

FAULT RUPTURE HAZARD ALONG A SECTOR WITH ASEISMIC CREEP IN URBAN AREA (EASTERN SICILY)

Imposa, S., De Guidi, G.,Scudero, S., Grassi, S.

University of Catania, Department of Biological, Geological and Environmental Sciences, Earth Science Section, Corso Italia 57, 95129, Catania, Italy

Introduction

The hazard connected with the surface propagation of a fault rupture during a seismic event is a widely discussed topic in the literature and its importance in Italy has emerged particularly after the 2009 L'Aquila (Italy) earthquake (Boncio et al., 2010; EMERGEO Working Group, 2010). The area of Mt. Etna volcano is considered as the most critical in Italy because of the high geological predisposition to surface faulting in relation to the high urbanization (Guerrieri et al., 2009).

An active fault whose coseismic displacement can intercept the ground surface is defined as capable (Machette, 2000; Galadini et al., 2012). The faults characterized by aseismic slip (creep), either episodic or constant over time, should be considered similar to the capable faults. In a largely urbanized area like the lower eastern slope of Mt. Etna also affected by high level of seismic strain release, the risk related to surface faulting (coseismic and aseismic) is very high (Blumetti et al., 2007; Guerrieri et al., 2009). The displacement between the two fault blocks can dislocate, rotate or cause structural damage to buildings and infrastructure and lifelines located along or in proximity of the fault line.

In this study we precisely map the segments associated with an active fault system in the lower eastern slopes of Etna, we characterize the damaged zone by means of several geophysical surveys (environmental noise, GPR, seismic tomography, ReMi) and, finally we try to assess the criteria for a rupture surface faulting hazard zonation, essential for any land use planning and management.

Geological and tectonic setting

A system of active normal faults with main directions trending NNW and NNE, affects the eastern slope of the volcano (Fig. 1) (Monaco et al., 1995; Bousquet and Lanzafame, 2004); these segment originated, both in recent and historical times, earthquakes with magnitude up to 4.5. Because of shallow foci depth (<2-3 km) earthquakes have often caused harsh, even though localized, damages (Azzaro, 1999). The Late Pleistocene strain rates derived from geological markers, range from 1-2 mm/a (Monaco et al., 1997).

Recent GPS and interferometric data show that the eastern flank of the volcano is rapidly moving eastwards with velocity up to several cm/a (Solaro 2010; Bonforte et al., 2011; Guglielmino et al., 2011). This extension process, accompanied by subsidence in some coastal areas (Branca et al., 2014), has been

interpreted as a sliding of the whole eastern flank (see Azzaro et al., 2013 for a complete review) driven by gravity, load of magmatic intrusions or various fluids, tectonic forcing, or a combination of these (Azzaro et al., 2013; Mattia et al., 2015; Scudero et al., under review).

Flank sliding would be confined to the north by the movement of the left-lateral Pernicana fault, while to the south it would be partially accommodated by the Trecastagni - Tremestieri – San Gregorio fault system with prevailing right-lateral kinematics (Lo Giudice and Rasà, 1992; Solaro et al., 2010; Bonforte et al., 2010; Chiocci et al., 2011); finally the differential deformation within the eastern flank is accommodated through the movements of rigid blocks outlined by the pre-existing faults. Flank sliding is thought to be a recent (last 60 years) and shallow process (Branca et al., 2014; Mattia et al., 2015).
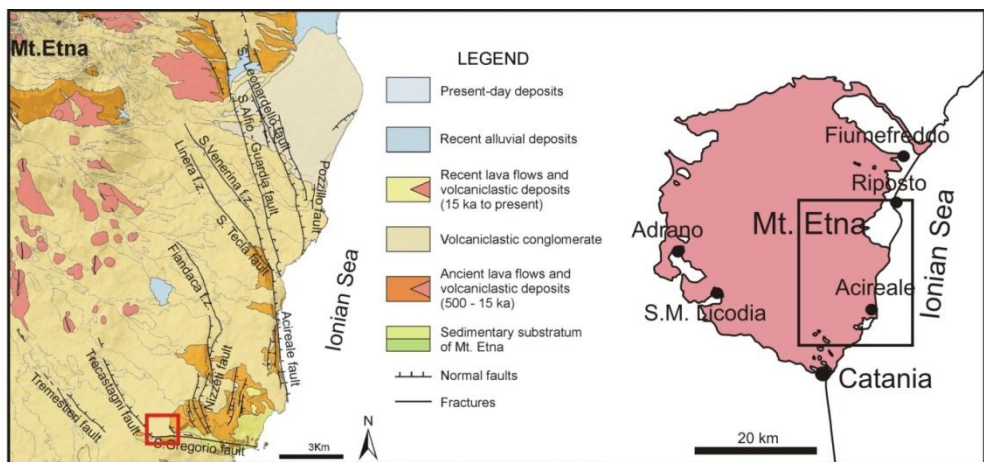
Figure 1.Geological and tectonic map of the eastern flank of Mt. Etna (modified after Monaco et al., 2010); the red box indicates the studied areas.

Ground ruptures

The San Gregorio fault extends roughly E-W for about 5 km inland (Monaco et al.2010) and continues also in the Ionian offshore (Chiocci et al., 2011). The structure is divided into three main segments with prevailing right lateral kinematics, and many other secondary segments. The absence of a sharp and defined morphology suggests that the lineament activated in more recent time with respect to the other faults, probably in response to the sliding process (Mattia et al., 2015). The fault is entirely lacking in instrumental seismicity, displacement occurs exclusively through creep episodes (Monaco et al., 2010). This study examines in detail the western segment, since it affects a large urbanized area.

Unlike other faults of Mt. Etna, whose long-term activity has produced cumulative scarps reaching tens to hundred meters, the morphological evidence of the San Gregorio fault is poor because to the lateral kinematics. The traces of the fault (or damage) zones have been mapped with precision within the urban areas

after an accurate and detailed survey of damages to artefacts and infrastructures caused by the fault displacement. The damages mainly consists of shallow to deep cracks affecting the walls of buildings (both infilling and bearing walls), fractures and rotations of retaining walls, sidewalks, curbs and paving. Fractures and cracks are usually aligned along bands with variable width ranging from 2 to more than 40 m. The maximum offset observed is ~30 cm and is probably the result of several creep episodes.

In addition to the damaged zones located along the fault trace we detected secondary damaged zones. Because of their arrangement with respect to the main fault, some of them are interpretable as Riedel's R or T type fractures in a right lateral shear zone; others are probably part of the NNW to NNE system. We mapped ground ruptures for a total length of about 3.8 km within the urban area of San Gregorio di Catania. Table 1 summarizes the geometric and kinematic characteristics of each damaged zone.

Geophysical surveys

The physical and mechanical properties of the hosting rocks are influenced by the presence of faults. To reconstruct the 3D geological structure of the fracture zones we applied different geophysical techniques: ground penetrating radar (GPR), seismic tomography, refraction microtremor (ReMi) survey and ambient noise recordings. All those methods are widely used in the investigation of active faults because they allow modelling the buried geological structure in terms of thickness of strata, geometry of discontinuities and seismic waves velocity propagation. In addition their integration allows the best possible resolution and a comprehensive interpretation (Imposa et al., under review). We performed 8 GPR sections, 1 tomographic survey, 1 ReMi section, and 533 ambient noise recordings arranged to form 26 sections. The results show features related to the occurrence of a fault: low velocity zones highly fractured areas, dislocated markers. Geophysical data always agree with field observation: damaged zone at depth is never larger than detected on the ground.

Table 1.Geometric and kinematic parameters of the mapped damaged zones.

Name	L (m)	D max (m)	Main kinematics	Behaviour	Long term slip rate (mm/a)	Short-term slip rate (mm/a)	Ref.
Catira - Cantarella	1600	5(v)	oblique dextral	creeping	0.3 (v; 15 ka)	5 – 7.5 (l)	Azzaro et al., 2012; this work
Salesiani	390	-	right lateral	creeping	-	-	this work
Macello	1080	3	normal	creeping	0.2 - 0.75 (15 – 4 ka)	0.4 – 0.7	this work
Morgioni	730	-	extensional (?)	creeping	-	1 - 3	this work

Surface Fault Rupture Hazard zoning

The presence of capable faults concerns two distinct topics: i) the potential interaction of the dislocation with artifacts, particularly their foundations; ii) the assessment and the zonation of the Surface Fault Rupture Hazard (SFRH; Boncio et al., 2012) and the definition of belts encompassing the potential occurrence of a ground rupture (setback). In this study we will discuss the latter issue.

Setbacks are the areas where the existing artifacts are susceptible to damage following a surface propagation of the rupture and they also define the minimum distance from the fault to build new critical infrastructures or any artefact that could suffer the rupture (Bryant and Hart, 2007). Many variables play a role in the assessment of setbacks and it is difficult to define general criteria. For a single fault system the following should be considered: fault geometry (lateral extension, dip angle, associated segments, tip or overlay zones), fault kinematics (dip, lateral or oblique slip), and the topography (Mc Calpin, 1987).

As general rule, a new rupture will tend to mark exclusively pre-existing ruptures where the greatest part of the slip is accommodated (Borchardt, 2010) and the width of the damaged zone is not strictly proportional to earthquake magnitude (or to maximum displacement) (Batatian, 2002; Boncio et al., 2012). Ground rupture could also occur at larger distances, but in any case on secondary structures that can be mapped if the scale is sufficiently detailed, so that they can be considered as independent fault in turn. (Boncio et al., 2012). It is essential to assess the scale of approach for SFRH zoning. The more detailed the scale and the fault zone is, the less are the uncertainties and the narrower could be the setback.
It is also essential to define a temporal scale for the process (Galadini et al., 2012).

The probability of a rupture on an undisturbed soil is low for rock older than the activation of the fault even for very active ones; conversely the probability of a new fracture is relatively high for young soils adjacent to moderately active faults (Borchardt, 2010). Setback should therefore follow a concept of "maturity" of the fault; Borchardt (2010) defines a statistically fault "mature" when it cumulates 30 or more slip events. In a mature fault the displacement will be always accommodated along the main rupture and the damaged zone will stop widening (Borchardt, 2010; Petersen et al., 2011); in this case, theoretically, it is not necessary to define a setback. In this study we decided to distinctly examine and characterize the detected fracture zones in order to better define the SFRH and the setbacks. We are aware that it is counterproductive to define setback unnecessarily wide, when it might be more effective to plan structural mitigation of the infrastructure where limited effects are expected (Borchardt, 2010).

In the last few years in Italy the discussion on the SRH zoningis rising (Boncio et al., 2012; Peronace et al., 2013) because of the lack of enough detailed regulation (GdL, M. S, 2008). In the literature the setback for normal faults are asymmetric based on the evidence that in normal faults the associated fracture density is wider in the hangingwall rather than the footwall. The ratio between setbacks in the two blocks varies from 1:3 to 1:5 (Boncio et al., 2012; Peronace at al., 2013; Guerrieri et al., 2014). In strike slip faulting the probability of rupture is

considered equal in the two fault block (Petersen et al., 2011), therefore setbacks are symmetric (Peronace et al., 2013; Guerrieri et al., 2014). Those authors propose setbacks depending on the level of understanding of the fault but that are never narrower than 30m even for the well assessed fault zones.
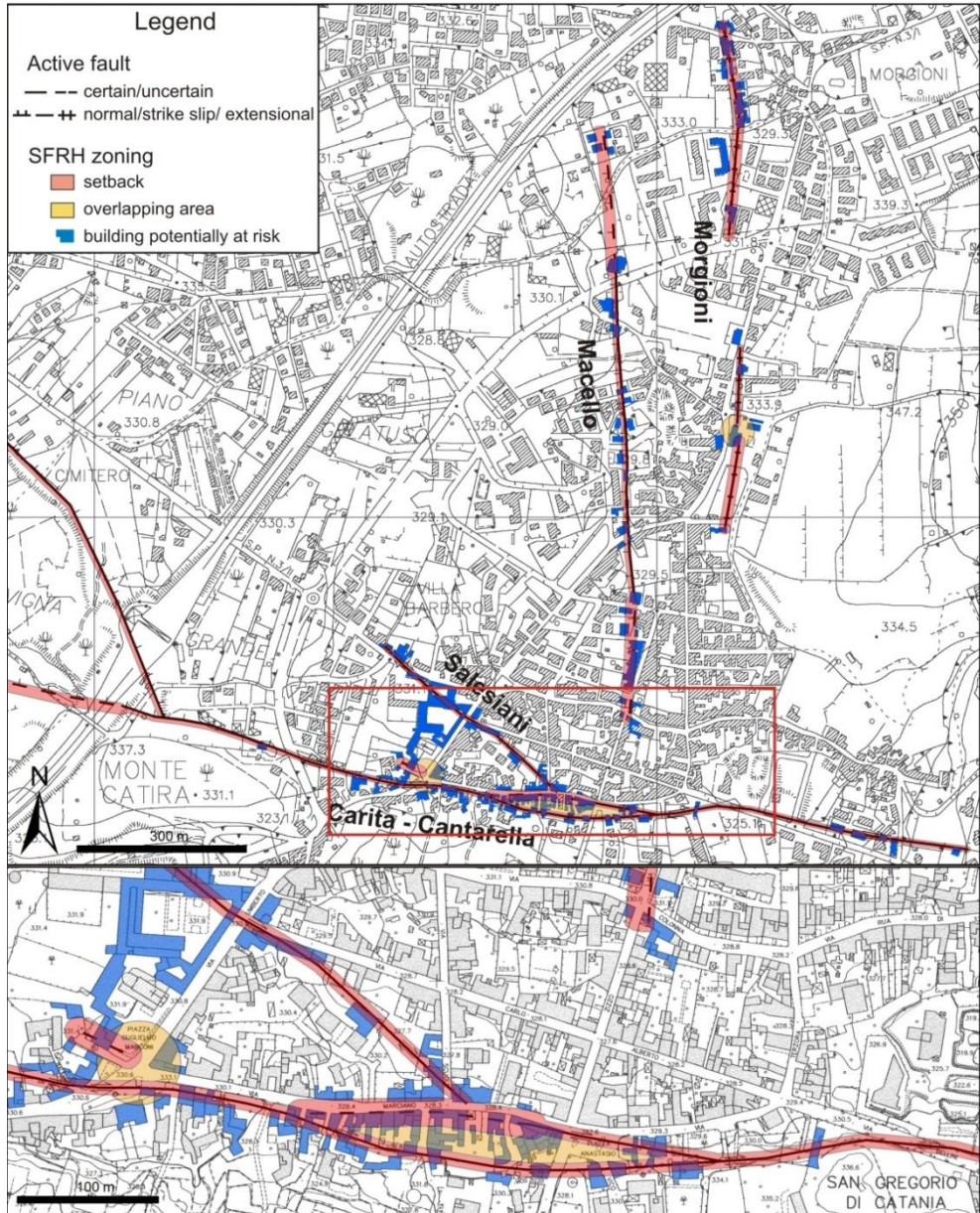
Figure 2.Example of SFRH in San Gregorio area: general view and detail.

The amount of detailed information collected on the fault makes the assessment of some general criteria for the SFRH zoning possible. We have been able to map also minor cracks or fractures associated to the main fault zone and we can consider negligible any mapping error that would be considered defining setback width. We can clearly consider the fault zone in San Gregorio area as mature because they mark pre-existing structures showing long-term activity, conversely in the Acitrezza area the fault system cannot be considered mature. For mature fault zone we propose setback of 10 m both for normal and strike slip fault extending 5m aside from the limit of the fault zones for strike slip ruptures. The same setback extends 2m in the footwall and 8 m in the hangingwall in normal fault zone, where uncertain faults were reported (dashed lines), setbacks were doubled. In the overlapping areas we propose a susceptibility zone 30 m wide.

Conclusive remarks

The multidisciplinary approach combining and integrating the classic surface survey with different geophysical methods has enabled obtaining a very accurate model of the geological structure especially in the first 15 m in depth. Therefore, we could define setbacks for the investigated fault zones. In San Gregorio area 174 buildingsintersect the setbacks and then are potentially involved in ruptures (Fig. 2). Ruptures associated with documented creep events are identified and reported. However, we cannot exclude definitively that future displacement could occur outside the assessed setback (Bryant and Hart, 2007). Ground ruptures associated to secondary effects (differential compaction, landslides, etc.) are not included in our analysis. Other potentially active faults could exist somewhere else in the mapped area and further investigations are recommended before planning any critical infrastructure.

Acknowledgements

References

Azzaro, R. (1999). Earthquake surface faulting at Mount Etna volcano (Sicily) and implications for active tectonics.J. Geodyn. 28(2), 193-213.

Azzaro, R., Bonforte, A., Branca, S., and F. Guglielmino (2013). Geometry and kinematics of the fault systems controlling the unstable flank of Etna volcano (Sicily). J. Volcanol. Geotherm. Res. 251, 5-15.

Azzaro, R., Branca, S., Gwinner, K., and M. Coltelli (2012). The volcano-tectonic map of Etna volcano, 1: 100.000 scale: an integrated approach based on a morphotectonic analysis from high-resolution DEM constrained by geologic, active faulting and seismotectonic data. Ital. J. Geosci. 131(1), 153-170.

Batatian, D. (2002). Minimum standards for surface fault rupture hazard studies. Salt Lake County Geologic Hazards Ordinance.

Boncio, P., Galli, P., Naso, G., and A. Pizzi (2012). Zoning surface rupture hazard along normal faults: insight from the 2009 Mw 6.3 L'Aquila, Central Italy, earthquake and other global earthquakes. Bull. Seism. Soc. Am. 102(3), 918-935.

Bonforte, A., Guglielmino, F., Coltelli, M., Ferretti, A., and G. Puglisi (2011). Structural assessment of Mount Etna volcano from Permanent Scatterers analysis.Geochem.Geophys.Geosyst.12(2).

Borchardt, G. (2010). Establishing appropriate setback widths for active faults.Env.Eng. Geosci. 16(1), 47-53.

Bousquet, J. C., and G. Lanzafame (2004). The tectonics and geodynamics of Mt. Etna: synthesis and interpretation of geological and geophysical data. Mt. Etna: volcano laboratory, 29-47.

Branca, S., De Guidi, G., Lanzafame, G., and C. Monaco (2014). Holocene vertical deformation along the coastal sector of Mt. Etna volcano (eastern Sicily, Italy): Implications on the time–space constrains of the volcano lateral sliding. J. Geodyn. 82, 194-203.

Bryant, W. A., and E. W. Hart (2007).Fault-rupture hazard zones in California.Special Publication, 42, 7-2.

Chiocci, F. L., Coltelli, M., Bosman, A., and D. Cavallaro (2011). Continental margin large-scale instability controlling the flank sliding of Etna volcano.Earth Planet. Sci. Lett. 305(1), 57-64.

EMERGEO Working Group. (2009). Evidence for surface rupture associated with the Mw 6.3 L'Aquila earthquake sequence of April 2009 (central Italy). Terra Nova.

Galadini, F., Falcucci, E., Galli, P., Giaccio, B., Gori, S., Messina, P., Moro, M.,Saroli, M., Scardia, G., and A. Sposato (2012). Time intervals to assess active and capable faults for engineering practices in Italy.Eng. Geol. 139, 50-65.

GdL, M. S. (2008). Indirizzi e criteri per la microzonazione sismica. In Conferenza delle Regioni e delle Province autonome–Dipartimento della Protezione Civile, Roma.

Guerrieri, L., Blumetti, A. M., Di Manna, P., Serva, L., and E. Vittori (2009). The exposure of urban areas to surface faulting hazard in Italy: a quantitative analysis. Boll. Soc. Geol. It. 128(1), 179-189.

Guerrieri, L., Blumetti, A. M., Comerci, V., Franz, L., Michetti, A.M., Eutizio, V., and S. Leonello (2014). Fault Displacement Hazard in urban areas in Italy: a first assessment. 5th INQUA Meeting on Paleoseismology, Active Tectonics and Archeoseismology (PATA), 21-27 September 2014, Busan, Korea.

Guglielmino, F., Nunnari, G., Puglisi, G., and A. Spata (2011). Simultaneous and integrated strain tensor estimation from geodetic and satellite deformation measurements to obtain three-dimensional displacement maps.Geoscience and Remote Sensing, IEEE Transactions on, 49(6), 1815-1826.

Imposa, S., De Guidi, G., Grassi, S., Scudero, S., Barreca, G., Patti, G., and D. Boso.Applying geophysical techniques to investigate a segment of a creeping fault in the urban area of San Gregorio di Catania, southern flank of Mt. Etna (Sicily, Italy).Under review on J. Appl. Geophys.

Lo Giudice, E., and R. Rasà (1992). Very shallow earthquakes and brittle deformation in active volcanic areas: The Eatnean region as an example. Tectonophys. 202(2), 257-268.

Machette, M. N. (2000). Active, capable, and potentially active faults—a paleoseismic perspective.J. Geodyn. 29(3), 387-392.

Mattia, M., Bruno, V., Caltabiano, T., Cannata, A., Cannavò, F., D'Alessandro, W., Di Grazia, G., Federico, C., Giammanco, S., La Spina, A., Liuzzo, M., Longo, M., Monaco, C., Patanè, D., and G. Salerno (2015). A comprehensive interpretative model of slow slip events on Mt. Etna's eastern flank.Geochem.Geophys.Geosyst. 16(3), 635-658.

McCalpin, J. P. (1987). Recommended setback distances from active normal faults. In Proceedings of the Symposium on Engineering Geology and Soils Engineering (Vol. 23, pp. 35-56).

Monaco, C., De Guidi, G., and C. Ferlito (2010). The morphotectonic map of Mt. Etna.Ital. J. Geosci. 129(3), 408-428.

Monaco, C., Petronio, L., and M. Romanelli (1995). Tettonica estensionale nel settore orientale del Monte Etna (Sicilia): dati morfotettonici e sismici. Studi Geol. Camerti, 2, 363-374.

Monaco, C., Tapponnier, P., Tortorici, L., and P. Y. Gillot (1997). Late Quaternary slip rates on the Acireale-Piedimonte normal faults and tectonic origin of Mt. Etna (Sicily). Earth Planet. Sci. Lett. 147(1), 125-139.

Peronace, E., and Boncio, P., Galli, P., and G. Naso (2013).Faglie attive e capaci negli studi di microzonazione sismica: definizioni e procedure di zonazione. In 32° ConvegnoNazionale GNGTS (Vol. 2, pp. 293-299).

Petersen, M. D., Dawson, T. E., Chen, R., Cao, T., Wills, C. J., Schwartz, D. P., and A. D. Frankel (2011). Fault displacement hazard for strike-slip faults. BulL. Seism. Soc. Am. 101(2), 805-825.

Solaro, G., Acocella, V., Pepe, S., Ruch, J., Neri, M., and E. Sansosti (2010). Anatomy of an unstable volcano from InSAR: Multiple processes affecting flank instability at Mt. Etna, 1994–2008. J. Geophys. Res.: Solid Earth (1978–2012), 115(B10).

Scudero, S., De Guidi, G., Imposa, S. and G. Currenti. Modelling the long-term deformation of the sedimentary substrate of Mt. Etna volcano (Italy).Under final review on Terra Nova.

SEISMIC AND TSUNAMI HAZARD ASSESSMENT OF A COASTAL ACTIVE FAULT CONSTRAINED WITH THE HISTORICAL CALABRIA 1905 EARTHQUAKE (SE TYRRHENIAN SEA)

Loreto, M.F.[1], Brutto F.[2], Muto F.[3], Armigliato A.[4], Pagnoni G.[5], Sandron D.[6], Tiberi L.[7], Tinti S.[8], Zgur F.[9]

[1] *Institute of Marine Sciences – CNR, Via. P. Gobetti 101 – Bologna- Italy, filomena.loreto@bo.ismar.cnr.it*

[2] *Dipartimento di Biologia, Ecologia e Scienze della Terra (DiBEST)- University of Calabria, Arcavacata di Rende (CS) - Italy, fabrizio.brutto@gmail.com*

[3] *Dipartimento di Biologia, Ecologia e Scienze della Terra (DiBEST)- University of Calabria, Arcavacata di Rende (CS) - Italy, francesco.muto@unical.it*

[4] *Dipartimento di Fisica e Astronomia (DIFA) – University of Bologna, Viale Carlo Berti Pichat, 8*
40127 Bologna – Italy, alberto.armigliato@unibo.it

[5] *Dipartimento di Fisica e Astronomia (DIFA) – University of Bologna, Viale Carlo Berti Pichat, 8*
40127 Bologna – Italy, gianluca.pagnoni3@unibo.it

[6] *Istituto Nazionale di Oceanografia e di Geofisica Sperimentale (OGS), Borgo Grotta Gigante, 42C - 34010 - Sgonico (TS) – Italy, dsandron@inogs.it*

[7] *Department of Mathematics and Geosciences (DMG) - University of Trieste, Via Weiss 4, 34127 - Trieste Italy, lara.tiberi@gmail.com*

[8] *Dipartimento di Fisica e Astronomia (DIFA) – University of Bologna, Viale Carlo Berti Pichat, 8*
40127 Bologna – Italy, stefano.tinti@unibo.it

[9] *Istituto Nazionale di Oceanografia e di Geofisica Sperimentale (OGS), Borgo Grotta Gigante, 42C - 34010 - Sgonico (TS) – Italy, fzgur@ogs.trieste.it*

Summary

Italy is one of the most seismically active regions in Mediterranean and one of the countries with the longest record of historical earthquakes in the world. Over the last decades the scientific community invested great energy and resources for seismic and tsunami hazard assessment, that can actually improve with knowledge of those active structures capable of generating destructive earthquakes and, if located offshore, also tsunamis. A more reliable hazard assessment of the exposed regions can be done if forecasting models can be constrained with instrumental or historical data. This is the case of the 1905 Calabria earthquake, which was destructive and was followed by tsunami waves. A recent geophysical survey allowed to identify an active structure, named Sant'Eufemia Fault, located offshore within the Sant'Eufemia Gulf (SE Tyrrhenian Sea) and facing the western Calabria. Numerous observations and models support the hypothesis that this

structure could be the seismogenic source of the 1905 earthquake and, being active, capable to trigger a new event.

Analyzing all available geophysical data, we defined the most credible geometry of the Sant'Eufemia fault: 40 km length and 2.3m of slip rate. Using empirical relationships available in the literature, we assigned to this fault a width equal to 17km and the potential for an Mw 7 earthquake. Using these parameters we performed shacking scenarios imaging a fault plane with a single centered asperity and uniform Seismic Moment (M_0) distribution. We produced both the Peak Ground Acceleration (PGA) and the Peak Ground Velocity (PGV) maps, that can be compared with intensities distribution of the 1905 Calabria earthquake. Seismic hazard assessment is also analyzed taking into account soils type distribution interacting with shaking. This fault is also used to perform tsunami modelling and to compare the numerical results with the historical data available on run-up and inundation. Main results:the Sant'Eufemia fault is reasonably compatible with the historical information on the 1905 event; and an eventual tsunami wave impact on the western Calabrian shoreline is better constrained.

We consider the thorough assessment of the different types of hazards associated with the Sant'Eufemia fault as a very important result for the Tyrrhenian coasts of Calabria, which have not received so far the attention reserved to other Italian coastal areas despite the growing infrastructure facilities and tourism activities.

Introduction and Geological Setting

The Sant'Eufemia Gulf (Figure 1b) lies between the Calabrian arc and the southeast Tyrrhenian basin, which is the Neogene back-arc basin of the Apennines subduction system (Patacca and Scandone, 2004, and references therein). The Calabrian arc is an independent, continental block that bridges theNE-trending southern Apennines (to the north) with the approximately E-trending SicilianApennines (to the south; Bonardi et al., 2001). The rapid southeast-ward migration of the Calabrian Arc and the abundant seismicity recorded at different depths support the hypothesis that subduction of the oceanic crust is still active beneath the Calabrian block and is laterally constrained by two main tear faults, the Tindari fault (to the south) and the likely Sangineto line (to the north; Van Dijk and Scheepers, 1995; Rosenbaum et al., 2008). Calabrian Arc is laterally segmented by main WNW-trending shear zones that have accommodated rotational movements (Malinverno and Ryan, 1986; Knott and Turco, 1991) from the late Miocene (Van Dijk and Scheepers, 1995) to the Recent (Tansi et al., 2007). Since middle Pleistocene times, the Calabrian arc experienced a rapid uplift up to ~1 mm/yr (Westaway, 1993; Tortorici et al., 2003), in part accommodated by major NE-SW oriented normal faults (Ghisetti, 1984; Monaco and Tortorici, 2000).

Mediterranean region is characterized by active geodynamic processes that during the past generated highly destructive events such as the 365AD Crete tsunami (Altinok et al., 2011), the 1693 AD Sicilian tsunami, or the 1908 Messina earthquake / tsunami (Tinti and Maramai, 1996), and others. The historical

earthquake catalogue of Italian region (Figure 1a; Rovida et al., 2011) is studded by numerous events considered highly destructive amongst which the 1905 Calabria earthquake (Tinti and Maramai, 1996). This event although considered minor,if compared to the 1693 or 1908 ones, claimed 557 casualties, more than 2000 injured (Baratta, 1906), and about300,000 people were left homeless. Moreover, this event was followed by tsunami wave that, albeit modest, was reported by contemporary observers both in the open sea and along the coasts of south Italy (Platania, 1907).The detailed review of the historical tsunamis generated along the Italian coasts (Tinti and Maramai, 1996) images the Calabria, together with eastern Sicily, as the region with the highly risk level. The fault generating this event was been for long time under discussion in terms of magnitude and seismogenetic source location (Loreto et al., 2013, and references therein).Based on the recent shacking scenarios simulation, Sandron et al. (2015) restrict the seismogenetic sources to two most probable faults: the Sant'Eufemia Fault; and the Vibo Valenzia Fault. While based on tsunami simulations, Pagnoni et al. (2014) propose as most probable tsunamogenic fault the Capo Vaticano Fault and less probable the Sant'Eufemia Fault. Combining all information: geophysical, geological, and models, we decide to better explore the Sant'Eufemia Fault as the most probable source of the 1905 earthquake.

The aim of this work is to assess the georisks of the Calabrian coasts overlooking the SE Tyrrhenian Sea, through the seismological models: shacking scenarios and tsunami simulation, generated by the new interpreted active fault crossing the Sant'Eufemia Gulf (Figure 1b), constrained by the Intensity distribution and tsunami effects reported for the 1905 Calabria earthquake. The 1905 Calabria earthquake is an interesting case study for risk assessment in an area currently characterized by growth of infrastructure facilities and tourism activities.

Results

Comparing the historical records of the 1905 event with the seismological and tsunami simulations of a newly interpreted active normal fault located in the Sant'Eufemia Gulf, we could assess the hazard of lands overlooking the SE Tyrrhenian Sea. Loreto et al. (2013) identified a 25 km long, N31°-striking normal fault,named Sant'Eufemia Fault, using a multidisciplinary dataset acquired within the Sant'Eufemia Gulf (Loreto et al., 2012). This fault outcrops at the seafloor of 8kmlength (Figure 1c), corresponding to the central segment of the fault plane, while along the northern rim lies buried below recent marine sediments (see Figure 10 in Loreto et al., 2103). Using the high resolution morpho-bathymetric data, we sampled a series of bathymetric profiles orthogonally oriented to the fault plane (Figure 1c) and used to estimate the slip rate associable to the last earthquake (MB P in Figure 1). The average (linear media method) of measured slip rate on fault plane is of 2.3m (see last plot in Figure 1), assuming a unique slip movement controlled by the 1905 earthquake also filtered by the erosion effect.
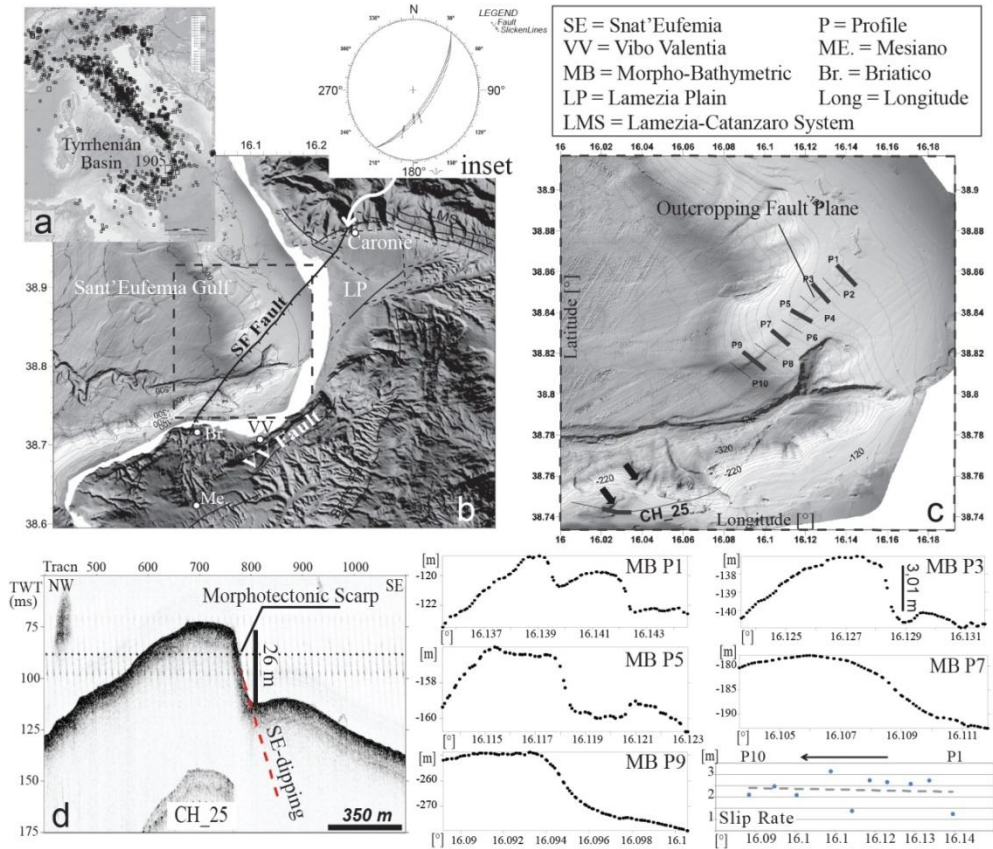
Figure 1. a) Italian earthquakes from CPTI11 catalogue including events since 1000 AD (Rovida et al., 2011), the larger square corresponds to the 1905 Calabria earthquake. b) Morpho-structural map of the western Calabria including high resolution morpho-bathymetry (ISTEGE project; Loreto et al. 2012) and SRTM 90m resolution on-land data form (Jarvis et al., 2008; http://srtm.csi.cgiar.org). Stereographic plot of normal faults measured close to Caronte Terme are reported in the inset. c) Morpho-bathymetric map showing the fault plane trace at the seafloor and sampled bathymetric profiles plotted below. Blue thick arrows mark a morphotectonic scarp. d) CH_25 sub-bottom chirp profile, acquired using Benthos CAP-6600 with a sweep ranges between 2 and 7 kHz, crossing a deep morphotectonic scarp.

Recent on-land structural survey on outcropping units, carried out by Brutto et al. (2015) in the frame of the PhD work, allowed of identifying a group of NE-SW striking normal faults close the Caronte Terme (Figure 1b, inset), which result in agreement with the offshore normal fault. Accordingly, we extend northward the Sant'Eufemia Fault closing it against the morphological barrier in literature associated to a transcurrent faults system. Southward, the chirp profile CH_25 images a 26m-deep scarp, SE-dipping plane. Being this scarp well imaged also on the morpho-bathymetric map (thick blue arrows in Figure 1c), the geological feature controlling this scarp has a NE-SW orientation. This scarp well

113

agree with the likely southward prolongation of the Sant'Eufemia normal Fault. Finally, the morphological trend of subaerial area, narrowed between Briatico, Vibo Valentia and Mesiano, is affected by numerous slumps triggered by the 1905 earthquake (Chiodo and Sorriso-Valvo, 2006) and by subsidence associated to the tilting of the Capo Vaticano Promontory (Pepe et al., 2013). All these morpho-tectonic elements allowed us to extend the Sant'Eufemia fault southward and northward, resulting thus ca. 40 km long.

Analysis of shacking scenarios, performed using seven source models (Sandron et al., 2015, and references therein) in literature associated to the 1905 Calabria earthquake, allowed to better constrain the geometry of fault plane source, namely a fault planemore than 25km-long, NE-trending and affected by a single central asperity, located in the area between the Sant'Eufemia Gulf and the central Calabria. Considering the new geological and geophysical elements we performed a new PGA (Pick Ground Acceleration) and PGV (Pick Ground Velocity) scenarios with input a fault plane 40 km-long, 17 km-wide along dip and estimated M7 (Wells and Coppersmith, 1994).The PGV values (Figure 2a) shows a typical butterfly distribution with high values in the northern and eastern areas, where Intensity values map (Figure 2b) shows highest IX-X MCS (Mercalli-Cancani-Sieberg) values. Velocity values rapidly decrease southward.
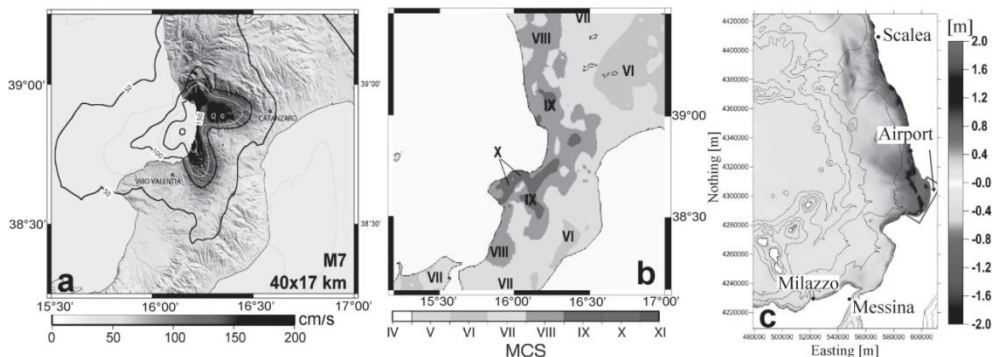
Figure 2. a) PGV (Pick Ground Velocity) map assuming a uniform Seismic Moment (M_0) distribution along the fault plane 40km-long, 17km-wide along dip, with a single centred asperity. The estimated magnitude of the earthquake is M7 enucleating in the centre of the fault plane. b) Intensity map of the 1905 Calabria earthquake. c) Tsunami wave simulation, final stage, triggered by the Sant'Eufemia normal fault, estimated slip rate of 2.3m.

Similarly, a tsunami simulation of an event triggered along Sant'Eufemia Fault, with a 2.3m of slip rate is performed by using the the program UBOTSU-FD. This code solves linear Navier-Stokes equations in shallow water approximation by a finite difference numerical method. Final stage of tsunami simulation (Figure 2c) images a maximum wave elevation of ca. 2m along the northern part of the Gulf. The tsunami wave propagates along northern and southern coasts and open-sea with average values of ca. 0.8m.

Discussions

On-land geological and offshore geophysical data combined with seismological and tsunamigenic models, constrained with historical 1905 earthquake data, allowed us to assess the hazard of central-western Calabria region, considered one of the Italian regions with highest vulnerability. The good fitting amongst PGV values distribution and Intensity values map (Figure 2a, b) in the eastern and northern area strongly supports the hypothesis that the Sant'Eufemia Fault is the causative fault of the 1905 earthquake further confirming the new interpretation of the fault,extended on-land. Thus, this hypothesis better agrees with the estimated magnitude (Martini and Scarpa, 1982; Gruppo di Lavoro CPTI04, 2004)and with on-land observed morphological features. Moreover, the higher velocity values observable in the Lamezia plain (Figure 2a) could be favoured by soil type D presence, represented by loose, coarse and fine deposits (Di Capua et al., 2011) which could produce an amplifying effect increasing acceleration and thus damage in case of an earthquake trigger by this fault. In Lamezia plain, the missing of X MCS values (Figure 2b) could be due to the missing of infrastructures at the time of 1905 earthquake time.Further phenomena that could be justified by the presence of weak soils are slides and slumps, which abound in the Capo Vaticano Promontory amongst Briatico, Vibo Valentia and Mesiano (Chiodo and Sorriso-Valvo, 2006), these could strongly increase Intensity values recorded at that time. Tsunami modeling of the Sant'Eufemia Fault (Figure 2c) shows the maximum wave elevation of about 2m mainly from the internal shoreline of the Gulf moving to northward.

Even if far from the Sant'Eufemia Gulf the wave elevation rapidly decreases down to 0.8m, it results well in agreement with anomalous wave recorded at Milazzotidal station, and with 0.1m oscillationsrecorded at Messinatidal station. Higher wave elevation values in the northern shoreline, as at Scalea, agree with high inundation of 30m on-land. This good fitting between tsunami simulation and recorded data at the 1905 event time (Platania, 1907) further give a confirmation that the Sant'Eufemia Fault is the most probable causative fault of the 1905 Calabria earthquake.Tsunami simulation allows to identify the coastal area highly exposed to a tsunami event, corresponding mainly to the northern part of the Gulf where the Lamezia plain opens.

This area and all the near coast zone along Capo Vaticano promontory and northward up to Scalea are characterized by numerous touristic infrastructures and commercial activities, amongst which one can count even the Airport (Figure 2c). These areas are currently more populated and under interesting economic development, which increases its potential risk. Integrated analysis of all available data and of seismological and tsunami modelling allow us to assess the potential risks of the western Calabria that facing the SE Tyrrhenian Sea if the active Sant'eufemia Fault could trigger an earthquake with an estimated magnitude of Mw 7 comparable with the historical 1905 event.

Acknowledgements

References

Altinok, Y., B. Alpar, N. Özer, and H. Aykurt (2011). Revision of the tsunami catalogue affecting Turkish coasts and surrounding regions. NHESS, 11(2), 273-291.

Baratta, M.(1906). Il grande terremoto calabro dell'8 settembre 1905. Atti della Societa Toscana di Scienze Naturali, Memorie, 22.

Bonardi, G., W. Cavazza, V. Perrone, S. Rossi (2001). Calabria-Peloritani Terrane and Northern Ionian Sea. In: Martini, L.P., Vai, G.B. (Eds.), Anatomy of an Orogen: The Apennines and Adjacent Mediterranean Basins. Kluwer Academic Publication, 287–306.

Brutto, F, M. Francesco, M. F. Loreto, V. Tripodi and S. Critelli (2015). Plio-Quaternary tectonic evolution of the western Catanzaro Trough (Calabria, South Italy). In EGU General Assembly Conference Abstracts(Vol. 17, p. 12572).

Chiodo, G., and M. Sorriso-Valvo (2006). Frane sismo-indotte: casistica e fenomeni innescati dal terremoto dell'8 settembre 1905. I. Guerra (Editor), 8 (1905), 207-224.

Di Capua, G., G. Lanzo, V. Pessina, S. Peppoloni and G. Scasserra (2011a). The recording stations of the Italian strong motion network: Geological information and site classification, Bull. Earthq. Eng. 9, 1779–1796, doi: 10.1007/s10518-011-9326-7.

Ghisetti, F. (1984). Recent deformations and the seismogenic source in the Messina Strait (southern Italy), Tectonophysics 109, 191–208.

Gruppo di Lavoro CPTI, 2004. Catalogo Parametrico dei Terremoti Italiani, versione 2004 (CPTI04). INGV, Bologna (http://emidius.mi.ingv.it/CPTI/).

Jarvis A., H.I. Reuter, A. Nelson, E. Guevara (2008). Hole-filled seamless SRTM data V4, International Centre for Tropical Agriculture (CIAT), available from http://srtm.csi.cgiar.org.

Knott, S. D., and E. Turco (1991). Late Cenozoic kinematics of the Calabrian arc, southern Italy, Tectonics 10, no. 6, 1164–1172.

Loreto, M. F., F. Zgur, L. Facchin, U. Fracassi, F. Pettenati, I. Tomini, M. Burca, P. Diviacco, C. Sauli, and G. Cossarini, et al. (2012). In search of new imaging for historical earthquakes: A new geophysical survey offshore western Calabria (southern Tyrrhenian Sea, Italy), Boll. Geofis. Teor. Appl. 53, no. 4, 385–401.

Loreto, M. F., U. Fracassi, A. Franzo, P. Del Negro, F. Zgur, and L. Facchin (2013). Approaching the seismogenic source of the Calabria 8 September 1905 earthquake: New geophysical, geological and biochemical data from the S. Eufemia Gulf (S Italy), Mar. Geol. 343, 62–75, doi:10.1016/j.margeo.2013.06.016.

Malinverno, A. and W. B. F. Ryan (1986). Extension in the Tyrrhenian Sea and shortening in the Apennines as result of arc migration driven by sinking of the lithosphere, Tectonics 5, 227–245.

Martini, M. and R. Scarpa (1982). Italian earthquakes since 1900. Proc. E. Fermi Summer School in Geophysics.Springer-Verlag, Varenna.

Monaco, C. and L. Tortorici (2000). Active faulting in the Calabrian arc and eastern Sicily. J. Geodyn., 29, 407–424.

Pagnoni, G., Armigliato, A., Tinti, S., Loreto, M. F., & Facchin, L. (2014). What is the fault that has generated the earthquake on 8 September 1905 in Calabria, Italy? Source models compared by tsunami data. In EGU General Assembly Conference Abstracts (Vol. 16, p. 12142).

Patacca, E. and P. Scandone(2004). The Plio-Pleistocene thrust belt — foredeep system in the Southern Apennines and Sicily (Italy). In: U. Crescenti, S. D'Offizi, S. Merlini, L.Lacchi (Editors), Geology of Italy. Soc. Geol. It, Roma, pp. 93–129.

Pepe, F., G. Bertotti, L. Ferranti, M. Sacchi, A.M. Collura, S. Passaro and a. Sulli (2013). Pattern and rate of post-20 ka vertical tectonic motion around the Capo Vaticano Promontory (W Calabria, Italy) based on offshore geomorphological indicators. Quatern.Int., 30, 14.

Platania, G. (1907). I fenomeni in mare durante il terremoto di Calabria del 1905. Società tipografica modenese.

Rosenbaum, G., M. Gasparon, F. P. Lucente, A. Peccerillo, and M. S. Miller (2008). Kinematics of slab tear faults during subduction segmentation and implications for Italian magmatism, Tectonics 27, no. 2, TC2008, doi: 10.1029/2007TC002143.

Rovida, A., R. Camassi, P. Gasperini, M. Stucchi (2011). CPTI11, the 2011 version of the Parametric Catalogue of Italian Earthquakes. Milano, Bologna. http://emidius.mi.ingv.it/CPTI.

Sandron, D., M.F. Loreto, U. Fracassi and L. Tiber (2015). Shaking scenarios from multiple source models shed light on the Mw 7 Calabria 8 September 1905 earthquake (S Italy). Bulletin of the Seismological Society of America.

Tansi, C., F. Muto, S. Critelli and G. Iovine (2007). Neogene-Quaternary strike-slip tectonics in the central Calabrian Arc (southern Italy). J. Geodyn., 43, 393–414.

Tinti, S. and a. Maramai (1996). Catalogue of tsunamis generated in Italy and in Côte d'Azur, France: a step towards a unified catalogue of tsunamis in Europe. Annali di Geofisica XXXIX (6), 1253–1299.

Tortorici, G., M. Bianca, G. De Guidi, C. Monaco, and L. Tortorici (2003). Fault activity and marine terracing in the Capo Vaticano area (southern Calabria) during the Middle-Late Quaternary, Quaternary Int. 101/102, 269–278, doi: 10.1016/S1040-6182(02)00107-6.

Van Dijk, J.P. and P.J.J Scheepers (1995). Neotectonic rotations in the Calabrian Arc; implications for a Pliocene-Recent geodynamic scenario for the Central Mediterranean. Earth Sci. Rev., 39, 207–246.

Wells, D. and K. Coppersmith (1994). New empirical relationship among magnitude, rupture length, rupture width, rupture area and surface displacement. Bullettin of Seismological Society of America 84, 974–1002.

Westaway, R. (1993). Quaternary uplift of southern Italy, J. Geophys. Res. 98, no. B12, 741–772.

SUBMARINE LANDSLIDES OF THE CENTRAL MEDITERRANEAN SEA: STATE-OF-THE-ART AND CURRENT CHALLENGES

Micallef, A.[1], Cunarro Otero, D.[2]

1 Departmentof Physics, University of Malta, Msida, Malta,
aaron.micallef@um.edu.mt
[2] University of Las Palmas de Gran Canaria, Spain,
daniel.cunarro101@alu.ulpgc.es

Submarine landslides are one of the most important offshore geohazards - they destroy seafloor installations, generate tsunamis and deform shorelines. In the last three decades, large scale surveying and research programmes, based on geophysical mapping, seafloor sampling, in situ geotechnical characterisation, and numerical simulations, have demonstrated that landslides are ubiquitous elements of submarine landscapes and investigated their geomorphology, landslide dynamics and mechanics, and deposit architecture.

The Mediterranean Sea is an active, complex and peculiar region that hosts a wide range of geological environments. Submarine landslides are very common along all Mediterranean continental margins (Urgeles and Camerlenghi, 2013). Because of high coastal populations and density of seafloor infrastructure, the central Mediterranean region is highly vulnerable to these offshore geohazards.
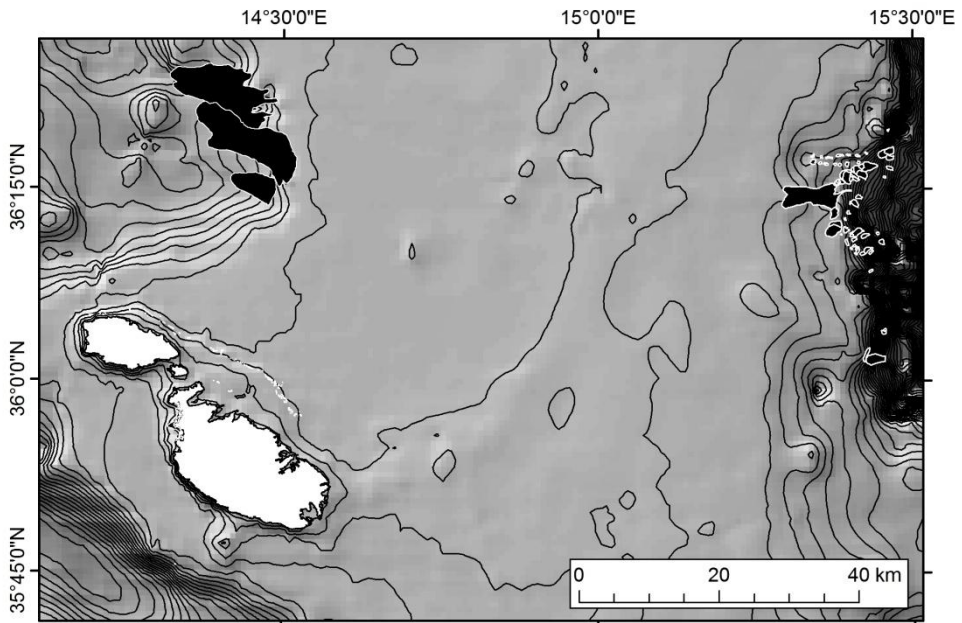
Figure 1. Known submarine landslides offshore the MalteseIslands (shaded in black).

In this paper we will focus on the most significant advances made in submarine slope instability research in the central Mediterranean Sea. We provide an overview of known submarine landslide occurrence and dynamics and their relevance to known natural disasters (Figure 1).

We identify the most outstanding research questions in submarine slope instability research – e.g. the preconditioning factors, triggers, prediction and evolution of submarine landslides, the generation of tsunamis, and the role of weak layers, hydrogeology and global climate change in slope failure – and propose how these can be addressed in the central Mediterranean Sea. This entails a strategy based on improved subseafloor characterisation and physical modelling, in situ monitoring and repeat surveys, and the more widespread use of statistically relevant datasets and 3D seismic geomorphology.

Acknowledgements

References

Urgeles, R., and A. Camerlenghi (2013). Submarine landslides of the Mediterranean Sea: Trigger mechanisms, dynamics, and frequency-magnitude distribution, Journal of Geophysical Research. 1181-19.

SITE CHARACTERIZATION AT ALGIERS CITY USING PEAK GROUND AND SPECTRAL ACCELERATIONS

Mobarki, M.[1], Talbi, A.[1]

[1]*Departement étude et surveillance sismique, CRAAG BP 63 Bouzaréah 16340 Algérie, mourad.mobarki@gmail.com*

[1]*Departement étude et surveillance sismique, CRAAG BP 63 Bouzaréah 16340 Algérie, abdelhak_t@yahoo.fr*

Introduction

In this work an equivalent linear model for different soils is used in response analysis. Then, different models are constructed based on borehole logs, velocity profiles and geotechnical data. The equivalent linear site response analysis program EERA (Bardet et al 2000) has been used to synthesize soil profiles, and then accelerations are input in EERA to get the reaction of soil stratigraphic log under seismic movement at rock level. Different outputs are registered at soil surface. This procedure has been applied to three sites at Algiers city, namely these sites are Bab el Oued (BEO), El Mouradia (EM), and Dar El Beida (DEB). We introduced filtered acceleration with $PGA = 0.1$ g as input. Input and output PGA and spectral acceleration (S_a) at a given depth and at the surface are compared and found consistent with site nature.

In most cases, contemporary catastrophic earthquakes as Izmit (Turkey, 1999, Mw=7.6), Kobe (Japan, 1995, Mj=7.3), Boumerdès (Algeria, 2003 Mw=6.7), Kashmir (Pakistan, 2005, Mw=7.6), and Sichuan (China, 2008, Mw=7.9) show the fragility of our urban environments when facing the destructive shaking. In China, Algeria, Turkey or in Italy, we observed a lot of similarities in building damages with high damage in fragile buildings including old buildings in bricklaying or in earth resist least. Schools suffered often high shaking. This picture is complicated with diffuse zone of destruction without any clear geographical repartition. . On the other hand, apart from these usual standard observations, there is an obvious scientific logic if better mastered and better controlled it would allow reducing earthquake damage on urban zones. Fortunately, there is an increasing interest on seismology and seismotectonics among the Algerian scientific community, especially in seismic risk assessment to urban area and its possible reduction. In this study, obtained results are presented as acceleration data corresponding to input and output layers of profile. Discussion in carried out using comparison between peak ground acceleration at surface and depth together with spectral acceleration analysis.

Geological and tectonic context

Algiers (Algeria) is integrated into the alpine chain mountains and is essentially structured by the plain of the basin Mitidja. It can be considered as a basin type structure intra mountainous, bounded on the south by the area of the

sheets forming Tellien Atlas. The sedimentary basin extends from Mitidja Eo-Miocene to Quaternary. During the Pliocene, the sea deposited interbedded of blue marl sandstone with thickness reaching about 1000 m. In the East, the Mitidja is bordered by outcrops of base-type granitoid appearing in Boumerdes and along the fault Thénia. Tellien Atlas is the most remarkable entity from seismotectonic perspective. It consists of a series of mountain ranges and valleys parallel to the coast, with systems of faults and folds induced by a compressive tectonic regime with NW-SE crustal shortening (Boudiaf, 1996). The inter-plate convergence movement is characterized by a NNW-SSE towards very close to horizontal (Deverchère et al., 2005).

Result and Discussion

The superposing of acceleration at input and surface give us important information on the state of the site effect (Fig1a). At the site DEB, EM and BEO, the ratio of PGA registered at surface area upon the one registered at depth is respectively 1.52, 1.62 and 1.04 for the three above considered sites. Another way to estimate seismic hazard of buildings and structures is response spectral acceleration curve. Spectral acceleration, commonly noted Sa, is the maximum acceleration of a single degree of freedom oscillator with different natural frequencies with unique damping ratio. Figures 1b compare S_a with 5% damping ratio at the ground surface with the one at bedrock. Results show that the S_a increases for high frequencies (between 0.2 sec and 0.5 sec). The Table 1 below list the result obtained for the three sites considered in this study.
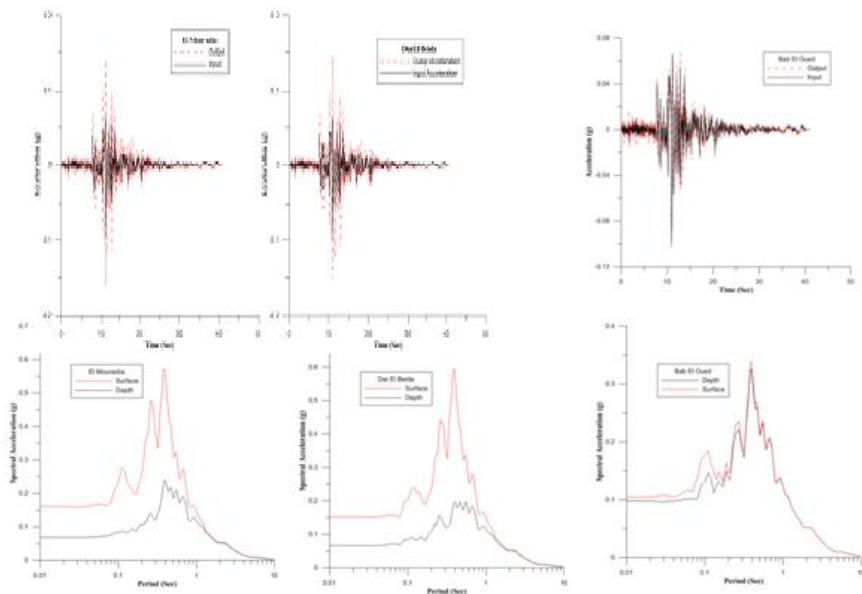
Figure 1. comparisons: of the superposing Acceleration (a) of the spectral acceleration (b) at depth and surface

Table 1. The main results of PGA and S_a on site.

Site	PGA(g) @	PGA (g) @	S_a(g) @	S_a(g) @
BEO	0.1	0.104	0.33	0.34
DEB	0.1	0.152	0.2	0.5
EM	0.1	0.162	0.24	0.57

Conclusion

This study shows importance of site characterization from the study of soil responses as peak ground acceleration (*PGA*) and spectral acceleration (*S_a*). More detailed analysis on how deep soil sites respond to ground shaking is necessary to help engineers and scientists understand the ground movements in the Algiers city. Additional studies should be carried on, especially for large urban site with large population and old structure to help the construction of microzonation maps in such case, we suggest that our procedures need to be evaluated in details in order to produce accurate representation of actual ground-motion response.

References

Bardet et al (2000)..“EERA: A Computer Program for Equivalent-linear Earthquake site Response Analysis of Layered Soil Deposits,” University of Southern California, Department of Civil Engineering, http://geoinfo.usc.edu/gees.

Boudiaf A. (1996) ''Étude sismotectonique de la région d'Alger et de la Kabylie (Algérie),'' Thèse de Doctorat, Université de Montpellier II- Sciences et Techniques du Languedoc.

Deverchere et al (2005) Deverchere J, Yelles K, Domzig A, Mercier De Lepinay B, Bouillin J-P,Gaullier V,Bracene R;Calais E,Savoye B, Kherroubi A, LeRoy P, Pauch et Dan. 'Active thrust faulting offshore Boumerdes, Algeria, and its relations to the 2003 Mw 6.9 earthquake,'' geophysical research letters

THE MOST IMPORTANT ENVIRONMENTAL EFFECTS TRIGGERED BY HISTORICAL EARTHQUAKES FROM 17TH TO 19TH CENTURY IN THE APULIA REGION (CENTRAL MEDITERRANEAN SEA)

Nappi, R.[1], Gaudiosi, G.[1], Alessio, G.[1], De Lucia, M.[1], Porfido, S.[2]

[1]*Istituto Nazionale di Geofisica e Vulcanologia, Sezione di Napoli - Osservatorio Vesuviano, Napoli, Italy.*
rosa.nappi@ingv.it, germana.gaudiosi@ingv.it, giuliana.alessio@ingv.it, maddalena.delucia@ingv.it
[2]*CNR-IAMC Napoli, Italy,sabina.porfido@iamc.cnr.it*

Introduction

The Apulia (Southern Italy) has been hit by several low energy and a few high energy earthquakes from 17th to 19th century. The aim of this study is a critical revision of the historical and recent seismicity of the Apulian region and surrounding seismogenetic areas, for re-evaluating the macroseismic effects in MCS scale and ground effects in natural environment according to the ESI 2007 scale (Michetti et al., 2007; Guerrieri et al., 2015). In particular, the February 20, 1743 earthquake, the strongest of the Salento area and the July 30, 1627 earthquake, the strongest of the Gargano promontory have been reviewed. Moreover we have evaluated the most important effects on land in the Salento and Gargano area. The use of both traditional MCS macroseismic intensity scale and the ESI 2007 scale gives a more accurate image of the earthquakes (Porfido et al., 2007) and allowed us to better constrain the seismic hazard assessment in the Salento peninsula.

Geodynamic Setting

The central area of the Mediterranean basin is a plate-boundary region of high seismicity and complex tectonics, dominated by frequent earthquake activity occurring mostly in the Ionian Sea and Western Greece. The geodynamic framework of the Apulian area is characterized by the subduction of the Ionian slab beneath the Calabrian Arc; such compressive regime is still active (Caputo et al., 1970; Castello et al., 2006). Particularly the Apulia region, NW-SE elongated, represents the emerged part of the Adriatic foreland domain shared by the Apennine chain to the west, and the Dinaride-Hellenide chain to the east (Moretti and Royden, 1988). As regards the tectonic setting of the Apennine-Dinaride converging region and surroundings, according to Gambini and Tozzi (1996) the major structural lineaments to be considered are: the Scutari-Pec Line; the Pescara-Dubrovnik dextral shear Line; the North Gargano Fault Zone; the Mattinata Gondola Fault Zone; the South Salento-North Kerkira Fault Zone; the right-lateral Cephalonia Transform Fault (see map in Gambini and Tozzi, 1996).

The rigid Apulian foreland block has been deformed through several normal faults, NW-SE and NNW-SSE trending, some of them presently active since they dislocate the sea floor by about 200–300 m; moreover, major E-W strike-slip and oblique-slip fault zones divide Apulia into structural blocks behaving independently, among them the Gargano Promontory, the Murge Ridge and the Salento Peninsula are relevant.

Seismicity of the Apulia Region

Apulia is a region with relatively moderate seismicity surrounded by regions with destructive seismicity: to the east the coast of Albania and the Ionian Islands (western Greece); to the west the Calabrian arc and the southern Apennines chain (Slejko et al.,1999). The historical and recent seismicity in the Apulia region is characterized by a greater frequency of earthquakes in the northern sector compared to the southern one (Fig. 1). The strongest historical earthquakes from 17th to 19th century occurred in the Apulian region from Gargano to Salento area were: July 30, 1627 (Gargano, Imax=X MCS); December 8, 1889 (Gargano, Imax=VII MCS); March 20, 1731 (Foggia, Imax=IX MCS); September 10, 1087, (Bari, Imax=VI-VII MCS); May 11, 1560 (Barletta-Bisceglie, Imax=VIII MCS); October 26, 1826 (Manduria, Imax=VI-VII MCS); January 20, 1909 (Nardò, Imax=VI MCS) and February 20, 1743, (Ionian sea, Imax=IX MCS) (CPTI11, Rovida et al., 2011; SHEEC, Stucchi et al. 2013, Grünthal et al., 2013). It is noticeable that the 1627, 1731, 1743 and 1889 earthquakes have also generated considerable seismo-induced environmental effects such as tsunami deposits along the Apulian coasts, landslides, liquefaction phenomena and hydrological changes (Margottini, 1982; De Simone, 1993; De Martini et al., 2003; Mastronuzzi et al., 2007; Maramai et al., 2014).

Felt reports in the far field

The whole Apulia region has also been struck by strong earthquakes of neighbouring seismogenetic areas located in the Southern Apennines, Adriatic and Ionian Sea, Albania and Greece. Several ground effects, mostly hydrological variations, have been triggered in Northern Apulia by the July 23, 1930 Irpinia earthquake (Imax=X MCS) and the November 23, 1980 Irpinia-Basilicata earthquake (Imax=X MCS) (Porfido et al. 2002, Porfido et al. 2007).

It is well known that earthquakes with epicentre in the central-eastern Mediterranean (Greece, Ionian Islands) well propagate throughout the Italian peninsula, and in particular in the southern regions, where the intensity degrees are higher, sometimes exceeding the limit of damage. Some well documented examples of Greek earthquakes strongly felt in the whole Apulia region were: the August 27, 1886 earthquake (epicenter in Peloponnesus, Greece) (Margottini 1982; Papazachos et al., 2003); the May 28, 1897 earthquake (epicenter in Creta – Cypro); the June 26, 1926 earthquake (epicenter between Creta and Cipro, Imax=X MCS), felt all over the Southern Italy; the August 28, 1962 earthquake (epicentre in Peloponnesus area) (Margottini 1982; Serva & Michetti, 2010).

It is noteworthy that earthquakes located in the Southern Apennines were powerfully felt in the whole Apulia region; among the strongest historical events of the Campania-Lucania Apennines we mention the 1456 (Imax =XI MCS), 1694 (Imax =XI MCS) and 1857 (Imax=XI MCS) earthquakes. More recently, the July 23, 1930 (Imax=X MCS) and the November 23, 1980 (Imax=X MCS) Irpinia earthquakes gave rise to several ground effects, mostly hydrological variations, in the Apulian region. In details, intensity I=VI-VII MCS was reached due to the 1930 seismic event, while I=VI MSK was estimated for the 1980 earthquake (Porfido et al 2002, Porfido et al. 2007).
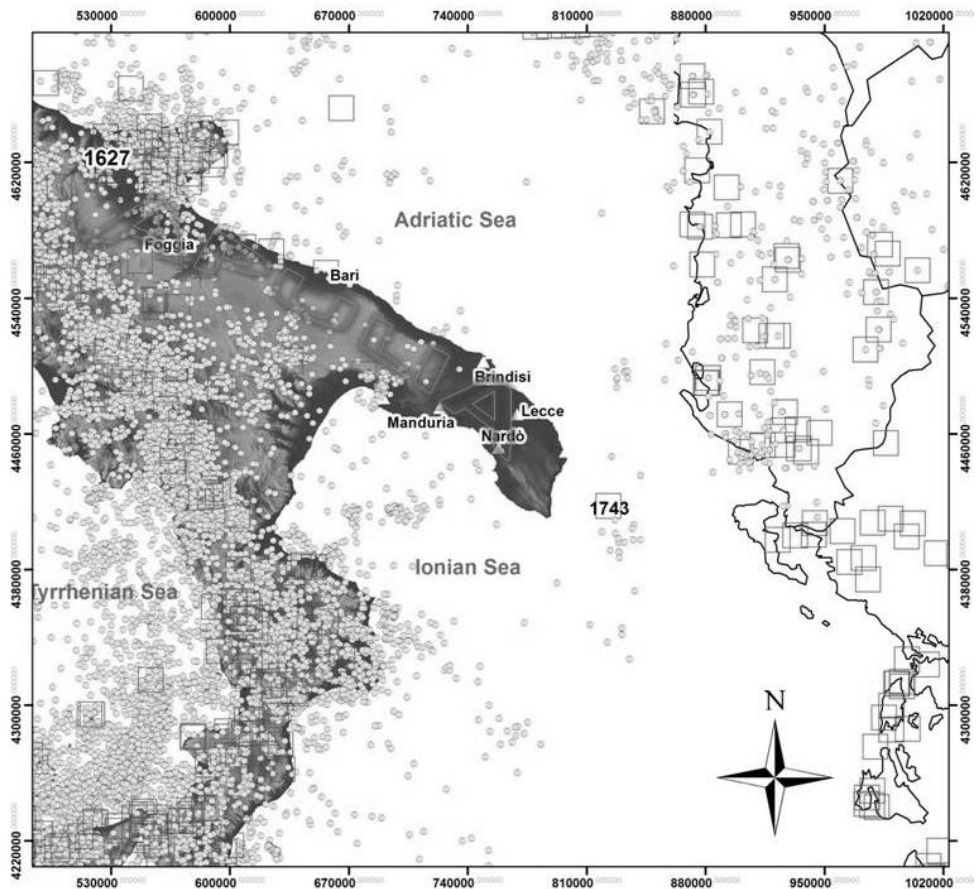
Figure 1. The map shows the spatial distribution of historical and recent seismicity extracted from: CPTI11 (Rovida et al, 2011), squares; SHEEC, (Stucchi et al., 2013; Grunthal et al., 2013) dots.

Earthquake Environmental Effects (EEE): case studies

For an appropriate mitigation strategy in seismic areas, it is fundamental to consider the role played by seismically induced effects on ground, such as active faults (size in length and displacement) and secondary effects (the total area

125

affected). With these perspectives the February 20, 1743 Nardò strong earthquake (Mw=6.9) (Salento, Southern Italy) has been reviewed. Moreover, a preliminary evaluation of environmental effects induced by the July 30, 1627 Gargano destructive earthquake (Mw=6.6) has been carried out in order to evaluate its macroseismic field according to the ESI scale.

The 1743 Salento earthquake caused about 180 dead, of which 150 in the town of Nardò. Heavy damage affected particularly the towns of Nardò (Lecce) and Francavilla Fontana (Brindisi) (Margottini, 1981, 1985). The seismic event was also felt on the western coast of Greece, on the Malta island, in Southern Italy and in some localities of Central and Northern Italy. The 1743 earthquake also generated a tsunami, which deposits are distributed along the southern Adriatic coastline of Salento (Mastronuzzi et al., 2007; Galli and Naso, 2008).This earthquake is described in a large amount of historical documents and seismic catalogues, however the location and geometry of the seismogenetic source is still a subject of scientific debate.

On the basis of recent scientific papers, (Margottini, 1981; Margottini, 1985; Ferrari, 1987; De Simone, 1993; Boschi et al., 1995; Galli & Naso, 2008, De Lucia et al., 2014; Nappi et al., 2015; Porfido et al, 2015) and historical documents revision (De Giorgi, 1898; Baratta, 1901), a new estimation of the 1743 MCS intensity values of some localities has been carried out. Furthermore, a critical review of historical sources, especially archival documents coeval to the 1743 earthquake, found in different National Archives in Italy and in local church archives, has been performed.

On the basis of the MCS scale, our re-evaluation has assigned the value of X MCS intensity to the town of Nardò, whose previous intensity value was IX MCS according to Margottini, 1981, 1985; Boschi et al., 1995; Guidoboni et al., 2007, and IX - X MCS according to Galli & Naso, 2008; moreover, the value of IX MCS was assigned to Francavilla Fontana, VIII MCS to Castrignano del Capo, Leverano, Mesagne, Tuturano, Manduria, Racale, Salve, and VII MCS to the localities of Calimera, Copertino, Lecce, Oria, Ostuni, Seclì (Fig. 2). For a more complete evaluation of the earthquake from a macroseismic point of view, it is essential to take into account both the direct information derived from archival and historical sources and also the indirect geomorphologic data analysis concerning the relative environmental earthquake effects.

For our re-evaluation of the 1743 earthquake on the basis of the ESI scale, the tsunami phenomenon along the southern Adriatic coastline of Salento has been the most important environmental effect (Mastronuzzi et al., 2007; Mastronuzzi et al., 2011). Accordingly, for the town of Brindisi the ESI intensity value has been raised up from VIII to IX, due to the damage of the harbour mole caused by the tsunami. Moreover, it has been possible to assess the ESI intensity values of VIII$\geq$ I $\geq$ X for the localities of Torre Sasso (Tricase) and Torre Sant' Emiliano (Otranto), along the coastline of the Salento peninsula, on the basis of the tsunami blocks dimensions consisting of large boulders with a maximum weight of about 70 tons (Mastronuzzi et al., 2007). Ground effect phenomena triggered by the 1743

earthquake also occurred in the town of Nardò where variations of the water flow rate of wells together with variations of chemical-physical properties of water were observed.

A wide area that includes Albania, Greece and Malta island (Ambraseys, 2009; Galea, 2007) suffered also significant ground seismo-induced effects. Indeed, in the northern area of the island of Kefalonia (Greece) changes of chemical-physical properties of water occurred, in Castel Sant'Angelo (Corfù, Greece) and Malta island landslides took place, and in Butrinto fortress (Albania) ruptures and probably liquefaction phenomena were observed (Fig.2).
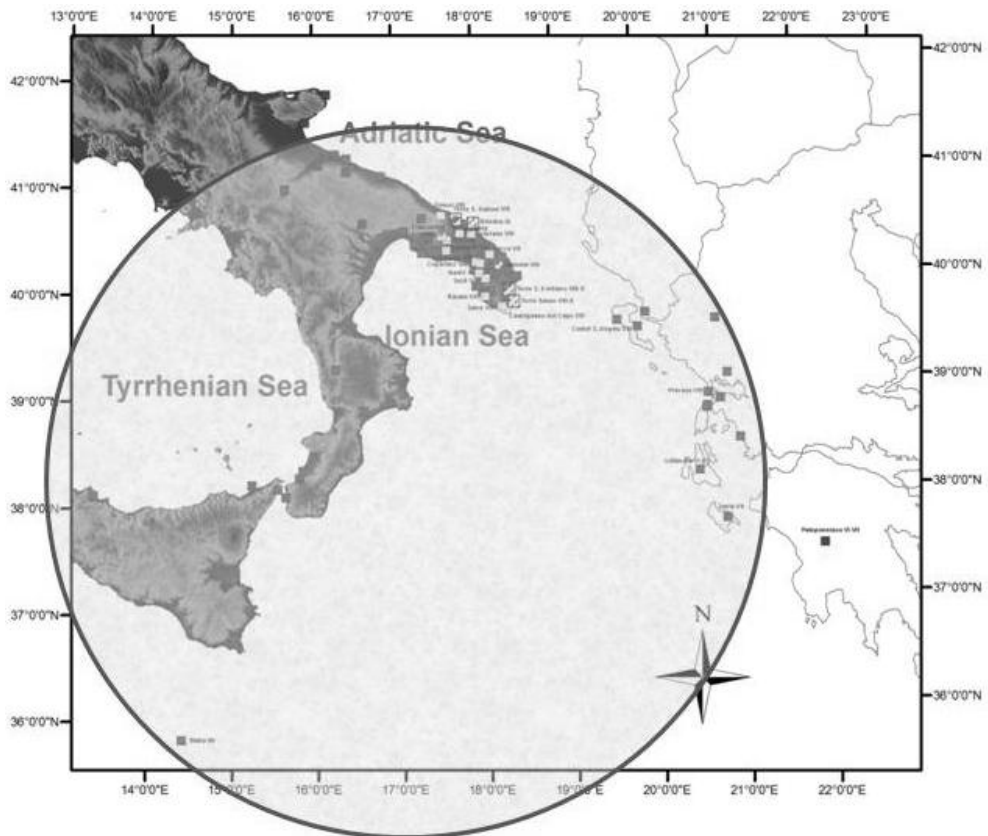
Figure 2. Map of the intensity values of the 1743 Salento earthquake: CFTIMED, 2007 MCS intensity values (black squares); re-evaluated MCS Intensity values in this study (white squares); re-evaluated ESI Intensity values in this study (white striped squares).

The July 30, 1627 earthquake hit the Gargano peninsula in the northeastern part of the Apulia region. It is considered the strongest event in this area reaching the X MCS degree. This earthquake was followed by four large aftershocks and destroyed several villages in the northern Gargano. The strongest

damages were located between S. Severo town and Lesina lake area. The total number of casualties is very different according to the source of information and fluctuates between 30.000 and 5.000 dead. A reliable number of victims could be obtained from the Lucchino chronicle reporting 4500 dead for the towns of Apricena, Lesina, San Paolo di Civitate, San Severo, Serracapriola, Torremaggiore. The most damaged localities were Apricena, Lesina, San Paolo di Civitate, San Severo e Torremaggiore where most of the buildings collapsed. Severe and well documented damages of churches, monastery and ecclesiastic properties have been reported.

Table 1. Localities where environmental effects of the 1627 earthquake have been detected.

Locality	IMCS	Earthquake Environmental effects
San Severo (FG)	10	Hydrological changes
Atri	n. d.	Landslides
Caramanico	n.d.	Landslides, Ground crack
Chieuti	9	Landslides
Fortore	n. d.	Liquefaction phenomena
Fossacesia	7	Hydrological changes
Lesina	10	Liquefaction phenomena?
Ripalta	9-10	Hydrological changes, Liquefaction phenomena
Roseto Valfortore	7-8	Landslides, Ground crack
S. Paolo di Civitate	10	Landslides, Ground crack, Hydrological changes, Liquefaction phenomena
San Severo	10	Landslides
Termoli	8-9	Hydrological changes
Torremaggiore	10	Landslides
Troia	7-8	Liquefaction phenomena
Lesina Lake	n.d	Tsunami, Liquefaction phenomena
Manfredonia	n.d	Tsunami
Fiume Sangro Mouth	n.d	Tsunami
San Nicandro	9	Tsunami

Uncertain data regards damages of the private houses, often reported inside coheval reports. The least damaged area includes the far-off coastal zones of the Gargano promontory, like Manfredonia in the south and Termoli in the north. The 1627

earthquake was felt in the Tremiti islands to the east of Gargano, and in many areas of the Campania region and the Daunia Apennines to the west, as well as in the town of Naples.

The environmental effects triggered by the 1627 seismic event (Tab. 1), documented by coeval reports and archival documents, have been observed mainly near San Paolo di Civitate and along the Fortore river flow: collapses, fractures in the ground, overflowing, gas emissions, springs appearance and disappearance, water level variations inside the wells. Landslides and variations of the hydrological regime occurred far away the epicentral area in many places, liquefaction phenomena happened near the town of Troia. Tsunami waves hit the coast sector facing the Lesina lake, the Manfredonia littoral and the mouth of the Sangro river. Nearby the Saro river (the present Lighthouse) the sea withdrawal was of about 90 meters. Nearby the Fortore river mouth, at first the sea withdrew of about 2 miles (over 3 km), successively it flowed over the coast. The tsunami caused flooding of the plane between Silvi and Mutignano, and inundation of the Sannicandro Garganico country; no victims have been reported.

Preliminary results

The critical analysis of the documentary and historical sources, besides the geomorphologic evidences of effects due to the strong 1743 Salento earthquake, have allowed us to remodel a quite different scenario for this event leading to differently assessed intensity values for some localities, and also to new original estimations of intensity values for other zones. Actually, strong earthquakes occurred in the far field respect to the Salento area, like the significant seismic events that have repeatedly hit Greece and Albania in the last centuries, have also caused heavy damages and serious tsunami effects in the Apulia region and Salento peninsula, despite the apparently low energy seismicity characterizing these areas, in comparison with other seismic areas of Italy. Consequently, the seismic hazard of the Salento peninsula must be re-evaluated and further study should be dedicated to this area, considering also a possible revision of the seismic classification.
The analysis of environmental effects of the 1627 Gargano earthquake is still preliminary in our study and has to be considered work in progress.

Acknowledgements

References

Ambraseys, N.(2009). Earthquakes in the Mediterranean and Middle East. Press. Cambridge University. 901
Baratta, M., (1901). I terremoti d'Italia, Torino.

Boschi, E., G. Ferrari, P. Gasperini, E. Guidoboni, G. Smriglio, and G. Valensise (1995). Catalogo dei forti terremoti in Italia dal 461a.C. al 1980. INGV-SGA.

Caputo, M., G.F. Panza, and D. Postpischl (1970). Deep structure of the Mediterranean Basin. Journal of Geophysical Research,75, 4919-4923.

Castello, B., G. Selvaggi, C. Chiarabba, and A. Amato (2006). CSI Catalogo della sismicità italiana 1981-2002, versione 1.1.INGV-CNT. Roma. http://csi.rm.ingv.it/.

De Giorgi, C. (1898). Ricerche su i terremoti avvenuti in Terra d'Otranto, Mem. Pont. Acc. Naz. Lincei. 15, 96-154.

De Lucia, M., G. Alessio, G. Gaudiosi, R. Nappi, and S. Porfido (2014). A review of the Intensity values for the 1743 Salentoearthquake. Rend. Online Soc. Geol. It. Suppl. 1, 31, 608 p. doi: 10.3301/ROL.2014.140.

De Martini, P.M., P. Burrato, D. Pantosti, A. Maramai, L. Graziani and H. Abramson (2003). Identification of tsunami deposits and liquefaction features in the Gargano area (Italy): paleoseismological implications, Annals of Geophysics, 46, 883-902.

De Simone, E. (1993). Vicende sismiche salentine, Edizioni del Grifo. 152 p.

Ferrari, G.(1987). Some aspects of the seismological interpretation of information on historical earthquakes. In: Proc. Workshop on historical seismicity.(Margottini, C. and Serva, L., eds).

Galea, P.(2007). Seismic history of the Maltese islands and considerations on seismic risk,Annals of Geoph., 50, 725-740.

Galli, P., G. Naso (2008). The "taranta" effect of the 1743earthquake in Salento (Apulia, Southern Italy), Boll.Geofisica Teorica Applicata. 49, (2), 177-204.

Gambini, R. and M. Tozzi (1996). Tertiary geodynamic evolution of the Southern Adria microplate, Terra Nova. 8, 593-602.

Grünthal, G., R. Wahlström, and D. Stromeyer (2013). The SHARE European Earthquake Catalogue (SHEEC) for the time period1900-2006 and its comparison to the European Mediterranean Earthquake Catalogue (EMEC), Jour. Seism.. 17, (4),1339-1344 doi: 10.1007/s10950-013-9379 y.

Guerrieri, L., E. Esposito, S. Porfido, A.M. Michetti, E. Vittori (2015). La scala di intensità sismica ESI 2007 (Italian), in Mem. Descr. Carta Geologica d'Italia, XCVII, 21-30.

Guidoboni, E., G. Ferrari, D. Mariotti, A. Comastri, G. Tarabusi, and G. Valensise (2007). CFTI4Med, Catalogue of Strong Earthquakes in Italy (461 B.C.-1997) and Mediterranean Area (760 B.C.-1500). INGV-SGA, http://storing.ingv.it/cfti4med/

Maramai, A., B. Brizuela, and L. Graziani (2014). The Euro-Mediterranean Tsunami Catalogue. Annals Geoph., 57(4) S0435; doi 10.4401/ag-6437.

Margottini, C.(1981). Il terremoto del 1743 nella penisolasalentina, CNEL-ENEL, Congr. annuale P.F.G. Udine 12-14 maggio 1981.

Margottini, C. (1982). Osservazioni su alcuni terremoti con epicentro in Oriente. Campo macrosismico in Italia del terremoto Greco del 1903, CNEN-RT/AMB. 82 (3).

Margottini, C., (1985). The earthquake of february 20,1743, in the Ionian Sea, In: Atlas of isoseismal maps of Italianearthquakes. CNR-PFG. 114, 2A, 62 p.

Mastronuzzi, G., C. Pignatelli, P. Sansò, and G. Selleri (2007). Boulderaccumulations produced by the 20th of February, 1743 tsunami along the coast of southeastern Salento (Apulia region, Italy), Mar. Geol. 242, 191-205.

Mastronuzzi, G., R. Caputo, D. Di Bucci, U. Fracassi, V. Iurilli, M. Milella, C. Pignatelli, P. Sansò, and G. Selleri (2011). Middle-Late Pleistocene Evolution of the Adriatic Coastline of Southern Apulia (Italy), In: Response to Relative Sea-Level Changes,Geog. Fisica e Din. Quat. 34, 207-221.doi: 1O.4461/GFDQ.2011.34.19.

Michetti, A.M., E. Esposito, L. Guerrieri, S. Porfido, L. Serva, R. Tatevossian, E. Vittori, F. Audemard, T. Azuma, J. Clague, V. Comerci, A. Gurpinar, J. Mc Calpin, B. Mohammadioun, N.A. Mörner, Y. Ota, E. and Roghozin, (2007). Intensity Scale ESI 2007, Mem. Descr. Carta Geologica d'Italia. 74, 53 p.

Nappi, R., G. Gaudiosi, G. Alessio, M. De Lucia, and S. Porfido (2015).A contribution to seismic hazard assessment of the Salento Peninsula (Apulia, Southern Italy), Misc. 6th INQUA Paleos., Active Tectonics and Archaeoseismology, INGV 27,ISSN 2039-6651, 317-320

Papazachos, B.C. and C. Papazachou (2003). The earthquakes of Greece, Ziti publications. Thessaloniki. Greece. 286 p. (inGreek).

Porfido, S., E. Esposito, E. Vittori, G. Tranfaglia, A. M. Michetti, M. Blumetti, L. Ferreli, L. Guerrieri, and L. Serva (2002). Areal distribution of ground effects induced by strong earthquakes in the Southern Apennines (Italy), Surv. Geophy. 23 (6), 529-562.

Porfido, S., E. Esposito, E. Vittori, G. Tranfaglia, L. Guerrieri, and R. Pece (2007). Seismically induced ground effects of the 1805, 1930 and 1980 earthquakes in the Southern Apennines (Italy), Ital. Jour. Geosc. 126, (2), 333-346.

Porfido, S., R. Nappi, M. De Lucia, G. Gaudiosi, G. Alessio, and L. Guerrieri (2015).The ESI scale, an ethical approach to the evaluation of seismic hazards, Geoph. Res. Abs.17, EGU2015-11732-2, 2015

Rovida, A., R. Camassi, P. Gasperini, and M. Stucchi (2011).CPTI11,la versione 2011 del Catalogo Parametrico dei Terremoti Italiani, http://emidius.mi.ingv.it/CPTI. doi:10.6092/INGV.IT-CPTI11.

Serva, L., A. and M. Michetti (2010). Shakeistics: l'eredità degli studinucleari in Italia per la valutazione del terremoto di riferimento per la progettazione degli impianti. InsubriaUn. Press. Fot. Varesina. 48 p.

Stucchi, M., A. Rovida, A.A. Gomez Capera, P. Alexandre, T. Camelbeeck, M.B. Demircioglu, V. Kouskouna, P. Gasperini, R.M.W. Musson, M. Radulian, K. Sesetyan, S. Vilanova, D. Baumont, D. Fäh, W. Lenhardt, J.M. Martinez Solares, O. Scotti, M. Zivcic, P. Albini, J. Battlo, C. Papaioannou, R. Tatevossian, M. Locati, C. Meletti, D. Vigano, and D. Giardini (2013). The European Earthquake Catalogue (SHEEC) 1000-1899. Jour. Seis. doi:10.1007/s10950-012-9335-2.

LEARNING MORE ABOUT 1990 DECEMBER 13TH IN SOUTH-EASTERN SICILY: EARTHQUAKE SCENARIOSIN THE SIRACUSA URBAN AREA, ITALY

Panzera F., D'Amico S.[1], Lombardo G.[2]

[1]*Dipartimento di Scienze Biologiche, Geologiche e ambientali,Università di Catania, Italy,fpanzera@unict.it*
[2]*Department of Geosciences,University of Malta, Malta*

Introduction

  A deterministic scenario aiming to estimate the expected ground motion in south-eastern Sicily is assessed for the Siracusa urban district. The study areais made up by a thick crustal plateau belonging to the Africa foreland domain that eastward is separated from the Ionian Basin by the Malta–Hyblean fault system. Such tectonic structure, trending NW-SE, together with the NE-SW striking normal fault system, located inland (Scicli line), characterize at regional scale the tectonics of south eastern Sicily. Seismotectonic information and interpretations available suggest that both fault systems can be identified as possible sources for the seismic activity that affected in historical time the town of Siracusa.

  In particular, the largest seismic event is represented by the MW 7.4 shock occurred in 1693 and felt in all southern Italy (Rovida et al., 2011). The seismicity recorded during the last twenty years show epicentres sparsely located in all the area and the most important moderate size instrumental seismic event occurred on December 13th 1990. This shock was felt throughout Sicily with a maximum seismic intensity of VII-VIII (Locati et al., 2011). Although its moderate magnitude (MW=5.7; Rovida et al., 2011), it caused the collapse of a few buildings, about 20 persons were killed and about 15,000 were left homeless.

Geologic setting

  In the Siracusa area the substratum outlines a horst structure formed by a Meso-Cenozoic carbonate sequence with interbedded volcanics (Grasso &Lentini, 1982) cropping out in the northern part of the town (Fig. 1a). The Cretaceous volcanics locally represent the deepest term which is unconformably covered by a sub-horizontal carbonate sequence that stands for the lithotype more frequently cropping out in the Siracusa town. This sequence is distinguished in two main units, having similar geotechnical features, known in the literature as Mt. Climiti and Mt. Carruba formations. The former, having thickness ranging between 20 and 80 m, lies on the Cretaceous volcanics and consists of compact and well cemented calcarenites. The latter, with an average thickness of about 20 m, is characterized by alternating calcarenites and marlstones. In some sites the carbonate sequence is directly overlaid by sub-horizontal poorly consolidated calcarenites up to 20 m thick (Tortorici, 2000) whereas, in the southern part of the study area, sands and

sandy clays, up to 20 m thick, overlie the carbonate bedrock. Finally, alluvial deposits fill up the graben of the "Pantanelli" plain (see Fig. 1a) whilst detritus, having thickness of about 6-8 m, due to anthropic activity and historical ruins, is mainly outcropping in the Ortigia peninsula, the historical part of the town.
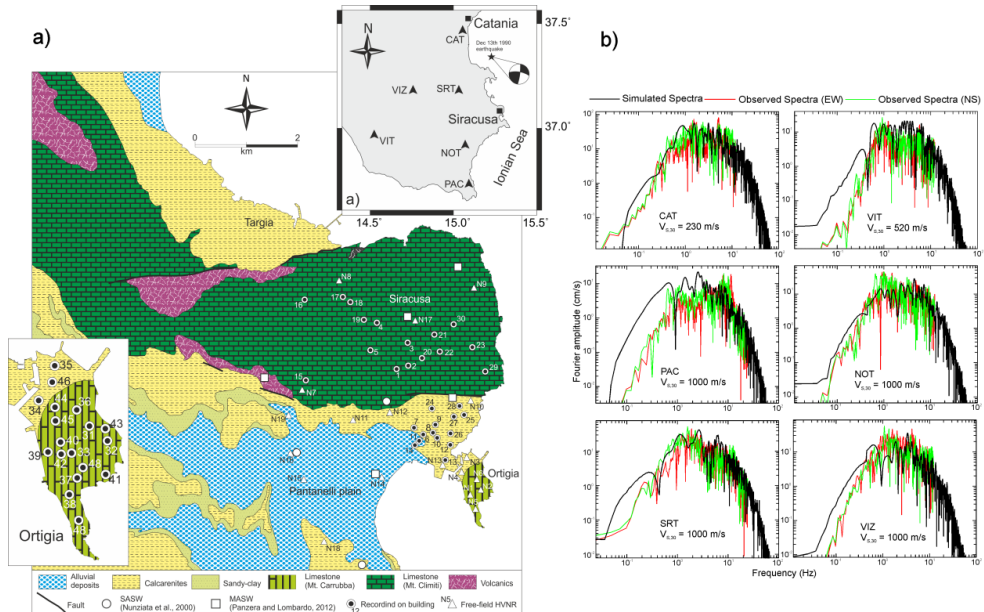
Figure 1. a) Geolithologic map of Siracusa urban area with the location of experimental measurements. In the lower left inset the location of buildings surveyed in Ortigia is shown. The upper right inset refers to geographic location of the scenario earthquake and spatial distribution of seismic stations in the study area. b) Simulated and observed Fourier spectra for the seismic stations. $V_{S,30}$ used for simulation are taken from ITACA (ITalian ACcelerometric Archive) database (website: itaca.mi.ingv.it).

Methodology

In the present study, we simulated the M_W=5.8 earthquake that occurred on 13th December 1990 off-shore of eastern Sicily (Amato *et al.* 1995; Di Bona *et al.* 1995; Rovida *et al.* 2011) on the Malta escarpment fault system. In order to predict the expected ground motion parameters in terms of peak ground acceleration (PGA), peak ground velocity (PGV) and Spectral Acceleration (SA) as a function of distance and magnitude we used the extended-source model code (EXSIM; Akinci *et al.* 2013; D'Amico *et al.* 2012; Boore 2009; Motezedian & Atkinson 2005). The dimensions of the fault were derived from the Wells and Coppersmith (1994) relations. We predicted the expected ground PGA, PGV and SA (at different frequencies) as a function of distance, magnitude and site-soil conditions. The Fourier acceleration amplitude spectrum of the ground motion at a distance *r*

from a source of seismic moment can be written as the product of the source spectrum S, the propagation term G and the site amplification term:

$$A(f, r, M) = S(f,M) \, G(r,f) \, Site(f) \quad (1)$$

In the finite fault simulation, the source term $S(f,M)$ is represented by a rectangular plane fault, whose dimensions are proportional to the moment magnitude M_W. The fault is discretized into a grid of rectangular sub-faults and the rupture is considered to begin at the centre of one of the sub-faults and to spread with a rupture velocity 0.8 times the shear wave velocity at the source. The acceleration time series from each sub-fault is derived by the inverse Fourier transform, and the time history at the site is obtained by summation of the individual time series, with appropriate time delays.
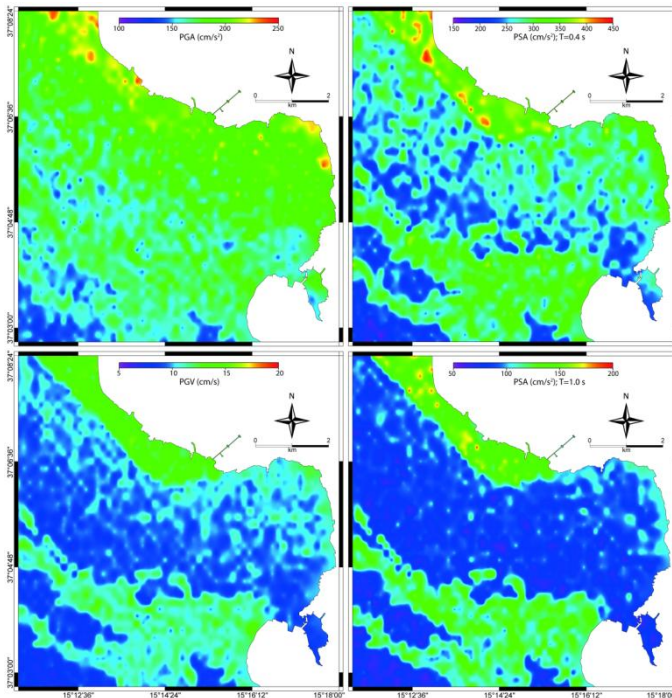
Figure 2. Contours of PGA, PGV and acceleration response spectral ordinates at 0.4 and 1.0 s period obtained for the 1990 earthquake scenario.

The propagation term $G(r,f)$ takes into account the geometrical spreading and the inelastic attenuation term. The regional propagation parameters for southeast Sicily (Scognamiglio et al., 2005) were also used. An important input parameter is the stress drop, which, if not properly calibrated, may cause differences in the ground motion levels, especially at short distances. In order to correctly represent the source characteristics we adopted a stress drop value of 210 bar as suggested by Di Bona *et al.* (1995). Furthermore, in order to create a reliable earthquake scenario we also considered the term *Site(f)* in the equation (1) to take

into account the effects due to the local geology. A generalized site response concept is indeed useful to create a detailed shaking map for a region where the different outcropping lithologies are known. In our simulation, to create a reliable earthquake scenarios, we considered the potential seismic effect due to the local geology using the site classification in term of V_{S30}, deriving the data from Nunziata *et al.* (2000) and Panzera & Lombardo (2013). The performance of our simulations were tested by computing the Fourier Amplitude spectra and comparing them with data of the Italian seismic network of strong motion stations, located in South eastern Sicily (see Fig. 1b and inset map in Fig. 1a for the seismic station locations). It can be easily observed that simulated spectra are in close agreement with those of the observations, therefore confirming that simulations provide reasonable estimates of the general shape and amplitudes of the spectra.

Results

Figure 2 shows the contouring of PGA, PGV and the PSA (at 5% critical damping) for periods of 0.4 and 1.0 sec, obtained through the EXSIM procedure for the considered scenario earthquake. They sets into evidence the important role played,in addition to the lithologic setting, by the azimuth and the source-to-site distance. The PGA values tend indeed to decrease towards the South, although they remain quite high due to the presence of soft sediments in the Pantanelli plain. On the other hand, the PGV map highlights the role played by the lithology especially in areas where the basement is mostly covered by soft sediments having thickness up to 50 m as in Targia area and the Pantanelli plain (see Fig. 1a). Using the relationship between the Mercalli–Cancani–Sieberg macroseismic intensity (I_{MCS}) and PGV proposed by Faenza & Michelini (2010) for Italian territory, our simulate values range between intensity VI and VIII, that are in good agreement with the intensity (VI-VII I_{MCS}) estimated for the 1990 earthquake (Locati *et al.* 2011). As concerns the effect of distance on the PSA evaluated at the selected periods (0.4 and 1.0 sec) it is interesting to observe that at periods of 0.4 s the PSA reaches values 150-450 cm/s^2. We have to remember that most of the RC and MA buildings erected in Siracusa consist of 2-4 stories, so that their fundamental period ranges between 0.2 and 0.4 s and consequently, they might suffer significant damage especially if not properly built or retrofitted. In terms of spectral accelerations, the MA building will be subject to an effect that is about 1.5 times greater than the RC one (see Fig. 2). So that it is important to take into account the source-to-site distance influence at lower periods rather than for periods of 1.0 s. On the other hand, a substantial hazard exists in the long period spectral ordinates for Targia and Pantanelli plains where large strains in the near surface terrains can imply the possibility of damage on tall and flexible structures.

To test out the results coming from the ground motion contour maps previously described, we compared them with findings from free-field horizontal to vertical noise spectral ratio (HVNR) obtained from records performed on the main lithotypes outcropping in the Siracusa area. HVNR show a good agreement with results coming from the analysis of the scenario earthquake. These outcomes

validate indeed the presence of local amplification effects on thick sedimentary terrains, pointing also out some critical behaviour in connection with some spots of the limestone formation, especially in Ortigia, and in sites where detritus outcrops. In conclusion, we have observed that major damage occurred during the 1990 earthquake are located in the Ortigia downtown area. This can be considered as the consequence of both the poor quality of some buildings and the local amplifications taking place especially on the sedimentary terrains. Such findings rather suggest that adetailed zonationoflimestoneshould be performed to identifyareas where the presence of detritus or significant rock fractures imply that they are susceptible to seismic amplification.

References

Akinci A, D'Amico S, Malagnini L, Mercuri A (2013) Scaling earthquake ground motions in western Anatolia, Turkey Phys Chem Earth. doi: 10.1016/j.pce.2013.04.013

Amato A, Azzara R, Basili A, Chiarabba C, Cocco M, Di Bona M, Selvaggi G (1995) Main shock and aftershocks of the December 13, 1990 Eastern Sicily earthquake. Ann Geofis 38(2): 255-266

Boore DM (2009) Comparing stochastic point-source and finite-source ground-motion simulations: SMSIM and EXSIM. Bull Seism Soc Am99:3202-3216

Di Bona, M, Cocco, M, Rovelli A, Berardi R, Boschi E (1995) Analysis of strong-motion data of the 1990 Eastern Sicily earthquake. Ann Geofis 38(2): 283-300

D'Amico S, Akinci A, Malagnini L (2012) Predictions of high-freqeuncy ground-motion in Taiwan based on weak motion data. Geophys J Int 189: 611-628, doi: 10.1111/j.1365-246X.2012.05367

Faenza L, Michelini A (2010) Regression analysis of MCS intensity and ground motion parameters in Italy and its application in ShakeMap. Geophys J Int 180:1138–1152

Grasso M, Lentini F (1982) Sedimentary and tectonic evolution of the eastern Hyblean Plateau (southeastern Sicily) during late Cretaceous to Quaternary time. Paleogeogr Paleoclimatol Paleoecol 39: 261–280

Locati M, Camassi R, Stucchi M (2011) DBMI11, the 2011 version of the Italian Macroseismic Database. Milano, Bologna, http://emidius.mi.ingv.it/DBMI11

Motazedian D, Atkinson GM (2005) Stochastic finite-fault modelling based on a dynamic corner frequency. Bull Seism Soc Am 95: 995-1010

Nunziata C, Centamore C, Natale M, Spagnuolo R (2000) Caratterizzazione sismica delle onde di taglio dei terreni superficiali di Noto, Augusta e Siracusa. In: Decanini L, Panza GF (eds) Scenari di pericolosità sismica ad Augusta, Siracusa e Noto, CNR-Gruppo Nazionale per la Difesa dai Terremoti, Roma pp 55-67

Panzera F, Lombardo G (2013) Seismic property characterization of lithotypes cropping out in the Siracusa urban area, Italy. Eng Geol 153: 12–24

Rovida A, Camassi R, Gasperini P, Stucchi M (2011) CPTI11, the 2011 version of the Parametric Catalogue of Italian Earthquakes. Milano, Bologna, http://emidius.mi.ingv.it/CPTI

Tortorici L (2000) Geologia delle aree urbane della Sicilia Orientale. In: Decanini L, Panza GF (eds) Scenari di pericolosità sismica ad Augusta, Siracusa e Noto, CNR-Gruppo Nazionale per la Difesa dai Terremoti, Roma, pp 43-54

A REGIONAL EARTHQUAKE EARLY WARNING SYSTEM: PRESTO@CE3RN

Pesaresi, D.[1], Picozzi, M.[2], Živčić, M.[3], Lenhardt, W.[4], Mucciarelli, M.[1], Elia, L.[2], Zollo, A.[2], Gosar, A.[3]

[1]*OGS CRS, Borgo Grotta Gigante 42/C 34010 Sgonico (TS) ITALY, dpesaresi@inogs.it*
[2]*RISSC Università "Federico II" di Napoli – AMRA,via Cintia 80126 Napoli ITALY, matteo.picozzi@unina.it*
[3]*ARSO, Vojkova 1b 1000 Ljubljana SLOVENIA, mladen.zivcic@gov.si*
[4]*ZAMG, Hohe Warte 38 1190 Vienna AUSTRIA, wolfgang.lenhardt@zamg.ac.at*

Introduction

With the aim of monitoring the seismic activity in the eastern sector of the Alps, since 2001 OGS (Istituto Nazionale di Oceanografia e di Geofisica Sperimentale, Bragato et al., 2011) in Udine (Italy), the Agencija Republike Slovenije za Okolje (ARSO) in Ljubljana (Slovenia), the Zentralanstalt für Meteorologie und Geodynamik (ZAMG) in Vienna (Austria), and the University of Trieste (UniTS) have been collecting, analyzing, archiving and exchanging seismic data in real time. The data exchange has proven to be effective and very useful in the case of seismic events at the borders between Italy, Austria and Slovenia, where the poor coverage of individual national seismic networks precluded a precise earthquake location. The usage of common data from the integrated networks improves significantly the overall capability of real-time event detection and rapid characterization in this area. Furthermore, in 2014, OGS, ARSO, ZAMG and UniTS signed a memorandum of understanding naming the cooperative network as the Central and Eastern European Earthquake Research Network (CE3RN) (Bragato et al., 2014).

Recently, in order to extend the seismic monitoring in north-eastern Italy, Slovenia and southern Austria towards earthquake early warning applications, OGS, ARSO and ZAMG teamed up with the RISSC-Lab group (http://www.rissclab.unina.it/) of the Department of Physics at the University of Naples Federico II in Italy.

An Earthquake Early Warning System (EEWS) is a real-time system integrating seismic networks and software capable of performing real-time data telemetry and analysis in order to issue alert messages within seconds from the origin of an earthquake and before the destructive S-waves generated by the event reach the users. When accompanied by appropriate training and preparedness of the population, an EEWS is an effective and viable tool for reducing the exposure of a population to seismic risk (Satriano et al., 2008 and 2010b). The collaboration among OGS, ARSO, ZAMG and RISSC-LAB focuses on testing the EEW platform PRESTo (PRobabilistic and Evolutionary early warning SysTem: http://www.prestoews.org/) in north-eastern Italy, Slovenia and Austria at the

network CE3RN, and represents the first attempt worldwide of implementing a trans-national EEWs. PRESTo is a stand-alone software system that processes live accelerometric streams from a seismic network to promptly provide probabilistic and evolutionary estimates of location and magnitude of detected earthquakes while they are occurring, as well as shaking prediction at the regional scale (Satriano et al., 2010a).

Since 2014 PRESTo has run on OGS, ARSO and ZAMG data, by collecting and analysing in real time the data streams from 20 stations (Fig. 1, Picozzi et al., 2014a, 2014b and 2015). In the following, first we briefly present the CE3RN project and we summarise the characteristics of EEWS and PRESTo, then we report on the performance of the EEW system during this first testing phase.
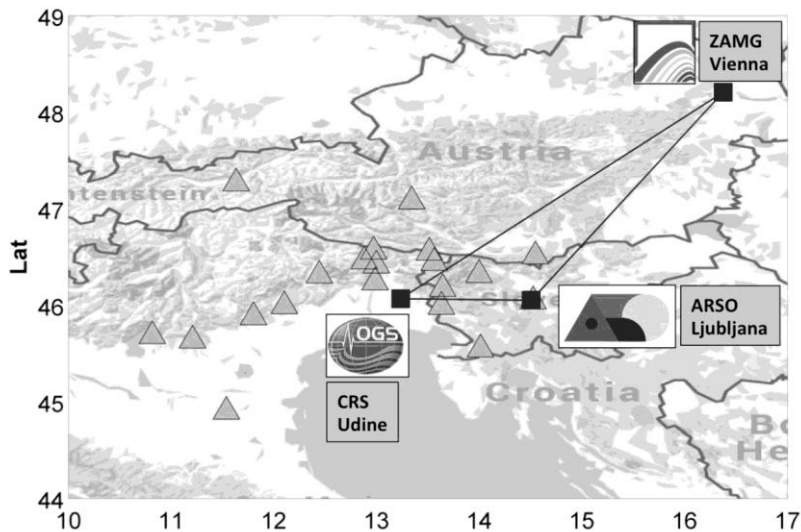
Figure 1. CE^{3}RN institutions involved in the EEW experiment (squares), real-time accelerometric stations (triangles).

Earthquake early warning systems and PRESTo

EEWS typically follows two basic approaches: "regional" (or network based), and "on-site" (or a single station). Regional EEWS are based on the use of a seismic network located near one or more expected epicentral areas, whose aim is to detect and locate an earthquake, and to determine its magnitude from the analysis of the first few seconds of the arriving P-waves at multiple stations close to the epicentre (Satriano et al., 2010b). On the other hand, on-site EEWS are based on seismic sensors deployed directly at the target site and exploit only the information carried by the faster early P-waves to infer the larger shaking related to the incoming S and surface waves. One key parameter for an EEWS is the lead time, i.e. the time available to perform safety measures at distant targets once an earthquake has been promptly detected and characterised, and an alarm has been issued. The lead time for regional EEWS is defined as the travel-time difference

between the arrival of the first S-waves at the target site and the P-waves recorded in the source area, after accounting for the necessary computation and data transmission times. In onsite EEWS, the lead time is equal to the difference in S- and P-wave arrival times at the target itself.

PRESTo is a free and open source, highly configurable and easily portable platform for earthquake early warning (Iannaccone et al., 2010). PRESTo processes the real-time accelerometric data streams from the stations of a seismic network to promptly detect the P-wave arrival, provide the probabilistic and evolutionary estimates of location and magnitude of earthquakes while they are occurring, as well as the shaking prediction on a regional scale. Alarm messages containing the continuously updated estimates of source and ground motion at target parameters, and their associated uncertainties, are sent over the Internet, and can thus also reach distant vulnerable infrastructures before the arrival of destructive waves, enabling the activation of automatic safety procedures.

PRESTo performance on CE[3]RN

Since the beginning of 2014, PRESTo (version 0.2.7) has been under experimentation in the transnational area including north-eastern Italy, Slovenia and Austria. During this preliminary test phase, in order to avoid overloading the Antelope system managing the CE[3]RN, a dedicated SeisComP server has been set up at the OGS CRS data centre in Udine with the aim of collecting and converting in SeedLink the data of 20 accelerometric stations from the Antelope system (Fig. 1), and pushing them towards a dedicated PRESTo system at RISSC-Lab in Naples. After an initial period during which we tested different setups of the system parameters, since the end of March 2014 we have been experimenting with the velocity model used for routine earthquake analysis and bulletin production at OGS (OGS, 1995–2014); a minimum number of five stations required to trigger within 12 s for event declaration; the coefficients of the empirical correlation laws between the peak displacement (Pd) measured on short time windows of P-waves and the earthquake magnitude (M) estimated by Lancieri and Zollo (2008); and the Akkar and Bommer (2007) ground motion prediction equation. Since the station distribution has a key role in determining the resilience of a system, that is to say the network rapidity in issuing EEW alerts, we estimated for the CE[3]RN Network the time of the first alert and the blind-zone extent when three stations have triggered. The analysis was carried out considering a grid of virtual seismic sources (i.e. a node each of 0.05 for a total of 9801 nodes) with a fixed depth at 6.4 km. Concerning the real-time testing of the EEWS, since the end of May 2014, that is to say when a stable configuration of the EEWS was found, PRESTo (version 0.2.7) detected in real time 23 earthquakes, while one event was missed.

The performance of the system in locating the earthquakes has in general been very good, with 18 events out of 23 located within 10 km of the authoritative value. Only in one case is the discrepancy between 10 and 50 km, and in four cases it is larger than 50 km.
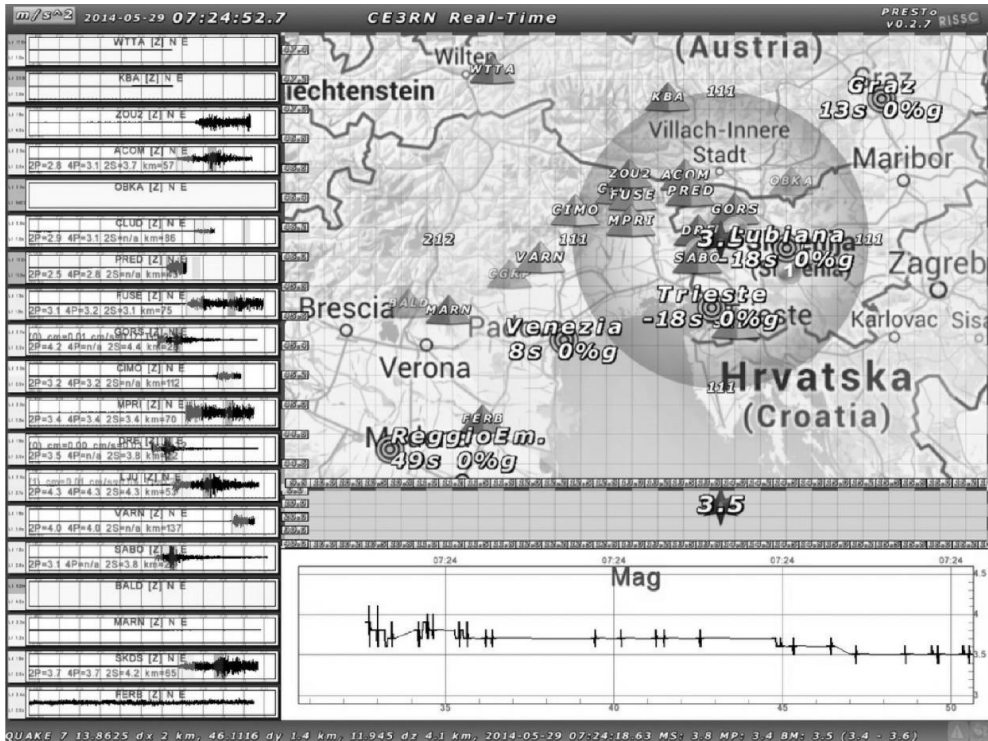
Figure 2. Snapshot of the PRESTo system during the 29 May 2014 M_{LD} 3.8 Slovenian earthquake.

Conclusions

During the period May–December 2014, PRESTo detected in real time 23 earthquakes in the magnitude range 1.7 to 4.1, of which 14 were correctly detected, while 4 and 3 events resulted in missed and false alerts, respectively. Despite the testing period still being too short to come up with definitive conclusions, it seems that the EEWS given by the integration of PRESTo and CE[3]RN is efficient with respect to earthquakes that occur nearby the area with higher station density.

Nevertheless, more testing and an improvement in the system are necessary to cope with events occurring out of the network, and in general where it has a lower station density. With respect to this last issue, we are evaluating to increase the network density, including in the EEWS also stations with velocimetric sensors.

Acknowledgements

References

Akkar, S. and J. J. Bommer (2007). Empirical prediction equations for peak ground velocity derived from strong-motions records from Europe and the Middle East, Bull. Seismol. Soc. Am., 97, 511–530.

Bragato, P. L., G. Costa, A. Gallo, A. Gosar, N. Horn, W. Lenhardt, M. Mucciarelli, D. Pesaresi, R. Steiner, P. Suhadolc, L. Tiberi, M. Živčić, and G. Zoppé (2014). The Central and Eastern European Earthquake Research Network – CE3RN, EGU General Assembly 2014, 27 April–2 May 2014, Vienna, Austria.

Bragato, P. L., P. Di Bartolomeo, D. Pesaresi, M. P. Plasencia Linares, and A. Saraò (2011). Acquiring, archiving, analyzing and exchanging seismic data in real time at the Seismological Research Center of the OGS in Italy, Annals of Geophysics, 54(1), 67-75, doi:10.4401/ag-4958.

Iannaccone, G., A. Zollo, L. Elia, V. Convertito, C. Satriano, C. Martino, G. Festa, M. Lancieri, A. Bobbio, T. A. Stabile, M. Vassallo, and A. Emolo (2010). A prototype system for earthquake early-warning and alert management in southern Italy, Bull. Earthq. Eng., 8, 1105–1129, doi:10.1007/s10518-009-9131-8.

Lancieri, M., and A. Zollo (2008). Bayesian approach to the realtime estimation of magnitude from the early P and S wave displacement peaks, J. Geophys. Res., 113, B12302, doi:10.1029/2007JB005386.

OGS (1995-2014). Bollettino della Rete Sismometrica del Friuli–Venezia Giulia e del Veneto, OGS (Istituto Nazionale di Oceanografia e di Geofisica Sperimentale), Centro di Ricerche Sismologiche, Udine, Italy.

Picozzi, M., L. Elia, A. Gosar, W. Lenhardt, M. Mucciarelli, D. Pesaresi, M. Živčić, and A. Zollo (2014). Testing the "PRESTo" Early Warning Algorithm in North-Eastern Italy, Austria and Slovenia: update analysis, in: Proceedings of the Second European Conference on Earthquake Engineering and Seismology, Istanbul, Turkey, 24-29 August 2014, doi:10.13140/2.1.2396.0962.

Picozzi, M., L. Elia, D. Pesaresi, A. Gosar, W. Lenhardt, M. Mucciarelli, M., Živčić, and A. Zollo (2014). Application of the "PRESTo" Earthquake Early Warning (EEW) and Alert Management System in North-Eastern Italy, Slovenia and Austria: experience with the CE3R Network, in: Proceedings of XXXIII GNGTS, Bologna, Italy, 25-27 November 2014, ISBN 978-88-940442-0-1, Tema 2: Caratterizzazione sismica del territorio, 464-469, ISBN 978-88-940442-2-5, doi:10.13140/2.1.2242.2087.

Picozzi, M., L. Elia, D. Pesaresi, A. Zollo, M. Mucciarelli, A. Gosar, W. Lenhardt, and M. Živčić (2015). Trans-national earthquake early warning (EEW) in north-eastern Italy, Slovenia and Austria: first experience with PRESTo at the CE3RN network, Adv. Geosci., 40, 51-61, doi:10.5194/adgeo-40-51-2015.

Satriano C., L. Elia, C. Martino, M. Lancieri, A. Zollo, and G. Iannaccone (2010). PRESTo, the earthquake early warning system for Southern Italy: concepts, capabilities and future perspectives, Soil Dynam. Earthq. Eng, http://dx.doi.org/10.1016/j.soildyn.2010.06.008.

Satriano, C., A. Lomax, and A. Zollo (2008). Real-Time Evolutionary Earthquake Location for Seismic Early Warning, Bull. Seismol. Soc. Am., 98, 1482–1494, doi:10.1785/0120060159.

Satriano, C., Y.-M. Wu, A. Zollo, and H. Kanamori (2010). Earthquake early warning: Concepts, methods and physical grounds, Soil Dynam. Earthq. Eng., 31, 106–108, doi:10.1016/j.soildyn.2010.07.007.

SUBMARINE EARTHQUAKE GEOLOGY AS A TOOL FOR SEISMIC HAZARD ASSESSMENT IN THE CENTRAL MEDITERRANEAN SEA: POTENTIAL, LIMITS, TECHNIQUES AND RESULTS

Polonia, A.[1], Romano, S.[1], Vaiani, S.[2], Gasparotto, G.[2], Torelli, L.[3], Gasperini, L.[1]

[1]*Institute of Marine Sciences (ISMAR-CNR), Bologna, Italy,*
alina.polonia@ismar.cnr.it

[2]*Dipartimento di Scienze Biologiche, Geologiche e Ambientali, University of Bologna, Italy stefano.vaiani@unibo.it*

[3]*Dipartimento di Fisica e Scienze della Terra "Macedonio Melloni", University of Parma, lutor@unipr.it*

Introduction

Paleoseismology is the investigation of individual earthquakes from their geological signatures such as those produced directly along the rupture plane, and those produced indirectly (landslides and, in general, mass wasting processes in the vicinity of faults). If dateable material is recovered from stratigraphic horizons that experienced successive ruptures, slip rate and time separation between large earthquakes can be reconstructed. Earthquake geology has been widely applied to major continental faults over the past decades. While paleoseismology has become a primary tool for seismic hazard evaluation on land, only few paleoseismological studies have been attempted on submarine fault systems, mainly because of the limited resolution of the available geophysical techniques used at sea. Rapid developments in imaging and sampling techniques have now made such studies possible. Submarine paleoseismological studies have the following advantages compared to those undertaken on land: (i) marine sedimentation is generally more continuous in time and space, allowing for regional stratigraphic correlations; (ii) offshore data can be acquired more quickly. Innovative techniques have been developed to make submarine paleoseismology feasible (see bibliography below). They include (i) high-resolution morphobathymetric images of the sea floor, (ii) 3-D and pseudo-3D high resolution seismic reflection imaging, and (iii) detailed stratigraphic reconstruction of the sedimentary record. Although submarine geophysical data have lower resolution than trenching, they provide complete spatial coverage of fault structures, both horizontally and vertically. This will allow accurate long time-scale, high-resolution reconstruction of fault-zone evolution. During the last years, during a number of oceanographic expeditions with R/V CNR Urania, we applied such methodology to the Calabrian Arc (CA) and surrounding areas of the central Mediterranean Sea which is characterised by a very high seismic and tsunami hazard since it has been struck repeatedly by very strong historical earthquakes and tsunamis (365, 1169, 1542, 1624, 1693, 1783, 1905, 1908, often associated with destructive tsunami).

Interplay between seismic shaking, tsunamis and mass flows

Submarine geohazards such as major earthquakes, tsunamis, volcanic eruptions, volcanic flank collapse and submarine landslides are isolated and exceptional events capable of producing large-volume turbidites that result from catastrophic submarine slope failures and the associated downslope mass transport of enormous quantities of sediment from continental shelves and slopes to the deep sea.

In this study we analyse Africa/Eurasian convergence processes in the Ionian Sea (Polonai et al., 2011) and the interplay between tectonics and sedimentation through an integrated approach involving the interpretation of geophysical data at different scales and well targeted sediment samples. The CA region has been struck repeatedly by destructive historical earthquakes (1908, 1905, 1783, 1693, 1159) but knowledge of causative fault source parameters is relatively poor. In our approach, high penetration multi-channel seismic data unravelled the overall geometry and tectonic evolution of the subduction complex while single fault strand dynamics have been reconstructed through the analysis of high resolution geophysical data. On the other hand, the integrated analysis of sediment samples collected in the abyssal plain and slope basins, highlight the occurrence of anomalous sedimentary deposits (i.e. turbidites, debris flow and mass wasting deposits) during historical times and the likely relationships between active tectonics and sedimentation.

Ionian Sea seismoturbidites: 1908, 1693 and 1908 earthquakes

Gravity cores contain the eastern Mediterranean hemipelagic sequence interbedded with redeposited units characterised by coarse and/or graded layers. Three recent turbidite sequences have been analysed in two different cores. Sedimentological and micropaleontological findings together with radiometric dating below and/or above key-layers outlined that turbidite emplacement may be related with the occurrence of major earthquakes in the area (1169, 1693 and 1908 events). Sediment composition deduced by mineralogical analysis and SEM observations unravel the source region of the different turbidite beds and identify the links between sedimentary or tectonic preconditioning factors and the occurrence of the catastrophic event (Polonia et al., 2013a). Our findings suggest that during historical times 90% of sedimentation in the deep sea basins is related to catastrophic events and, similarly to other active margins, the turbidites deposited in the Ionian Sea may be considered the result of paleo-earthquakes occurrence. The surveying techniques and approaches used in this study have therefore the potential of documenting earthquake ruptures of fault segments, extending the earthquake record far before the known history. Moreover, the regional analysis of sediment samples is useful to understand if the recurrence time of major catastrophic events is constant and which portions of the Arc have experienced great earthquakes in the past thus improving hazard evaluations and

the fundamental understanding of earthquake process in this highly populated region of the central Mediterranean.

The AD 365 Crete earthquake

Destructive earthquakes/tsunamis have affected repeatedly the circum Mediterranean highly populated coastal regions. A record of these past events can be provided by large-volume turbidites or megaturbidites, detected in the marine sedimentary record. Megaturbidites have been identified in the Ionian basin (central Mediterranean) that is located between two tectonically active subduction zones (i.e. the Calabrin Arc to the North and the Hellenic Arc to the East). The uppermost megabed, has been named "Homogenite" (Kastens and Cita, 1981) or "Augias turbidite" (Hieke, 1984). Its well defined stratigraphic position, above the regional marker sapropel bed S1, has been interpreted as evidence that it was deposited in a single, basin-wide event capable to put into suspension simultaneously sediment at a basin-wide scale. Absence of absolute dating of the megabed and of a detailed chronostratigraphy of the deposits above and below the turbidite, have allowed a number of different correlations of this megaturbidite with the 3500 yr BP Minoan eruption of Santorini and related tsunamis in the Aegean Sea (Kastens and Cita, 1981), to the 7.600 ± 130 yr B.P. collapse of a flank of the Etna Volcano (Pareschi et al., 2006) or to the 365 earthquake in the Mediterranean (Vigliotti, 2008). Based on studies of sediment cores we collected from the Ionian sea floor (mineralogy, micropaleontology, elemental and isotopic geochemistry and radiocarbon dating), we show that the Homogenite/Augias turbidite (HAT), up to 20-25 m thick, was related to multi-source turbidity flows triggered by the 365 AD tsunami (Polonia et al., 2013b). We were able to reconstruct the different units deposited in response to the 365 AD Cretan earthquake/tsunami and the results confirm that the HAT is a unique instance of deep sea tsunami deposit. Backwash flows and related gravity-driven processes are the primary means of downslope sediment transport. An older similar deep sea megaturbidite was deposited in the Ionian Sea about 15.000 years B.P., implying a large recurrence time of such extreme sedimentary events in the Mediterranean Sea.

Conclusions

The Ionian Sea is a landlocked basin where convergence between Africa and Eurasia produced the emplacement of two opposite verging subduction/rollback systems (i.e. the Calabrian and the Hellenic Arcs). It is one of the most seismically active regions in the Mediterranean Sea and has been struck repeatedly by destructive historical earthquakes, often associated with tsunamis.Slab tearing in a pre-collisional setting is reflected in dynamic topography with high uplift rates of the coastal mountain belts, accompanied with a great sediment discharge to the continental margins. This increases the susceptibility to mass failures implying a strong interplay between active tectonics, seismic shaking, mass flows and tsunami generation. We investigated the effects of historic

144

earthquakes on abyssal marine sedimentation through the analysis of the turbidite record in tectonically controlled basins. Holocene resedimented units in the deep Ionian Sea represent more than 90% of the total thickness of the sedimentary record. We dated the most recent turbidite sequences using different radiometric methods and the results suggest that turbidite emplacement was triggered by major historic earthquakes and tsunamis recorded in the region (i.e. AD 365 Crete and AD 1169, 1693 and 1908 Italian earthquakes). Textural, micropaleontological, geochemical and mineralogical signatures reveal that turbidite beds are stacked sandy units, which have different compositions suggesting coeval multiple failures. They are characterized by organic-rich sandy layers, containing a mixture of lithic clasts, plant fragments and displaced benthic foraminifera derived from several sources and bathymetric ranges. Structure and composition of each turbidite unit, combined with geochemical and isotopic analysis on organic carbon, are being refined to unravel the relative contribution of seismic shaking and tsunami wave loading on mass flow processes generation. Turbidites may be considered as the sedimentary earthquake code within the background pelagic sedimentation (Polonia et al., 2015). Deciphering this code aims at reconstructing paleo-seismicity during several earthquake cycles, a time span long enough to perform reliable seismic and tsunami hazard assessment in tectonically active coastal regions.

References

Hieke, W., 1984, Thick Holocene homogenite from the Ionian abyssal plain (Eastern Mediterranean): Marine Geology, v. 55, p. 63–78.

Kastens, K.A., and Cita M.B., 1981, Tsunami-induced sediment transport in the abyssal Mediterranean Sea: Geological Society of America Bulletin, v. 92, p. 845–857.

Pareschi, M.T., Boschi, E., and Favalli, M., 2006, Lost tsunami: Geophysical Research Letters, v. 33, p. L22608.

Polonia, A., Torelli, L., Mussoni, P., Gasperini, L., Artoni, A. and Klaeschen D., 2011, The Calabrian Arc subduction complex in the Ionian Sea: Regional architecture, active deformation, and seismic hazard, Tectonics, 30, TC5018, doi:10.1029/2010TC002821.

Polonia, A., Torelli, L., Gasperini, L., and Mussoni, P., 2012, Active faults and historical earthquakes in the Messina Straits area (Ionian Sea), Nat. Hazards Earth Syst. Sci., 12, 2311-2328, doi:10.5194/nhess-12-2311-2012.

Polonia, A., Bonatti, E., Carmelenghi, A., Lucchi, R.G., Panieri, G., and Gasperini, L., 2013a, Mediterranean megaturbidite triggered by the AD 365 Crete earthquake and tsunami: Scientific Reports, 3, Article number 1285, doi:10.1038/srep01285.

Polonia, A., Panieri, G., Gasperini, L., Gasparotto, G., Bellucci, L.G., and Torelli, L., 2013b, Turbidite paleoseismology in the Calabrian Arc Subduction Complex (Ionian Sea): Geochemistry, Geophysics, Geosystems, v. 14, no. 1, doi 10.1029/2012GC004402.

Polonia, A., Romano, S., Çağatay, M.N., Capotondi, L., Gasparotto, G., Gasperini, L., Panieri, G., and Torelli, L., 2015, Is repetitive slumping during sapropel S1 related to paleo-earthquakes?: Marine Geology, v. 361, p. 41–52.

THE 1976 GUATEMALA EARTHQUAKE REVISED. MACROSEISMIC DATA FOR AN APPROPRIATE SEISMIC HAZARD ASSESSMENT

Porfido S.[1], Caccavale M.[2], Spiga E.[3], Sacchi M.[4]

[1]*CNR-IAMC, Calata Porta di Massa, Interno Porto, 80133 Napoli, Italy .*
Sabina.Porfido@iamc.cnr.it
[2] *CNR-IAMC, Calata Porta di Massa, Interno Porto, 80133 Napoli,*
Italy.Mauro.caccavale@iamc.cnr.it
[3] *Independent Researcher, Avellino, Italy, spiga.efisio@gmail.com*
[2] *CNR-IAMC, Calata Porta di Massa, Interno Porto, 80133 Napoli, Italy-*
Marco.sacchi@iamc.cnr.it

Preface

The recent tragic news from Nepal, hit by a devastating earthquake of magnitude 7.8, on April 25th, 2015 reveal, once again, a dramatic seismic scenario: the loss of thousands of lives and the destruction of the architectural heritage of entire cities and villages, dramatic environmental effects triggered by the earthquake. Among these, especially landslides have played a major role, by changing the morphology of some valleys, erasing villages, obstructing rivers, creating new lakes and destroying vital infrastructures. The contribution that the scientific community can offer is with no doubt manifold. It includes, assistance in the reconstruction of a cultural heritage and provides all the scientific methods for the mitigation of seismic risk of the region. In this perspective, the study of earthquakes can be examined through the intensities assessment evaluation, not only on the basis of damage caused to buildings and artefacts, but also by taking into account the seismic-induced effects, on natural landscape, such as primary and secondary environmental effects triggered by earthquakes, according to the new macroseismic scale ESI 2007 (Michetti et al., 2007). This would, indeed, be a fundamental contribution to the mitigation of seismic risk of territories affected by earthquakes, as it may provide a more realistic and ethically correct scenario of damage, based on a set of criteria that are largely independent from the socio-economic issues.

Introduction and methodology

Guatemala has repeatedly suffered from several dramatic earthquakes during the last century. The most destructive event associated with the Motagua fault, occurred on February 4th, 1976 (M=7.5), that caused 23,000 deaths, and 77,200 injuries and produced severe damage over a wide area of the country. The seismic sequence was characterized by a main shock at 04 09:01 UTC, M 7.5 followed by a few days of important aftershocks (Mb = 5.8), such as February 6th, and March 7th, 1976, near Guatemala City (Person et al., 1976). The estimated intensity was relatively low (Imax= IX MM, only in few localities), despite the high degree of damage and the spectacular environmental effects triggered by the

earthquake, including a 230 km strike-slip fault with average displacement of 1.1 m, a large number of landslides, numerous liquefaction phenomena, ground cracks and ground deformation spread over an area of about 18,000 (Espinosa,1976; Plafker, 1976; Harp et al., 1976).

The aim of this study is to analyse the primary and secondary earthquake environmental effects, in order to assess the local intensities according to the ESI scale 2007 (Michetti et al., 2007) thus drawing the new macroseismic field for a more appropriate strategy in the future strategy of seismic hazard evaluation of the region. The ESI 2007 (Environmental Seismic Intensity) scale (Michetti et al., 2007; Audemard et al., 2015), ratified by the INQUA (International Union for Quaternary Research) during the XVII Congress in Cairns (Australia) is a new macroseismic scale that measures the seismic intensity on the basis of the effects induced by earthquakes on the environment. The ESI scale integrates the traditional macroseismic scales, of which it represents the evolution, allowing to assess the intensity parameter also where buildings are absent or damage-based diagnostic elements saturate, solely on the bases of environmental effects.The ESI scale is a 12-degree scale: each degree reflects the corresponding strength of an earthquake and provides a measure of the Intensity on the basis of its characteristics. The main advantage of the ESI 2007 scale is the classification, quantification, and measurement of several known geological, hydrological, geomorphological and botanical features that are associated with each intensity degrees. The scale has been tested in the case of several modern, historical and paleoearthquakes (Silva et al. 2008; Reicherter et al. 2009; Lekkas 2010; Papanikolaou 2011; Encyclopedia of Natural Hazards, Bobrowsky (Ed) 2013, Audemard et al., 2015; Porfido et al., 2015b).

Geological framework and historical seismicity

The tectonic setting of the Central American region is characterized by the interaction of three major lithospheric plates: the Cocos, the Caribbean and the North American plates. In this region relative plate motions varies between 2-9 cm/yr and is accompanied by active volcanism and shallow and intermediate seismicity. The largest earthquakes are produced along the subduction zone of the Cocos and Caribbean plates in the Middle America Trench of the Pacific Ocean (Benito et al. 2012). Over the past 40 years, Guatemala and neighboring areas have experienced 50 events with Mw $\geq$ 6, out of which 2 with Mw > 7 (USGS data). Large earthquakes are also produced along the boundary between the North American and the Caribbean plates, defined by a zone of large left lateral strike–slip faults (Chixoy-Polochic fault, Motagua fault etc.) that run through the Guatemala from the Swan Fracture Zone in the Caribbean Sea. The earthquakes generated along these transcurrent faults, have a great importance for seismic hazard in Central America, more than the subduction-related earthquakes, because of their shallow hypocentres and the proximity of many cities and villages to these active structures. The most destructive event in this region was the earthquake associated with the Motagua fault, that occurred on 4th of February 1976 causing

23,000 deaths, and 77,200 injuries. The total number of houses destroyed was 258,000, and 1.2 million people were left homeless (Espinosa, 1976). Destructive historical earthquakes have been reported in detail for Guatemala since 16th century (Espinosa, 1976; Ambraseys & Adams 1996). There are at least 18 events, with 5.6≤M≤7.9 that induced environmental effects, mostly slope movements, followed by ground cracks, ground settlements, hydrological changes, topographic changes, tsunami and in some cases surface faults. In addition to the aforementioned event 1976, the largest earthquakes occurred in 1902 (M=7.5) and in 1942 (M=7.9).

The event of 19th April 1902 had its epicentre in Quetzaltenango. It triggered landslides and ground fractures within the epicentral area, in Sololà and along the slope of the Agua and Cerro Quemado volcanoes. Significant slope movements dammed the Naranjo and Ixtacapa Rivers, while in Ocos liquefaction and settlement phenomena were observed. The earthquake of August 6th, 1942 earthquake, with the epicentral zone off the southern coast of Guatemala, also induced many landslides and destruction along the west-central highlands in the country. Slope movements affected the Pan-American Highway and secondary roads. Many ground settlements, especially in the western Pacific coast region also occurred (Ambraseys & Adams 1996; Bommer &. Rodrıguez 2002).

The 4th February, 1976 earthquake

This earthquake (Mw = 7.5) had its epicentre near Los Amates, about 157 km NE of Guatemala City, and according to Espinosa et al. (1976) the maximum estimated intensity was IX MM in Gualan, in the Mixco area and in the centre of Guatemala City, in spite of the high level of damage, testified by the total destruction (100 % of houses) of a series of towns and villages, such as Gualan, Parramos, Patzicia, El Progreso, Rabinal, San Jose Poaquil, San Martin Jilotepeque, etc. and notwithstanding the large and spectacular environmental ground effects induced by event (Espinosa et al. 1976; Harp et al, 1976; Plafker et al., 1976). In order to assess local intensities according to the ESI 2007 scale we have analysed the earthquake environmental effects (EEE) reported from several papers (Harp et al. 1981, Harp et al. 2011; Hoose et al., 1976; Plafker et al. 1976; Plafker 1976 etc). Localities with diagnostic EEEs are24 (Table 1). The resulting ESI intensities range between VII and XI.ESI intensities have been evaluated on the basis of primary effect (e.g. surface faulting) as well as secondary effects (slope movements, liquefaction and ground rupture features). A main strike-slip fault was identified in the Motagua Valley and the mountainous area West of the valley, from Quebradas to Patzaj, with a total length of 230 km, and maximum horizontal displacement of 3.40 m with an average value of ca. 1 m (Plafker et al. 1976). Secondary surface faults were observed in the Mixco area and in the western part of Guatemala City, with total length of about 10 km and maximum displacement of a few centimeters (Plafker et al. 1976). According to Harp et al. (2011), secondary effects were mostly represented by landslides (estimated in a number of ca. 50.000), including falls, debris slides and flows, which involved rocks as well as

thick pumiceous pyroclastic deposits over an area of ca. 16,000 km^2 of total area affected.

Table 1. The localities affected by Earthquake Environmental Effects: SF Surface Faulting, SM Slope Movements, GC Ground Cracks, L Liquefaction phenomena, GS Ground Settlements, and the macroseismic evaluation according to the ESI2007 and MM scales.*Locality out of Guatemala.

Locality	Type of effect	ESI Intensity	MM Intensity
Cabanas	SF, GC	XI	VIII
Chuarrancho	SF, GC	XI	VIII
El Progreso	S F, GC	XI	VIII
Gualan	SF, GC	XI	IX
Quebradas	SF, GC, L	XI	VIII
Subinal	SF, GC	XI	VIII
Estancia de la Virgen	SM, GC	X	VIII
San Martin Jilotepeque	SM, GC, L	X	VIII
San Josè Poaquil	SM, GC	X	VIII
Puerto Barrios	SF, GS, GC	IX	IX (VI)
Finca San Carlos	SF, SM, GC	IX	VIII
Guatemala City	SF, SM, GC	IX	VII-VIII
Los Choloyos	SM, L, GC	IX	VII-V
Mixco Area	SF, GC, SM	IX	VII-VIII
Rio Blanco	SM, GC	IX	VII
Rio Cotzibal	SM, GC	IX	VIII
Rio Los Cubes	SM, GC	IX	VIII
Rio Naranjo	SM, GC	IX	VIII
Rio Polima	SM, GC	IX	VIII
Rio Ruyalchè	SM, GC	IX	VIII
Rio Teocinte	SM, GC	IX	VIII
Lake Amatitlan	SM, L, GC, GS	VIII	V (VII)
Lake Atitlan	SM, L, GC, GS	VII	V (VI)
Lake Ilopango*	SM, L, GC	VII	V

Slope instability involved the bedrock as well as a thick cover of volcanoclastic deposits mostly deriving from small to moderate-size and in some cases large-size slope failure (V>100.000 m^3). Lateral spreads and liquefaction phenomena occurred in the Motagua valley, along Atlantic coast of Guatemala and Honduras, as well as along the shores of Lakes Amatitlan, Atitlan and Ilopango, in El Salvador.

Discussion and conclusions

In this study we have reviewed the relevant literature concerning macroseismic, geological and seismic scientific studies of the 1976, Guatemala earthquake (Mw 7.5), (Espinosa 1976; Harp et al. 1976; Plafker et al. 1976; Plafker 1981) in order to highlight effects of this event on the natural environment. For localities characterized by surface faulting, the ESI scale degree has been assessed by taking into account the total length of the fault segment and the maximum displacement observed, as well as others coseismic effects. The attribution of the ESI degree for the secondary effects (mostly landslides), was reference to the volume of mobilized material the extent of the area involved (Porfido et al., 2012; Porfido et al., 2015a). The towns of Cabanas, Chuarrancho, El Progreso, Gualan, Quebradas, Subinal suffered the XI ESI, Estancia de la Virgen, San Martin Jilotepeque and San Josè Poaquil where the earthquake triggered complex and large landslides with V>10^6 m^3 of mobilized material the estimated Intensity was the X ESI. Guatemala City and Mixco, San Martin Jilotepeque, along with the localities of Finca San Carlos, Los Choloyos, Rio Blanco, Rio Cotzibal, Rio Los Cubes, Rio Naranjio, Rio Polima, Rio Ruyalchè and Rio Teocinte reached the IX ESI. The VIII degree ESI has been attributed to the villages of La Playa and El Sauza, located approximately 185 km away from the epicentre and 40 km from the Motagua fault, where diffused phenomena of lateral spreads affected many houses and settlements causing severe damage. Finally, far from the main fault, 206 km and 158 km from the epicentre, on the lake Ilopango in El Salvador, liquefaction phenomena were observed, suggesting the assessment of the VII ESI.
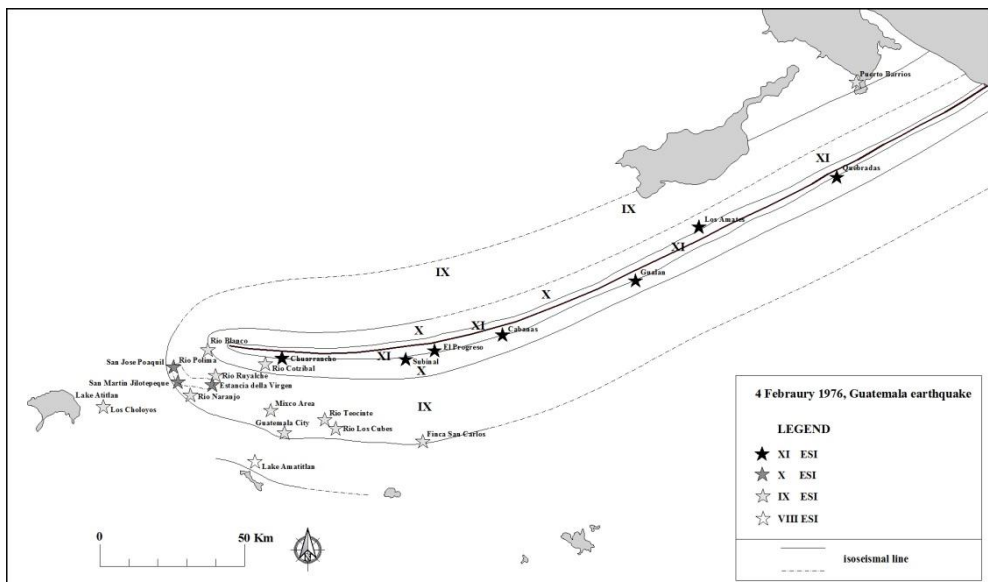
Figure 1. Guatemala 1976 earthquake: isoseismal lines based on the ESI2007 Intensity

The analysis of primary and secondary effects has permitted the evaluation of seismic intensity in 24 localities (Table 1.). Moreover a new epicentral Intensity,

characterized by I_o=XI ESI was establish and a new macroseimic map of the event was constructed. The epicentral intensity (I_0) of the 1976 Guatemala earthquake has been assessed by taking in account the total length of the surface faulting and the total area of ground effects. According to the ESI scale, $I_0 = XI$ corresponds to 230 km total rupture length and maximum horizontal offset of 3.40 m. This is in good agreement with the total area of ground effects estimated of ca. 18,000 km, characterized by landslides, ground cracks and ground settlements. The macroseismc field based on the ESI intensity shows a direct correlation with the fault zone at the surface (Fig. 1). The general pattern of ESI isoseismal lines is compatible with the rupture mechanism of the Motagua fault and its propagation from ENE to WSW. This trend had been already highlighted by instrumental seismological data (Person et al., 1976), that showed a higher concentration of the area damaged by the earthquake towards the south-western edge of the Motagua fault. The XI ESI degree isoseismal line substantially encircles the restricted area along the fault zone. The area of X ESI degree has been defined on the basis of intensity evaluation from the localities of Estancia de la Virgen, San Martin Jilotepeque,and San Josè Poaquil,to the south-west of the fault zone, and on the basis of the hypothesized trend of isoseismal line. The IX ESI is characterized by assessment of intensity from a series of localities to the south of the western part of the fault, such as Finca San Carlos Guatemala City Los Choloyos Mixco Area Rio Blanco Rio Los Cubes Rio Cotzibal and one site located to north of the eastern edge of the fault (Puerto Barrios).

In conclusion, this study confirms the importance of collecting primary and secondary EEE in order to define the nature of earthquake, and provides a mean for a more reliable evaluation of the epicentral intensity. In the case of 1976 Guatemala earthquake, the use of ESI scale yields a value of two degrees higher than previous estimates which is definitely more consistent with the scenario of the actual damage caused by the earthquake. The adoption of the ESI scale also provides a perspective for a definition of seismic hazard in Guatemala. Further steps in the research activity will include a systematic review of major earthquakes of the region addressed to the comparison of the estimated ESI intensities with instrumental peak ground acceleration values (e.g. Giner-Robles, 2015)

References

Ambraseys, N.N. and R.D. Adams (1996). Large-magnitude Central American earthquakes, 1898– 1994, Geoph. J. Inter.127, 665– 692.

Audemard, F., T. Azuma , F. Baiocco, S. Baize, A.M. Blumetti, E. Brustia, J. Clague, V. Comerci et Alii (2015). Earthquake Environmental Effect for seismic hazard assessment: the ESI intensity scale and the EEE Catalogue, Mem. Descr. Carta Geologica d'Italia, v. XCVII, ISPRA, L. Guerrieri (Ed)

Bommer, J.J and C.E. Rodriguez (2002). Earthquake-induced landslides in central America, Eng. Geol., 63, 189-220, ISSN: 0013-7952

Benito, M. B., C. E. Lindholm, Camacho et al. (2012). A New Evaluation of Seismic Hazard for the Central America Region, Bull. Seism. Soc. Am.,102, 2, 504–523.

Espinosa, A.F. (Ed.) (1976). The Guatemala Earthquake of February4, 1976: A Prel.Rep. USGS P. P. 1002.

Encyclopedia of Natural Hazards (2013). Bobrowsky, P. T. (Ed), Springer, XLI, ISBN 978-90-481-8699-0.

Espinosa, A.F., R. Husid, and A. Quesada (1976). Intensity and source parameters from filed observations. The Guatemalan Earthquake of February 4, 1976. USGS P. P. 1002, 52– 66.

Giner-Robles, J.L., P.G. Silva , J. Elez , M.A Rodríguez-Pascua, R. Pérez-López, E. Rodríguez-Escudero (2015)

Relationships between the ESI-07 scale and expected PGA values fromthe analysis of two historical earthquakes (≥ VIII EMS) in East Spain:Tavernes 1396 AD and Estubeny 1748 AD events, in Misc.27 6th INQUA Meeting on Paleos., Active Tectonics a Archaeoseismology, ISSN 2039-6651, 185-188.

Harp, E.L., R.C. Wilson, and G.F. Wieczorek (1981). Landslides from the February 4, 1976, Guatemala earthquake, USGS Prof. Pap., 1204 A.

Harp, E. L., D.K. Keefer, H. P. Sato, and H. Yagi (2011). Landslide inventories: The esential part of seismic landslide hazard analyses, Eng. Geology, v. 122.

Lekkas, E. L., (2010). The 12 May 2008 Mw 7.9 Wenchuan, China, earthquake: macroseismic intensity assessment using the EMS-98 and ESI 2007 scale and their correlation with the geological structure, Bul. Seism. Soc. Am., doi:10.1785/0120090244

Hoose, S.N., R. C. Wilson, and J. H. Rosenfeld (1978). Liquefaction-caused ground failure during the February 4, 1976, Guatemala earthquake.

Michetti, A.M., E. Esposito, L. Guerrieri, S. Porfido, L. Serva, R. Tatevossian, E. Vittori, F. Audemard, T. Azuma, J.Clague, V. Comerci, A. Gurpinar, J. McCalpin, B. Mohammadioun, N.A. Mörner, Y. Ota and E. Roghozin (2007). Intensity Scale ESI 2007, Mem. Descr. Carta Geologica d'Italia, Roma, 74, 53.

Papanikolaou, I. D. (2011).Uncertainty in intensity assignment and attenuation relationships: How seismic hazard maps can benefit from the implementation of the Environmental Seismic Intensity scale (ESI 2007), Quat. Intern., http://dx.doi.org/10.1016/j.quaint.2011.03.058

Person, W, W.Spence, and J. W. Dewey (1976). Main event and principal aftershocks from teleseismic data, in The Guatemala Earthquake of February4, 1976: A Prel. Rep.-USGS P. P. 1002, A.F. Espinosa (Ed).

Plafker, G., M.G. Bonilla, and S.B. Bonis (1976). Geologic effects. The Guatemalan Earthquake of February 4, 1976, USGS P. P. 1002, 38– 51.

Plafker, G. (1976). Tectonic aspects of the Guatemala 4 February 1976, Science, Vol. 193 n. 4259, 1201-1208.

Porfido, S., E. Esposito, L. Guerrieri., E. Vittori, G. Tranfaglia, and R. Pece (2007). Seismically induced ground effects of the 1805, 1930 and 1980 earthquakes in the Southern Apennines (Italy), Ital .J. Geo., 126, 2, 333-346.

Porfido, S., E. Esposito, E. Spiga, and S. Mazzola (2012). Application of the ESI Scale: Case study of the February 4, 1976 Guatemala earthquake, INQUA-IGCP 567 Proc. Morelia (Mexico), 3, 147-150.

Porfido, S., E. Esposito, M. Sacchi, F. Molisso and S. Mazzola (2015a). Impact of Ground Effects for an appropriate mitigation strategy in seismic area: the example of Guatemala 1976 earthquake, Engineering Geology for Society and Territory, 2, DOI: 10.1007/978-3-319-09057-3_117

Porfido, S., R. Nappi, M. De Lucia, G. Gaudiosi, G. Alessio, and L. Guerrieri (2015b).The ESI scale, an ethical approach to the evaluation of seismic hazards, Geoph. Res. Abs.17, EGU2015-11732-2, 2015

Reicherter, K., A.M. Michetti, and P.G. Silva (Eds) (2009). Paleoseismology: Historical and prehistorical records of earthquake ground effects for seismic hazard assessment, Geol. Soc. London, SP 316

Serva, L., A.M. Blumetti, E. Esposito, L. Guerrieri, A.M. Michetti, K. Okumura, S. Porfido, K. Reicherter, P. G. Silva, and E. Vittori (2015). Earthquake Environmental Effects, intensity and seismic hazard assessment: the lesson of some recent large earthquakes, in Mem. Descr. Carta Geologica d'Italia, XCVII.

Silva, P. G., M. A. Rodríguez Pascua, R. Pérez-López, T. Bardaji, J. Lario, P. Alfaro, J.J. Martínez-Díaz, K. Reicherter, J. Giménez García, J. Giner, J.M. Azañón, J.L. Goy, and C. Zazo (2008). Catalogacion de los efectos geologicos y ambientales de los terremotos en Espana en la Escala ESI 2007 y su aplicacion a los estudions paleosismologicos. Geotemas, 6, 1063-1066.

Website: http://earthquake.usgs.gov/

PROBABILISTIC SEISMIC HAZARD ANALYSIS FOR MOLDAVIAN AND TURKEY TERRITORIES

Burtiev, R.

Institute of Geology and Seismology, 3 Academie str. Chisinau, Moldova. 2028.
burtiev_rashid@mail.ru, burtievrashid@gmail.com

Introduction

Cluster analysis is applied for seismic zoning of the Turkish territory. The optimal solution in 50 clusters is established. The PSHA procedure based on the four-dimensional Markovian model of a seismic regime of zones is proposed. Seismic hazard is described by the probability of earthquake occurrence of any number and intensity in the course of a given time interval at some point. It is assumed that the intensity of shaking caused by an earthquake from some seismic zone has conditional normal distribution. An algorithm of assessment of the seismic hazard on a territory within the range of several seismic zones is proposed. Seismic hazard analysis is carried out in standards of degree of EMS-98 scale of intensity and EUROCODE 8.

Assessment of seismic hazard

The condition probability to be estimated by formula for degree EMS 98 scale:

$$p_r^k = P(I^k / E_r) = P\left\{(I \geq I^k)/E_r\right\} = \frac{1}{\sigma\sqrt{2\pi}} \int_{I^k}^{12} e^{-\frac{(I-\bar{I})}{2\sigma^2}} \, dI \tag{1}$$
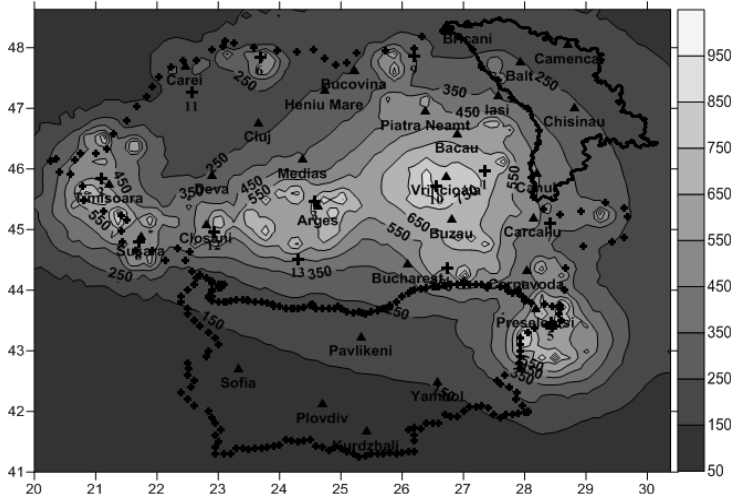
Figure 1. Seismic hazard map of the territory of Moldova, Romania and Bulgaria (13 clusters).

for peak ground acceleration:

$$p_i^k = P\left(\ln pga \geq \ln pga_k \middle/ E_i\right) = 1 - \frac{1}{\sigma\sqrt{2\pi}} \int_{\ln pga_k}^{\ln pga_{max}} e^{-\frac{(\ln pga - g(m,r,h))^2}{2\sigma^2}} \, d\ln pga$$

154

Figure 2. Seismic hazard map of Turkey (50 clusters).

Legend of map (fig.1,2) – symbols: ▲ - is the name of city; + the centre of clusters with number below (seismic zones); right column is color scale.

Acknowledgements

References
Burtiev R.Z., (1985), Seismic hazard mapping based on multi-dimensional Markov model of a seismic regime, *Gerlands Contributions to Geophysics (Gerlands Beitrage zur Geophysik)*, **95**, 499-508.
Rashid Burtiev (2012). Evaluation of seismic hazards from several seismic zones. Environmental Engineeri   and Management Journal. 12, 32-42.

PROS AND CONS OF SEISMIC HAZARD ANALYSIS

Romeo, R.W.

Departmentof Earth Sciences, University "Carlo Bo", Scientific Campus, 61029 Urbino (Italy), roberto.romeo@uniurb.it

Introduction

The paper addresses the main advantages and shortcomings of seismic hazard analysis as resulting from some common misunderstandings of the SHA outcomes by the final users, and from a not good practice by the practitioners, whose main drawbacks and possible solutions are discussed.

Every human activity is characterized by a more or less conscious (or unconscious) assumption of the risks that a possible failure may produce. In fact, neither a long-experienced job, a repetitive action nor a well-trained hobby can assure a safe and expected result. Therefore risk is an intrinsic part of our life to the extent that it represents the possible, even if unpredictable, negative outcome of any action. What is really important isn't therefore to try to avoid the risk at any cost, but rather to know in advance what is the amount of risk implied by a certain action in order to knowingly assume if the action can be undertaken or not.

Risk is expressed in terms of losses per unit time (e.g., € or $ per year, casualties per year, and so on), where the value of the loss is given by the fragility and the amount of the exposed assets, and the time is given by the frequency of the threatening event. The potentially damaging event (threat) is known as the hazard. For instance, the hazard of a deadly car crash is the traffic, of a respiratory disease is the air pollution, of a seismic damage to structures is the ground motion. The variation in time of the severity of none of these hazards can be precisely known in advance, neither the intensity of the traffic or the quality of the air or the seismic shaking, and this is why the hazard is better expressed by a probability to exceed a threshold severity within a reference time than by a conservative but strongly uncertain assumption of the expected severity.

Probabilistic Seismic Hazard Analysis (PSHA) has become a tool to assess the probability of a ground motion exceedance within a reference time for a variety of purposes: 1) for the land use planning; 2) for the design of new structures or the retrofitting of existing ones; 3) for the assessment and mitigation of risk; 4) for policies and strategies of insurance coverage; and others.

Nonetheless, despite the diffusion of the PSHA practice, many misunderstandings still exist either among the insiders and the users, such as: 1) misleading of the basics of PSHA as in the case of the misinterpretation of the term return period, when someone says "How can you predict ground motion values for return periods longer than the earthquake recurrence intervals?", ignoring that the former applies to exceedance (or, conversely, non-exceedance) probability of ground motion at the site while the latter applies to the frequency of earthquake occurrence; 2) the apparent dichotomy between probabilistic and

Deterministic Seismic Hazard Analysis (DSHA), which brings people to divide themselves into two parties, the Tory (let's say the DSHA supporters) and the Labour (let's say the PSHA supporters), each one affirming the supremacy of one approach over the other, when they are integrative rather than alternative. In fact, different approaches for the assessment of seismic hazard can be adopted, depending on the target of the seismic hazard analysis, let's say for planning purposes, for risk assessment and mitigation policies, or for seismic design either of conventional structures or critical facilities; 3) the misconception that PSHA necessarily implies a Poisson process, that means earthquakes follow a process showing independence, stationary and orderliness, is not true since a Poisson distribution hasn't necessarily been generated by a Poisson process, as in the case when a Poisson distribution can result from random operations (e.g., sampling) performed on a set of non-Poisson processes, or when the computed hazard is not time-independent, as it is the case of the application of the renewal processes; 4) and many others of less even if of not minor concern.

Last but not least, the increasing request of seismic hazard analyses for a variety of purposes as shortly listed above, in conjunction with the availability of relatively user friendly computer programs, bring often to a misuse of such a practice that can be summarized in the following key-points: 1) the appropriate choice of the seismic source model, which affects the spatial distribution of hazard more strongly than other more reputed important matters; 2) the inappropriate application of the disaggregation tool when joined to the wrong seismic source model; 3) true and false alternative choices used to explore the epistemic uncertainties and expanded into logic trees; 4) the correct way to communicate seismic hazard results.

Despite PSHA practice dates back to the 1970s, only in very recent years some papers were published aimed to clarify some relevant matters of seismic hazard, most of them stimulated by the criticism moved to PSHA as an unrealistic tool to predict the hazard. Among others, the paper by Abrahamson [1] and his following EERI distinguished lecture in 2009, address many of the shortcomings of a good practice of seismic hazard. Therefore, the aim of this paper is not to repeat those but to highlight some of the critical matters and choices that may bring to a bad practice when improperly applied or may lead to criticism from the users. The task is accomplished through appropriate examples derived from the experience and the application to real cases.

References

Abrahamson, N. (2006). Seismic hazard assessment: problems with current practice and future developments. Proc. of the 1st Eur. Conf. on Earthquake Engineering and Seismology, Geneva, Switzerland, 3-8 September 2006.

SEISMIC HAZARD DEAGGREGATION FOR SELECTED EGYPTIAN CITIES

Sawires, R.[1,2], Fat-Helbary, R.E.[3], Peláez, J.A.[2], Ibrahim, H.A.[1], Hamdache, M.[4], Panzera, F.[5]

[1] *Department of Geology, Assiut University, 71516 - Assiut, Egypt, rashad.sawires@gmail.com*

[2] *Department of Physics, University of Jaén, Jaén, Spain, japelaez@ujaen.es*

[3] *Aswan Regional Earthquake Research Centre, 152 - Aswan, Egypt, fat_helbary2@yahoo.com*

[4] *Départment d'Etudes et Surveillance Sismique, CRAAG, Algiers, Algeria, m_hamdache@hotmail.com*

[5] *Dipartimento di Scienze Biologiche, Università degli studi di Catania, Italy, panzerafrancesco@hotmail.it*

Probabilistic seismic hazard analysis in terms of peak ground acceleration and spectral acceleration values was conducted to assess the seismic hazard across the Egyptian territory. Eighty-eight potential seismic sources (for shallow- and intermediate-depth seismicity) in and around Egypt were identified and characterized based on an updated and unified earthquake catalogue spanning the time period from 2200 B.C. until 2013. Earthquake recurrence relationships were developed, from both instrumental and historical data, for the defined seismic sources. Six well-known ground motion attenuation models were selected to model the ground motion for the different tectonic environments in and around Egypt. Finally, a logic tree design was setup, after a sensitivity analysis, to consider the epistemic uncertainty in different inputs (b-value, maximum expected magnitude and ground motion attenuation model).

In the current study, we show the seismic hazard deaggregation results, in terms of distance and magnitude, for the most important cities in Egypt to help understanding the relative contributions of the different seismic sources. Seismic hazard deaggregation for peak ground acceleration (PGA) and 0.2, 1.0 and 2.0 s spectral accelerations (SA), and for 10% probability of exceedance in 50 years (return period of 475 years), is computed in detail. The results of the mean and modal magnitude and distance values, for the control earthquake, for different spectral periods, are also computed. Our results were obtained using a magnitude interval of 0.5 and a distance interval of 25 km.

In general, the results at most of the cities, indicate that the distance to the seismic sources which mostly contributes to the seismic hazard is mainly controlled by the nearby seismic sources (especially for PGA). However, the more distant earthquake events contribute more to the hazard for larger spectral periods (for 1.0 and 2.0 s SA). For example, for Cairo, a distance value of 0-25 km have been obtained for the control earthquake for PGA, SA (0.2 s), SA (1.0 s) and SA (2.0 s), and magnitude values of 5.0-5.5 MW for the first three periods and 6.0-6.5 MW for the last one. However, for Port Said (located along the Mediterranean Sea

coast), values of 7.0-7.5 MW and 375-400 km for the control earthquake has been obtained for all spectral periods. A significant result of this type of work is that seismic hazard deaggregation provides useful data on the distance and magnitude of the contributing seismic sources to the hazard in a certain place, which can be applied to generate scenario earthquakes and select acceleration records for seismic design.

AN INTEGRATED APPROACH FOR LANDSLIDE HAZARD ASSESSMENT ON THE NW COAST OF MALTA

Soldati, M.[1], Devoto, S.[2], Foglini, F.[3], Forte, E.[4], Mantovani, M.[5], Pasuto, A.[6], Piacentini, D.[7], Prampolini, M.[8]

[1]*Department of Chemical and Geological Sciences, University of Modena and Reggio Emilia, Via Campi 103, 41125 Modena, Italy, soldati@unimore.it*

[2]*Department of Mathematics and Geosciences, University of Trieste, Via Weiss 2, 34127 Trieste, Italy, sdevoto@units.it*

[3]*Institute of Marine Sciences, National Research Council (ISMAR-CNR), Via Gobetti 101, 40129 Bologna, Italy, federica.foglini@bo.ismar.cnr.it*

[4]*Department of Mathematics and Geosciences, University of Trieste, Via Weiss 2, 34127 Trieste, Italy, eforte@units.it*

[5]*Research Institute for Geo-Hydrological Protection, National Research Council of Italy, Corso Stati Uniti 4, 35127 Padova (Italy), matteo.mantovani@irpi.cnr.it*

[6]*Research Institute for Geo-Hydrological Protection, National Research Council of Italy (IRPI-CNR), Corso Stati Uniti 4, 35127 Padova (Italy), pasuto@irpi.cnr.it*

[7]*Department of Earth, Life and Environment Sciences, University of Urbino, Campus Scientifico "E. Mattei",61029, Urbino, Italy, piacentini.daniela@libero.it*

[8]*Department of Chemical and Geological Sciences, University of Modena and Reggio Emilia, Via Campi 103, 41125 Modena, Italy, mariacristina.prampolini@unimore.it*

Introduction

This contribution presents the outputs of multidisciplinary research carried out along the north-western coast of Malta aiming at landslide hazard assessment. The investigated area extends on a surface of 15 km2 and it is situated between Paradise Bay and Il-Pelegrin promontory. Elevation ranges from the sea level to about 120 m of altitude. The stability conditions of this stretch of coast are deeply controlled by a linkage of different factors, such as tectonics and lithology, which control the landslide onset. Landslides certainly make up a predominant geomorphological feature in this area and they have been investigated in detail by means of mapping, monitoring and modelling since 2005 by a composite team of Italian researchers supported by Maltese institutions.

Geological setting

The Maltese archipelago is composed of Tertiary limestones, clays and marls capped by very thin superficial deposits, such as red soils or colluvial sediments. In the north-western part of Island of Malta, two geological units are dominant and influence the types of landslides: Upper Coralline Limestone and Blue Clay Formation.

Figure 1. Geographical setting of the investigated area and examples of block slides: A) north-western area of Marfa Ridge; B) stretch of coast between Rdum id-Delli and Ras Il-Wahx; C) Il-Qarraba peninsula.

Inland the Upper Coralline Limestone produces a barren grey pavement, bordered by vertical cliffs of varying heights, which range from a few metres to over 30 m. The underlying Blue Clay forms gentler and sometimes terraced slopes that in some cases reach directly the sea. The different mechanical behaviour of clays and limestone favours the development of impressive lateral spreading and block sliding phenomena, which occur in particular along the north-western sector of Marfa Ridge, at Ras Il-Wahx and at Ghajn Tuffieha Bay (Fig. 1).

Block slides are particularly widespread on the large terraces which slope gently towards the sea. Other types of landslides are earth flows, earth slides, affecting clayey slopes, as well as rock falls and topples, which are favoured primarily by persistent fissures and cracks of tectonic origin enlarged by lateral spreading (Devoto et al., 2013a).

Landslide investigation

In order to recognize, inventory and map coastal slope movements, a geomorphological survey was conducted at a scale of 1:5000. This phase of research also included a check of the existing bibliography and maps. Geomorphic information deriving from land surveying was integrated and controlled by multitemporal aerial photo interpretation. Field surveys permitted to observe directly landforms, processes and deposits whereas orthophotos helped to understand their evolution and to map particular morphological features of landslides identified on the ground, such as cracks related to limestone fragile behaviour. Parallel to structural escarpments, vertical fissures and cracks situated on karst plateau can exceed 200 m length.

In order to evaluate the state and style of activity of lateral spreading and block sliding phenomena, different monitoring techniques were applied. In particular, two GPS networks have been operating since 2005 which enabled to define the investigated mass movements as active. The latter can be classified as extremely slow, according Cruden and Varnes classification (1996). All surveying data were digitized at a scale of 1:5000, compiled and stored in an AutoCAD Map® software and mapped using the symbology of the legend proposed by the Italian Working Group for Geomorphological Mapping of the Italian Geological Service (1994). The final product is a detailed geomorphological map at a scale of 1:7500 including the coastal area between Paradise Bay and the Great Fault (Devoto et al., 2012). This map may represent a useful and comprehensive tool for identifying geomorphological risk along the coast.

Integrated landslide monitoring

Integrated monitoring techniques have been adopted to investigate lateral spreads and block slides in order to define the kinematics and the triggering mechanisms. These phenomena may evolve into faster movements, which can determine catastrophic failures (i.e. block slides), or they can favour a series of collateral landslides (i.e. sudden block slides, flows, falls and topples) occurring at the edges of the areas affected by spreading (Pasuto and Soldati, 2013). In this

context, the coupling of traditional and innovative monitoring techniques makes up a reliable solution for the detection and survey of active deformations due to rock spreading, with promising perspectives in terms of hazard assessment and mitigation (Magri et al., 2008; Devoto et al., 2013b; Mantovani et al., 2013).

An example of site analysed through different methods is the Il-Qarraba peninsula (Fig. 1C). This peninsula is composed by a limestone plateau surrounded by an extensive block slides deposit with a subcircular shape and connected to the land through an isthmus made up of Blue Clay that is eroded by the marine action. At this site a GNSS network has been working since 2006 and tape extensometer measurements have been carried out since the end of 2009. Moreover, to support and confirm the monitoring results, interferometric analyses (satellite SAR) and geophysical investigations (GPR and Electrical Resistivity Tomographies - ERT) were carried out (Devoto et al., 2013b; Mantovani et al., 2014).GNSS monitoring is taking place with reference to eight benchmarks located both on the plateau and on rock masses and blocks detached due to rock spreading and block sliding. Considering the extremely slow rate of deformation, the static relative positioning technique was employed in order to achieve more accurate results. Surveys have been carried out twice a year at the end of the wet and dry seasons, in order to investigate the relationship between recorded displacements and rainfall. Since the very beginning, it was clear that rock spreading was active over a large area, and the series of readings carried out showed continuous evidence of activity (Magri et al., 2008; Devoto, 2012; Devoto et al., 2015). The interferometric analyses took into account ERS radar images, to evaluate the deformation eventually occurred before the realization of the GNSS control network, and images acquired from ENVISAT and Terra SAR-X satellites, in order to define the present state of deformation and to integrate and validate the results achieved with the monitoring system. This kind of analysis allowed also to evaluate any change in rate of deformation, state and style of activity. In the site of Il-Qarraba, the interferometry highlighted displacements ranging between -3,5 mm to +0,5 mm in 9 years with the same style of activity (Piacentini et al., in press).

ERT profiles acquired with a multielectrodes (48) system allowed to evaluate the thickness of limestones and to highlight some tectonic structures. GPR data were acquired using 300 and 500 MHz shielded antennas. The investigation was concentrated on blocks showing significant vertical and planar displacement in order to obtain a precise imaging of the rock mass and to reconstruct the 3D discontinuity network (Mantovani et al., 2013). The integration of results obtained with this multi-technical integrated approach have been of fundamental importance for describing quantitatively the evolution of lateral spreading and block sliding affecting Il-Qarraba and the other monitored sites.

Landslide susceptibility analysis

The results from Permanent Scatterer Interferometry were used as input data in the Weight of Evidence (WofE) model to produce a landslide susceptibility map, validated through field survey and GNSS measurements (Piacentini et al., in press)
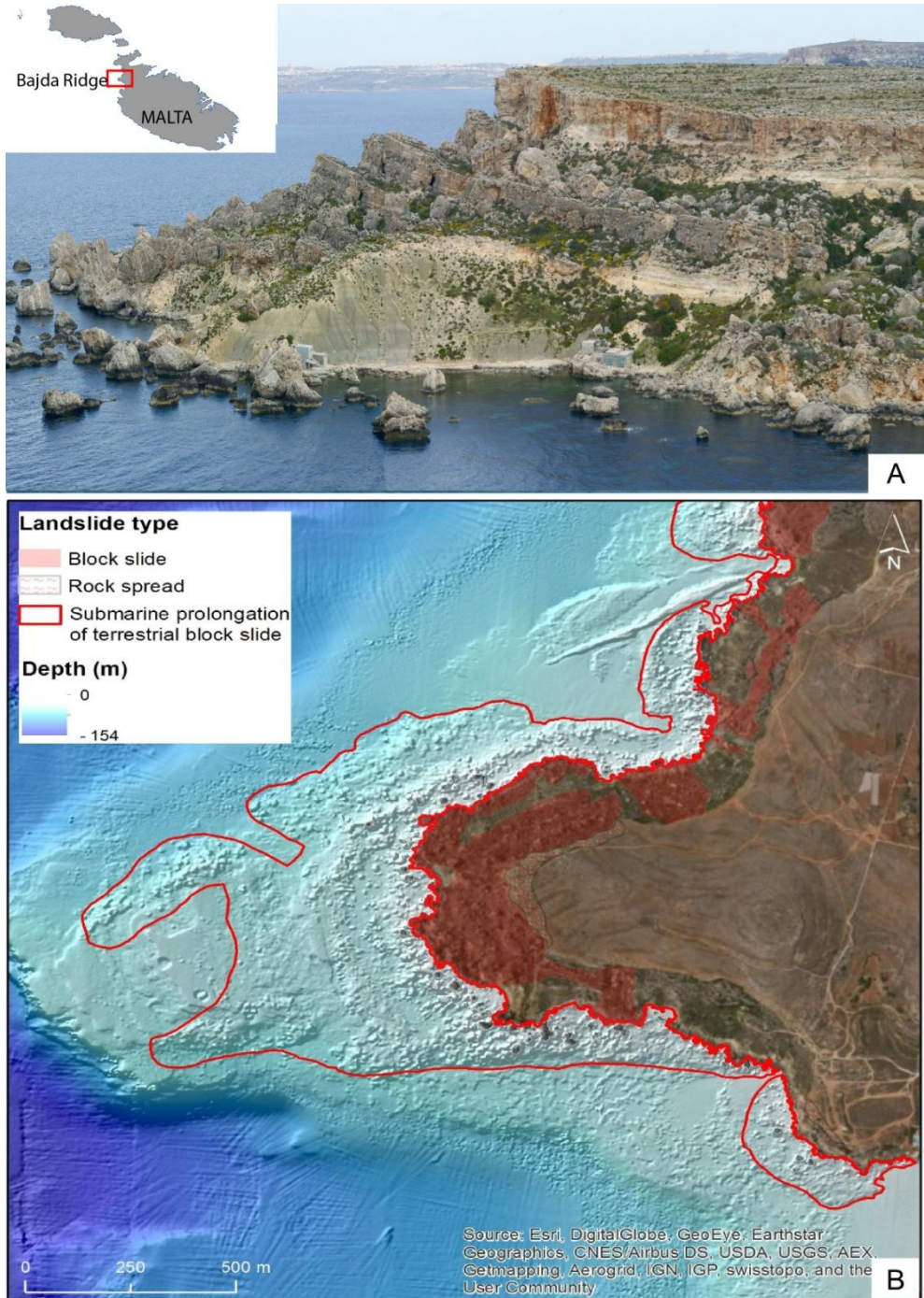
Figure 2. Ras Il-Wahx block slide at Bajda Ridge (A); landslide deposits largely extending under the sea level are evident (B).

and resulting in a reliable method to produce susceptibility maps at medium and regional scale. Geomorphological data were compared with the model output with a satisfying fitting between the inventoried block slides and the spatial distribution of high landslide susceptibility classes. In particular, the active block slides affecting the northern part of Marfa Ridge, at Il-Prajjet, in the coastal sector between the southern part of Ghadira Bay and Ras Il-Wahx promontory (Figure 9) and at Il-Qarraba peninsula have been correctly identified by the model. Finally, the model outputs were quantitatively compared with the surface displacements derived from GNSS campaigns reported in Mantovani et al. (2013) with a positive feedback. The landslide susceptibility map of the north-western coast of Malta can be considered as an easy-to-use tool for the implementation of further hazard analyses and land management activities.

Coupling terrestrial and marine datasets

A deep understanding of the processes acting on the coastal areas (such as landslides) is crucial for coastal hazard assessment, especially landslide hazard assessment and mapping. To this aim, integrated investigations of emerged and submerged areas resulting in geomorphological mapping represent an innovative way to provide the necessary knowledge for preventing hazards and reducing risks, understanding the evolution of the processes in a framework of climatic changes.
A Multibeam survey has recently been carried out offshore the north-western coast of Malta to acquire high resolution bathymetry (2 m) and backscatter data. A LiDAR-derived DEM was used to cover the gap between the bathymetric survey and the land (courtesy of the AcquaBioTech Group).The seafloor sediments were analysed through the analysis of the reflectivity (backscatter) data exploiting the TexAn software (University of Bath, UK) to produce a sediment distribution map. The submerged geology was inferred drawing geological section exploiting the Geological Map of Malta published by the Oil and Exploration Directorate (1993). Morphological features of the seafloor were recognized and mapped thanks to bathymetry analysis and geomorphological interpretation. A series of these features were emerged during the Last Glacial Maximum, when the sea level was about 130 m lower than at present (Lambeck et al., 2011; Micallef et al., 2013). An integrated geomorphological map of emerged and submerged coastal areas of north-western Malta was produced, which is also crucial to understand the geomorphological evolution of the archipelago since the Last Glacial Maximum (LGM). It should be emphasized that the most relevant features offshore the north-western coast of Malta are landslide deposits which are the continuation of terrestrial ones below the sea level down to a depth of about 50 m (Fig. 2). In most cases the largest part of the block slide deposits is under the sea level.

Conclusions and perspectives

The multidisciplinary and integrated research carried out (and still ongoing) along the north-west coast of Malta has allowed (i) the reconstruction of

the geomorphological evolution of the area, (ii) the characterization of slope instability phenomena there occurring, and (iii) the definition of the areas which are more susceptible to landslide processes.

The outputs of the research have provided the basis for defining future scenarios of evolution, which are essential for landslide hazard assessment in an area which is visited by many tourists and locals throughout the whole year.

At present no time constraints are available for past landslide activity in the study area. Landslide dating would be however needed to provide a more precise temporal frame to the overall geomorphological evolution of the north-western coast of Malta. To this aim, a recent geomorphological campaign enabled to collect samples from scarps and blocks that are presently under dating using cosmogenic nuclides (36Cl) at the University of Exeter, UK. Achieving information on the temporal occurrence of landslides will be beneficial in outlining future evolution scenarios which are crucial for land planning and civil protection.

Acknowledgements

References

Devoto, S., (2012). Cartografia, monitoraggio e modellizzazione di frane lungo la coasta nord-occidentale dell'isola di Malta. PhD dissertation, Università degli Studi di Modena e Reggio Emilia, Italy.

Devoto, S., Biolchi, S., Bruschi, V. M., Furlani, S., Mantovani, M., Piacentini, D., Pasuto, A. and Soldati, M., (2012). Geomorphological map of the NW Coast of the Island of Malta (Mediterranean Sea), Journal of Maps, 8(1), 33-40.

Devoto, S., Biolchi, S., Bruschi, V.M., González Díez, A., Mantovani, M., Pasuto, A., Piacentini, D., Schembri, J.A. and Soldati, M. (2013a). Landslides Along the North-West Coast of the Island of Malta. In Margottini, C., Canuti, P., Sassa, K. (Editors), Landslide science and practice, Vol. 1, Springer-Verlag, Berlin Heidelberg, 57-63.

Devoto, S., Forte, E., Mantovani, M., Mocnik, A. Pasuto, A., Piacentini, D. and Soldati, M., (2013b). Integrated Monitoring of Lateral Spreading Phenomena Along the North-West Coast of the Island of Malta. In Margottini, C., Canuti, P., Sassa, K. (Eds), Landslide Science and Practice, Vol. 2, Springer-Verlag, 235-241.

Devoto, S., Mantovani, M., Pasuto, A., Piacentini, D. and Soldati, M., (2015). Long-term monitorning to support landslide inventory maps: the case of north-western coast of the Island of Malta. In Lollino, G., Giordan, D., Crosta, G.B., Corominas, J., Azzam, R., Wasowski, J., Sciarra, N. (Editors), Engineering Geology for Society and Territory, Volume 2, Springer International Publishing, Switzerland, 1307-1310.

Gruppo di Lavoro per la Cartografia Geomorfologica (1994). Carta geomorfologica d'Italia – 1:50.000 – Guida al rilevamento. Servizio Geologico Nazionale, Quaderni serie III, vol 4, 42p.

Lambeck, K., Antonioli, F., Anzidei, M., Ferranti, L., Leoni, G. and Silenzi, S., 2011. Sea level change along the Italian coasts during Holocene and prediction for the future. Quaternary International, 232, 250–257.

Magri, O., Mantovani, M., Pasuto, A., and Soldati, M., (2008). Geomorphological investigation and monitoring of lateral spreading along the north-west coast of Malta, Geografia Fisica e Dinamica Quaternaria, 31(2), 171-180.

Mantovani, M., Devoto, S., Forte, E., Mocnik, A., Pasuto, A., Piacentini, D. and Soldati, M., (2013). A multidisciplinary approach for rock spreading and block sliding investigation in the north-western coast of Malta, Landslides, 10(5), 611-622.

Mantovani, M., Piacentini, D., Devoto, S., Prampolini, M., Pasuto, A., and Soldati, M., (2014). Landslide susceptibility analysis exploiting Persistent Scatterers data in the northern coast of Malta, Proceedings International Conference "Analysis and Management of Ghnaging Risks for Natural Hazards", 18-19 November 2014, Padua, Italy. AP19 1-8.

Micallef, A., Foglini, F., Le Bas, T., Angeletti, L., Maselli, V., Pasuto, A. and Taviani, M., 2013. The submerged paleolandscape of the Maltese Islands: Morphology evolution and relation to Quaternary environmental change. Marine Geology, 335, 129–147

Oil and Exploration Directorate, 1993. Geological map of the Maltese Islands. Valletta: Office of the Prime Minister.

Pasuto, A., and Soldati, M., (2013). Lateral Spreading. In Shroder, J.F., Marston, R.A., Stoffel, M. (Editors). Treatise on Geomorphology, Vol 7, Mountain and Hillslope Geomorphology, Academic Press, San Diego, 239-248.

Piacentini, D., Devoto, S., Mantovani, M., Pasuto, A., Prampolini, M. and Soldati, M., in press. Landslide susceptibility modelling assisted by Persistent Scatterers Interferometry (PSI): an example from the north-western coast of Malta. Natural Hazards.

SCENARIOS OF DEBRIS FLOW MODELLING BEFORE AND AFTER THE BUILDING OF MITIGATION WORKS: CASE STUDY IN VAL CANALE VALLEY (FRIULI VENEZIA GIULIA, ITALY)

Boccali C.[1], Calligaris C.[1], Lapasin R.[2], Zini L.[1], Cucchi F.[1]

[1]*Departmentof Mathematics and Geosciences, University of Trieste, via Weiss 2, Trieste, Italy, cboccali@units.it*

[2]*Departmentof Engineering and Architecture, University of Trieste, P.le Europa 1, Trieste, Italy, romano.lapasin@di3.units.it*

Introduction

Debris flows are rapid gravity-induced flows of high-concentration granular-liquid mixtures, consisting of clay, silt, sand and boulders with a variable quantity of water. Due to their high speed and energy, they represent a severe hazard in mountain regions. In this study we investigate the properties and the dynamic of a debris flow that occurred in 2003 in ValCanale valley (Friuli Venezia Giulia, Italy). On August 29th 2003 many debris flows were activated along different tributaries of the Fella river basin (North-East Italy). After that huge event a program of debris flow risk analysis was started and through the use of FLO-2D software, a new outline of the hazardous areas was obtained.

For the present research, the simulations based on the parameters collected after the event on the DTM of 2003 were used as back analysis, whereas new simulations were performed using parameters derived from samplings and laboratory analyses completed during 2013 on a more detailed DTM, available from laser scanner data, collected in 2008 by the Civil Defence of Friuli Venezia Giulia Region. The present work aims to create future possible flooding scenarios on the actual morphology and to test the effectiveness of the mitigation measures, built up after the 2003 event.

Study area

The area of Fella watershed (Figure 1), with the whole north-eastern part of the Friuli Venezia Giulia Region as well, on 29th August 2003, was hit by a high intensity rainfall. This intense convective system produced rainfall peaks of about 390 mm in 6 hours (Marchi et al., 2009). In that occasion, the main part of the tributaries of the Fella River gave rise to debris flow phenomena, on the right and left side, causing the obstruction of the main roads present in the valley and two fatalities.The estimated damages were around one billion Euro (Tropeano et al., 2004).

One of the right tributaries of the Fella river, called "Solari" stream (Figure 1C), during the 29th August event overflowed and a large amount of debris reached

a road downstream, impeding the access at the small hamlet of Cucco, in the municipality of Malborghetto-Valbruna.

Eyewitnesses report that the event occurred into at least two pulses, separated from each other by periods of low torrential activity (Silvano et al., 2004). The hydrograph, derived through the hydrologic model KLEM, tested by Borga et al. (2007), evidences three main discharge peaks between 3 and 10 pm, the major of which happened at 6 pm. The cumulate rainfall exceeds 250 mm. The return period of the rainfall amounts, measured on 29th August 2003 by a rain gauge located 10 km far from the Solari stream, was close to 800 years for duration between 3 and 12 hours (Norbiato et al., 2007).

The Solari stream is constituted by two paths merging in a single gorge 100 m before the outlet on the alluvial fan. The fan is around 40° steep on the top and its gradient decreases up to the confluence with the main valley. The two paths differ in morphology and average size of the debris material. The right one is narrow and is constituted of dolomitic clasts of average size equal to $0.5 - 1 \, m3$; the left stream is twice wider and steeper than the other, the debris is commonly beyond the angle of repose and is composed by pebbles and gravel leant on finer material. At the confluence of the two streams the debris is very heterometric, with a maximum size of $1 \, m3$. The source area is completely surrounded by fractured rocky cliffs, generated mainly by the intense tectonic stresses. This agent ensures a continuous debris production that can be mobilized by water, both from rainfall and seepage.Silvano et al. (2004) estimate 4-6 m depths of mobilizable material.
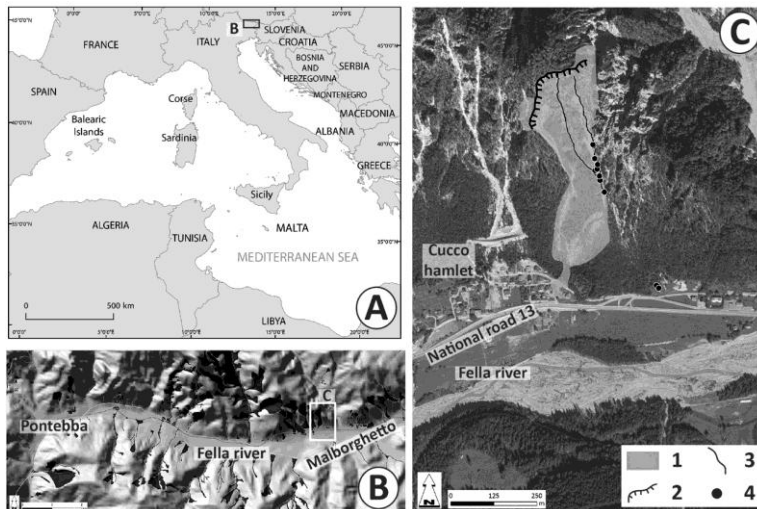
Figure 1. Study area. (A) Geographical setting; the letter and the square indicate the location of the map (b). (B) Shaded relief of the ValCanale valley and its tributaries. The black polygons represent debris flows occurred during the 29th August 2003 event; the letter and the square indicate the location of the map (c). (C) Aerial photo of the Solari watershed; the legend symbols are accompanied by numbers indicating: 1, Delimitation of the 2003 debris flow; 2, Edge of the main scarp; 3, Main flow paths; 4, Sampling points.

Material characterization

In order to obtain a complete characterization of the watershed and its material, we defined grain-size and mineralogical properties of 12 samples collected along the stream, both in source and in deposition area (Figure 1C). After that, the rheological behavior was defined by measures with a controlled stress rheometer. The so-derived rheological parameters were used for the numerical simulation on the latest DTM.

An overall analysis of the grain-size distribution points out that the clay to silt content ranges from 3.75 to 16 per cent of the fraction finer than 32 mm. No trend of grain-size distribution was observed comparing the different sampling points, however it is possible to identify a decrease of the fraction finer than 62.5 micron downstream, according to Bardou et al. (2007).

The genetic homogeneity of the samples was confirmed by the mineralogical analysis. In each sample, dolomite is dominant and there is a lack of other minerals; only a very small percentage of kaolinite was recognized for seven samples, collected in the source area.

All samples collected in the source area were prepared at different solid volumetric concentrations (Cv, from 44 to 64 per cent, by volume) and analyzed using a controlled stress rheometer (RheostressHaake RS150, Haake GmbH, Germany) equipped with a parallel plate geometry (35 mm diameter). The yield stress and viscosity, essential parameters for characterizing and modelling debris flow, were estimated through the application of correlation models. A convenient extrapolation technique is based on viscoplastic flow models (Nguyen and Boger, 1992):among the many models proposed by the literature,the simple Bingham model can be profitably used for correlating the experimental data collected in the shear flow region.By correlating values of yield stress and viscosity obtained at different solid volumetric concentration, it is possible to derive four coefficients, that express the dependence of viscosity and yield stress from the solid concentration, by means of exponential law (Table 1).

Table 1.The fitting coefficientsα, β, γ, δ of the samples collected along the Solari stream. The relative equations are $\eta = \alpha exp\,(\beta C_v)$ and $\tau = \gamma exp\,(\delta C_v)$.

Sample	α	β	γ	δ
PC3_0	7E-11	43.98	2E-09	52.36
PC3_10	1E-11	47.19	5E-07	34.81
SOL2	1E-08	36.98	6E-10	57.78
SOL3A	1E-15	65.36	3E-08	44.02
SOL3B	1E-13	57.86	6E-07	38.75
SOL4	5E-08	35.07	4E-09	54.40
SOL5	2E-12	51.30	3E-12	64.97
SOL6	2E-10	42.57	4E-10	54.06
SOL7	7E-11	43.96	3E-07	40.22
SOL8	2E-13	58.09	9E-12	63.84

Numerical simulations: scenarios and results

Even if the phenomenon along the Solari stream is not remembered as one of the most dangerous and destructive, it was chosen as test site for comparing the simulation results obtained on the existing morphology in 2003, at the time of the alluvial event, with the ones obtainable on the actual morphology of the stream. After the alluvial occurrence, in fact, Solari watershed suffered a complete transformation in order to mitigate the risk of the area: at the confluence of the stream with the alluvial fan a weir was located, now partially destroyed. An artificial channel downstream conveys the debris towards SE and many thresholds were created in order to brake the flows and support the deposition of the larger material. The retention basin, placed at the bottom of the fan, has a storage capacity of around 15,000-18,000 m3. Downstream of the basin a disposal channel ensures the liquid phase flow to the Fella River.
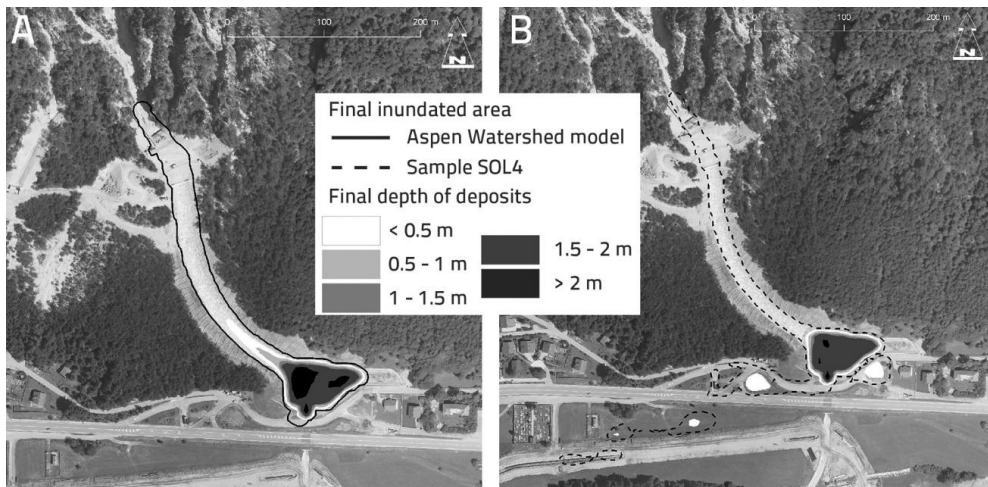
Figure 2.Simulated scenarios on DTM of 2008. (A) Rheological parameters from Aspen Watershed model. (B) Experimental rheological data (sample SOL4).

First of all, for the present research, a back analysis was performed on DTM of 2003 using 15 couples of rheological parameters, chosen from the ones available on literature (Dai et al., 1980; Kang and Zhang, 1980; O'Brien and Julien, 1988; Major and Pierson, 1992; Sosio et al., 2007), trying to reconstruct the real scenario, outlined during field survey just after the alluvial event and through the analysis of aerial photos. Among all the models, Aspen Watershed (O'Brien and Julien, 1988) was selected. The simulated debris volume was equal to 3,674.99 m3, with a final inundated area of 27,525 m2. Secondly, the same parameters were used for simulations on the DTM of 2008: the volume was calculated to be 3,676.57 m3, with a final inundated area of 10,625 m2. In this scenario all the debris stops into the retention basin at the bottom of the fan (Figure 2A). Figure 2B represents a possible scenario of event on 2008 DTM using rheological parameters derived by the experimental data of the sample SOL4 (Table 1). The calculated

volume was 3,677.57 m3 and the final inundated area was 25,175 m2. The values of the sample SOL4 were chosen among all other tested ones because they give rise to a more plausible event, even if all the simulations with the experimental data produce an overestimation of the final inundated area and a partial overflowing of the basin. The overflowed material reaches and overpasses two roads downstream. However, as pointed out by both scenarios on 2008 DTM, the artificial channel is able to convey all the material downstream, protecting the wooded fan and the eastern part of theCucco hamlet.

Conclusions

The hazard induced by debris flows is well known in mountain regions, especially in the Alps, where these phenomena affect commonly second order streams, creating risks for humans and their settlements. In 2003 the ValCanale valley was invested by a high intensity cloudburst that caused more than 1,000 debris flows. After that event, the authorities started a program of risk analysis and many mitigation measures were built up along and at the bottom of debris flow streams and alluvial fans.

The present research aims, firstly, to repeat the modelling on the morphology existing at the time of the alluvial event, in order to define the better parameters for delineating a real scenario; secondly, new simulations were performed on the actual morphology, in order to verify the efficiency of the mitigation works.

The efficiency was well confirmedby the simulations performed using the literature rheological model (Aspen Watershed). In this case the almost complete filling of the retention basin was observed, that is congruent with the actual disposition of the debris inside the basin.

Conversely, the modelling using the experimental rheological data does not permit to highlight the capability of the deposition basin and points out an overestimation of the inundated area. The differences between the simulations are probably connected with issues encountered during the rheological analysis, in particular at low solid concentration. The observed and calculated conditions underline an unreal liquid-like behaviour of the debris flow that is probably the cause of the greater expansion of theflow during the simulation.Given these observations, it is possible to conclude that in case of another event similar to the one occurred in 2003, the area directly interested by the Solari stream will be in a good state of safeness and the mitigation works will correctly work and defend human infrastructures and settlements.

Acknowledgements

References

Bardou, E., P. Boivin, and H.R. Pfeifer (2007). Properties of debris flow deposits and source materials compared: implication for debris flow characterization, Sedimentology 54 469-480.

Borga, M., P. Boscolo, F. Zanon, and M. Sangati (2007). Hydrometeorological analysis of the 29 August 2003 flash flood in the Eastern Italian Alps, J. Hydrometeorol. 8 1049-1067.

Dai, J., W. Chen, and B. Zhou (1980).An experimental study of slurry transport in pipes, in Proceedings of the International Symposium on River Sedimentation Li B. (Editor), Chinese Society for Hydraulic Engineering, Beijing, 195-204.

Kang, Z., and S. Zhang (1980). A preliminary study of the characteristics of debris flow, in River Sedimentation Li B. (Editor), Chinese Society for Hydraulic Engineering, Beijing, 225-226.

Major, J.J., and T.C. Pierson (1992).Debris flow rheology: experimental analysis of fine-grained slurries, Water Resour. Res. 28 841-857.

Marchi, L., M. Cavalli, M. Sangati, and M. Borga (2009). Hydrometeorological controls and erosive response of an extreme alpine debris flow,Hydr. Proc. 23 2714-2727.

Nguyen, Q.D., and D.V. Boger (1992).Measuring the flow properties of yield stress fluids, Annu. Rev. Fluid Mech. 24 47-88.

Norbiato, D., M. Borga, M. Sangati, and F. Zanon (2007).Regional frequency analysis of extreme precipitation in the eastern Italian Alps and the August 29, 2003 flash flood, J. Hydr. 345 149-166.

O'Brien, J.S., and P.Y. Julien (1988).Laboratory analysis of mudflow properties.J. Hydr. Engn. 114 877-887.

Silvano, S., F. Cucchi, V. D'Agostino, and L. Marchi (2004). Attività tecnico scientifica per l'analisi delle condizioni di rischio idrogeologico a seguito degli eventi alluvionali del 29 Agosto 2003 in località Cucco in comune di Malborghetto Valbruna e per la definizione degli interventi indispensabili per la messa in sicurezza delle abitazioni soggette a pericolo alluvionale, Rapporto interno elaborato per la Protezione Civile della Regione Autonoma Friuli Venezia Giulia.

Sosio, R., G.B. Crosta, and P. Frattini (2007). Field observations, rheological testing and numerical modelling of a debris-flow event, Earth Surface Processes and Landforms 32 290-306.

Tropeano, D., L. Turconi, and S. Sanna (2004). Debris flows triggered by the 29 August 2003 cloudburst in Val Canale, Eastern Italian Alps, International Symposium INTERPRAEVENT, Riva (TN), Italy, 121-132.

SITE CHARACTERISATION AND RESPONSE STUDY IN RABAT, MALTA

Farrugia, D.[1], Paolucci, E.[2], D'Amico S.[1], Galea P.[1]

[1] Department of Geosciences, University of Malta, daniela.farrugia@um.edu.mt
[2] Department Dipartimento di Scienze Fisiche, della Terra e dell'Ambiente,
Università degli Studi di Siena, Siena, Italy

Introduction

The investigation of local ground conditions is an important part of seismic hazard assessment (Fäh et al., 2003). Local geology can greatly alter the seismic waves from earthquakes by amplifying their amplitude, changing the frequency content and increasing the shaking duration during an earthquake (Kramer, 1996). Sedimentary structures hosting dense settlements are likely to suffer from heavy damage, even though they can be situated away from the epicentre of the earthquake (Zor et al., 2010). The main parameters responsible for such effects are the shear-wave velocity (VS) structure and thickness of the sedimentary cover, the impedance contrast between the soft sediments and the underlying bedrock as well as the geometry of their interface (Parolai et al., 2006). Site response studies contribute to earthquake-hazard mitigation strategies such as seismic risk assessments, emergency response-preparedness and land use planning by considering existing and proposed buildings (Zor et al., 2010).

Since 1530, an earthquake intensity of VII on the European Macroseismic Scale (EMS-98) scale was experienced on the Maltese archipelago at least four times, with the major source of seismic hazard being the northern segment of the Malta Escarpment. Earthquake activity can also be attributed to active fault zones in the Sicily Channel and the Hellenic Arc. Even though the latter is situated relatively far away from the islands, an earthquake in 1856, with an epicentral location around 1000 km away from the islands, caused significant damage to buildings, with many houses suffering serious cracks to their walls (Galea, 2007). The public perception about seismic risk remains one of negligence and complacency and up to date, no comprehensive seismic site response study has been done on the islands.

This study is the first of a series of site response analyses which are to be carried out. It is divided in two parts. Firstly, a series of ambient noise measurements were done at a site in Rabat (Malta) to investigate and evaluate different techniques for estimating one-dimensional shear-wave velocity profiles. The chosen site is characterised by outcropping Blue Clay overlying the harder Globigerina Limestone. The data from the first investigations then serve as input to the equivalent-linear analysis programme SHAKE2000 (Ordonez, 2002) which is used for the site response analysis. In this research work, some advantages and limitations of chosen surface-wave techniques are also assessed. Moreover, any difference between equivalent profiles (satisfying the same experimental data) in site response results is investigated.

Geophysical investigations to obtain the shear-wave velocity profile
Methodology

Three different array techniques were first tested at the chosen site which presents the ideal geology for such studies: a velocity profile, in which VS increases with depth. The first part of the study is aimed at testing the capabilities and limitations of the three techniques which are: the Modified Spatial Auto-Correlation (MSPAC, Bettig et al., 2001), Extended Spatial Auto-Correlation (ESAC, Okada, 2003) and f-k method (Capon, 1969). Three different array configurations, an array of 17 geophones arranged in an L-shape and circle respectively and 42 geophones in an L-shaped configuration, were also tested out in the field.

A series of three-component measurements were also conducted to obtain the H/V curve (Nakamura, 1989). Chosen dispersion curves were then jointly inverted with the H/V curve using two different inversion algorithms, the Neighbourhood Algorithm (NA) and the Genetic Algorithm (GA). Five different profiles interpreting the geology of the site were obtained and compared.

Results

A comparison of the dispersion curves using MSPAC and ESAC shows that the two methods, based on the SPAC method (Aki, 1957), are in good agreement. However, it was observed that the f-k method tends to overestimate the Rayleigh-wave velocities at low frequencies, as is also reported in other studies (Zor et al., 2010; Picozzi et al., 2009).

The short L-shaped and circular arrays gave similar results, which can indicate that the wave-field was isotropic, while as expected, the dispersion curve of the longer array consisted of data in the lower frequencies. Table 1 presents a summary of the five best fitting profiles obtained from five separate inversion. The shear-wave velocity of the Globigerina Limestone at this site can be considered to be around 900-1000 m/s, with only NA1 being an outlier, since a velocity of 750 m/s was obtained. This range is similar to that obtained by Pace (2011) and Panzera et al. (2013) in Xemxija and some other sites in Malta using MASW and H/V modelling.

The thickness of the clay obtained for all the models is around 40-50 m. The only model which estimated a 60 m depth to bedrock is GA1. The calculated VS30 values for each profile are 257 m/s, 292 m/s, 307 m/s, 309 m/s and 323 m/s, thus classifying the site as belonging to the class C according to the EC8 classification (Bisch et al., 2012).

Since the recorded ambient noise with the longer L-shaped configuration is richer in low frequencies, the VS profiles GA2 and NA2 were used to perform site response analysis in the next part of this study. NA3 was eliminated since the MSPAC curve is very similar to the ESAC one.

Table 1: The results obtained from the five different inversions. GA stands for Genetic Algorithm while NA for Neighbourhood Algorithm and these refer to the type of algorithm used for the inversion. The Dispersion curve and Configuration columns show the chosen curves used for the inversion

	Dispersion Curve	Configuration		BC	GL
GA1	*ESAC*	*Circle*	V_S	350 m/s	940 m/s
			H	62 m	n/a
GA2	*ESAC*	*L-shape*	V_S	325 m/s	900 m/s
		42 geophones	*H*	40 m	n/a
NA1	*MSPAC*	*Circle*	V_S	325 m/s	750 m/s
			H	37 m	n/a
NA2	*ESAC*	*L-shape*	V_S	370 m/s	990 m/s
		42 geophones	*H*	45 m	n/a
NA3	*MSPAC*	*L-shape*	V_S	375 m/s	925 m/s
		42 geophones	*H*	51 m	n/a

Site Response Analysis using SHAKE2000

Idriss and Seed (1967) first proposed the equivalent linear approach for site response analysis that calculates an approximate nonlinear response through a linear analysis with soil layer properties adjusted to account for the softening during earthquake shaking (Bolisetti et al., 2014).

As an input for the analysis, the following information has to be provided:
1. A one-dimensional representation of the profile
2. Shear modulus reduction and damping ratio vs. strain curves
3. An acceleration time history

Results obtained in the first part of the study were used to construct the profiles (GA2 and NA2) while the curves used for the different stratigraphic materials have been selected among the available standard ones incorporated in SHAKE2000. Three acceleration time histories, representative of a large, medium and small earthquake, were chosen. These are: the 1693 M7.4 earthquake (simulated by Abela (2014), peak acceleration 0.041g), the 1990 M5.4 earthquake (PGA=0.0356g) and 2014 M4 earthquake with a PGA of 0.000388g (ITACA database http://itaca.mi.ingv.it). Data from the last two earthquakes is real and was recorded by stations in Sicily with epicentral distances being similar as those of Malta, and situated on bedrock.

Figure 1 and 2 show the response spectra with 5% damping ratio and amplification spectra for each profile and bedrock obtained for the 1693 input, while in Table 2 the PGA and spectral accelerations at periods which at periods of 0.1 s, 0.2 s, 0.3 s and 1 s are presented

The first resonance peak of the amplification spectrum is almost equal in frequency and very similar in amplitude, however this agreement decreases with frequency.
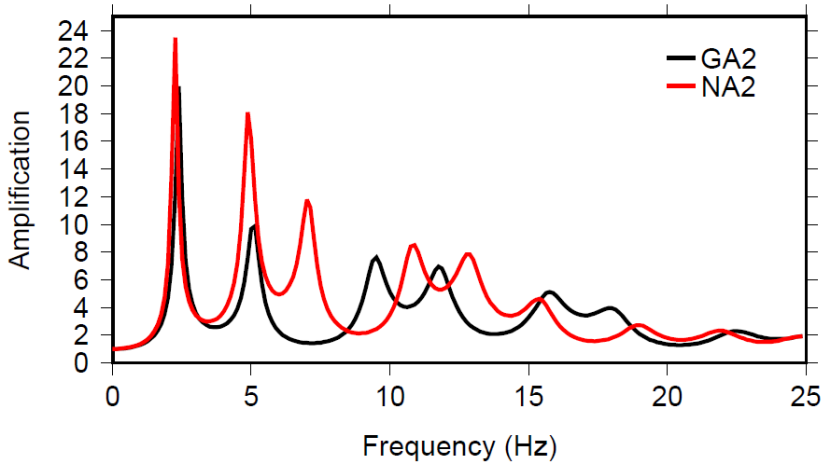
Figure 1: Amplification spectrum for the simulated 1693 earthquake
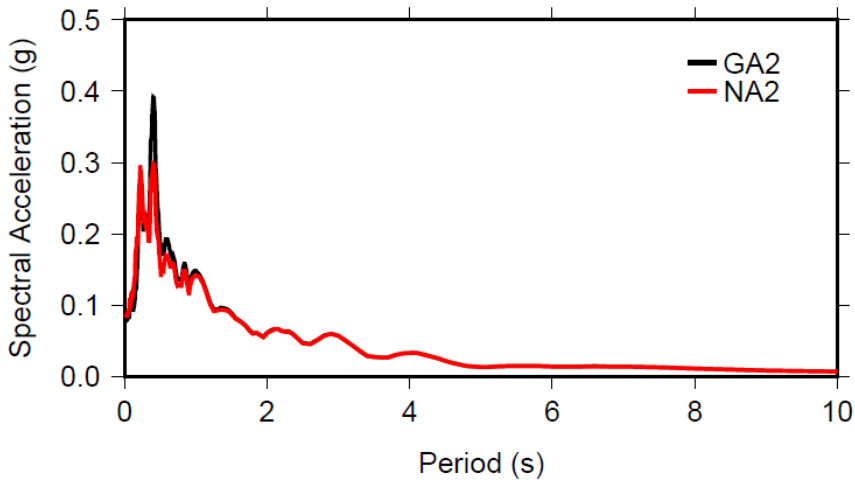
Figure 2: The response spectra for 5% damping at the surface for the simulated 1693 earthquake.

It is observed that the peak ground acceleration (PGA) for the 1693 input motion is about 0.08 g. The maximum spectral acceleration for GA2 is around 0.4 g and corresponds to a period of 0.4 s (2.5 Hz) which is very close to the fundamental period of the soil deposit as found experimentally using single-station ambient noise techniques (H/V). For NA2, the maximum spectral acceleration is approximately 0.3 g and also occurs at both 0.22 s and 0.4 s. Even though the input V_S profiles differed slightly due to the non-uniqueness of surface-wave techniques and the fact that they were obtained from two different inversion runs, this did not reflect any significant differences in the final seismic site response results

Table 2: The main results obtained from the site response analysis for a simulated 1693 event

Model	PGA (g)	Amplification	SA at 0.1 s	SA at 0.2 s	SA at 0.3 s	SA at 1 s
GA2	0.08064	1.967	0.14843	0.22923	0.22173	0.11366
NA2	0.08699	2.122	0.1415	0.25456	0.20558	0.11755

Conclusion

The main objectives of this research were to measure shear wave velocity, estimate site response and calculate response spectra and spectral acceleration at a chosen site in Malta. Different surface wave techniques were used to obtain a one-dimensional V_S profile for the site and after choosing two profiles, the effect of the soft Blue Clay in modifying ground response was obtained by conducting one dimensional equivalent- linear ground response analysis using the software SHAKE2000. Three input motions were tested and the results are presented in terms of response spectrum, amplification spectrum and PGA.

It has been shown that lithographic sequence as in Rabat plays an important role in amplifying ground motion as a significant difference between the input ground motion at the bedrock and that at the surface was observed.

Acknowledgements

References

Abela, K. (2014). M.Sc. Dissertation, University of Malta

Aki, K. (1957). Space and time spectra of stationary stochastic waves, with special eference to microtremors. Bulletin of the Earthquake Research Institute, 35: 415-456.

Bettig, B. P. Bard, F. Scherbaum, J. Riepl, F. Cotton, C. Cornou, and D. Hatzfeld. (2001). Analysis of dense array noise measurements using the modified spatial auto-correlation method (SPAC): Application to the Grenoble area. Bollettino di Geofisica Teorica ed Applicata, 42: 281-304.

Bolisetti, C., A.S. Whittaker,et al., H.B. Mason, I. Almufti, and M. Willford (2014). Equivalent linear and nonlinear site response analysis for design and risk assessment of safety-related nuclear structures, Nuclear Engineering and Design, 275: 107-121

Bisch, P., E. Carvalho, H. Degee, P. Fajfar, M. Fardis, P. Franchin, M. Kreslin, A. Pecker, P. Pinto, A., Plumier, H. Somja, and G. Tsionis (2012). Eurocode8: Seismic Design of Buildings. Worked examples. Publications Office of the European Union, 2012.

Capon, J. (1969). High-resolution frequency-wavenumber spectrum analysis. Proceedings of the IEEE 57: 1408-1418.

Fäh, D., F. Kind, and D. Giardini. (2003). Inversion of local S-wave velocity structures from average H/V ratios, and their use for the estimation of site-effects. Journal of Seismology, 7: 449-467.

Idriss, I.M., and H.B., Seed (1967). Response of Horizontal Soil Layers During Earthquakes. Soil Mechanics and Bituminous Materials Research Laboratory, University of California, Berkeley, Berkeley, CA.

Kramer, S. (1996). Geotechnical Earthquake Engineering. Dorling Kindersley (India) Pvt. Ltd.

Nakamura, Y. (1989). A method for dynamic characteristics estimations of subsurface using microtremors on the ground surface. Quarterly Report of the Railway Technical Research Institute Nguyen, 30: 25-33.

Okada, H. (2003). The Microtremor Survey Method. Geophysical Monograph Series No. 12, Society of Exploration Geophysicists, Tulsa, Oklahoma.

Ordonez, G. (2002). SHAKE 2000, A computer Program for the 1-D Analysis of Geotechnical Earthquake Engineering Problems. California, Berkeley.

Pace, S., F. Panzera, S. D'Amico, P. Galea., and G. Lombardo (2011). Modelling of ambient noise HVSR in a complex geological area- Case study of the Xemxija Bay Area, Malta in: Slejko, D. and Rebez, A.(eds.), Riassunti Estesi Delle Comunicazioni, 30° Convegno Nazionale GNGTS, Trieste, Italy, 299-302.

Panzera, F., S. D'Amico, P. Galea., G. Lombardo, M.R. Gallipoli, and S. Pace (2013). Geophysical measurements for site response investigation: preliminary results on the island of Malta. *Bollettino di Geofisica Teorica ed Applicata,* **54**,111–128.

Parolai, S., S. M. Richwalski, C. Milkereit, and D. Fäh. (2006). S-wave velocity profiles for earthquake engineering purposes for the Cologne area (Germany). Bulletin of Earthquake Engineering, 4: 65-94.

Picozzi, M., A. Strollo, S. Parolai, E. Durukal, O.Özel, S. Karabulut, J. Zschau, and M. Erdik. (2009). Site characterization by seismic noise in Istanbul, Turkey. Soil Dynamics and Earthquake Engineering, 29: 469-482.

Zor, E., S., Özalaybey, A. Karaaslan, M. C. Tapirdamaz, S. C., Tarancioğlu, and B. Erkan. (2010). Shear-wave velocity structure of the Izmit Bay area (Turkey) estimated from active-passive array surface wave and single-station microtremor methods. Geophysical Journal International, 182: 1603-1618.

SEISMIC CHARACTERIZATION OF SOILS IN THE CITY OF LORCA (SE SPAIN) FROM AMBIENT NOISE MEASUREMENTS

Garcia-Fernandez, M.[1], Albarello, D.[2], Jimenez, MJ[3],Massini, F.[4], Lunedei, E.[5]

[1] *Institute of Geosciences, CSIC, UCM, Spain, mariano.garcia@csic.es*

[2] *Dip.Sc. Fisiche, della Terra e dell'Ambiente, Università di Siena, Siena,Italy, dario.albarello@unisi.it*

[3] *Institute of Geosciences, CSIC, UCM, Spain, mj.jimenez@csic.es*

[4] *Dip. Sc. Fisiche, della Terra e dell'Ambiente, Università di Siena, Siena,Italy, nuvolacamy@gmail.com*

[5] *Dip.Sc. Fisiche, della Terra e dell'Ambiente, Università di Siena, Siena,Italy, lunedei@unisi.it*

A 5.2 Mw earthquake shook the city of Lorca, in Murcia region (SE-Spain) on 11 May 2011 at 18:47 local time. The main shock was preceded by a large 4.5 Mw foreshock, about two hours before. The strongest aftershock, around four hours later, reached Mw 3.9. The event caused 9 fatalities and more than 300 people were injured in a town with a population of around 60,000 in an area of 7 km2. Around 1,000 buildings, including residential, cultural heritage, schools, government buildings, healthcare, security facilities, etc., were damaged with different degree. Damage was concentrated in several areas of the town where around 40% of buildings were affected. In the historical centre 16% of buildings were damaged. Historical heritage was severely affected including old churches and medieval wall towers. Nearby towns and provinces were not seriously affected. Earthquakes are not infrequent in Murcia region, where Lorca city is located. Several events in the historical record reached maximum intensity EMS-98 VIII (e.g., one in 1674 and two in a 1911 sequence), while in the last 10 years a number of events have occurred in the same region in 1999, 2002, and 2005 of magnitudes 4.8, 5.0 and 4.7, respectively. These three events reached intensities EMS98 VI-VII, causing damage and economic losses in several towns in the region.

Within the two years following the 2011 5.2 Mw earthquake in Lorca, several ambient vibration measurement campaigns, both single-station and multi-station array configurations, were performed in order to constrain seismic properties of the subsoil in the city and its surroundings. Single-station ambient-vibration records were obtained at 79 sites in Lorca, mainly in its urban area. Additionally, at 13 sites, 9 three-directional digital tromographs were deployed in 2-D array configurations, characterized by dimensions of the order of 100 m. Measurements in the vertical component were used to retrieve the relevant effective dispersion curve of Rayleigh waves by considering ESAC and f-k approaches. Furthermore, at each measurement point within the array, horizontal-to-vertical average spectral ratios (HVSR) were also computed. Moreover, polarization analysis was carried out, which allowed detecting possible anisotropies in the ambient vibration wavefield.

The dispersion and HVSR curves obtained at each site were ere jointly inverted by considering a genetic algorithm (GA) approach, assuming that the monitored ambient vibration wavefield is dominated by surface waves including both Love and Rayleigh waves with relevant higher modes. By this procedure, S-wave velocity profiles, along with the relevant uncertainties, were estimated at each site up to depths of the order of hundreds of meters. Preliminary results reveal that possible groundmotion amplification by local soils is not significant in most of the Lorca urban area and they also suggest the presence of significant lateral heterogeneities in the subsoil structure, resulting from past tectonic activity of major faults present in the region.

GEOPHYSICAL SURVEYS TO STUDY A LANDSLIDE BODY (NORTH-EASTERN SICILY)

Imposa, S.[1], Fazio, F.[2], Grassi, S.[1], Cino, P.[3], Rannisi, G.[2]

[1] *University of Catania, Department of Biological, Geological and Environmental Sciences,*
Earth Science Section, Corso Italia 57, 95129, Catania, Italy
[2]*Geo Dixi, via Alfonzetti 46, 95131, Catania*, Italy
[3]*Freelance geologist, Messina*, Italy

Introduction

Two field surveys, performing recordings of environmental noise combined with a MASW survey were carried out in 2010/11 and 2015. in an area affected by landslide, near the village of Tripi (Messina) (Fig. 1a). The Tripi area is greatly affected by instability phenomena triggered by intense rainfalls on the particular geological and morphological characteristics of the territory, characterized by very steep slopes (Fig. 1b).The Tripi country with its hamlet "Casale" are among the centers, in Sicily, at higher hydrogeological risk, since the landslides and rockfalls that often mobilize, put at risk the population and the structures (P.A.I.- Hydrographic basin of the Mazzarrà creek).

The landslide studied in this work activated on December 14th, 2009, just north of the Tripi village, threatening the main road between this center and its hamlet Casale, the landslide then re-activated again on February 21st, 2012.
On December 22nd, 2010 and January 18th, 2011, 36 measures of noise were carried out. They were located along 3 different profiles within the landslide body arranged orthogonal to the movement direction, and a MASW survey located near the profile performed at lower altitude.

During the second field survey performed on April 28th, 2015, 34 environmental noise recordings on 3 profiles were acquired; two section partially mark those performed 5 years earlier and, even in this case, an investigation MASW. The main purpose is to obtain information for the geometric reconstruction of the landslide slip surface and to observe the possible variations over time.

Geological and tectonic setting

The study area is located on the border between the northeastern sector of the Nebrodi mountains and the northwestern sector of Peloritani mountains, that is the southernmost tip of the Calabrian-Peloritan arc, that connects the Apennines with Sicilian Maghrebids. The geology is characterized by metamorphic units of medium and high grade (Lentini et al., 2000) (Fig. 1c).

From a tectonic point of view, is an area of broad Late Quaternary, regional uplift, approximately trending NE-SW and dipping towards NE, bounded at its edges by the Ionian and Tyrrhenian zones down from systems of normal faults oriented NE-SW (Messina-Giardini system) and ENE-WSW (peritirrenic

system), referring to the phase essentially relaxing that took place in the Upper Pliocene-Pleistocene (Caliri et al., 1993; Lentini et al.,2000).

This stratigraphic and structural edifice show a tangential compressive deformative stress to main south convergence that has created a system of folds, layers of cover and structural axes movements generally orientated E-W, including transverse structures with functions of cinematic " junction" represented by fault transpressive system with a discrete component vertical orientated NW-SE (Caliri et al., 1993; Lentini et al., 2000). The morphology of the area around Tripi is characterized by very steep slop and deeply incised valleys. Watersheds are short and with high slope, and were affected by intense recent geomorphological dynamic. In fact, analysis of maps of Hydrogeological Plan of the Sicilian Region, referring to the hydrographic river basin of the creek "Mazzarra" and attached maps show that the area is affected by instability phenomena of collapse.

Figure 1. a) Location of Tripi (Messina) Sicily; b) the picture show at right the Tripi village and at left the hamlet Casale, yellow dashed line point out the landslide; c) geological and tectonic map of Tripi area (Lentini et al., 2000); d) location profiles on the study area.
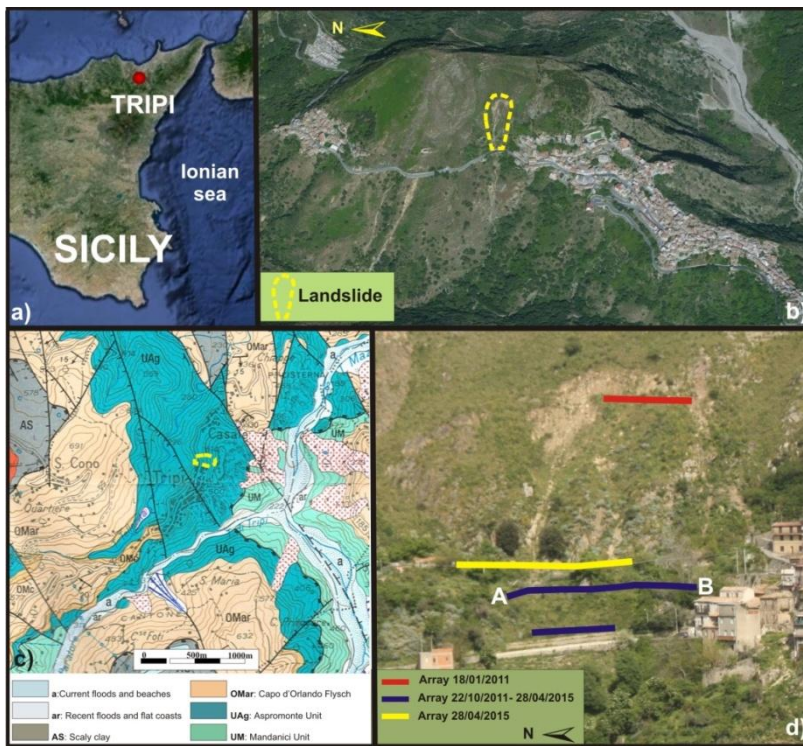
Geophysical Surveys

To achieve the objective, we used the acquisition of noise processed with the technique of Nakamura (1989), integrating the results with a MASW; the joint

fit of the dispersion curve, obtained from the analysis MASW with spectrum HVSR, result of microtremor measures, has allowed to get a Vs profile with depth. Environmental noise recordings were acquired, with preset spacing along alignments in order to obtain seismo-stratigrafic sections that could allow the reconstruction of sliding plane through the detection of impedance contrast caused by the passage between the bedrock and the landslide body.

The "passive seismic single-station" methodology, providing information on the local seismic response, is based on the acquisition of environmental seismic noise, characterized by low energy and amplitude (Okada, 2003). It consists in calculating the spectral ratio between the average of the horizontal and vertical components of the signal. This method was applied for the first time by Nogoshi and Igarashi (1970) and, subsequently, it became popular thanks to Nakamura (1989). In recent years, several authors have highlighted how this methodology allows to obtain information on the stratigraphy of an investigated site (e.g. Field and Jacob, 1993; Lachet and Bard, 1994; Ibs-Von Shet and Wohlenberg, 1999; Delgado et al., 2000a; Parolai et al., 2002; Imposa et al., 2013).

In a simple two-layer system of soft sediments, with a shear-wave velocity Vs and a thickness H, covering a hardrock basement, the equation (1) links the resonance frequency "f" to the thickness "H" of the resonating layer, depending on the shear waves velocity:

$$f = n\ Vs/4H \qquad (1)$$

where n (= 1, 3, 5 ...) indicates the order of the mode of vibration (fundamental, first superior etc.), Vs and H represent the shear waves velocity and the thickness of the resonating layer respectively.

Equation 1 allows to understand how the H / V technique can also provide information on stratigraphic features. Indeed, starting from a noise measurement providing f, knowning the Vs of the coverage, the depth of the main seismic reflectors or vice versa can be estimated (Ibs-Von Seht and Wohlenberg, 1999; Delgado et al., 2000b; Gosar and Lenart, 2010). Each peak in the H / V graph corresponds to a possible reflector (seismic-stratigraphic level) that presents an impedance contrast compared to the neighbour levels. In this case, the impedance contrast is associated to the landslide slip surface.

In this surveys a total number of 70 environmental noise samplings, distributed along six profiles, with regular spacing of 5 m, except for the profile done at higher altitude, where it was used a spacing of 4 m, were sampled in order to obtain a two-dimensional "impedance contrast" section. The profile has been located in perpendicular direction to that of landslide movement (Fig. 1d).

The recordings of environmental noise were carried using 6 portable digital seismographs series TROMINO® (Micromed S.p.a.), equipped with three electrodynamic orthogonal sensors (velocimeters) responding in the band 0.1 ÷ 1024 Hz. Seismic noise has been acquired following a standard procedure (Castellaro et al., 2005), with a sampling frequency of 128 Hz, amplified and digitalized to 24-bit equivalent, and recorded for 20 minutes. This allowed obtaining "stable" H/V ratios and ensured that the recorded signal was the result of

"dominant" sources. Recordings were processed through the software package Grilla® (Micromed).

During the two acquisition campaigns we also proceeded to the execution of two MASW, to estimate the various seismic waves velocities in the subsurface and reach, in particular, to the definition of an average velocity of the uppermost layers necessary for the development of impedance contrast sections (Fig. 2a-c).

The methodology MASW was introduced by the Kansas Geological Survey (Park et al., 1999); the energization is effected at various distances and with various repetitions (stacking technique), the signals obtained are algebraically added in order get a signal clearly stronger than environmental noise. The MASW technique is based on the registration of Rayleigh surface waves in the time domain and the subsequent analysis in the frequency domain to reconstruct the trend of shear waves velocity in the subsoil; the measuring of S waves velocity through the use of surface waves is possible because the two velocity Vs and Vr in the same medium differ by few percentage units (Richart et al., 1970; Achenbach, 2000).

The seismic signal was acquired through a digital multi-channel array, SoilSpy Rosina, Micromed S.p.A., able to record continuously; the array formed by 12 vertical geophones to natural frequency of 4.5 Hz, with spacing of 5 meters, for a total length of 55 m. The time series acquired by the multichannel system SoilSpy, was drawn in frequency - phase velocity domain (slant-stack, and Fourier transform) in order to discriminate the energy associated with Rayleigh waves .

The maximum energy associated with Rayleigh waves defines the dispersion curve trend, that associates to each frequency the propagation wave velocity. The 1D seismic stratigraphic models (Fig. 2b-d), showing the variation of shear wave velocity at depth, were obtained through mutual "constraints" of depth resulting from conjunct fit between the dispersion curve, obtained from MASW technique and HVSR spectrum, obtained from noise recordings**.**

Results

Based on processing of the acquired data you may notice a slight deepening of the impedance contrast between sections obtained from recordings made in December 2010-January 2011 and those made five years later. A good agreement between the depth where it is found the most significant velocity change and the depth of the impedance contrast can also be observed, this can therefore associated with the passage between the detrital material in landslide and the underlying substrate, thereby permitting the identification of the trend of probable sliding surface.

The section shown as example in figure 2, along the profile AB (Fig. 1) identifies an important seismic refractor associable with the slip surface. The depth of the surface, was approximately 3 m on December 2010 and about 4 m 5 years later, in April 2015. Above this surface, the deposits have very low shear wave velocity (Fig. 2b-d), around 200 m/s, associable to deposits involved in the landslide. Under these deposits the shear wave velocity increases rapidly, around 500-600 m / s, this is associated with the bedrock.

Data processing allowed to obtain information about the sliding surface depth through an interpretation of geometric reconstruction of the track along the alignments of profiles that take into account the strong impedance contrasts associated with the transition between the body landslide and substrate; it was also obtained Vs variations with depth profiles, which allows to evaluate the shear waves velocity of landslide material and bedrock.
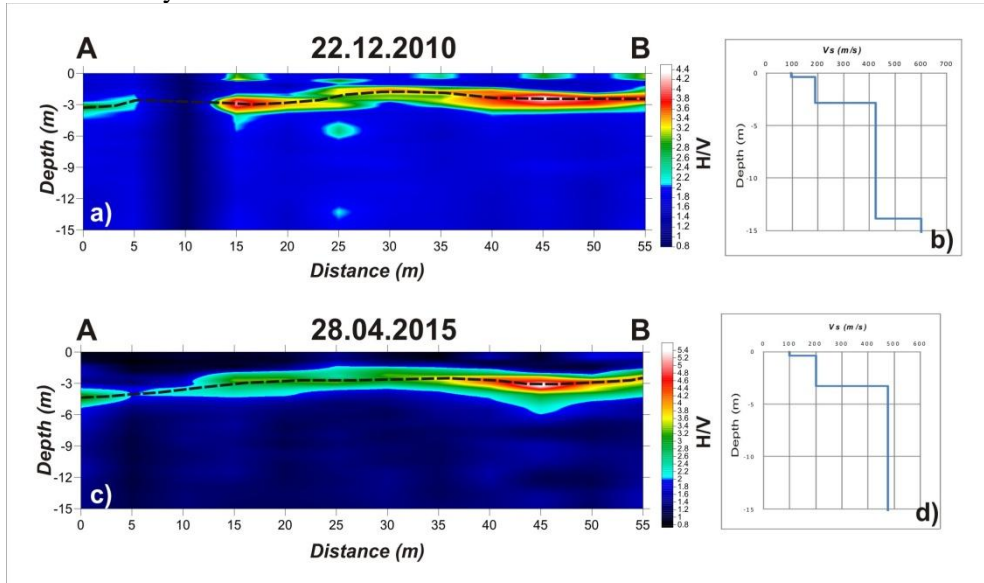
Figure 2. a)-c) Example of impedance contrast sections,at two different acquisition times; the dashed black lines show the trend of the sliding surface; b)-d) velocity values vs depth.

Acknowledgements

References

Achenbach, J. D. (2000). Calculation of surface wave motions due to a subsurface point force: An application of elastodynamic reciprocity. The Journal of the Acoustical Society of America, 107(4), 1892-1897.

Amorosi, A., Castellaro, S., and F. Mulargia (2008). Single-Station Passive Seismic Stratigraphy: inexpensive tool for quick subsurface investigations. Geoacta, 7, 29-39.

Caliri, A., Carbone, S., Carveni, P., Catalano, S., Lentini, F., Strazzulla, S., Romeo, M., Vinci, G., and G. Vinciguerra (1993). Carta geologica del Golfo di Patti (Sicilia settentrionale). 1:25.000. S. EL. CA.

Castellaro, S., Mulargia, F., and L. Bianconi (2005). Passive seismic stratiraphy: a new efficient, fast and economic technique. Geologia Tecnica e Ambientale, 3, 76-102.

Delgado, J., Lopez Casado, C., Estevez, A., Giner, J., Cuenca, A., and S. Molina (2000a). Mapping soft soils in the Segura river valley (SE Spain) : a case study of microtremors a san exploration tool. J. of Appl. Geophys., 45, 19-32

Delgado, J., Lopez Casado, C., Giner, J., Estevez, A., Cuenca, A., and S. Molina (2000b). Microtremors as a geophysical exploration tool: applications and limitations. Pure, 157, 1445–1462.

Field, E.H., and K. Jacob (1993). The theoretical response of sedimentary layers to ambient seismic noise. Geophys. Res. Lett., 20–24, 2925–2928.

Gosar, A., and A. Lenart (2009). Mapping the thickness of sediments in the Liubljana Moor basin (Slovenia) using microtremors. Bull. Earthquake Eng. (2010), 8, 501-518.

Ibs-Von Seht, and J. Wohlenberg (1999). Microtremor measurements used to map thickness of soft sediments. Bull.Seism. Soc. Am., 89 (1), 250-259.

Imposa, S., Fazio, F., Grassi, S., and G. Rannisi (2013). Studio della risposta di sito in un area del versante meridionale del Mt. Etna . In: Geofisica Applicata, 2, 409-416, Trieste , 19 - 21 Novembre.

Lachet, C., and P.Y. Bard (1994). Numerical and theoretical investigations on the possibilities and limitation of Nakamura's technique. J. Phys. Earth, 42, 377-397.

Lentini, F., Carbone, S., Catalano, S., and Messina (Provincia) (2000). Ass. territorio. Servizio geologico. Carta geologica provincia Messina. Scala 1:50.000. S. EL. CA.

Nakamura, Y. (1989). A method for dynamic characteristics estimation of subsurface using microtremor on the ground surface. Quarterly Report of Railway Technical Research Institute. Rept., 30, 25–33.

Nogoshi, M., and T. Igarashi (1970). On the propagation characteristics of the microtremors. Journal of the Seismological Society of Japan, 24, 24-40.

Okada, H. (2003). The microtremor survey method. Geophysical monograph series, no. 12. Society of Exploration Geophysics.

Park, C. B., Miller, R. D., and J. Xia (1999). Multichannel analysis of surface waves. Geophysics, 64 (3), 800–808.

Parolai, S., Bormann, P., and C. Milkereit (2002). New relationships between Vs, thickness of sediments and resonance frequency calculated from H/V ratio of seismic noise for the Cologne area. Bull. Seism. Soc. Am., 92, 2521-2527.

Regione Siciliana, Assessorato Territorio e Ambiente. Piano Stralcio di Bacino per l'Assetto Idrogeologico (P.A.I.) – Bacino Idrografico del Torrente Mazzarrà (010).

SEISMIC SITE RESPONSE AT LAMPEDUSA ISLAND, ITALY

Panzera F., Sicali S. ,Lombardo G.
Dipartimento di Scienze Biologiche, Geologiche e Ambientali,Università di Catania– Italy,fpanzera@unict.it

Introduction

Recently, a joint Italo-Maltese research project (Costituzione di un Sistema Integrato di ProtezioneCivileTransfrontalieroItalo-Maltese, SIMIT) was financially supported by the European community with the aim to improve the geological and geophysical information in the area between the south-eastern Sicilian coast and the islands of Lampedusa and Malta with a final purpose to mitigate natural hazards.

Although this region lies onthe Sicily Channel Rift Zone, a seismically active domain of Central Mediterranean, the knowledge about seismotectonic and local seismic response is at present quite unsatisfing. In the frame of SIMIT project, the island of Lampedusa (Pelagian archipelago) was investigated through a multidisciplinary approach including, besides a geophysicalmethods, structural, morphologic and lithologic analyses as well. Results of geological-structural surveys were, in particular used to understand the local seismic response of the distinct outcropping terrains and its influence on the dynamic behavior of existing buildings. Ambient noise recordings were used as seismic input, processing the data collected through spectral ratio techniques. Polarization of the horizontal component of motion was also investigated in order to set into evidence possible directional effects.

Geologic and structural setting

Lampedusa is an E-W elongated island located in the central Mediterranean sea, about 200 km south of the Sicilian coastline and 150 km East of Tunisia. The island consists of a 11 km long carbonate shelf that reaches the maximum topographic elevation of 133 m a.s.l. From the structural point of view, Lampedusa belongs to the Pelagian block, a foreland domain at the northern edge of the African plate, formed by a 6–7 km thick Meso-Cenozoic shallow to deep-water carbonate successions (Civile et al. 2008; 2013). The island is found inside the Sicily Channel,at the southern shoulder of a Plio-Quaternary foreland rift zone that exhibits deep, NW-SE trending, fault-controlled structural depressions (e.g. the grabens of Pantelleria, Linosa and Malta).

As revealed by the available seismic database (INGV 1981-2013), the rift zone is characterized by a moderate seismicity, mostly located in the Linosagraben, with shallow events (h < 25 km) and magnitude ranging from 2 to 4 (Civile et al., 2008). In this scenario, Lampedusa represents a small horst structures formed by Neogene –Quaternary carbonate sequences (Grasso and Pedley, 1985) characterized by the following lithologic units: Carbonate lithoclastbreccias of late

Pleistocene-Holocene age; Aeolian dunes formed of bioclasticgrainstones of late Pleistocene; Wave-cut platform and sand raised beaches (late Pleistocene, Tyrrhenian); Bioclasticgrainstones (early Pleistocene); Limestones of the Lampedusa Formation that is constituted by the VallonedellaForbice, Capo Grecale and CalaPisana members of Tortonian–Early Messinian age (see Fig. 1a). Following Grasso and Pedley (1985), major tectonic lineaments are located in the eastern part of the island.Structural measurements performed along the cliff revealed that the area is deformed by a NW-SE oriented wrench zone (CalaCreta fault) composed of sub-vertical fault segments accompanied by a damaged zone consisting of fractures with pervasive pattern. Faults consist mostly of NW-SE oriented and SW-dipping reverse structures with slickenside on planes indicating a left-lateral component of motion (Lombardo et al., 2014).
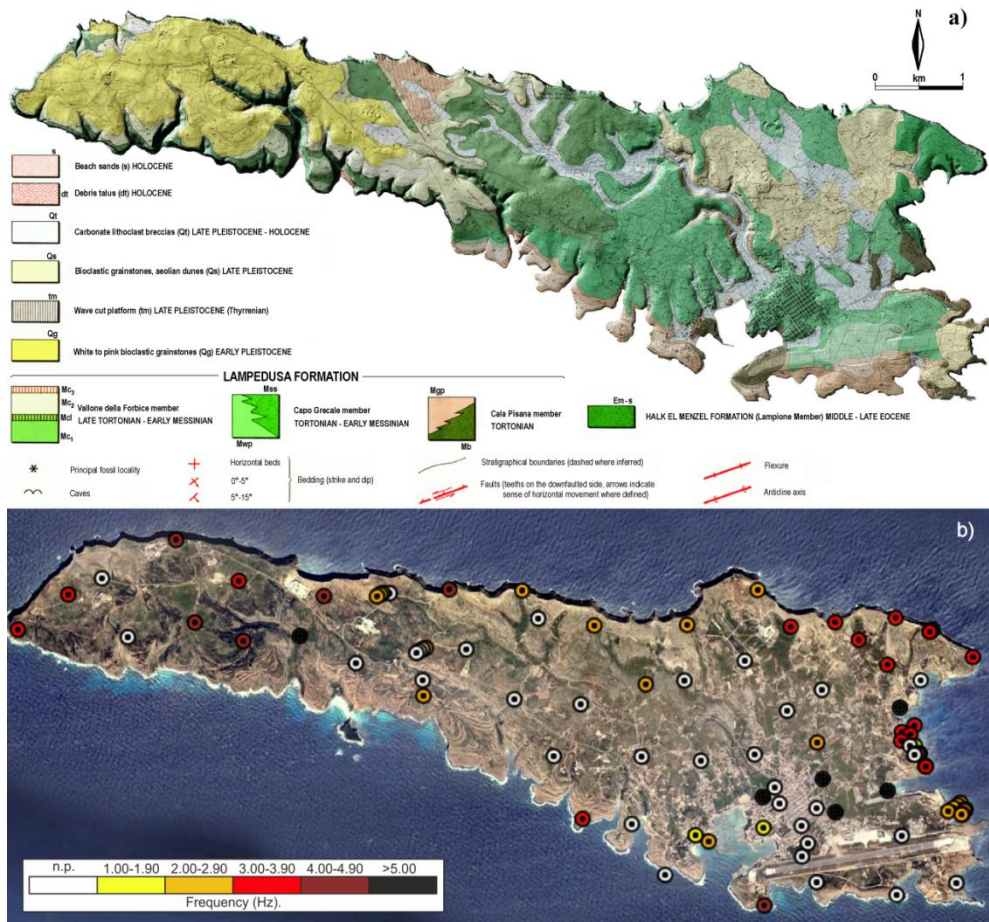

Figure 1.a) Geologic map of the Lampedusa island (modified from Grasso and Pedley 1985); b) Location of ambient noise recording sites and related fundamental frequencies experimentally detected.

Another tectonic lineaments (Aria Rossa fault), is detected in the central part of the island. It consist of a NW-SE oriented fault with no evident fault plane but a series of second order fractures and a topographic irregularity with a quite sharp change in the outcropping lithology.

Methodology

Ambient noise recordings were performed in eighty measurement sites (Fig. 1b) that were almost homogeneously spaced along a grid having size of about 600 m, taking into account the outcropping lithology. Data were collected through aTromino, a 3-component velocimeter particularly suitable for a cheap and speedy field measurements survey. Time series of 20 minutes length were recorded using a sampling rate of 128 Hz and processed through the Horizontal to Vertical Noise spectral Ratio technique (HVNR). Time windows of 20 s were considered and the most stationary part of the signal was selected excluding transients associated to very close sources. In this way the Fourier spectra were calculated in the frequency range 0.1-30.0 Hz and smoothed using a proportional 20% triangular window. Following the criteria suggested by the European project Site EffectS assessment using AMbient Excitations (SESAME 2004), only the spectral ratio peaks having amplitude greater than two units, in the frequency range 0.5-15 Hz, were considered significant.

Experimental spectral ratios were also calculated after rotating the horizontal components of motion by steps of 10 degrees starting from 0° (north) to 180° (south) in order to investigate about the possible presence of directional effects. In this study we also applied the time-frequency (TF) polarization analysis proposed by Vidale (1986) and exploited by Burjánek et al. (2012). This technique can provide quite robust results, overcoming the bias that could be introduced by the denominator spectrum in the HVNR calculation. For each time-frequency pair, polarization is characterized by an ellipsoid and it is defined by two angles: the strike (azimuth of the major axis projected to the horizontal plane from North) and the dip (angle of the major axis from the vertical axis). Another important parameter is the ellipticityof the particle motion that, according to Vidale (1986), is defined as the ratio between the length of the minor and major axes: this parameter approaches 0 when ground motion is linearly polarized as typically observed for body waves. Polarization strike and dip obtained all over the time series analyzed are cumulated and represented using polar plots where the contour scale represents the relative frequency of occurrence of each value, and the distance to the center represents the signal frequency in Hz.

Description of Results and Concluding Remarks

The results obtained set into evidence that major spectral ratio peaks are detected in the frequency range 2.0 - 4.5 Hz. Going into more details, we observe that these peaks often do not reach two amplitude units(left panel in Fig. 2a). Such behavior is more evident both in the south-eastern part of the island, as well as in its central and western portion. Comparison with the Lampedusa lithology points

out that in these areas the most ancient and rigid terrains outcrop. These findings are therefore in good agreement with the stiffness of the limestone formations extensively outcropping in the plateau located in the central part of the island. More pronounced spectral ratio peaks (right panel in Fig. 2a)are detected in the measurement sites located in proximity of the outcrops of more recent and soft deposits, as well as along the transects crossing the CalaCreta fault, which marks out the eastern boundary of the island.Similarly, marked spectral ratio peaks are observed inthe transects performed perpendicularly to the strike of the morphologic escarpments existing in the north eastern side of the island (central panel in Fig. 2a). We can therefore affirm that since Lampedusa is almost entirely formed by calcareous deposits, the amplification effects are mostly caused by either morphological features or tectonic structures.

In Figure 2b examples of the local seismic response observed nearby the CalaCreta fault are shown. A clear spectral ratio peak at about 2.5 Hz is evident in the measurement sites. This peak seem to be strongly directional, with maximaalmost perpendicular to the fault strike. The polarization of the horizontal components of motion, evaluated in the measurement sites located nearby the fault lines, show indeed that the largest amplifications occur at high angle from the fault strike (Lombardo and Rigano, 2006; Panzera et al., 2012). On the other hand, measurements performed at increasing distance from the fault zone do not show a similar behavior, therefore suggesting that the observed directional effects can be ascribed to the fault fabric (Panzera et al., 2014).

We can finally affirm that the use of ambient noise records showed to be a reliable and not expensive technique for a quick characterization of the local seismic response and the experimental evaluation of building fundamental periods, as well as investigations about possible soil-to-structure interactions. This kind of studies appear to be particularly useful to governmental agencies tasked with emergency response and rescue. Indeed, performing a detailed geologic study, together with the evaluation of the local seismic response and the dynamical properties of buildings in the island of Lampedusa has given significant suggestions about potential critical conditions due to soil-structure interaction and local amplification phenomena.

The results obtained can be summarized as follow:
- A detailed survey, especially performed in the areas of major interest from the geological point of view, such as landslide prone areas was carried out;
- The complexity of the near-surface geology, as well as the morphology strongly influence the local amplification of the ground motion and the occurrence of directional effects.
- Major amplification effects take place on the soft deposits that partially fill up the incisions of old pre-existing streams and mostly in the neighboring of both morphologic escarpments and faults. On the contrary, HVNR with not significant spectral ratio peaks are observed on the calcareous plateau.
- Rotated spectral ratios and polarization analysis highlight the presence of evident directional effects in proximity of both faults and cliffs. The polarization of the

wave-field assumes major values at wide angles (between 60°-90°) with respect to the structures strike.
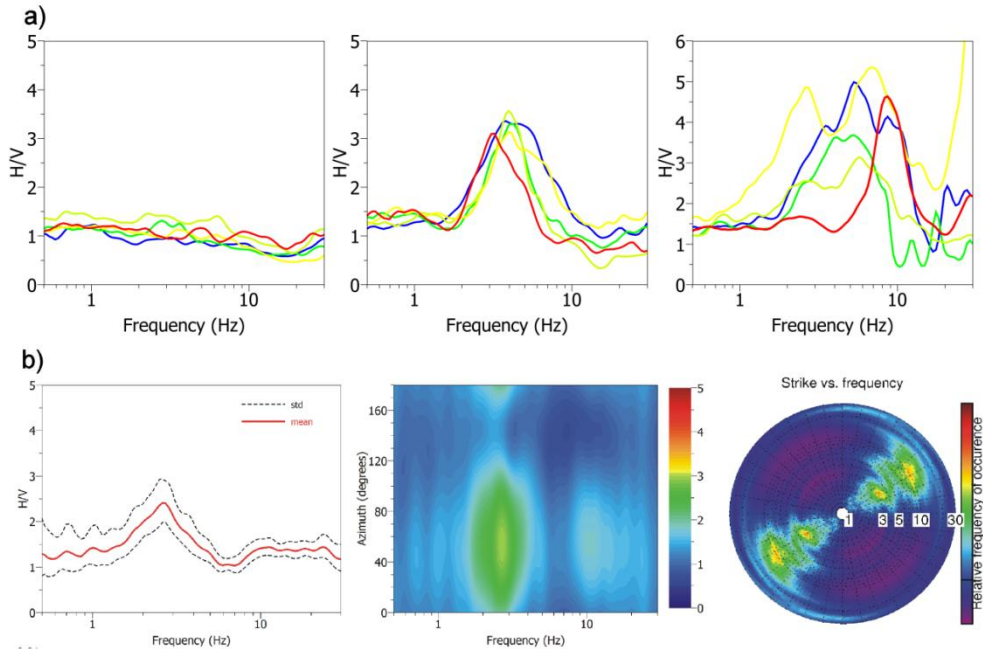
Figure 2.a) Examples of HVNR results subdivided in three groups. left panel flat HVNR; central panel HVNR with a clear peak at about 3.5 Hz,observed in sites located near the cliff areas; right panel HVNR characterized by high frequencies fundamental peak in sites in which outcrops soft deposits. b)Examples of HVNR, directional resonance diagrams and polar plot of polarization azimuthobtained in the CalaCreta fault area.

Acknowledgements

References

Burjànek, J., Moore, J.R., Molina, F.X.Y., and D. Fäh (2012).Instrumental evidence of normal mode rock slope vibration, Geophys, J. Int. 188, 559-569.

Civile, D., Lodolo, E., Tortorici, L., Lanzafame, G., and G. Brancolini (2008).Relationships between magmatism and tectonics in a continental rift: the Pantelleria Island region (Sicily Channel, Italy), Marine Geology 251, 32-46.

Civile, D., Lodolo, E., Alp, H., Ben-Avraham, Z., Cova, A., Baradello, L., Accettella, D., Burca, M., and J. Centonze (2013). Seismic stratigraphy and structural setting of the Adventure Plateau (Sicily Channel), Mar. Geophys. Res. DOI 10.1007/s11001-013-9205-5

Grasso, M., and H.M. Pedley (1985).The Pelagian Islands: a new geological interpretation from sedimentological and tectonic studies and its bearing on the evolution of the central Mediterranean sea (Pelagian Block), Geol. Romana24, 13-34.

Lombardo, G., Panzera, F., Salamanca, V., Sicali, S., Baldassini, N., Barreca, G., Di Stefano, A., Monaco, C., and S. D'amico (2014). Detailed geophysical and geologic study in the Lampedusa Island: SIMIT Project. In: Gruppo Nazionale di Geofisica della Terra Solida. D. Slejko et alii eds, Atti del 33° Convegno Nazionale G.N.G.T.S.. vol. 2, Caratterizzazione sismica del territorio, p. 203-209,:Casa Editrice Stella Arti Grafiche, Trieste, ISBN: 978-88-940442-2-5.

Lombardo, G., and R. Rigano (2006).Amplification of ground motion in fault and fracture zones: observations from the Tremestieri fault, Mt. Etna (Italy), Journal of Volcanology Geothermal Research 153, 167-176.

Panzera, F., Lombardo, G., D'amico, S., Di Stefano, A., Galea, P., and C. Monaco (2012).Evidence of directional site effects on fault zones: observations from south-eastern Sicily and Malta, European Seismological Commission 33-rd General Assembly, Moscow, August 19-24. Book of Abstracts, 411-412.

Panzera, F., Pischiutta, M., Lombardo, G., Monaco, C., and A. Rovelli (2014).Wavefield polarization in fault zones of the western flank of Mt. Etna: observations and fracture orientation modeling, Pure Appl. Geophys. DOI 10.1007/s00024-014-0831-x.

SESAME (2004).Guidelines for the implementation of the H/V spectral ratio technique on ambient vibrations: Measurements, processing and interpretation, SESAME European Research Project WP12, deliverable D23.12, 2004; http://sesame-fp5.obs.ujf-grenoble.fr/Deliverables 2004

Vidale, J.E. (1986).Complex polarization analysis of particle motion, Bull. Seism. Soc. Am. 76, 1393–1405

DYNAMIC CHARACTERIZATION AND DECONVOLUTION ANALYSIS FOR SOME SITES OF THE ITALIAN ACCELEROMETRIC NETWORK (RAN)

Paolucci, E.[1], Albarello, D.[2], Lunedei, E.[3], Peruzzi, G.[4],
Papasidero, M. P.[5], Francescone, M.[6]

[1]*Dipartimento di Scienze Fisiche, della Terra e dell'Ambiente, Università di Siena, Via Laterina 8, Siena, Italy, enricopaolucci83@gmail.com*
[2]*Dipartimento di Scienze Fisiche, della Terra e dell'Ambiente, Università di Siena, Via Laterina 8, Siena, Italy, dario.albarello@unisi.it*
[3]*Dipartimento di Scienze Fisiche, della Terra e dell'Ambiente, Università di Siena, Via Laterina 8, Siena, Italy, lunedei@unisi.it*
[4]*Dipartimento di Scienze Fisiche, della Terra e dell'Ambiente, Universià di Siena, Via Laterina 8, Siena, Italy, peruzzi31@student.unisi.it*
[5]*Dipartimento di Scienze Fisiche, della Terra e dell'Ambiente, Università di Siena, Via Laterina 8, Siena, Italy, michele.papasidero23@gmail.com*
[6]*Dipartimento di Scienze Fisiche, della Terra e dell'Ambiente, Università di Siena, Via Laterina 8, Siena, Italy, mib87@hotmail.it*

Introduction

This work is part of the DPC-INGV-S2 research project devoted to improving mid-long term seismic hazard assessment in Italy (https://sites.google.com/site/ingvdpc2012progettos2/home). One of its main aims is the empirical testing of seismic hazard estimates proposed so far for the Italian area (Albarelloet al., 2015). To this purpose, several sites belonging to the Italian accelerometric network (RAN) active for long time (at least for 25 years) are considered and the probabilistic "forecasts" provided by each hazard estimate for that site is compared with observations (for a general discussion of the testing methodology see Albarello and D'Amico, 2015).

Since hazard estimates are generally provided for reference soil conditions, only accelerometric sites of type A (by following NTC, 2008), which represent a subset of the considered sites, could be used for testing. Furthermore, site soil classification for the most part of these stations was provided on the basis of large-scale (1:100000) geological maps only, and this inaccurate soil classification may bias results of testing. To face this problem, the first phase of the work has been devoted to estimating the S-wave velocity (VS) profile at all the sites and to provide a site characterization in terms of VS,30. Thus, to exploit as much as possible available information, observations at non-reference sites were deconvolved (e.g., Kramer, 1996) for the local seismic response to obtain accelerometric records "equivalent" to those relative to reference site conditions.

Results relative to nine accelerometric sites are presented here: eight of them are located in Central Italy (Cagli, Cascia, Castel Viscardo, Matelica, Peglio,

Rincine, Senigallia, Sirolo) and one in Southern Italy (Gildone). By following the procedure described in Pileggiet al. (2011), the VS profile at these locations has been estimated by performing ambient vibration measurements both in single-station and multiple-station configuration. For each non-reference site, the free computer program STRATA (https://nees.org/resources/strata) has been used to de-convolve the ground motion by considering the mono-dimensional seismo-stratigraphical model obtained by the passive seismic study.

Ambient vibration monitoring

Several single-station, analysed by the HVSR technique (Nakamura, 1989; SESAME, 2004), and one multiple-station (seismic array) measurements, analysed by both ESAC (Ohoriet al., 2002; Okada, 2003) and f-k (Lacosset al., 1969; Capon, 1969) techniques, have been performed at each site. In one site, two arrays have been realized, while in another one, an active MASW measurement has also been carried out (vide infra). As regards single-station acquisitions, ambient vibrations have been recorded using a three-directional digital tromographTromino®Micromed (http://www.tromino.eu/); for seismic arrays, vertical geophones (4.5 Hz) and a BrainSpy 16 channel digital acquisition system by Micromed have been used. Acquisition duration of single-station measurements was of 20 or 30 minutes, with a sampling frequency of 128 Hz, while passive seismic arrays recorded at 128, 256 or 512 Hz, in any case for 20 minutes. HVSR curves allow to evaluate the possible presence of seismic resonance phenomena, while from seismic array records Rayleigh-wave dispersion curves are obtained.

Jointly with each ambient-vibration monitoring, a geological/geomorphological survey has been carried out at a local scale (1:5000 or 1:10000), with the aim to better identify the geometry and to characterize the main lithological units where seismic impedance contrasts may occur (cf. Pileggiet al., 2011). In the cases where the RAN stations are located on outcropping stiff soil (Cagli, Cascia, Rincine), it has not been possible to deploy seismic arrays in the exact correspondence of the stations due to the rough topography: in these situations, geologic survey was particularly useful to identify alternative sites characterized by a strict geologic correspondence with the site of interest. Topographical conditions have caused a similar problem for the station of Peglio.

As fully described in Pileggiet al. (2011), passive seismic surveys on stiff-rock sites suffer from significant drawbacks. In fact, in these geological settings, ambient vibrations are characterized by very low powers of surface waves (particularly evident in vertical ground motion) in the whole frequency range of interest (1-20 Hz). Moreover, when relatively high phase velocities exist (such as the ones expected at stiff-rock sites), ambient vibrations can be characterized by large wavelengths with respect to the overall dimension of the array (Fotiet al., 2011; Pileggiet al., 2011). These effects may hamper retrieving clear dispersion curves in some of the analysed rock sites. At Cagli, a reasonable dispersion curve has been obtained for relatively high frequencies (10-25 Hz) only, while at Rincine it has not been possible to obtain any kind of dispersion curve, both using ESAC

and f-k procedures. In this latter case, an active seismic prospecting has been necessary: by using the MASW technique (Park et al., 1999), a dispersion curve that confirms the presence of Rayleigh-wave velocity values greater than 800 m/s at high frequencies (about 20 Hz) has been obtained.

As regards the seismic array analysis, dispersion curves obtained by ESAC and f-k technique are, in general, very similar. Just in one case (Sirolo) the curves produced by these two techniques have been merged to "build" a single curve, because the ESAC curve is acceptable for relatively low frequencies (3-6 Hz) while the f-k one is so for higher frequencies (6-14 Hz). In the remaining cases, the choice of the dispersion curve to be used in the joint inversion procedure (vide infra) has been done by considering the shape regularity and the frequency coverage of the obtained ones.

To assess the VSprofile for the sites whose Rayleigh-wave velocity values are lower than 800 m/s, a joint inversion of a site-representative HVSR curveand of the Rayleigh-wave dispersion curve has been performed in each of them, by using a Genetic Algorithm procedure (e.g., Albarelloet al., 2011). Since other geophysical measurements and borehole data are not available in the studied places, information provided by geological/geomorphological surveys has been used to constrain the inversion process. At each site, the inversion procedure has been repeated several times (>10) in order to estimate possible uncertainties affecting the resulting profiles. The overall variability for the S-wave velocity profile of each site has been assessed by using the extreme values of the set of solutions (profiles obtained by the inversion procedure) whose misfit is not greater than two times the misfit value associated to the best fitting model. These variability ranges have then been used in the deconvolution procedure (vide infra). The best profile of each site has been used to estimate the VS,30and therefore to reclassify the site on the base of this parameter.

Deconvolution analysis

When the stations are located, according to the realized reclassification, on reference sites, the ground-motion recorded by them can be directly used for validating seismic hazard estimates. For the other stations, recorded ground-motion has been de-convolved by considering the seismic response of shallow low-velocity layers from the surface to the seismic bedrock where the ground motion has to be assessed.

The de-convolution has been performed, in a 1D scheme (in which the shallow subsoil is constituted by a stack of horizontal homogeneous and isotropic viscoelastic layers), by means of the free software STRATA (https://nees.org/resources/strata), doing both linear and equivalent linear analysis. STRATA requests the definition of a stratigraphy where each stratum is characterized by: thickness, some statistical properties of S-wave velocity (extremal values, means and variance), the kind of material and its viscosity properties. Results discussed in the previous section have been used to fix these parameters.

First of all, a seismo-stratigraphical profile has been built by correlating the geological section of the area around each station with the VSprofiles derived from relative inversions. This step has been useful in order to link each geological unit to a density value as well as to a damping and a bulk modulus reduction curves. Density values and dynamic curves have been chosen from data derived from seismic microzoning studies in similar lithological units, in the same geological context and geographic area. Only for depths exceeding 40 metres, dynamic curves by EPRI (1993) have been used, in order not to overestimate damping values (usually derived from analysis in shallow samples). Variability ranges in S-wave velocity profiles have been used to establish minimum and maximum values for the bedrock depth, as well as the statistical properties of VSin each strata. Variability of modulus reduction and damping curves have been reproduced by following Darendeli (2001).

For each station where the de-convolution has been made, the ground motion to be de-convolved has been provided by other research units participating in the project, and consists in a set of selected earthquake events.

Statistics about peak ground acceleration (PGA) and acceleration spectral amplitude (SA) at 0.15, 1 and 2 s have been extracted for each site, based on an ensemble of 100 de-convolution runs for each earthquake record, to account for uncertainty affecting the local seismic stratigraphy. For each earthquake, the two horizontal components have been considered separately, taking into account both the geometric mean and the maximum of PGA and SA of each run. Then the median and the 75th percentile of the ensemble have been computed. An example of obtained results (relative to the site of Castel Viscardo) is reported in Table 1.

Table 1. Results for the station of Castel Viscardo: 75th percentile of PGA and SA values are reported for the maximum of horizontal components; surface values are derived from accelerometric registration, while bedrock values are derived from equivalent linear analysis with STRATA; in the last column is reported the ratio between each couple of values.

	Earthquake event	**Surface** (cm/s^2)	**Bedrock** (cm/s^2)	**Surface / Bedrock**
PGA	IT-1992-0001	34.655	22.780	1.521
SA at 0.15s	IT-1994-0002	84.138	54.049	1.557
SA at 1s	IT-1994-0002	3.381	2.537	1.333
SA at 2s	IT-1994-0002	0.804	0.480	1.675

Acknowledgements

References

Albarello D., Cesi C., Eulilli V., Guerrini F., Lunedei E., Paolucci E., Pileggi D., Puzzilli L.M. (2011). The contribution of the ambient vibration prospecting in seismic microzoning: an example from the area damaged by the 26th April 2009 L' Aquila (Italy) earthquake. *Boll. Geofis. Teor. Appl.*, 52, 3, 513-538, doi:10.4430/bgta0013.

Albarello D., Peruzza L., D'Amico V. (2015). A scoring test on Probabilistic Seismic Hazard Estimates in Italy. *Nat. Hazards Earth Syst. Sci.*, 15, 171-187, doi:10.5194/nhess-15-171-2015.

Albarello D., D'Amico V. (2015). Scoring and testing procedures devoted to Probabilistic Seismic Hazard Assessment. *Surv. Geophys.*, Volume 36, Issue 2, Page 269-293, doi:10.1007/s10712-015-9316-4.

Capon J. (1969). High-resolution frequency-wavenumber spectrum analysis. *Proc. IEEE*,**57**(8), 1408–1418.

Darendeli M. B. (2001). Development of a new family of normalized modulus reduction and material damping curves. Austin, Texas: The University of Texas.

EN 1998-1 Eurocode 8 (2004). Design of structures for earthquake resistance – part 1: general rules, seismic actions and rules for buildings [Authority: The European Union per regulations 305/2011, Directive 98/34/EC, Directive 2004/18/EC].

EPRI (1993). Guidelines for Determining Design Ground Motions.EPRI TR-102293, http://www.epri.com/search/Pages/results.aspx?k=Guidelines%20for%20Determining%20Design%20Basis%20Ground%20Motions:%20Volumes%201-5.

Foti S., Parolai S., Albarello D., Picozzi M. (2011). Application of surface wave methods for seismic site characterization. *Surv. Geophys.*, 32, 6, 777-825, DOI 10.1007/s10712-011-9134-2.

Rathje E. M., Kottke A. (2013). Strata. Available online at http://nees.org/resources/strata.

Kramer S.L. (1996).Geotechnical Earthquake Engineering.Prentice Hall, New Jersey, USA.

Nakamura Y. (1989).A method for dynamic characteristics estimation of subsurface using microtremor on the ground surface. *QR Railway Technical Research Institute*, 30, 25 - 33.

Ohori M., Nobata A., Wakamatsu K. (2002).A comparison of ESAC and FK methods of estimating phase velocity using arbitrarily shaped microtremor arrays. *Bulletin of Seismological Society of America*, 92, 6, 2323 - 2332.

Okada H. (2003). The microtremor survey method. Geophysical Monograph Series, SEG, 129 pp.

Lacoss K.T., Kelly E.J. and Toksöz M.N. (1969).Estimation of seismic noise structure using arrays. *Geophysics*, 34, 1, 21 – 38.

NTC (2008). Norme Tecniche per le Costruzioni. DM 14 gennaio 2008. *Gazzetta Ufficiale*, n. 29 del 4 febbraio 2008, Supplemento Ordinario n. 30. Istituto Poligrafico e Zecca dello Stato, Roma (in Italian), available online at http://www.cslp.it/cslp/index.php?option=com_content&task=view&id=66&Itemid=20.

Park C.B., Miller RD.., Xia J. (1999). Multichannel analysis of surface waves. *Geophysics*, 64:800–808.

Pileggi D., Rossi D., Lunedei E., Albarello D. (2011). Seismic characterization of rigid sites in the ITACA database by ambient vibration monitoring and geological surveys. *Bull. Earthq. Eng.*, 9, 1839-1854, doi:10.1007/s10518-011-9292-0.

Site Effects Assessment using Ambient Excitations (SESAME) European project (2004). Deliverable D23.12, Guidelines for the implementation of the H/V spectral ratio technique on ambient vibrations: measurements, processing and interpretation; deliverable D13.08, Final Report WP08, Nature of noise wavefield.

PRELIMINARY RESULTS FROM AN INTEGRATED SHALLOW GEOPHYSICAL INVESTIGATION IN THE NORTH-EASTERN SECTOR OF THE MALTA ISLAND

Pischiutta, M.[1], Villani, F.[2], Vassallo, M.[2], Galea, P.[3], D'Amico, S.[3], Amoroso, S.[2], Cantore, L.[2], Di Naccio D.[2], Mercuri, A.[1], Rovelli, A.[1], Famiani, D.[1], Cara, F.[1], Di Giulio, G.[2], Akinci, A.[1]

[1]*Istituto Nazionale di Geofisica e Vulcanologia, Roma, Italy.*
[2] *Istituto Nazionale di Geofisica e Vulcanologia, L'Aquila, Italy.*
[3]*Department of Geosciences, University of Malta, Msida, Malta*

Introduction

In the framework of the project "SIMIT" and under an agreement between Istituto Nazionale di Geofisica e Vulcanologia (INGV) and DPC of the Regione Siciliana, seismic hazard estimates were performed, resulting in the distribution of the expected peak ground acceleration values (PGA). These estimations refer to stiff-rock sites, and do not include the contribution of the site-local geological condition. In order to take the subsoil response into account in the hazard assessment of the Maltese islands, on November 2014 we performed several geophysical investigations including seismic and electrical 2D-tomography, MASW profiles, 2D arrays and single-station measurements using ambient noise (see Figure 1). The final goal was to combine different geophysical methods which allow the reconstruction of geometries at depth (tens of meters) and the evaluation of shear-wave velocities in the most common geological formations outcropping on the islands. The geology of Malta is characterized by a succession of Tertiary marine sediments, from the bottom to the top: Lower Coralline Fm.; Globigerina Limestones; Blue Clay Fm., Green Sand Fm., Upper Coralline Fm. Moreover the velocity profile has been related to Vs30 parameter that is used to classify soils by the European seismic code (Eurocode8, 2003).

Previous studies performed in Malta by several authors have pointed out that even rock-sites can show site amplification as the effect of cliff-edge and unstable boulder collapse (Panzera et al. 2012; Galea et al., 2014) as well as to the strong impedance contrast between the Blue Clay Fm and the Globigerina Limestone Fm buried under tens of meters of the Upper Coralline Limestone Fm (Vella et al., 2013). Both these situations are quite common in the Northern sector of Malta Island that is characterized by a wide plateau of Upper Coralline Fm. bordered by steep cliffs with large slope failures, representing a threat for human activity in the area. The presence of the stratigraphic contact between the Blue Clay Fm and the Globigerina Limestone Fm under the Upper Coralline Limestone is responsible for an amplitude peak between 1 and 2 Hz.

We decided to focus the attention on the problem of amplification at sites where the Upper Coralline Limestone outcrops. In fact in southern sector of the
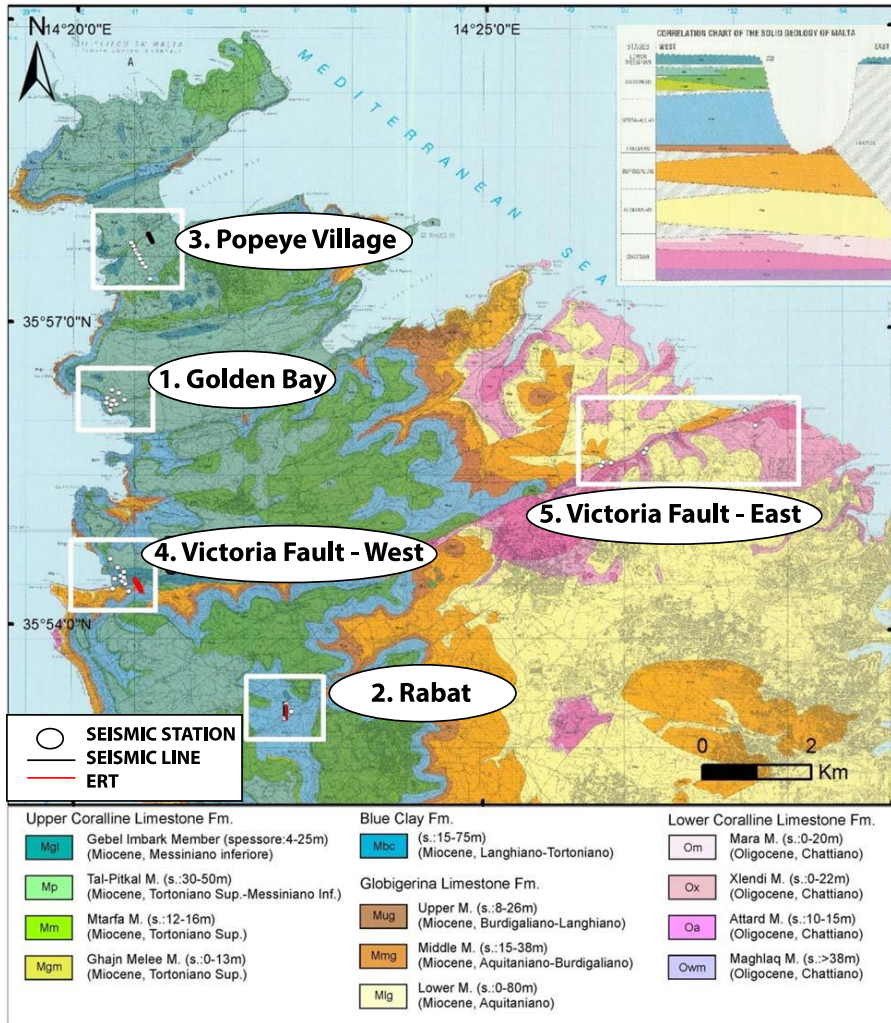
Geophysical Prospecting	ACTIVE INVESTIGATIONS			PASSIVE INVESTIGATIONS	
SITE	Seismic tomography	MASW	Electric tomography	Array measurements	Single station HVSRs
1.Golden Bay	-	-	-	X	X
2. Rabat	X	X	X	-	X
3.Popeye Village	X	X	-	-	X
4.Victoria Fault West	X	X	-	-	X
5.Victoria Fault East	-	-	-	-	X

Figure 1. Geologic map with location of the studied sites and geophysical prospecting carried out.

Malta Island where the Lower Coralline Limestone Fm and the Globigerina Limestone Fm outcrop, no site amplification has been observed so far. All the survey sites are close to a set of NE-trending normal faults that are another common and persistent feature in Malta (Reuther, 1984; Pedley, 1987; Gardiner et al., 1994). These faults belong to the north Malta graben system where the main tectonic feature is the Victoria Line, a complex system of NE-trending strike-slip and normal faults with a prevailing normal component of slip (Putz-Perrier and Sanderson, 2010). For this reason we also decided to study two sites across the Victoria fault.

We finally selected the following sites: 1. Golden Bay; 2. Rabat; 3. Popeye Village; 4. Victoria Fault - West; 5. Victoria Fault - East. In each site we carried out different experiments depending on site-specific geological and logistic conditions. Site location and geology are shown in Figure 1 as well as geophysical investigations performed at each site. In the following sections we describe results of active (seismic and electrical 2D-tomography, MASW profiles) and passive (2D arrays and single-station measurements using ambient noise) geophysical investigations.

Results of active seismic and electrical investigations

We report preliminary results from the active seismic survey performed in site "Victoria Fault–West", across the Victoria Line close to the Fomm Ir-Rih Bay. The 142 m long, NW-trending seismic transect crosses a portion of the fault that does not outcrop because of extensive colluvial cover. The footwall hosts the Globigerina Limestone Fm., whereas the hanging wall hosts the Blue Clays and the Upper Coralline Fm. Probably, at this site the Victoria Line is made of several splays. We provide a high-resolution Vp tomogram (obtained through a non-linear inversion of first arrival traveltimes; see Improta et al. 2002 for details about the method) indicating that between 60 m and 120 m from the NW corner of the line a wide area of low Vp (< 1500 m/s) represents a possible interruption of a 10 m deep refractor. Although additional geophysical and structural investigation is needed, we interpret this feature as the effect of a shallow fault zone. There is no hint of recent faulting because the shallower layers seem undisturbed. The dispersion of surface waves indicates that the shallow layers have Vs slightly higher in the NW part of the profile with respect to the SE part (150-300 m/s and 120-200 m/s respectively). This seems in accordance with the presence of the Upper Coralline Fm. in the hanging wall and the Globigerina Limestone Fm. in the footwall.

In the site "2. Rabat" we performed an electrical resistivity tomography (ERT) across a N-trending, 256 m long line. The main purpose of the investigation was the determination of the thickness of the Blue Clay Fm. We inverted apparent resistivity data acquired with a Wenner configuration of quadrupoles. Our results indicate that the thickness of the Blue Clay Fm. in this site may exceed 40 m (resistivity in the 10-50 Ohm*m range), and probably the deeper part of the ERT section indicates at 45 m depth the transition with the underlying Globigerina Limestone Fm. We acquired also active seismic data parallel to the ERT line.
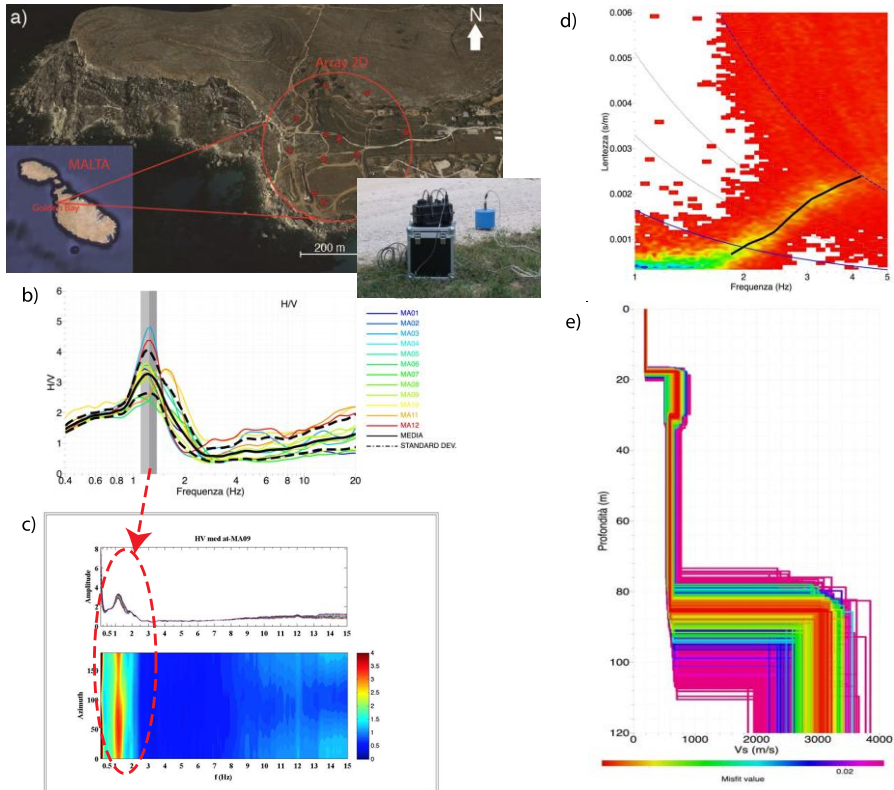
Figure 2 – Passive measurements performed at site "1. Golden Bay". Instrument and array geometry is shown in panel a). Panel b) HVSR calculated at stations, all showing a peak at 1.2 Hz. This peak has the same amplitude on N-S and E-W components, as shown in panel c). In Panel d) we report the dispersion curve obtained from f-k analysis. The Vs velocity profile resulting from the inversion is drawn in panel e).

Traveltime tomography is still in progress. MASW results indicate that the shallow subsurface is characterized by a roughly homogeneous Vs profile, in the 150-200 m/s range, and these values are typical of clayey deposits.

Results of passive seismic investigations

In the site "1. Golden Bay" we performed passive noise measurements using a 12-stations array with a spiral-shape, the minimum and maximum distances being 11 and 400 m, respectively in order to resolve 80-200 m at depth. Stations were composed of velocimetric Lennartz sensors Le3d-5s and Reftek R130 digitizer. Time synchronism was provided by GPS connection. At all stations, HVSRs show an amplitude 4 peak at about 1.2 Hz, that is caused by the impedance contrast between Globigerina Limestone Fm. and Blue Clay Fm., which is overlain by the outcropping Upper Coralline Limestone Fm. The dispersion curve obtained by applying the f-k analysis, was inverted to obtain the Vs velocity profile which is

characterized by 3 layers lying on the Globigerina Limestone bedrock (Vs≈3000 m/s): the first layer (Vs≈200 m/s; h≈18 m) is represented by superficial weathered limestones belonging to the Upper Coralline Fm.; the second layer (Vs≈700 m/s; H≈15 m) is associated to unweathered limestones of the Upper Coralline Fm.; the third layer (Vs≈600 m/s an h≈55m) represents the Blue Clay Fm. The analysis of directional amplification has shown that the 1.2 Hz peak is isotropic, the two horizontal component of ground motion NS and EW showing the same amplitude levels. Conversely, at frequency higher than 4 Hz, stations located closer to the cliff show a slight broadband directional amplification effect with a variable direction.

The same analysis was also applied to noise measurements carried out using 3 single stations at site "2. Rabat", where the Blue Clay Fm outcrops. Here the analysis of directional HVSR revealed the presence of a 2 Hz peak that, consistently to site "1. Golden Bay", is related to the impedance contrast between the Blue Clay Fm. and the underlying Globigerina Limestone Fm. The higher frequency observed at this site could be explained by a smaller thickness of the Blue Clay Fm. and to the absence of the Upper Coralline Fm. After investigating amplification at rock sites related to stratigraphic impedance contrasts we have focused our attention at amplification of rock sites close to fault zones and related to fractured rocks in the fault damage zone (Rigano et al., 2008; Di Giulio et al., 2009; Pischiutta et al. 2012, 2014; Panzera et al., 2014). We have chosen three sites (3. Popeye Village, 4. Victoria Fault-West and 5. Victoria Fault-East) where we have performed passive noise measurements using single stations realizing transect crossing the mapped faults. The Popeye Village prospecting results are not reliable because measurements were strongly affected by anthropogenic noise source resulting in narrow frequency amplitude peaks.

Preliminary results obtained at site "4. Victoria Fault-West" are encouraging because stations installed on the fault footwall do not show any directional amplification and stations at about 1.5 km far from the fault hanging wall show only the stratigraphic peak previously described. Conversely, stations installed on the fault hanging wall show a maximum amplification along NE-SW direction with amplitudes up to a factor of 4 in a broad frequency band (3-8 Hz). This same azimuthal direction was found on one measurement site at "5. Victoria Fault–East" site. Further investigations are needed to check the recurrence of this direction and to interpret its relation to fracture distribution in the fault damage zone.

Conclusions

With our preliminary geophysical investigation in the north-eastern sector of the island of Malta we were able to provide a subsoil characterization of some sites which represent a typical situation where the outcropping fractured limestones of the Upper Coralline Fm. overlies the plastic Blue Clay Fm.

Micro-tremor analyses revealed a typical peak in the H/V curves in the 1-1.5 Hz range, most probably related to the interface between the two formations.

Directional analyses close to some important fault zones revealed the presence of a recurrent NE-SW peak that needs to be thoroughly studied.

Shallow geophysical investigation of the Victoria Line close to the Fomm Ir-Rih Bay revealed a shallow fault zone, however further studies are needed to assess the possible recent activity of this complex fault system at this site.

References

Di Giulio, G., F. Cara, A. Rovelli, G. Lombardo, and R. Rigano (2009), Evidences for strong directional resonances in intensely deformed zones of the Pernicana fault, Mount Etna, Italy, J. Geophys. Res., 114, B10308, doi:10.1029/2009JB006393.

Gardiner, W., Grasso, M., Sedgeley, D., 1995.Plio-Pleistocene fault movement as evidence for mega-block kineatics within the Hyblean-Malta plateau, Central Mediterranean. J. Geodynamics, 19/1, 35-51.

Galea, P., D'Amico, S., Farrugia, D., 2014. Dynamic characteristics of an active coastal spreading area using ambient noise measurements—Anchor Bay, Malta, Geophys. J. Int. (2014) 199, 1166–1175.

Improta L., Zollo A., Herrero A., Frattini R., Virieux J. and Dell'Aversana P. 2002. Seismic imaging of complex structures by non-linear traveltime inversion of dense wide-angle data: Application to a thrust belt, Geophysical Journal International 151, 264–278, doi: 10.1046/j.1365-246X.2002.01768.x.

Panzera F., D'Amico S., Lotteri A., Galea P. and Lombardo G.; 2012: Seismic site response of unstable steep slope using noise measurements: the case study of Xemxija bay area, Malta. Nat. Hazards Earth Syst. Sci., 12, 3421–3431, doi:10.5194/nhess-12-3421-2012.

Pedley, H.M. 1987. Controls on Cenozoic sedimentation in the Maltese Islands. Review and reinterpretation. Memorie della Società Geologica Italiana, 38, 81–94.

Pischiutta, M., F. Salvini, J. Fletcher, A. Rovelli, and Y. Ben-Zion (2012), Horizontal polarization of ground motion in the Hayward fault zone at Fremont, California: Dominant fault-high-angle polarization and fault-induced cracks, Geophys. J. Int., 188(3), 1255–1272.

Pischiutta M., Pastori M., Improta L., Salvini F. and Rovelli A.: 2014: Orthogonal relation between wavefield polarization and fast S-wave direction in the Val d'Agri region: an integrating method to investigate rock anisotropy, J. Geophys. Res, 119, 1–13, doi:10.1002/2013JB010077.

Putz-Perrier, M., and Sanderson, D.J. (2010), Distribution of faults and extensional strain in fractured carbonates of the North Malta Graben. AAPG Bulletin, 94/4, 435–456.

Reuther,C .D.,1984. Tectonics of the Maltese Islands. Centro, 1(1), pp.1-20.

Rigano, R., F. Cara, G. Lombardo, and A. Rovelli (2008), Evidence of ground motion polarization on fault zones of Mount Etna volcano, J. Geophys. Res., 113, B10306, doi:10.1029/2007JB005574.

Vella, A., Galea, P. & D'Amico, S., 2013. Site frequency response characterization of the Maltese islands based on ambient noise H/V ratios, Eng. Geol., 163, 89–100

SALTWATER INTRUSION IN FRIULI LOW PLAIN

Zavagno, E.,Zini, L., Cucchi F.
Department of Mathematics and Geosciences – University of Trieste, via Weiss 2, Trieste, 34100 Italy, ezavagno@units.it

Introduction

In coastal areas, the interaction between seawater and fresh water is in a dynamic equilibrium andoccursboth in surface bodies (saltwater ingression) and in groundwater (saltwater intrusion in aquifers). Human actions and climatic changes, especially sea level rising, can alter this equilibrium leading to a contamination of the fresh water andsoils by seawater.

The shift of salt wedge towards inland can be a consequence of both natural and anthropogenic processes. Natural processes have generally slow effects, except in the case of tsunami, as in Sri Lanka (Villholth and Neupane, 2011). The sea level rising due to climatic changes (Mellouland Collin, 2006) and local subsidence along coastal areas cause a slow salt wedge shifting. Instead, human actions have rapid effects on the coast system. Examples of the human actions are the overexploitation of aquifer, the incorrect and extreme watercourse regimentation, the excavation of floodway canal and dredging for navigation. The salt wedge intrusion can lead to freshwater contamination and consequentlyto a decrease of water reserve, to coastal area desertification by ground salinization and to a loss of faunistic and floristic species.

Study area

The study area is adjacent to the GradoMarano lagoon (Figure 1a) in the Low Friuli Plain (Friuli Venezia Giulia region, NE Italy). Friuli plain is built up by fluvial, glacio-fluvial and marine deposits and is divided in two parts by a resurgence belt:High Plain and Low Plain. The High Plain consists mainly of gravels and sands, while silt and clay are prevalent in Low Plain. Theundifferentiated phreatic aquifer of the High Plain feeds the complex confined aquifer system of the Low Plain, which is an important water resource for a large population. Stratigraphic studies show the presence of 11 aquifers.Our study focused particularly on the shallowestone, located between 20 m and 80 mbelow ground level (b.g.l.). This aquifer, named "A", consistsof three permeable layers separated by two impermeable ones (Zini et al., 2011; Zini et al, 2013).

The Low Plain topographic gradient varies from 4‰ in the northern part to 0.5‰ in the southern part (Fontana, 2006). Large areas are near and below sea level (down to -4.3 ma.m.s.l.) in the extreme southern part.An important embankment belt was built in 20th century to protect and drain a vast area. The embankment belt divides the Low Plain from GradoMarano Lagoon. The latter is composed of the estuary deposits of Tagliamento and Isonzo Rivers, the main rivers of the Region. GradoMarano lagoon is exhaustively studied due tothe

IsonzoRiver strong mercury contamination from natural and human origin (Covelli et al., 2009).

The Stella, the Corno and the Aussa Rivers are the most important riversflowing from the resurgence belt towardsGradoMaranoLagoon. These rivers have peculiar characteristics: no solid transport, low temperature variationsand a delayed response to seasonal precipitations. The last 8 km of Corno and Aussa riverbeds were strongly modified during 19th and 20th centuries.The rivers wereboth straightened. During the second part of 20th century,Corno River was dredged to build an important harbour for local industry. In the last 25 years, several piezometers were completedfor groundwater quality monitoring (figure 1b).
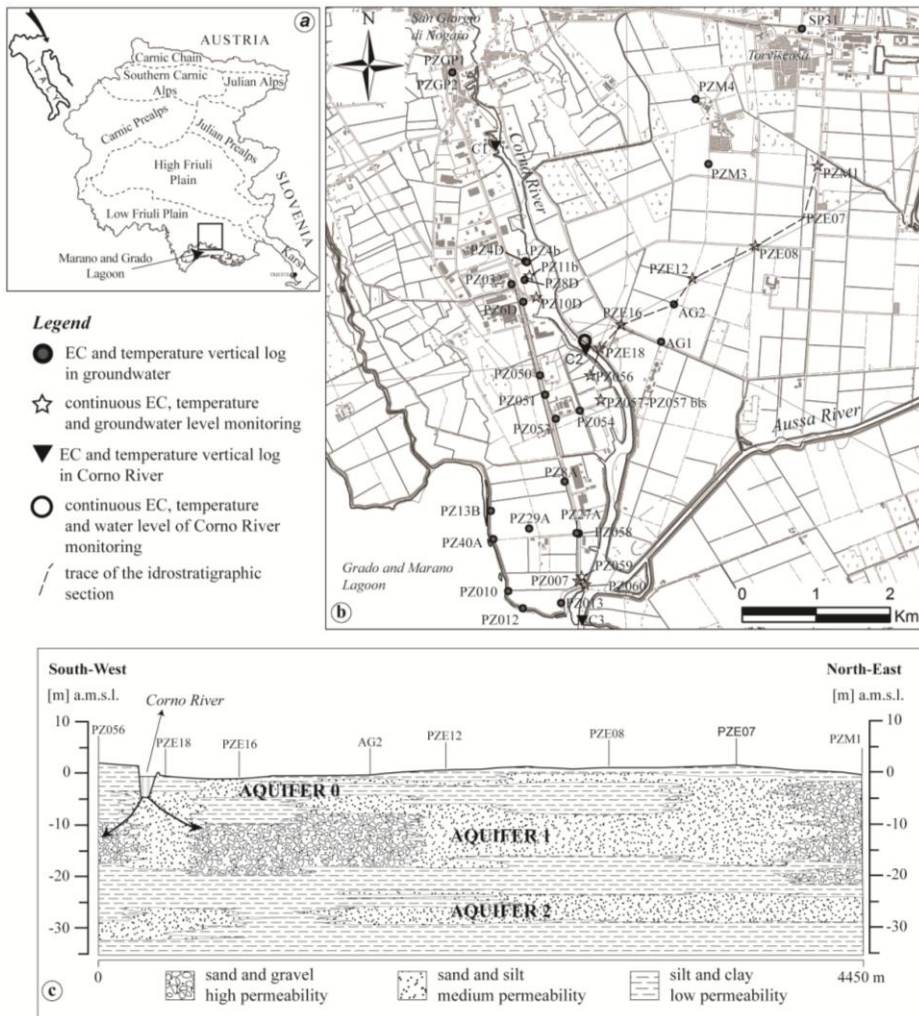

Figure 1: a) Study area location; b) Monitoring network and location of hydrogeological section; c) hydrogeological section.

The study focused on monitoring the CornoRiver and the surrounding shallowaquifers (0-25 m deep). A monitoring network has been planned in collaboration with ARPA FVG to verify the occurrence of a salt wedge and to assessthe relationships between CornoRiver and the surface aquifers. The study is linked to a research of ARPA FVG to understand the origin of anomalous values of some metals, especiallyiron, in water and soil (Pezzetta E., 2011).

Stratigraphic model

The stratigraphic data of 357 boreholes were elaborated using the RockWorks 14 (Rockware®) software. Each single borehole stratigraphy has been georeferenced and correlated with neighbouring ones to elaborate a tridimensional model.The size of the stratigraphic model is 18*14 km up to a depth of 35 m. Pixel size is 50*50*0.1 m. From the model, 15 geological sections were realized and furtheranalysed from a hydrogeological point of view.

This stratigraphic analysis is fundamental in order to recognize levels with different permeability. The obtained stratigraphic section allows identifying the high- (gravel, gravel and sand), medium- (sand, sand and silt) and low- (silt, silt and clay, clay) permeable layers (Figure 1c). We distinguished two main aquifers (Aquifer 1 and Aquifer 2) and aminor shallower one (Aquifer 0).

Aquifer 0 is not laterally continuous and itsmaximum thickness is 3.0-4.0 m. Its depth ranges between 0.0 and 5.0 mb.g.l. and occurs in deposits with high-medium permeability. Aquifer 1 is laterally continuous and can be 12 m thick. It is located between 8.0 and 20.0 mb.g.l. and it is constituted by deposits with high and medium permeability. Aquifer 2 is the deepest, its maximum thickness is 5 m and it is located between 25.0 and 35.0 mb.g.l.. It is not laterally continuous and consists of deposits with medium permeability. Aquifer 0 and Aquifer 1 are partly in connection.

Electrical Conductivity, Temperature and Water Level monitoring

A high mineralization of water is the main indicator of itssalinization;therefore,the electrical conductivity was selected as the first parameter for the water monitoring. Another important parameter is the temperature because, in this case, it represents a natural tracer,which allowsdistinguishing the seawater from freshwater. In fact, the water of Corno and AussaRivers shows minimaltemperature variationscompared to the seawater. Moreover, the water level plays a crucial role in the analyses of possible interactions between seawater and the aquifers.

The tidal flow can cause a change in the aquifer water level if sea and aquifer are connected. This relation is stronger when the connection is due to the presence of high permeable layers and/or to a low hydraulic loading of the aquifer. The electrical conductivity, temperature and water level were measured continuously (30 min. sampling rate)by means of five multi-parametric probes (CTD Divers, EijkelkampAgrisearch Equipment®). A Baro Diver

(EijkelkampAgrisearch Equipment®) was used for barometric compensation. The CornoRiver was monitored for 7 months (04/2011 – 11/2011).Theinstrument was placed into a punched PVC tube to protect it from current and impacts. The groundwater was monitored continuously in13 piezometers (two in the Aquifer 0 and 11 in the Aquifer 1), at least for one lunar cycle (28 days), in order to verify the tide influences (Figure 1b). Water level data were also collected manually.

One CTD Diver was used to obtainvertical logs of electrical conductivity and temperature in41 piezometers (7 in the Aquifer 0 and 34 in the Aquifer 1) and inthe CornoRiver(Figure 1b). The instrument was set to asamplingrateof 1 second and was slowly droppeddown by means of a cable into the aquifer. The vertical logs were collected in several tide conditions both in rivers and in piezometers, in order to check the sea influences.

Results

Electrical conductivity and temperature logs obtained along the Corno and Aussa Rivers show, near the mouth in the GradoMarano lagoon, high electrical conductivity already from the first centimetres of the water surface. The electrical conductivity values increase, with the deepening of the probe, up to seawater values in the bottom of the river. Upstream the behaviour is similarbut, at the river bottom, the electrical conductivity has lowervalues than the seawater. An example of three electrical conductivity logs (C1, C2 and C3), collected in Corno River, is shown in figure 2b. Both electrical conductivity and temperature logs show soft stratification of the water. In the hot season the temperature increases with depth, while in the cold seasons temperature decreases.The difference between the surface temperature and bottom temperature is higher during hot seasons. Far from the river mouth the freshwater has greater influence than near the mouth. The electrical conductivity and temperature logs highlight the effects of seawater ingression up to 8 km from the Corno River mouth.

In 12 piezometers the electrical conductivitylogs show typical seawatervalues between 5 and50 mS/cm. In general, the electrical conductivity shows a sharp increasewith depth to be opposed to the soft one in the rivers (figure 2a). The piezometers near the lagoon are exposed directly to the tide effects but only the PZ40A and PZ13B (Figure 1b) have electrical conductivity values above 5 mS/cm, while the others have values bellow 2 mS/cm (freshwater). Their EC is constant with depth. The EC measured in vertical profilesin the piezometersare not always correlatedwith the distance from the Corno River. The piezometer located farther north (PZ11b) shows values above 5 mS/cm (saltwater) and the AG1 piezometer contains salty water despite its distancefrom the Corno River.

The continuous water level data in the Corno River point out a clear lagoon feeding (Figure 2c). This is evidenced by the semi-diurnal tide effect perfectly correlated to the tide gauge station of MaranoLagunare levels. Instead, the temperature has a diurnal variation due toatmospheric influences.The electrical conductivity has no regular oscillation, the mean value is 6.8 mS/cm (salty water), but during high tides the EC can increase up to 30 mS/cm.
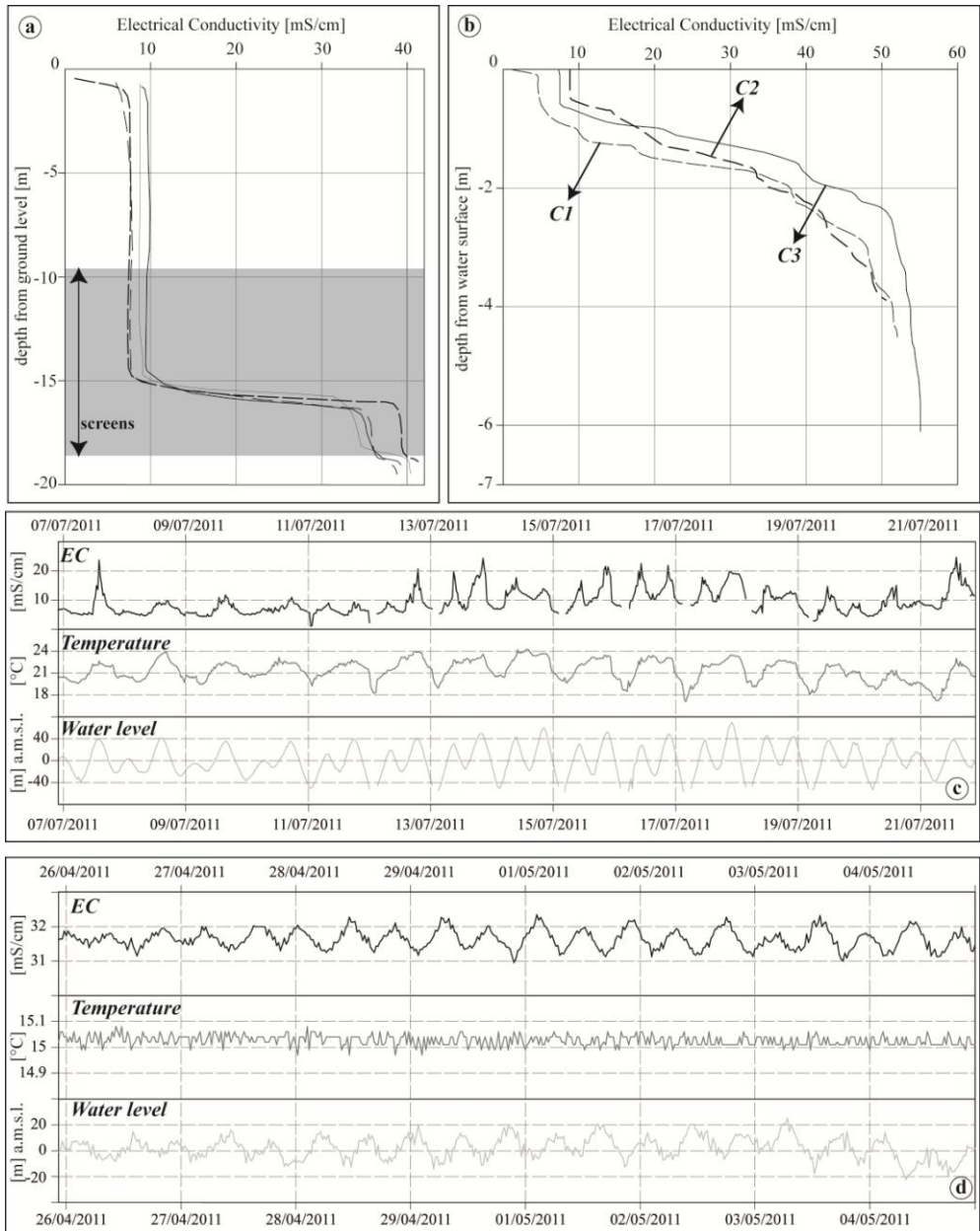
Figure 2: a) example of electrical conductivity vertical log in aquifer; b) example of electrical conductivity vertical log in Corno River; c) electrical conductivity, temperature and water level continuous monitoring in Corno River; d) electrical conductivity, temperature and water level continuous monitoring in aquifer.

The 13 continuously monitored piezometers exhibited different EC, level and temperature behaviours. PZ057bis, PZE16, PZE12, PZE08, PZM1 and PZ11b (Figure 1b) did not showtide-related oscillations of EC, temperature and water level. PZ060, PZ059, PZ056, PZ007 and PZ057 show a medium-low correlation with the Corno River considering the water level and the electrical conductivity data. PZE18 and PZ10D showeda high correlation with the river.PZE18 has a stable high EC value (49 mS/cm) and the piezometer water level has a good correlation with the Corno water level. PZ10D water level data has the higher correlation with water level of the Corno River.Electrical conductivity and water level data of the piezometer PZ060 show clear semidiurnal oscillations (fig. 1d).

This is interpreted as a sign of direct connection with the Corno River waters.The peaks of the two parameters are not simultaneous because of the delayed EC signal responseof about 4-6 hours compared to the instantaneous water-pressure transmission.This delay between EC and water level peaks,in the PZ10D and in other piezometers was not recorded.

Conclusions

The intensive anthropogenic alteration of the natural riverbed of the Corno River in the 20th centurycaused the ingression of the seawater up to 8 km from the mouth of the river.The water column in the last part of the Corno River is stratified with electrical conductivity values comparable to seawateron the bottom of the river.

The water level and electrical conductivity in the river show a semi-diurnal tide influence. Our study highlight the saltwater intrusion inside the superficial aquifers. Electrical conductivity profiles discard a direct correlation between the distance from the lagoon or the Corno Riverandthe presence of saltwater in the aquifer. This is attributable to thenatural heterogeneity of the deposits of different permeability. Alternatively this could be due to the reclaim and rectificationworks of the rivers.

The tide effect on the aquifer, as demonstrated by the correlation between their chemical-physical characteristics, proves the existence of a link between the Corno River and the aquifer. As the last dredging dates from 19 years ago, new dredging works started in the Corno River to bring back the riverbed to 7 m depth.

This operation could intensify the connection between the Corno River and theaquifers. Although theydo not representan important water resourceit is essential tomonitor the effects of the dredging, in order to check the evolution of the saltwater intrusion and to prevent a possible contamination of the deeper aquifers.

Acknowledgements

References

Covelli S., A.Acquavita, R. Piani, S. Predonzani, and C. De Vittor (2009). Recent contamination of mercury in an estuarine environment (Marano lagoon, Northern Adriatic, Italy). Estuar Coast Shelf S 82 273–284.

Fontana A. (2006). Evoluzione geomorfologica della bassa pianura friulana e sue relazioni con le dinamiche insediative antiche. MonografieMuseoFriulanoStoriaNaturale47, Udine, 288 pp.

Melloul A., and M. Collin (2006). Hydrogeological changes in coastal aquifers due to sea level rise, Ocean Coast Manage 49 281-297.

Pezzetta E., A.Lutman, I. Martinuzzi, C. Viola, G. Bernardis, and V. Fuccaro (2011). Iron concentrations in selected groundwater samples from the lower Friulian Plain, northeast Italy: Importance of salinity,Environ Earth Sci62 377-391.

Villholth K.G., and B.Neupane (2011). Tsunamis as Long-Term Hazards to Coastal Groundwater Resources and Associated Water Supplies, in Tsunami - A Growing Disaster Mohammad Mokhtari (Ed.), InTech, 87-104.

Zini L., C. Calligaris, F. Treu, D. Iervolino, and F. Lippi (2011). Risorse idriche sotterranee del Friuli Venezia Giulia: sostenibilità dell'attuale utilizzo, EUT edizioni, 90 pp.

Zini L., C. Calligaris, F. Treu, D. Iervolino, and F. Lippi (2013). Groundwater sustainability in the Friuli Plain, AQUA Mundi 41-54.

GPR PROSPECTING ON LARGE BURIED CRYPTS: THE CASE HISTORY OF THE CHURCH OF SANTA MARIA DEL SUFFRAGIO IN GRAVINA IN PUGLIA (APULIA, SOUTHERN ITALY)

Matera, L.[1], Ciminale, M.[2], Leucci, G.[1], De Giorgi, L.[1], Piro, S.[3], Persico, R.[1]

[1]*Institute for Archaeological and Monumental Heritage IBAM-CNR, via per Monteroni di Lecce, Lecce,Italy,*
matera@ibam.cnr.it; g.leucci@ibam.cnr.it; l.degiorgi@ibam.cnr.it;
r.persico@ibam.cnr.it

[2]*Department of Earth and Geo-environmental Sciences, University of Bari Aldo Moro, via Orabona, Bari, Italy, marcello.ciminale@uniba.it*

[3]*Institute of Technologies Applied to Cultural Heritage ITABC-CNR, Via Salaria, km 29.300, Monterotondo, Rome, Italy, salvatore.piro@itabc.cnr.it*

Introduction

In this paper we put into evidence some benefits but also some problems that can be met when large buried cavities are investigated by means of a GPR system. This is done with reference to the specific case history of the church Santa Maria del Suffragio, in Southern Italy, where the complexity and the size of the buried anomalies put into evidence some limits intrinsic to the GPR technique. Monitoring of historical monuments is an issue of interest both for cultural and safety issues. In particular, a non-invasive investigation of the architectural structures can be useful to address in a proper fashion a restoration work, possibly identifying meaningful fractures in walls and pillars, or ascents of humidity from the ground (Gabellone et al., 2013, Leucci et al., 2011). Moreover, hidden abandoned buried crypts are present in some cases, which can cause stability problem, especially during the execution of a restoration work, if not previously identified and, as far as possible, characterized. In many cases the involved buried anomalies are not just rectangular rooms with a flat floor and a flat ceiling, but rather they have irregular shapes, and neither the ceiling neither the floor is flat. In these conditions, different attenuations from point to point, as well as scattering phenomena and mutual electromagnetic interactions make quite challenging the problem of the reconstruction of the buried scenario. In particular, the classical focusing procedures based on migration algorithms might not provide satisfying results, because the migration is an algorithm essentially based on a linear approximation of the phenomenon of the scattering (Persico, 2014), which instead in complex scenarios becomes nonlinear (Persico et al., 2002). At the same time, also the classical visualization of the buried scenario by means of depth slices is not expected to provide very clear images, essentially for two reasons. The first one is that the horizontal cuts intercept only parts of the non-flat interfaces of the buried anomalies (ideally they intercept only curves of level, but practically the slices are averaged along a non-null range of time depths, as well known). The second reason

212

is that the propagation velocity is markedly different in the buried void volumes and in the surrounding soil, so that any time level cannot be correctly converted into a unique depth level. In other words, a flat time slice should be ideally converted in a curved depth slice, and vice-versa.

Notwithstanding, a careful lecture of the data can provide useful, even if in general incomplete, information. In the present work, we put in evidence these aspects with respect to a GPR prospecting performed in the church of Santa Maria delSuffragio in Gravina in Puglia (Southern Italy). This is a monument with an underlying large and accessible charnel house, which makes it a natural and meaningful test site.

The Monument

The Church of Santa Maria del Suffragio in Gravina in Puglia (Apulia region, southern Italy), also known as Church of the Purgatory, was built in 1654 by Ferdinand III Orsini as a mortuary family chapel. The Church is located in the old town of Gravina in Puglia. The portal of the facade consists of columns which represent three towers, superimposed on three floors, supported by three bears. On the tympanum two skeletons lie down, with a recline glance up to the sky, because the temple is dedicated to the death and to the cult of the dead. At the centre of the gable, the Orsini-Tolfa banner is present. The church has a single nave with three chapels on each side communicating with each other, and it is covered by a tripartite barrel vault. The church is also characterized by the presence of an underlying level obtained by digging the calcareous bedrock. It is a structure used as a charnel house, which consists of empty rooms with vaulted ceilings, placed at different heights and connected together by a system of corridors, ceilings directly dug in the bedrock or made with stonework, pillars and stairs.

GPR Survey

Within the activities of a Ph.D. course, handled jointly by the University of Bari and the Institute for Archaeological and Monumental heritage IBAM-CNR, a geophysical survey has been conducted. It was conceived within a larger research activity described elsewhere (Persico et al., 2014). The prospecting at hand allowed to test the detection of the charnel house plan as well as to identify the presence of any buried rooms in addition to those already known.

The floor of the church has been prospected investigating an area of about 240 square meters (20x12 m), according to the grid provided in Fig. 1a, where the dashed line refers to the plan of the church and the continuous contour describes the plant of the underlying charnel house. Crossed radar sections were performed with an interline spacing of 40 cm: 34 B-scans parallel to the short side of the church (labelled C1-C34) and 16 B-scans parallel to the long side of the church (laballed L1-L16). A pulsed RIS Hi Mod GPR system was used. The system is characterized by the presence of a double couple of antennas with nominal central frequencies 200 and 600 MHz, respectively. This means that, for each going through, the system gathers two signals, whose spectra are about centred at 200 and

600 MHz. In the case at hand, we have achieved the best results from the antennas at 200 MHz and will limit to show results relative to them.
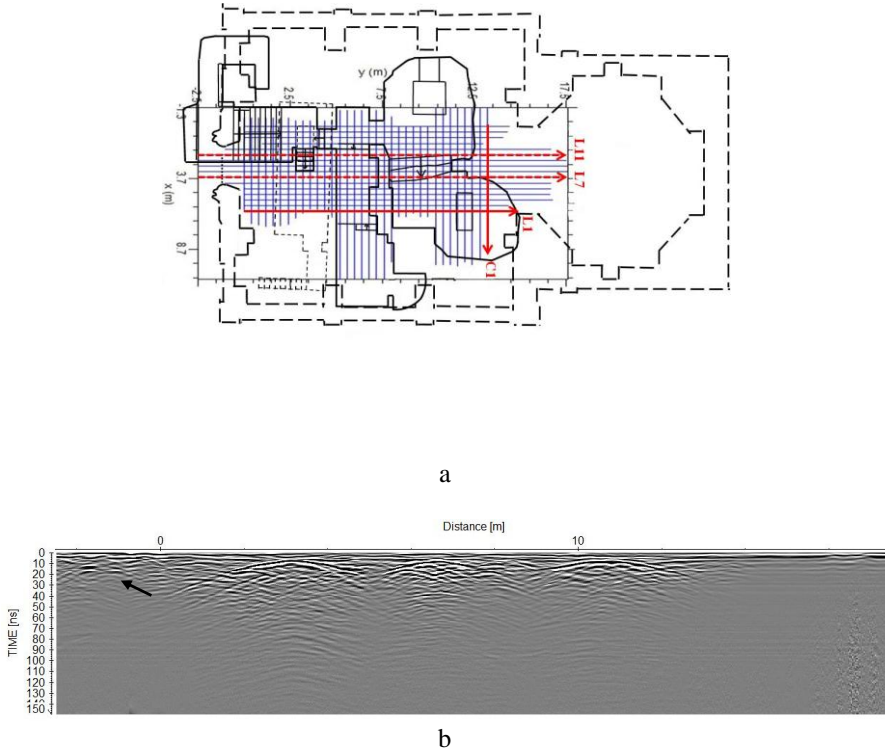

a

b

Figure 1. Panel a: The plan of the church (dashed line) and that one of the underlying charnel house (solid line) with the layout of the pulsed GPR survey; Panel b: Radar sections L11, recorded with the pulsed GPR system with the antenna at 200 MHz. The arrow indicates the signals referred to an anomaly towards the entry portal

A standard processing has been applied to the dataset using two commercial codes ReflexW (Sandmeier, 2009) and GPRSLICE (Goodman, 2013). The former was used to process the single collected B-scans, whereas the latter was exploited to obtain time-depth slices.

The processing steps applied to the data were the following: zero timing, background removal, gain vs. the depth and 1D filtering in order to mitigate the effects of the amplification of the signal vs. the depth. The migrated data did not allow any deeper interpretation of the buried scenario with respect to those non-migrated ones, because of the above mentioned large size, strength and geometrical complexity of the buried anomalies. Therefore, in the following non-migrated data are shown.

214

The average propagation velocity of electromagnetic waves in the non-void parts of the subsoil has been estimated to be of the order of 0.085 m/ns, on the basis of the diffraction hyperbolas present in the data.

Results

In the following sections some remarks about the main anomalies are reported. In particular, on the basis of the B-scan L11, reported in Fig. 1b, starting from the entry portal towards the central part of the main nave, it is possible to identify a shallow reflection in the first 20 ns (0.85 m), starting from about 10-15 ns (0.45-0.64 m). This reflectionis put into evidence with an arrow in Fig. 1b.

This anomaly is interesting for us, because it does not overlap to the map of the charnel house, and so it must be something external to it. Instead, coming the three subsequent arches correspond to three cylindrically vaulted ceilings of rooms of the underlying charnel house. Starting from the processed B-scans, time slices have been obtained with the software GPRSLICE as it is shown in Fig. 2. In particular, the ellipsis in Fig. 2a (slice at 9 ns) marks the anomaly outlined above, that disappears at 13.5 ns (Fig. 2b) and appears again at 108 ns (Fig. 2g) and remains at the deeper level of 117 ns (Fig. 2h). In particular, it is again marked with an ellipsis in Fig. 2h, whereas it is not marked in Fig. 2g in order not superpose it to the other depicted ellipsis, that will be commented in a while. This anomaly corresponds to that indicated with the arrow in Fig. 1b and that falls outside the underlying charnel house. The similarity of the geometrical shapes between the shallower and deeper parts make us deem that the shallow spot of Fig. 2a and the deeper ones of Figs. 2g-h are ascribable to the top and the bottom of the same structure, possibly constituted (or maybe filled up with) a material with high dielectric permittivity, which would make slower the propagation velocity of the waves in that area. Through Fig. 2b, moreover, we see the images of the three ceilings of the three consecutive rooms. The image is of course partial, because the ceilings are vaulted, and the third ceiling appears (toward to higher part of the image) appears cut in two parts. In particular, there is a piece of ceiling not identified in the slide. Indeed, as can be seen in the map, there are two steps between the two adjacent rooms of the charnel house, and the ceiling follows this difference of level.In the time slice at about 60 ns (Fig. 2c) and at 70 ns (Fig. 2d), it is possible to identify two distinct anomalies, marked with an ellipsis, that we deem to be ascribable to the floor of the two corresponding rooms of the charnel house. In Fig. 2e(slice at 79 ns), the alleged bottom of the central room of the charnel house is marked with an ellipsis. We deem this on the basis of the fact that the anomaly is continuous. For the same reason, we deem that the floor of the first room of the charnel house is identifiable with the ellipsis at 108 ns (Fig. 2g). For comparison, also the slice at 103 ns is shown (Fig. 2f) is shown. In Fig. 2f, in particular, we see that the anomaly close to the entrance is not still "reappeared" (its place is marked with an ellipsis) and we don't see continuous reflections that make us deem of a floor. Comprehensively, the slices suggest that the ceilings of the rooms of the charnel house are at about the same depth, whereas the floors are

at different levels, which corresponds to the ground truth because the different rooms are connected by steps, and the depth of the floors is greater in the area closest to the entrance of the church and smaller in the areas closest to the altar.
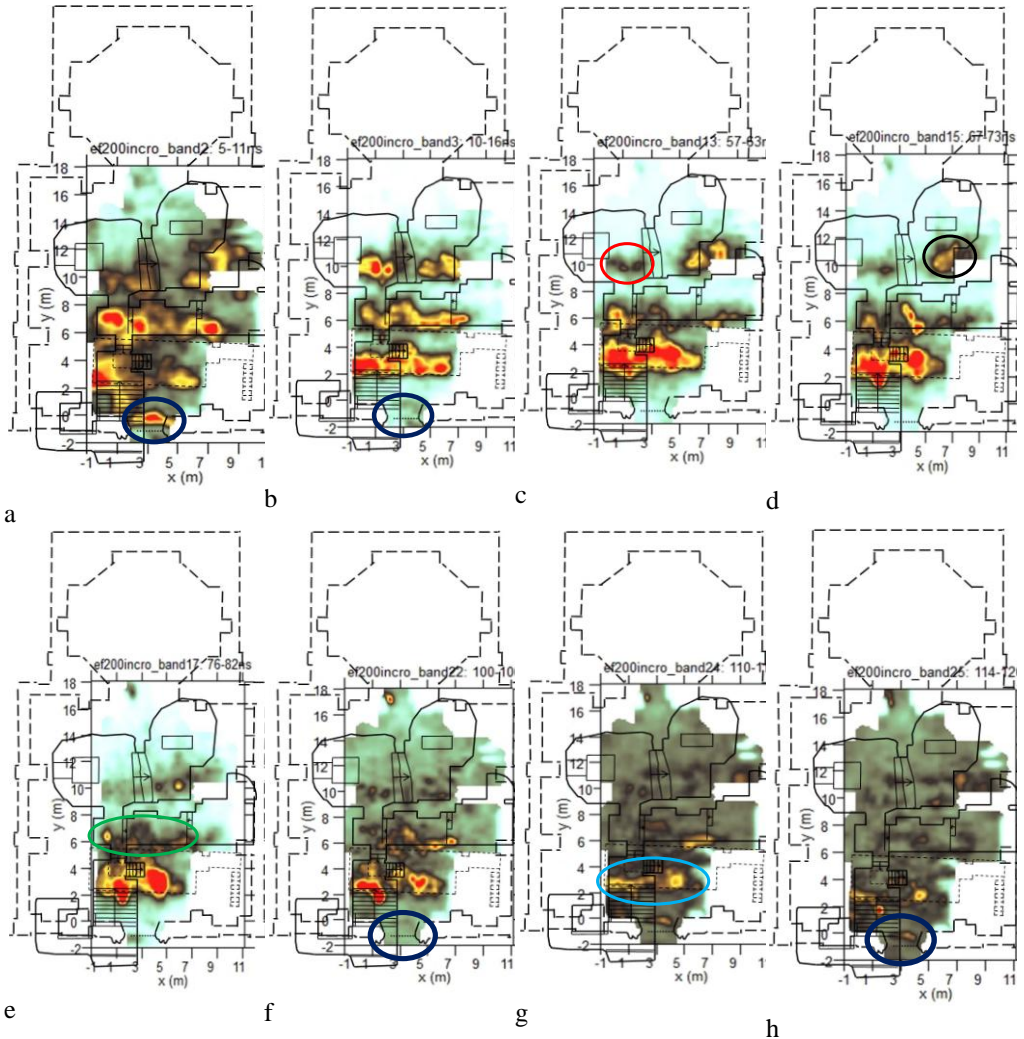
Figure 2. Depth slices at subsequent time depth levels. a: 9 ns; b: 13.5 ns; c: 60 ns; d: 70 ns; e: 79 ns; f: 103 ns; g: 108 ns; h:117 ns.

Of course, we are facilitated in the interpretation by the knowledge of the buried scenario, but the results shows that the buried rooms are anomalies whose shape is not easy to be interpreted in general, mainly because of the differences of levels present in them and because of the fact that their ceilings and floors are not necessarily uniformly flat. In particular, in the case at hand we identify the

presence of a big anomaly, and the data can make us "suspect" that this anomaly (given also the fact that it is under an historical church) is ascribable to a crypt divided into several rooms. However, the result do not enable us to track a reliable map of the buried charnel house.

We have also achieved three a three dimensional representations of the buried scenario by means of iso-surfaces, but for sake of space these will be shown at the conference.

Conclusions

In this contribution we have proposed the results of a GPR prospection performed in an historical monument. This historical monument constituted a natural test site for inferring some capabilities but also some limits of the GPR technique in this kind of situations. In particular, we appreciate that the instruments in able to "see" underground, but a fully correct interpretation of the data is customarily challenging. In particular, we can have differences of levels, steps, ceilings vaulted and excavated in the rock at different levels, and not necessarily parallel to each other. Moreover, the anomaly can be quite large, and the strong difference between the propagation velocity in the soil and in the void chambers can deform the achievable image dramatically. This means that the interpretation of the data should be prudent and should account for all the available a-priori information. In the case at hand, e.g., only the availability of the plant of the church and of the charnel house, and above all of their geometrical superposition, allowed to infer anomalies not ascribable to the charnel house.

References
Gabellone, F., Leucci, G., Masini, N., Persico, R., Quarta, G., Grasso, F. (2013). Nondestructive Prospecting and virtual reconstruction of the chapel of the Holy Spirit in Lecce, Italy, Near Surface Geophysics, vol. 11, n. 2, 231-238.
Goodman, D. (2013). GPR Slice Version 7.0 Manual. www.gpr-survey.com.
Leucci, G., Masini, N., Persico, R., Soldovieri, F. (2011).GPR and sonic tomography for structural restoration: the case of the Cathedral of Tricarico, Journal of Geophysics and Engineering, vol. 8,76-92.
Persico, R., Soldovieri, F., Pierri, R. (2002). Convergence Properties of a Quadratic Approach to the Inverse Scattering Problem, Journal of Optical Society of America Part A, vol. 19, n. 12, 2424-2428.
Persico, R. (2014). Introduction to Ground Penetrating Radar: Inverse Scattering and data processing. Wiley, ISBN 9781118305003.
Persico, R. Ciminale M., Matera L. (2014). A new reconfigurable stepped frequency GPR system, possibilities and issues; applications to two different Cultural Heritage Resources, Near Surface Geophysics, vol 12, n. 6, 793-801.
Sandmeier, K. J. (2011). Reflexw 6.0 Manual Sandmeier Software ZipserStrabe1 D-76227 Karlsruhe Germany.

Structures, Vulnerability and Risk

ON THE DEFINITION OF SEISMIC VULNERABILITY MAPS IN CROSS-BORDER MEDITERRANEAN AREAS

Cavaleri, L., Di Trapani, F., Macaluso, G., Bilello, C.
Department of Civil, Environmental, Aerospace and Materials Engineering,University of Palermo,VialedelleScienze, 90128, Palermo, Italy,
liborio.cavaler@unipa.it

Introduction

The chance to locate and quantify the major risks associated to natural catastrophic events on a territory allows the planning of adequate strategies and interventions by civil protection bodies involved in local and international emergencies. The seismic risk depends most of all by the vulnerability of buildings belonging to the urban areas. For this reason the definition, by a deep analysis of the territory, of instruments identifying and locating vulnerability, largely favours the activities of institutions appointed to safeguard the safety of citizens.

Seismic and hydro-geological risks constitute the major component of the activities involving assistance actions carried out by civil protection bodies because of their repetitiveness and the amount of human resources needed to face the emergencies. The possible coordinate action and cooperation between different countries is of fundamental importance, especially if the procedures are based on standardized rules and civil protection plans are characterized by consciousness of the territory and the associated risks. The promptness of the response is basic for the success of the operations. This feature is however not only achievable by practice exercises aimed to implement a responsiveness system to emergencies, but also through a deep understanding of the existing risks and the major exposure recognized for the urbanized contexts.

The challenge for the assessment of seismic vulnerability of buildings is not easy because it involves a large amount on constructions to investigate in a reasonable time. Several researchers, based on the post processing of data coming from the observation of damaged buildings, proposed simplified relationship linking a vulnerability index with the intensity of a seismic event (Benedettini and Petrini (1984), Braga et al. (1984), Angeletti et al. (1988), Casolo et al. (1993)). In other studies the interest has been addressed to the definition of fast assessment methods for the vulnerability index and the relative large scale application (Martinelli et al. (1999), Dolce et al. (2004), Dolce and Moroni (2005), Dolce and Martinelli (2005)).

In this summarythe outputs of the activity carried out within the research project "SIMIT-Development of an integrated cross-border Italian-Maltese civil protection network" are presented with specific reference to the assessment of the seismic vulnerability of buildings and definition of vulnerability maps in terms of vulnerability index and peak ground acceleration limit values. In agreement with the scope of the paper, the criteria adopted for the assessment of vulnerability and

definition of the vulnerability maps were calibrated to provide reliable predictions for typically small urban contexts, which are largely widespread in the Mediterranean area. The representative test site selected for the activities was the city centre of the island of Lampedusa. The choice was particularly suitable for the prefixed purposes because of the opportunity to operate on a large quantity of buildings concentrated in a small area with and characterized by a repetitiveness of the constructive typology. The final goal was to develop a standard procedure for the assessment of seismic vulnerability of small urban contexts widespread in the Mediterranean.

The specific research activity carried out on the island has been divided in 4 phases, characterized by a progressive level of depth of the analysis, listed below:

- Historical, critical, and typological analysis of the urban centre and typical buildings;
- Simplified assessment of seismic vulnerability of buildings by standard vulnerability forms;
- Choice and validation of a vulnerability model;
- Definition of fragility functions and vulnerability maps.

The historical-critical study was aimed at the recognition of the urban evolution of the city centre of Lampedusa over the time and of the regulations succeeded which have changed the constructive and typological framework of buildings. The subsequent typological analysis of the buildings, performed through several surveys, made it possible to categorize the recurring structural types within the city centre of the island and their similarities and differences in relation to periods of construction. Such preliminary activities permitted to collect fundamental information, necessary for a fast and effective assessment of the buildings vulnerability, carried out by the use of evaluation forms already known in the literature and commonly used in Italy (GNDT (1994))for the fast assessment of the vulnerabilitysingle buildings and building aggregates. The major output coming from the use of such kinds of vulnerability evaluation forms is constituted by possibility to determine a numerical vulnerability index, suitable to be adopted for the definition of the vulnerability maps.

The definition of the fragility curves, which provide a relationship between the intensity of the seismic event (synthetically represented by the Peak Ground Acceleration) and the structural damage, passes through a preliminary calibration, necessary to adapt the vulnerability model (index of vulnerability vs. PGA) to the characteristic building context. In the current study, the calibration operations were performed by an experimental dynamic monitoring campaign on two prototype buildings, followed by the realization of the numerical structural models consistent with the experimental results. The seismic assessment of the prototype buildings by static pushover analysis made possible the determination of the critical PGA values to be linked with indexes of vulnerability previously evaluated, in order to adapt the vulnerability model to the urban context of the island of Lampedusa. The final outputs are the fragility curves and the associated vulnerability maps for the urban

area of Lampedusa, presented in terms of index of vulnerability and critical peak ground accelerations.

The assessment of the seismic vulnerability of buildings

The assessment of seismic vulnerability has been carried out for masonry and reinforced concrete buildings belonging to the city centre of Lampedusa. For the sake of brevitythe procedure for the assessment described in the following regards only masonry buildings.

The recognition of vulnerability of masonry structures has been carried out by the evaluation forms developed by GNDT (1994). The need to correlate scientific information with on-site surveys has requested the use of so called "second level forms", since their compilation is not direct but requires a deeper investigation of the geometrical and mechanical characteristics, followed by the evaluation of specific parameters by a numerical calculation.

The assessment of the vulnerability by the 2nd level GNDT forms is based on the determination of a vulnerability index which is a conventional measure of the propensity of a building to undergo seismic damage. The index is numerically calculated as sum of vulnerability scores obtained by the analysis of 11 parameters considered fundamental for the identification of the seismic behavior of masonry buildings. The vulnerability index that is obtained allows to compare buildings and to establish graded lists or a map of vulnerability (as in the case of the present study).

Table 1.Parameters for the identification of vulnerability of masonry buildings in GNDT forms and related scores and weights.

	PARAMETER	Class C_{vi}				Weight
		A	**B**	**C**	**D**	p_i
1	Type and organization of the resisting system	0	5	20	45	**1.00**
2	Quality of the resisting system	0	5	25	45	**0.25**
3	Conventional resistance	0	5	25	45	**1.50**
4	Position of the building and foundations	0	5	15	45	**0.75**
5	Floors	0	5	25	45	**0.75**
6	Configuration in plan	0	5	25	45	**0.50**
7	Configuration in elevation	0	5	25	45	**1.75**
8	Walls maximum interaxis	0	5	25	45	**0.25**
9	Roof	0	15	25	45	**0.50**
10	Non-structural elements	0	0	25	45	**0.25**
11	Current conditions	0	5	25	45	**1.00**

The choice of GNDT forms has been determined on the following base requirements:

• Possibility of detecting pre-earthquake vulnerability
• Adequate amount of information about the parameters that affect the vulnerability;
•Compilation without specific investigations or detailed surveys on buildings;

• Consolidated use of the forms on the national territory;
• Possible adaptation of the forms to particular needs found in the area;
• Availability of the same type of forms masonry and RC structures.

The GNDT vulnerability assessment form for masonry buildings requires the determination of the 11 parameters reported in Table 1. Each parameter is associated with a class of vulnerability between A and D, where A represents the best condition detected and D the worst. At the same time a class of quality of the information used to establish the class of vulnerability, is assigned. The vulnerability classes are characterized by increasing scores and identified by the symbol cvi. The single parameters are moreover weighted by the weight pi, which establishes their influence on the overall assessment of the vulnerability.

The vulnerability index V is defined as:

$$V = \sum_i c_{vi} p_i$$

taking values between 0 and 328.5. The vulnerability index can be also normalized by its maximum value and assume values between 0 and 100.

The vulnerability model and its calibration

The definition of a relationship between the severity of the earthquake and the damage, through the vulnerability index *V*, is based on the observation that a building, subject to seismic actions of increasing severity, is typically characterized by a beginning stage of damaging, a phase of increase and a rapid decay up to the collapse. If one assumes the parameter *y=a/g*, which identifies the normalized ground acceleration, as index of the severity and the parameter *D* as index of the damage (between 0 and 1), identifying the loss of the economic value, the relationship may be represented by a fragility function.On this curve one can identify the accelerations corresponding to damage beginning $y_i$and collapse y_c. As proposed in Guagenti and Petrini (1989), a linearized fragility function has been used to reduce the problem of establishing the fragility function to the simple calculation of the values of $y_i$andy_c.

$$D(\,y,V\,) = \begin{cases} D = (\,y - y_i\,)/(\,y_c - y_i\,) \\ D = 0 \quad per\ y < y_i \\ D = 1 \quad per\ y > y_c \end{cases}$$

In particular the following functional relationship linking the early damage acceleration $y_i$and the collapse acceleration y_c to the vulnerability index according to Guagenti and Petrini (1989) was assumed:

$$y_i(\,V\,) = \alpha_i\,exp[\,-\beta_i(\,V\,)]$$

$$y_c(\,V\,) = \alpha_c + \beta_c(\,V\,)^\gamma$$

The equations reported above depend on 5 parameters whose calibration is of great importance for the reliability of the results and has to be performed by major investigations on typical buildings.

For this reason the calibration has been performed on the basis of an experimental investigation, which included the dynamic identification of 2 prototype buildings chosen to be adequately representative of the previously discussed features of the urban centre built. The final purpose was the definition of refined numerical models to be used for the determination of the critical PGA values (y_i and y_c) at the specific vulnerability levels characterizing the buildings.

The calibration process was performed according to the following steps

• Choice of the prototype building and assessment of the vulnerability index by GNDT forms;

• Dynamic identification of the buildings and definition of the numerical models;

• Evaluation of y_i and y_c values by static pushover analyses;

• Positioning $V – y(V)$ points and best fitting.

The buildings selected for the investigation were the City Hall of Lampedusa (BT "A") and the headquarters of the Marine Protected Area of Lampedusa (BT "B").

The numerical models

Structural models were performed using the software SAP 2000 NL. For the sake of brevity only the BT"A" model is reported here. A "frame-type" schematization of the masonry structure was adopted. Walls were modelled as beam/column elements with reference to their centroidal axis. Taking into account the presence of RC curbs at any level, it was assumed that the coupling masonry beams were flexurally resistant. The presence of concrete slabs allowed moreover to consider the rigid diaphragm constrain. The loads coming from the floors were distributed linearly on the beams at each level. Finally, the connections at the areas of overlap between the walls and the masonry beams were modelled as rigid elements. The nonlinearity was introduced by a shear – sliding hinge placed in the middle of each vertical elements. A 3D representation of the model is shown in Fig. (1).
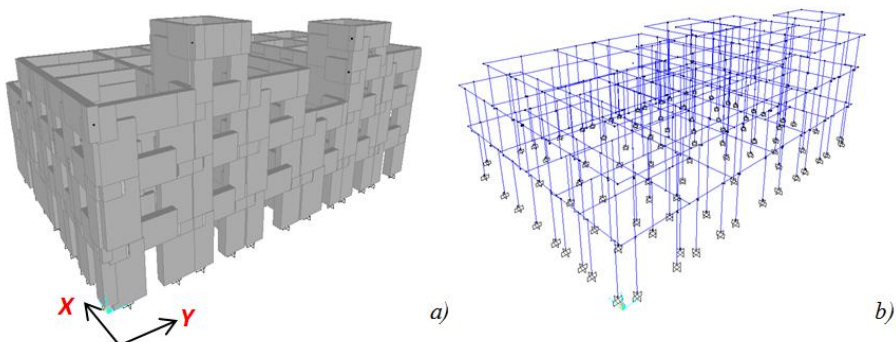

Figure 1.3D view of the structural model (BT"A"): a) solid scheme; b)unifilar scheme.

Pushover analyses were carried out in order to define the capacity of the structuresespecially in terms of early damage and collapse ground

accelerations.The analyses allowed to determine the reference critical accelerations for the prototype buildings BT"A" and BT"B". In particular, reference was made to minimum values respectively for accelerations of early damage and collapse. Joining PGA values and vulnerability indexes on a *V-y* plane, it was possible to calibrate the coefficients governing the *y(V)* relationships according to the model by Guagenti and Petrini (1989), providing suitable general expressions having validity for the buildings of the city centre of Lampedusa.

The vulnerability maps

The final output was reported in three maps. The first one (Fig. 2a) is the map of the vulnerability index, obtained by the application of the GNDT procedure to the masonry buildings investigated, which represent almost the totality within the urban centre. The map has a reference chromatic scale of the normalized vulnerability index going from cooler colours (blue - green), associated to a lower vulnerability, to warm colours (red-orange) associated to increasing vulnerability values.
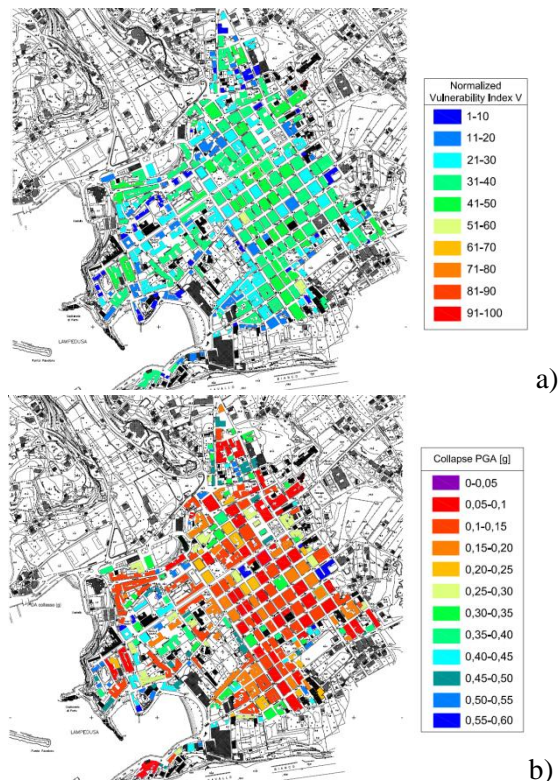

a)

b)

Figure 2.Vulnerability of the city centre of Lampedusa: a) Map of the vulnerability index; b) Map of the collapse PGA.

Two further maps were generated: collapse PGA map and early damage PGA map. For the sake of space only the collapse PGA map is reported in Fig. 2b. These maps were obtained after the calibration of the necessary parameters and regulating of the vulnerability model. Within these two maps the warmest colours were associated to the lowest values of ground acceleration, representative of the most critical conditions. Looking at the output expressed by the vulnerability index map, the overall condition does not present relevant criticalities. The average vulnerability is settled to mid-low values. On the contrary, the early damage and collapse PGA values are instead rather low. However, considering the expected PGA values, which are associated the low seismicity of the area, one can exclude, with good approximation, the possibility of the occurrence of catastrophic post-earthquake scenarios. It appears evident from the maps that the areas characterized by a greater vulnerability refer to the oldest urban disposition, which were also the most subject to further transformations during the time. The peripheral areas, consisting of newer buildings, resulted instead less vulnerable, consistently with the expectations coming from the initial assessments The overall framework that has emerged, for the case study of Lampedusa island, was in agreement with the predictions made by the assessment forms, in which a good general condition was recognized. The elements of major criticality detected regarded essentially the presence of aggregates building with strong irregularities in elevation. These buildings reached in fact the highest levels of vulnerability.

In accordance with the purposes, the major outputs obtained by the application of the proposed assessment procedureto the case of the island of Lampedusa gave a univocal representation of the seismic risk for its urban centre area.This procedureis suitable to bestandardizedin order to be largely forthe generation ofvulnerability mapsofsmallurbanareas in the Mediterranean.

Acknowledgements

References

BenedettiniD. and PetriniV. (1984). On seismic vulnerability of masonry buildings: proposal of an evaluation procedure, L' industriadelleCostruzioni 18, 66-78.

BragaF., DolceM. and LiberatoreD. (1984). Fast and reliable damage estimations for optimal relief operations, Proceedings Int. Symp. on Earthquake Relief in Less Industrialized Areas, Zurich,145-151.

AngelettiP., BellinaA., GuagentiE., MorettiA. and PetriniV. (1988). Comparison between vulnerability assessment and damage index, some results, Proceedings of the 9th World Conference on Earthquake Engineering, Tokyo-Kyoto,181-186.

CasoloS., GrimazS. and PetriniV. (1993). Scala deiGiudizisintetici di stimadeldannosismico. Scala G.S.D.e.m. 93", Internal Report, Dipartimento di Georisorse e Territorio, Universityof Udine, Italy.

MartinelliA., CorazzaL., CherubiniA., DolceM., Di PasqualeG. and PetriniV. (1999).Censimento di vulnerabilitàdegliedificipubblici, strategici e specialinelleregioniAbruzzo, Basilicata, Calabria, Campania, Molise, Puglia e Sicilia – RelazioneGenerale, Civil Protecion Department, Rome, Italy.

DolceM., MasiA. and Moroni C. (2004).Valutazionedellavulnerabilitàsismica di edificiscolasticidellaProvincia di Potenza, Proceedings of XI National Congress "L'ingegneriaSismica in Italia", Genoa, Italy.

DolceM., MoroniC. (2005). La valutazionedellavulnerabilità e del rischiosismicodegliedificipubblicimediante le procedure VC (vulnerabilità C.A.) e VM (vulnerabilitàmuratura), Civil Protection Department, Potenza, Italy.

DolceM. andMartinelliA. (2005).Inventario e vulnerabilitàdegliedificipubblici e strategicidell'Italiacentro-meridionale, Vol. II – Analisi di vulnerabilità e rischiosismico, INGV/GNDT".IstitutoNazionale di geofisica e Vulcanologia / GruppoNazionale per la DifesadaiTerremoti, L'Aquila, Italy.

GNDTGruppoNazionale per la DifesadaiTerremoti (1994). Schede di 1° e 2° livello di vulnerabilità e di rilevamentodeldanno (edifici in c.a. e muratura).

GuagentiE. andPetriniV. (1989).Ilcasodellevecchiecostruzioni: versounanuovaleggedanni-intensità. Proceedings of the 4th Italian National Conference on Earthquake Engineering, Milan, Italy, 1, 145-153.

PRELIMINARY ASSESSMENT OF THE SEISMIC VULNERABILITY OF LOAD-BEARING MASONRY BUILDINGS IN MALTA THROUGH NUMERICAL MODELLING.

Cicero C.[1], Borg. R. P.[2], Bonello M.[3], Lombardo G.[1]

[1]*Departmentof Civil Engineering and Architecture – University of Catania, Viale A. Doria 6, Catania (Italy), ing.chiaracicero@gmail.com, glombardo@dau.unict.it*
[2]*Departmentof Construction and Property Management, Faculty for the Built Environment, University of Malta, Tal-Qroqq, Msida MSD 2080, Malta, ruben.p.borg@um.edu.mt*
[3]*Departmentof Civil and Structural Engineering, Faculty for the Built Environment, University of Malta, Tal-Qroqq, Msida MSD 2080, marc.bonello@um.edu.mt*

Introduction

The seismic risk is Malta is perceived to be low, and no significant events have been recorded in recent years. In 1693, a major earthquake struck about 170 kilometres from Malta, devastating south-eastern Sicily, and causing serious damage in buildings in Malta with historical records of significant damage in Mdina but also in Valletta, Rabat and elsewhere.Research suggests that a similar earthquake on the same fault could occur every few hundred years.

The present study is part of a wider research initiative in Malta focusing on the vulnerability of buildings to seismic activity including the vulnerability of unreinforced masonry buildings, their characteristics contributing to seismic vulnerability and their effect on the adjacent structures. The integrity of a building during an earthquake depends on various factors including the materials used, structural systems, building height and building layout, position in a block and building-soil interaction. The urban landscape of Malta is characterised by a large density, mainly consisting of load-bearing masonry structures. The local globigerina limestone resources have been exploited over the years in the construction of buildings and stone masonry buildings are characteristic not only of historic areas which evolved over many years, but also recent development. Load-bearing masonry structures rely on globigerina limestone blocks (franka) and hollow concrete blocks.

The present study focuses on a specific load-bearing masonry typology developed in Malta during the past 40 years. Therefore the structural systems analysed are typically characterized by the following features: 3 to 4 floors above ground level, masonry load-bearing structure with rigid reinforced concrete slabs and a basement level "soft story". The study consisted in the assessment of the seismic vulnerability of the structural typology through structural numerical modelling and using a specific seismic analysis software tool: 3D Macro. The numerical modelling tool is based on a discrete element approach.

The following building characteristics have been assessed through the structural modelling: presence of long corridor adjacent to party wall / central corridor, with/without lateral walls, with/without the soft storey. Both single blocks and an aggregate of adjacent blocks have been considered in the assessment. Building configurations assessed included shared and independent party walls between properties, staggered floors in adjacent buildings and varying number of floors. The behaviour of the aggregate wasanalyzed with respect to various combinations of adjacent building types.

Analysis of Results and Discussion

In the preliminary analysis of this building typology using numerical modelling through 3D Macro, structural units, located in a specific urban area, namely Xemxija in Malta, have been analyzed (Fig.1). In a first phase of research, the influence of the soft storey has been assessed. In particular, the structural units have been modelled, using the specific software, 3D Macro, with and without the soft storey. The safety factor was obtained through the analysis and the results are reported in Table 1.Results obtained in this first phase of research show that the presence of the soft storey is a very influential indicator on the assessment of damage of the buildings, with the safety factor being reduced significantly.

Figure 1. Structural Units 1 and 2 (Xemxjia – Malta).

Table 1. The safety factors assessed for models analysed using 3D Macro

	with the soft storey	without the soft storey
Structural unit 1	71%	155%
Structural unit 2	83%	188%

Conclusion

In the subsequent phases, other indicators of vulnerability were assessed, namely: the presence of a long corridor adjacent to party wall / central corridor, with/without lateral walls. Both single blocks and an aggregate of adjacent blocks have been considered in the assessment. Building configurations assessed included shared and independent party walls, staggered floors in adjacent buildings and varying number of floors. The behaviour of the aggregate was analyzed with respect to various combinations of adjacent building types. The various combinations assessed in a structured manner, provide significant insights into the contribution of the individual indicators to the overall structural vulnerability of the block and the aggregate.

Acknowledgements

References

Borg R.P., Borg R.C., Borg Axisa G. (2008), The seismic risk of buildings in Malta. In Urban Habitat Constructions under Catastrophic events. Edited by Mazzolani .F et al, European Science Foundation,COST C26, University of Malta, Malta.

Caliò, F. Cannizzaro, M. Marletta and B. Pantò (2010),A discrete-element approach for the simulation of the seismic behavior of historical buildings, XVIII GIMC Conference.Siracusa, 22-24 September 2010.

ANALYSIS AND EVALUATION OF THE SEISMIC VULNERABILITY OF THE STRUCTURAL AGGREGATE.THE STUDY CASE OF ORTIGIA

Cicero C., Lombardo G.

Departmentof Civil Engineering and Architecture – University of Catania, Viale A. Doria 6, Catania (Italy), ing.chiaracicero@gmail.com, glombardo@dau.unict.it

Introduction

The historical urban tissue of many countries with relevant seismic risk, are mostly made of stone masonry load-bearing buildings, mostly built in ancient times without any seismic standard. An important element for the development of strategies for the prevention and the reduction of the seismic risk is the evaluation of the structural behavior under seismic actions.Forexisting buildings, the problem arises mainly in the assessment of their vulnerability.

The methodologies used for these assessments can have different levels of detail, depending on the quality and quantity of information that are acquired for each individual building. Considering the mitigation of seismic risk, these analysis should be performed on whole territories or municipalities, or on a significant number of buildings: this leads to the research of procedures for the vulnerability assessment that, starting from an expeditious acquisition of information, allow to realize a reliable estimate of the level of seismic damage.

A territorial analysis, that moves its investigation scale from the single structural unit to the urban center, cannot ignore the fact that the masonry buildings are often organized into nuclei of structural units that interact in complex ways: this makes even more difficult the approach, the development of analysis and the interpretation of results. One of the existing and more widespread methods for the evaluation of urban seismic vulnerability in Italy is the statistical method (based on statistical data and Braga matrices [1]). This is utilized by municipalities to elaborate the scenery of seismic risk as well and it is exclusively based on data related to the characteristics of the bearing structure and on the number of residents involved. In time, results obtained by this method did not coincide with the real effects that occurred during subsequent earthquakes. The difficulty of the study related to the seismic issue of the urban centers emerges for the first time in the manual for the compilation of 1st level GNDT forms. It reads [2] "it is therefore necessary to identify, at urban scale, the aggregate, which is constituted by a set of non-homogeneous structural elements and which can interact under a seismic action (or dynamic in general)" … "An aggregate may consist of one or more buildings grouped. It means that there must be a contact, or a link, more or less effective in buildings generally with different design characteristics [...] within aggregates, buildings are identified, these are defined as homogeneous structural units from sky to earth [...]". This definition highlightsthe characterof interdependenceof the buildingsin theiroverallconfiguration [3] and confers to the aggregate the role of analysis module for the study of urban vulnerability.

The recent Italian seismic code [4] has also introduced the need for recognition of the aggregate giving it a key role in the planning of measures for the conservation and safety of the city. The aggregate is defined as: "... consisting of a set of parts that are the result of an articulated and not unitary genesis, because of multiple factors ..." [5].

Recently, a new pre-earthquake analysis method has been defined (CLE - Boundary Condition for Emergency) [6] to manage the post-earthquake emergency. Five types of forms have been developed of which the AS-Structural Aggregate and the US-Structural Unit. The aggregate form (AS), being in an intermediate scale of analysis between the single building and the urban center, is an element of novelty. The form takes into account the factors resulting from contiguity between different structural units in addition to the main morphological, geometric, construction and structural elements of the aggregate.

Within the SIMIT project, a study has been carried out which led to propose a methodology [7]that can be considered innovative towards the complexity of historical buildings and versatile both for pre-earthquake analysis and for the planning of mitigation actions. The method, already applied in several urban centers, considers an essential and preliminary knowledge phase, carried out with a strong interdisciplinary approach and based on the on-site data collection, by the use of special survey forms (SeiV-US and SeiV-AS) [7],based on indicators of vulnerability, and implementation of minimum campaigns of experimental investigations. Starting from the available analytical information (historical, typological and structural), the seismic vulnerability of structural aggregates has been assessed through the application of procedures, based on the presence of the detected indicators of vulnerability.By the literature experience[8, 9],based on the observation after the seismic events, weightshave been calibrated and assigned to the indicators of vulnerability for US.Since for the structural aggregate does not exist a specific literature related on the indicators of vulnerability, to calibrate the weights to be assigned to the indicators we relied on the observation after the seismic events.

Objective of the present paper is tovalidatesome of the assigned weights to the indicators of vulnerability.To do this, a comparison will be conducted between the weights assigned by the experience and the results obtained by a specific software for the evaluation of the seismic vulnerability based on a discrete element approach (3D Macro). The study will be carry out on a representative aggregate of the ancient quarter of Ortigia (Siracusa – Italy).

Methodology

The current appearance of Ortigia is almost entirely determined by the eighteenth century reconstruction, which took place after the earthquake of 1693, and by the significant construction that took place during the nineteenth century. A progressive occupation of open spaces by spontaneous constructions occurred in accordance with a development for clogging. Ortigia is still subject to continuous

transformation, in fact variations, between adjoining structural units, occur for recasting between buildings or for fractionations [10].

To define aggregates and structural units it was necessary to conduct a laborious preliminary stage, in a settlement characterized by continual mutations, recasts and clogging hardly analyzable except with a solid documentary base (historical cadastral) and direct visits onsitethat has disclosed the historical development of tissue.

The aggregate object of this study (fig. 1) is composed by 15 structural units characterized by load-bearing masonry vertical structure and semi-rigid horizontal structures. The number of floors is lower than 5, the average height of the plans is lower than 3,5 m, the system of opening is incongruous, the average height is between 7 and 12 m, the coverage ratio is superior than 70% and the state of maintenance is adequate-good without structural damage.
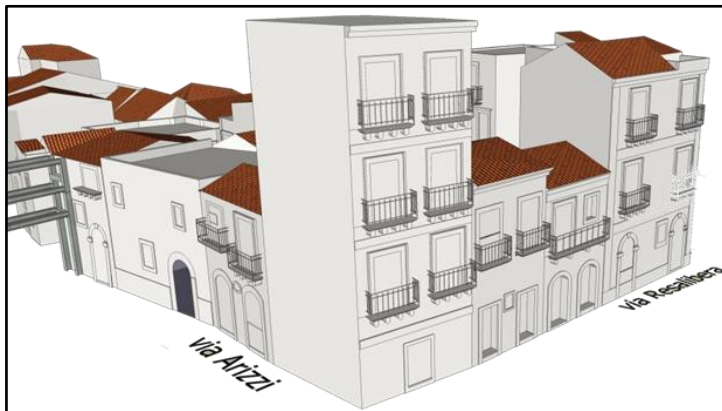

Figure 1.Aggregate object of this study.

The use of the new forms, based on indicators of vulnerability for US and AS (tab. 1-2), leads to the qualitative evaluation of the seismic vulnerability. The value of the weights assigned to the detected indicators added together, defines the index of seismic vulnerability. The higher index represents an higher seismic vulnerability.

*Table 1.Weight of the indicators of vulnerability for US.*

Indicators of Vulnerability (US)			
	Weight		Weight
Bearing vertical structure	1,5	Regularity of shape	1,25
Reinforcing elements (masonry building)	1,5	Juxtaposed elements or poorly connected	0,75
Bearing horizontal structure (masonry building)	1,25	System of openings	1,25
Location of the US in the aggregate	1	Presence of isolated columns	0,75
Specialist US	1	Presence of pilotis plans	0,75
Number of floors	0,75	Superelevations	1
Presence of basements (N. of floors > 5)	0,5	Structural damage	1,5
Average height of the plans	0,75	Maintenance status	1
Total height of US	0,5	Morphology of the ground	1,25
Single volume	1	Location of the US with respect to the slope	0,75

Table 2.Weight of the indicators of vulnerability for AS.

Indicators of Vulnerability (AS)			
	Weight		Weight
Presence of US with large spans	1	Juxtaposed elements or poorly connected	0,75
Average height	0,5	System of openings	1,25
Coverage ratio	1	Presence of isolated columns or pilotis plans	0,75
Regularity of shape	1	Superelevations	1
Recasts or clogging	0,75	Steeples, towers, chimneys	1
Misalignment of total height US	1,5	Deteriorated or damaged US	1,5
Misalignment of floors	0,5	Reinforcing elements	1,5
Misalignment of facade	0,5	Presence of ruins	1
Misalignment of internal space	0,5	Morphology of the ground	1,25
Slender header	0,5	Location of the AS with respect to the slope	0,75

In this phase, due to the use of the 3D Macro software, some indicators of vulnerability, related to the aggregate form, are analyzed. These are: presence of ruin, regularity of shape and misalignment of total height. In particular four cases will be modeled for the structural analysis: 1. Original state; 2. Presence of a ruin; 3 Irregularity of shape; 4. Alignment of total height (fig. 2).

3D Macro software is based on a discrete element approach. The basic element, developed for the simulation of the in-plane response, is constituted by an articulated quadrilateral (panel) with four rigid edges and four hinged vertices connected by two diagonal nonlinear springs (NLinks); each of the rigid edges can be connected to other elements by means of discrete distributions of nonlinear springs with limited tension strength (interfaces). This plane discrete element has been applied for the simulation of the nonlinear behavior of masonry buildings in which the masonry walls are subjected to in-plane forces, without taking into account the out-of-plane response [11].
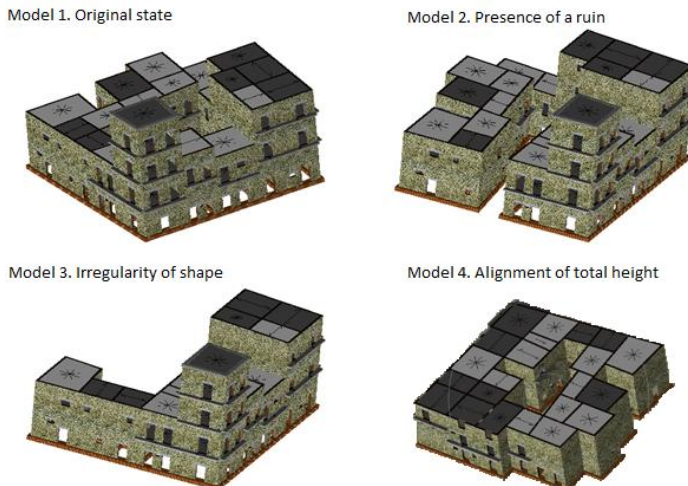
Figure 2.Models of the aggregate (3D Macro).

Results

The application of the new form SeiV-AShas lead to the qualitative evaluation of the seismic vulnerability of the aggregate as showed in table 3. The use of the new form SeiV-US has lead to an average index of the seismic vulnerability for the structural units equal to 4,9. These results confirm that the average value of the seismic vulnerability is not significant, that it does not represent the real seismic behaviour and that the seismic vulnerability of an aggregate cannot be defined as the sum of the vulnerability of the single buildings that make up it. In fact, the SeiV-ASforms takes into account other complex factors that come into play affecting the correlation between the structural units.

Table 3.Vulnerability assessment of the aggregate using the SeiV-AS form.

Detected indicators of vulnerability		Weight
Presence of US with large spans	NO	-
Average height	7 m<H<12 m	-
Coverage ratio	>=70%	1
Regularity of shape	YES	-
Recasts or clogging	YES	0,75
Misalignment of total height US	YES	1,5
Misalignment of floors	YES	0,5
Misalignment of facade	YES	0,5
Misalignment of internal space	YES	0,5
Slender header	NO	-
Juxtaposed elements or poorly connected	NO	-
System of openings	Incongruous	1,25
Presence of isolated columns or pilotis plans	NO	-
Superelevations	NO	-
Steeples, towers, chimneys	NO	-
Deteriorated or damaged US	NO	-
Reinforcing elements	NO	1,5
Presence of ruins	NO	-
Morphology of the ground	< 15°	-
Location of the AS with respect to the slope	Neither above nor below the slope	-
Index of vulnerability		7,5

Table 4 shows the results of this study. The values of the seismic vulnerability are represented in terms of Index of vulnerability, assessed with the SeiV-AS form, and in terms of Safety factors, assessed with the 3D Macro software. Moreover, the differences between the original state and the hypothesized models are represented. We can observe that, related to the indicators Presence of a ruin and Irregularity of shape, the ratio of the results obtained with the two used methods (SeiV-AS form and 3D Macro software) is consistent.

While, the ratio between the results obtained for the indicator Misalignment of total height is not consistent. This means that this indicatorsis more influentialon the damageability of the previous. In fact, through the observation of damage that occurred in the past, Guido Sarà affirms that a

widespread crisis mechanism was detected because of action ramming caused between adjacent buildings from not aligned heights [12].

Table 4. Vulnerability assessment for several models of aggregate using SeiV-ASform and 3D Macro software.

	Models	Index of vulnerability (SeiV-AS)		Safety factors (3D Macro)	
1.	Original state	7,5	-	56%	-
2.	Presence of a ruin	8,5	+1	43%	-13%
3.	Irregularity of shape	8,5	+1	46%	-10%
4.	Alignment of total height	6	-1,5	93%	+37%

Conclusions

The test in Ortigia highlighted that the compilation of the forms satisfy the request to be expeditious. In fact they allow you to reach to the optimum balance between the knowledge of the vulnerability and the effort required to obtain it.

In the future, this study will be deepened for the indicator Misalignment of total height and it will be extended to all the indicators of vulnerability, for US and AS. This will allow us to test the new forms (SeiV-US and SeiV-AS) and to understand if the identified indicators of vulnerability and their weights are able to describe damageability of urban centers. The evaluation of seismic vulnerability, along with exposure and hazard, is necessary to define the civil protection plans. At last, the results obtained are essential premises for the definition of guidelines. Moreover, it allows for the identification, in the aggregate, of particular points of weakness or strength after the earthquake, interpreted so as to constitute a comprehensive picture of earthquake damage to the urban centre.

Acknowledgements

References
[1] Braga F., Ramasco M., "Valutazione su base statistica delle Vulnerabilità sismica degli edifici di Pozzuoli", in Atti del 2° Convegno nazionale"L'ingegneria sismica in Italia", Rapallo, 1984
[2] AA.VV. (2007): Manuale per il rilevamento della vulnerabilità sismica degli edifici - Istruzione per la compilazione della scheda di 1° livello, GNDT - Gruppo Nazionale per la Difesa dai terremoti.
[3] Fera G., La città antisismica : storia, strumenti e prospettive della pianificazione territoriale per la riduzione del rischio, Roma, Gangemi, 1991

[4] Ministro delle infrastrutture, Ministro dell'Interno, Dipartimento della Protezione Civile, Decreto Ministeriale 14 Gennaio 2008, Nuove Norme Tecniche per le Costruzioni, Gazzetta Ufficiale n. 29 del 4 febbraio 2008 - Suppl. Ordinario n. 30

[5] Ordinanza 3274/2003, Testo integrato dell'Allegato 2 – Edifici –come modificato dall'OPCM 3431 del 3/5/05, capitolo 11.5.4.3.2

[6] Opcm n. 4007 del 29 febbraio 2012: contributi per gli interventi di prevenzione del rischio sismico per l'anno 2011

[7] Lombardo Grazia, Cicero Chiara (2014). Seismic safety of urban centers. Evaluation of the vulnerability for the existing building heritage. In: 40th IAHS World Congress on Housing: Sustainable Housing Construction. ISBN: 9789899894914, Funchal, 16-19 December 2014

[8] AA.VV. (2007): Manuale per il rilevamento della vulnerabilità sismica degli edifici - Istruzione per la compilazione della scheda di 2° livello

[9] A. Formisano, G. Florio, R. Landolfo, F.M. Mazzolani, (2011), Un metodo per la valutazione su larga scala della vulnerabilità sismica degli aggregati storici, Altro ministeriale.

[10] Giuffrè A., (1993): Sicurezza e conservazione dei centri storici. IlcasoOrtigia, Laterza, Bari.

[11] Caliò, F. Cannizzaro, M. Marletta and B. Pantò, A discrete-element approach for the simulation of the seismic behavior of historical buildings, in XVIII GIMC Conference Siracusa, 22-24 September 2010.

[12] Sarà G., (2014): Costruzioni in zona sismica, Dario FlaccovioEditore.

REPAIRING AND STRENGTHENING OF BUILDINGS IN ALGIERS CITY: AN EXAMPLE

Mohammed N. Farsi[1], Jean-Luc Chatelain[2], Bertrand Guillier[3]

[1] *Centre National de Recherche Appliquée en Génie Parasismique (CGS), Algiers, Algeria, mnfarsi@cgs-dz.org*

[2] *Institut de Recherche pour le Développement (IRD), Grenoble, France, jlchatel@ird.fr*

[3] *Institut de Recherche pour le Développement (IRD), Grenoble, France, bertrand.guillier@ird.fr*

Introduction

The building damaged by the magnitude 6.8 Boumerdes earthquake (Central North region of Algeria) of May 21st, 2003, is located in the COSIDER neighbourhood at Bordj-El-Bahri city, 30 km east of Algiers city and about 30 km west of Boumerdes city. It is composed an underground level of 2.5 m height and six stories of 3.0 m height (Figure 1). The resistant structure is made of 9 transversal RC shear walls of 15 cm thick and one longitudinal RC shear walls 20 cm thick. The floors have 15 cm thick RC slab. The building is founded on a 40 cm thick RC mat foundation. The principal and lateral façades are constituted by pre-cast RC elements.
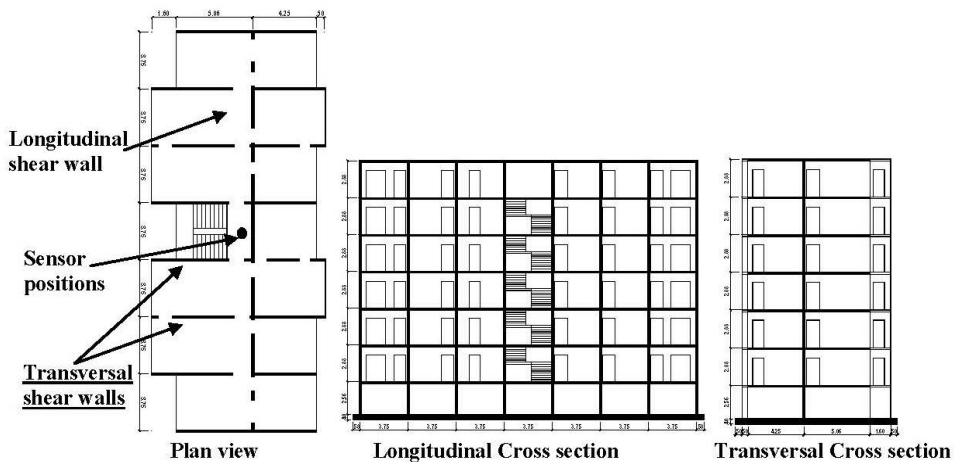

Figure 1: six-story RC shear wall building structure

Structural damage

The building is oriented, in its longitudinal direction, along the fault direction, i.e. in the same direction as the fault (Figure 4). In this longitudinal direction the building rigidity is insufficient because there is only one eccentric shear wall (Figure 1). The damages were located therefore on this shear wall at the first and the second levels and resulted in cracks of shearing that reached more than 10 cm of opening in some places (Figure 2). The buildings that are perpendicular to

the fault directional effect exhibit practically no damage due to the strong rigidity in the transversal direction. The reinforcement of this longitudinal shear wall is made by 2 tablecloths of diameter 12 mm steel bars constituting a mesh of 20 cm x 20 cm. Four steel bars forming a column of 20 cm x 20 cm cross section are put at each extremity to rigidify the openings.
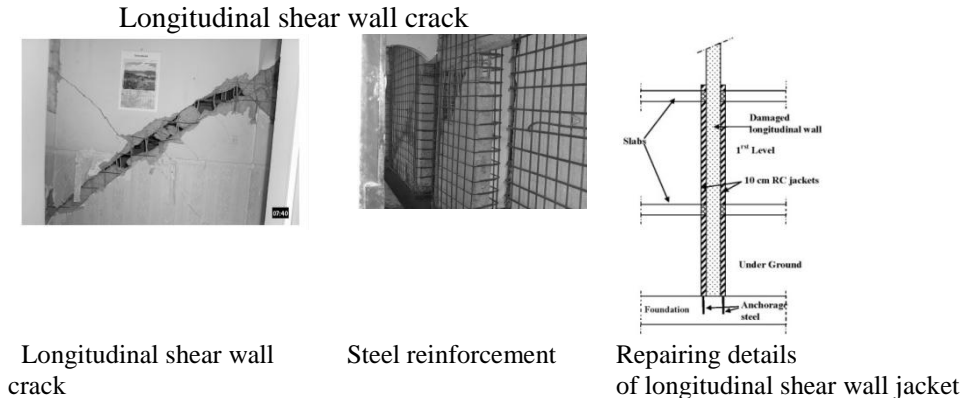
Longitudinal shear wall crack

| Longitudinal shear wall crack | Steel reinforcement | Repairing details of longitudinal shear wall jacket |

Figure 2: damaging and repairing of longitudinal wall

Dynamic analysis

A dynamic analysis has been done using a finite elements method to estimate the frequencies and the damping of the building before earthquake**.** The hypotheses considered are the following:

Density of concrete: 25 KN/m^3

Elasticity modulus of concrete: 2.3 10^7 KPa

Masses:- roof: 7.3 KN/m^2

- current story: 6.75 KN/m^2

Rigidity of soil: 50 000 KN/m3

Damping: 10%

The results of this analysis are discussed below.

Technique of retrofitting and strengthening

The jacketing technique was used to repair and to strengthen the damaged shear wall. This repair and the strengthen operation only concerned the underground level and the ground level, where the cracks have appeared. The jacket has 15 cm thick in the both sides of the wall with a steel reinforcement constituted by a 14 mm diameter bars forming a mesh of 20x20 cm (Figure 2).

Data acquisition and processing

Ambient vibration recordings were carried out using six 5-second 3C Lennartz seismometers, i.e. one at each floor of the building, installed in the stairwell (Figure 1), simultaneously recorded with a CitySark II-6 station

240

(Chatelain et al. 2000). The records were 30 minutes long with a sampling frequency of 200 sps. The gain was adjusted to obtain the best signal-to-noise ratio record for the 18 components.

Estimation of frequency and damping

The dynamic analysis using finite elements method showed that the first mode is in the transversal direction, the second mode is in the longitudinal direction and the third one is a torsional mode. The values of the frequencies are as follow:

Transversal direction (first mode): 3.71 Hz before earthquake and 3.76 Hz after retrofitting

Longitudinal direction (second mode): 4.26 Hz before earthquake and 4.30 Hz after retrofitting

The ambient vibration data analysis, based on an antitrigger procedure, has given the following frequencies and damping as shown in Table 1. The damping value considered in the dynamic analysis is 10% for shear wall resisting system according to Algerian the seismic code. For the analysis using ambient vibrations, damping was estimated using random decrement method. The different damping values are shown in Table 1:

Table 1: Frequencies and Damping values

	Transversal direction		Longitudinal direction	
	Frequency (Hz)	Damping (%)	Frequency (Hz)	Damping (%)
Before earthquake	3.73	7.84	4.13	7.79
Damaged state	3.09	2.13	2.07	1.70
After retrofitting	3.52	7.68	3.92	5.42

We note that the earthquake did not affect in an important way the building in the transversal direction. The retrofitting has increased very slightly the rigidity in this direction represented by the retrofitting of the wings of the transversal shear walls. In the longitudinal direction, the building had lost a significant part of its rigidity, about 50%, after earthquake occurrence. This is probably due to the coincidence between the building direction and the fault directional effect, i.e. the highest acceleration. The repairing and retrofitting, as explained above, have rigidified (3.92 Hz) in the longitudinal direction the building which has recovered practically its initial state (4.13 Hz). Based on these results we can admit that the repairing and retrofitting operation has been a success and the choice technique is good. However, looking on the modal shapes, we note that, if on the first level the building is more rigid than on the other levels (that is normal because of the retrofitting), on the third level exists a "fracture" which is probably due to no detected micro-cracks.

Conclusion

Frequencies and damping evaluations are very good techniques to detect the change in rigidity of a structure. A decrease of rigidity proves the existence of

damages in the structure. In the case of the present studied building, the frequency in the longitudinal sense that fell practically by half shows that the damages are important as can be evident from the photos. Periodical measure of the building frequency will permit to monitor the building's health over time. The techniques of repair and retrofitting that have been adapted are efficient since the building recovered its initial state, which means its initial capacity of resistance. The calculated frequencies with numeric modelling and the dynamic analysis are in the same order of those estimated from ambient vibrations. The damping input value (10% generally adapted for the structures in walls carriers made of reinforced concrete) in the numeric analysis is very far from those evaluated from the ambient vibrations. This is probably due to the bad quality of the materials and also to the soil-structure interaction. It is necessary to recognize also that the damping parameter is not easy to estimate with the frequency. Once again we note that the numeric modelling is far to reflect the real behaviour of a structure. It would be useful to carry out more investigations on the neighbourhood buildings and soils, to better understand what happened and to explain why the damages are so different from one building to another sometime soon.

References

Boutin C., Hans S., Erdin I., and Loriot M., (1999). Approche de la vulnérabilité sismique par l'étude du comportement de bâtiments réels, Rapport de recherche ENTPE, Lyon, 1999.

Chatelain, J. L., P. Guéguen, B. Guillier, J. Fréchet, F. Bondoux, J. Serrault, P. Sulpice and J.M. Neuville (2000). CityShark : A user-friendly instrument dedicated to ambient noise (microtremor) recording for site and building response studies, Seismological Research Letters, Vol. 71(6), 698-703.

Dunand F., Bard P.Y., Chatelain J.L., Guéguen Ph., Vassail T. & Farsi M.N. (2002). Damping and frequency from Randomdec method applied to in situ measurements of ambient vibrations. Evidence for effective soil structure interaction. Proceeding of the 12th European Conference on Earthquake Engineering, paper n° 869, Londres, 2002.

Farsi M. N., (1996). Identification des structures de génie civil à partir de leurs réponses vibratoires, Thèse de doctorat de l'Université Joseph Fourier, Grenoble, 1996.

Nakamura, Y., (1989). A method for dynamic characteristics estimation of subsurface using microtremor on the ground surface. QR of R.T.R., 30-1.

AMBIENT VIBRATIONS IN SEISMIC STUDYING THE UNESCO CULTURAL HERITAGE SITE OF SAN GIMIGNANO (ITALY)

Lunedei, E.[1], Peruzzi, G.[2], Albarello, D.[3]

[1]*Dipartimento di Scienze Fisiche, della Terra e dell'Ambiente - Università di Siena, Via Laterina 8, 53100 Siena (Italy), lunedei@unisi.it*
[2]*Dipartimento di Scienze Fisiche, della Terra e dell'Ambiente - Università di Siena, Via Laterina 8, 53100 Siena (Italy), peruzzi31@student.unisi.it*
[3]*Dipartimento di Scienze Fisiche, della Terra e dell'Ambiente - Università di Siena, Via Laterina 8, 53100 Siena (Italy), dario.albarello@unsi.it*

Introduction

San Gimignano is a village in Tuscany (Central Italy), whose historical hamlet is included in the UNESCO World Heritage List (http://whc.unesco.org/en/list/550). Several well-preserved medieval towers of considerable historical importance are in it and also represent a very important tourist attraction. Historical earthquakes are documented in the area and this makes these monuments potentially exposed to seismic damages. In order to improve the knowledge about the seismic risk of this cultural heritage, the Regione Toscana (Tuscany regional administration) promoted the RISEM project (RIschio Sismico negli Edifici Monumentali - seismic risk in monumental buildings; http://www.risem.unifi.it/), involving the universities of Florence and Siena. The project included three work packages. The first one was devoted to evaluate seismic hazard, including site response, in the San Gimignano hamlet. The second was devoted to the structural characterization of each tower by the use of historical documents and direct measurements. The third part was devoted to the estimate of possible damages expected at each tower as a consequence of possible future earthquakes.

In this frame, ambient-vibration monitoring was used in first and second work packages. In particular, measurements in streets, squares and fields were used to constrain the geological/seismic model to be used for site response assessment, while measurements inside the buildings contributed to evaluate dynamical response of the towers.

Ambient vibrations in microzonation

As concerns the first work package, a seismic microzonation of the San Gimignano historical centre was carried out. Passive seismic contributed to this task by measurements of the ambient vibration wavefiled both in single-station and multi-station configuration. A single-station measurement campaign was carried out by using a three component portable seismograph (Tromino®, http://www.tromino.eu/): measurement points are shown in Figure 1. Ambient-vibration measurements were processed to obtain HVSR (Horizontal-to-Vertical Spectral Ratio) curves (SESAME project, 2005; Picozzi et al., 2005; Albarello &

243

Castellaro, 2011), which allow detecting seismic resonance phenomena. Peak frequency f0 of HVSR curves, which estimates the resonance frequency attributed to the main impedance contrast in the subsoil, ranges from more than 8 Hz at south-west (where a few flat HVSR curves appear) to less that 1 Hz at to the north-east of the studied area, being included between 1 and 2 Hz inside the hamlet walls. This tendency indicates that the resonant interface gently deeps from the south-west (where the seismic bedrock outcrops) to the north-east of the San Gimignano hamlet.

Figure 1. Map of San Gimignano historical centre and surrounding area with the ambient-vibration single-station measurement points (white points).

Multi-station ambient-vibration measurements (passive seismic arrays) were carried out in order to constrain the S-wave velocity profile in the area above this resonant interface. Five arrays were laid out in the studied area, and their acquisitions were processed by the ESAC technique (Okada, 2003), to obtain Rayleigh dispersion curves. One of these arrays, located where the substratum

outcrops, points out the S-wave velocity of the bedrock. Whereas each one of the other Rayleigh dispersion curves were inverted, by means a genetic-algorithm procedure, jointly to the HVSR curve relative to a point near the array, obtaining the local S-wave velocity profile. These profiles, together with a profile relative to a pre-existent down-hole test located near the hamlet, were approximated by a single power law pattern in the form $V_S(z) = V_0 \cdot z^x$, where V_S is the S-wave velocity at the (adimensional) depth z. A fitting procedure gave the values $V_0 = 227$ m/s and $x = 0.25$. In this way (see, *e.g.*, Albarello *et al.*, 2011), the depth H of the resonant interface in correspondence of each single-station measurement point, was estimated by the formula:

$$H \cong \left[\frac{V_0(1-x)}{4f_0} \right]^{\frac{1}{1-x}} = \left[\frac{227(1-0.25)}{4f_0} \right]^{\frac{1}{1-0.25}} \cong 149 \cdot f_0^{-\frac{4}{3}}$$

with f_0 in hertz and H in metres. This allowed the definition of the overall pattern of the resonant surface representative of the seismic bedrock buried morphology.

Finally, specific abaci were used to estimate amplification factors in the studied area. They are abaci very recently adopted by *Regione Toscana* (http://www.rete.toscana.it/sett/pta/sismica/03normativa/microzonazione/microzon azione_regionale/specifiche/livello2/index.htm; Albarello and Peruzzi, 2014), which allow a quick estimate of the site amplification by just a few data: f_0 and the S-wave velocity profile at depth no more than 30 m.

Ambient vibrations in towers' characterization

As concerns the second work package, single-station ambient-vibration measurements were performed inside the medieval towers to identify the relative fundamental (elastic) resonance frequency. This parameter plays a role in realizing structural models of the towers. As a whole, twelve towers were monitored. For each of them, measurements were carried out in each accessible level as well as in the free-field at one or two sites just outside from each tower.

Standard Spectral Ratios (SSR) were obtained, for each level, as the ratio between the average spectral amplitudes of ambient vibrations obtained inside and outside the buildings along the three spatial directions (two horizontal, parallel to the building faces, and the vertical one). Peaks in the SSR curves are considered as representative of natural frequencies of the structure. In all the cases, a clear peak is detected in the SSR curves for each spatial direction, whose an example is shown Figure 2. In some cases, secondary peaks also appear, probably representative of higher modes or of interactions with other buildings located nearby. As several SSR curves were obtained for almost each tower, relative to its different levels, the range of the peak frequencies were considered as a lower bound for the relevant experimental uncertainty.

By assuming the linear relationship $T_0 = C_T \cdot h$ between the fundamental period along the horizontal directions ($T_0 = 1/f_0$) and the relative tower height h (Figure 2), obtained data allowed to estimate the coefficient as $C_T = 0.0144 \pm$

0.0004 s/m, a value in line with those obtained in different sites of the world for various kinds of buildings (masonry, concrete, etc.). As the measurements were asynchronous, no information was obtained about modal shapes.

Finally, data in Figure 2 clearly show that the main proper frequency of many studied towers falls close to the ground resonance frequency of the hamlet and this fact reveals a possible enhancement of the seismic risk for the medieval towers of San Gimignano.
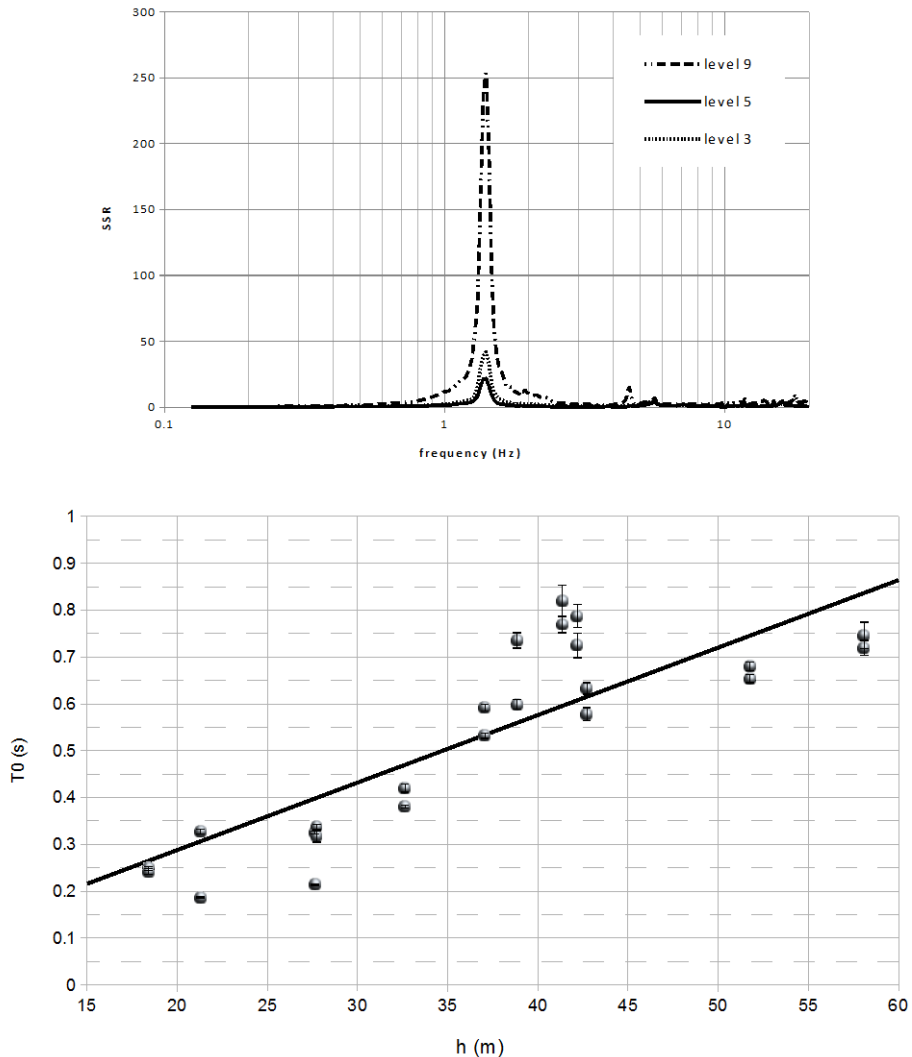

Figure 2. Example of SSR curves relative to different levels of a tower (top panel) and the trend of the towers' fundamental periods ($T_0 = 1/f_0$) versus the total towers' heights (lower panel), where the black line is the relationship $T_0 = C_T \cdot h$.

References

Albarello D., Cesi C., Eulilli V., Guerrini F., Lunedei E., Paolucci E., Pileggi D. and Puzzilli L.M. (2011). The contribution of the ambient vibration prospecting in seismic microzoning: an example from the area damaged by the 26th April 2009 l'Aquila (Italy) earthquake. *Boll. Geofis. Teor. Appl., 52(3), 513–538*, doi:10.4430/bgta0013.

Albarello D. and Castellaro S. (2011). Tecniche sismiche passive. *Ingegneria Sismica*, Anno XXVII, 2 (Suppl.), 32–63 (in Italian).

Albarello D. and Peruzzi G. (2014). Abachi regionali per amplificazioni litostratigrafiche finalizzati alla redazione di carte di microzonazione sismica di livello II. Available athttp://www.rete.toscana.it/sett/pta/sismica/01informazione/formazione/pubblicazioni/microzonazione/02_ps_locale/02_cap10.htm (in Italian).

Okada H. (2003). The microtremor survey method. Geophysical Monograph Series, SEG, 129 pp.

Lunedei E., Peruzzi G., Albarello D. (2014) Ambient vibrations in seismic studying the UNESCO cultural heritage of San Gimignano (Italy). Second European Conference on Earthquake Engineering and Seismology.

Lunedei E., Peruzzi G., Albarello D. (2014) Caratterizzazione dinamica delle torri di San Gimignano (Siena) mediante misure di vibrazioni ambientali. Atti del 33° convegno nazionale del GNGTS (Tema 2, Sessione 2.3), http://www2.ogs.trieste.it/gngts/ (in Italian).

Peruzzi G., Lunedei E., Albarello D., Pieruccini P., Firuzabadì D., Sandrelli F., Coltorti M., Fantozzi P. L. (2013). La Microzonazione Sismica di un sito UNESCO: il centro storico di San Gimignano (Siena). Atti del 32° convegno nazionale del GNGTS (Tema 2, Sessione 2.2), http://www2.ogs.trieste.it/gngts/ (in Italian).

Picozzi M., Parolai S. and Albarello D. (2005). Statistical analysis of Horizontal to Vertical Spectral Ratios (HVSR), *Bull. Seism. Soc. Am.*, 95(5), 1779–1786, doi:10.1785/0120040152.

Picozzi M. and Albarello D. (2007). Combining genetic and linearized algorithms for a two-step joint inversion of Rayleigh wave dispersion and H/V spectral ratio curves, *Geophys. J. Int.*, 169, 189–200.

Site Effects Assessment using Ambient Excitations (SESAME) European project, 2005. Deliverable D23.12, Guidelines for the implementation of the H/V spectral ratio technique on ambient vibrations: measurements, processing and interpretation.

SEISMIC IMPROVEMENT OF HISTORICAL MASONRY CONSTRUCTION BY STEEL TIES: A CASE STUDY

Mandara A.[1], Ramundo F.[2], Spina G.[2]

[1]*Department of Civil Engineering, Design, Design, Building and Environment, Second University of Naples, via Roma 29, 81031 Aversa (CE),Italy,alberto.mandara@unina2.it*
[2]*Consultant Engineer, Avellino, Italy*

Recent seismic events have emphasized the great vulnerability of the majority of masonry arrangements, mostly due to the low effectiveness of both walls and floor-to-wall connections. In the past, improving the safety of these structures has represented a priority need that often involved the execution of interventions which proved both ineffective and incompatible with the original structure. On the other hand, the need of preservation of historical constructions can represent an obstacle for the achievement of a satisfactory safety level. Therefore, it is necessary to develop methods capable of satisfying requirements of both safety and conservation. For this reason, a correct intervention methodology has to be set out which preserves the original character of the structure and eliminates, at the same time, the inherent causes of vulnerability by means of techniques compatible with original materials and architectural characteristics. In order to follow the principles of both safety and preservation, the design of seismic restoration interventions on masonry buildings, and in particular on those with historical features, often require reversibility and full compatibility with the structure to operate on. Tying systems allow satisfying both requirements.

A study on the seismic behaviour of in-plane loaded masonry walls strengthened with different tying systems is first presented in the paper. The work aims at the evaluation of the higher safety level produced by the increase of strength and ductility achieved thanks to the use of ties for strengthening masonry walls. Both serviceability and ultimate limit states have been investigated in the view of the modern performance based design. The design of ties has been carried out by means of a kinematic approach based on the possible collapse mechanisms. The effect of the improvement has been evaluated in terms of both strength and ductility.The output of the analysis represents a further demonstration on the effectiveness of such strengthening system. Calculations presented in fact, referred to a typical scheme of wall in a multi-storey masonry building, clearly show the significant improvement achievable with the use of steel ties. Also, they highlight the influence of ties arrangement within the wall on the global structural performance in terms of both strength and ductility.

The second part of the paper is then devoted to the case study represented by the former Borbonic Prison in Avellino, located in the Southern Italy. This building, erected at the beginnings of the XIX Century has been recently interested by a global refurbishment including the seismic improvement by means of steel

ties. The results of such intervention demonstrated the effectiveness of tying systems, whose reliability is guaranteed by experience, it having been used for a long time in repairing and strengthening of masonry. In addition, theyconfirmed the advantages of full reversibility and compatibility with the original masonry structure, as well as the possibility to be easily hidden and maintained at the same time.

References

Mandara, A., 2002. Strengthening techniques for buildings, in refurbishment of buildings and bridges.In F.M. Mazzolani& M. Ivanyi (Eds) Refurbishment of Buildings and Bridges.CISM publications, Chapter 4.

Mandara, A. &Mazzolani, F.M. 1998.Confining of masonry walls with steel elements.Proc. of the International IABSE Conference on Savings Buildings in Central and Eastern Europe. Berlin.

Mandara, A., Ramundo, F. &Spina, G., 2005.Strengthening of masonry walls by steel ties: analysis of performance levels under seismic actions.Proc. of the XX C.T.A. Conference - Ischia (Italy).

Mazzolani, F.M., 2002. Principles of rehabilitation and design criteria.In F.M. Mazzolani& M. Ivanyi (Eds) Refurbishment of Buildings and Bridges.CISM publications, Chapter 1.

Mazzolani, F.M. &Mandara, A., 2002.Modern trends in the use of special metals for the improvement of historical and monumental structures.Journal of Eng. Structures n.24.Elsevier.

D.M. 14-01-2008, NormeTecniche per le Costruzioni. Italian Ministry of Infrastrucutres, 2008.

Spina, G., Ramundo, F. & Mandara A. 2004. Masonry strengthening by metal tie bars, a case study. Proc. of SAHC Conference – Padova.

DYNAMIC IDENTIFICATION AND SEISMIC SAFETY OF TWO MASONRY BELL TOWERS

Ferraioli, M.[1], Abruzzese, D.[2], Miccoli, L.[3], Mandara, A.[4]

[1]*Department of Civil Engineering, Design, Design, Building and Environment, Second University of Naples, via Roma 29, 81031 Aversa (CE),Italy,massimiliano.ferraioli@unina2.it*

[2]*Department of Civil Engineering and Computer Science Engineering, University of Rome "Tor Vergata", via del Politecnico 1, 00133 Rome, abruzzese@uniroma2.it*

[3]*Division Building Materials, BAM Federal Institute for Material Research and Testing,Unter den Eichen 87, 12205 Berlin, Germany, lorenzo.miccoli@bam.de*

[4]*Department of Civil Engineering, Design, Design, Building and Environment, Second University of Naples, via Roma 29, 81031 Aversa (CE),Italy, alberto.mandara@unina2.it*

The recent experience of Italian seismic events provided wide observational information about typical behaviour, damage patterns and intrinsic vulnerability of monumental buildings. Evidence indicates that historical constructions are by far the most vulnerable from the seismic point of view. As a consequence, they demand for the definition of urgent strategies for the protection of cultural heritage from seismic hazard. The main goal of an in-depth knowledge of the structure should help to avoid inadequate, unsuitable or dangerous rehabilitation operations, as well as to select non-invasive and reversible techniques for the best exploitation of material and technology features. The definition of reliable models and methods for seismic risk assessment of historical constructions is today a very important topic. Typical problems of masonry structures concern aspects like inherent structural lacks, material degradation, geotechnical problems, buckling behaviour of slender elements and dynamic loading vulnerability. Modelling the mechanical behaviour of masonry may play an important role, due to both inherent material complexity and great scatter in mechanical properties. Effective procedures for the identification of the structural parameters from static and dynamic testing are thus required. In particular, dynamic measurements may be very useful for the identification of mechanical properties and soil restraints and, consequently, for the calibration of advanced numerical finite element models. The paper addresses two case studies of structural monitoring and seismic assessment of medieval masonry towers in Italy: the bell tower of Aversa and the bell tower of Capua. These monuments, placed in the Campania region, were monitored by means of full-scale environmental vibration testing. Measured responses are then used for modal identification with a typical finite element model updating technique based on vibration test results. Parameters optimization is carried out on the basis of a criterion which minimises a weighted error on modal properties. A satisfactory improvement in the determination of modal parameters is thus obtained, resulting in a close agreement between the

modal properties observed in dynamic tests and those calculated from numerical model. Seismic assessment is finally performed based on nonlinear static analysis of the tower under multimodal distributions of lateral loads. Results from nonlinear analysis indicate the potential collapse mechanisms and evidence dangerous structural weakness which may play a role in the seismic vulnerability of the towers.

References

Abruzzese, D., Miccoli, L. and Yuan, J. (2009). Mechanical behavior of leaning masonry Huzhu Pagoda. Journal of Cultural Heritage, 10: 480-486.

Peñaa, F., Lourenço, P.B., Mendes, N. and Oliveira, D.V. (2010). Numerical models for the seismic assessment of an old masonry tower. Engineering Structures, 32: 1466-1478.

Ferraioli, M., Mandara, A., Abruzzese, D. and Miccoli, L., (2012). Seismic assessment of two masonry medieval bell towers, Proc. 5th International Congress on "Science and Technology for the Safeguard of Cultural Heritage in the Mediterranean Basin", Roma.

SEISMIC VULNERABILITY OF MASONRY HERITAGE BUILDINGS IN MALTA

Mangion, A.[1], Torpiano, A.[2], Bonello, M.[3]

[1] *Department of Conservation and Built Heritage, University of Malta, Msida MSD 2080, Malta, andre.mangion.06@um.edu.mt*

[2] *Department of Civil and Structural Engineering, University of Malta, Msida MSD 2080, Malta, alex.torpiano@um.edu.mt*

[3] *Department of Civil and Structural Engineering &, University of Malta, Msida MSD 2080, Malta,, marc.bonello@um.edu.mt*

Introduction

The structural behaviour of masonry heritage buildings in Malta subjected to seismic action is a major risk in conserving such buildings. This is because Malta lies on a seismic zone which was subjected to high intensity earthquakes in the past (Galea, 2007). Many of the existing masonry heritage buildings were subjected to major earthquakes of 1693, 1743 and 1856, with repairs ranging from minor repairs to partial rebuilding (Abela, 1969; Galea, 2007). The survival of such buildings does not determine the degree of seismic resistance to any future strong tremor. The study will explore the possibility to determine the seismic vulnerability of masonry heritage buildings using Applied Element Method (AEM), a numerical structural modelling. Since AEM was never used to determine seismic vulnerability of masonry heritage buildings in Malta, simple masonry heritage building typology is being analysed in this study.

Numerical structural Modelling for Masonry Heritage buildings

Numerical structural modelling is widely used to analyse buildings and predict their behaviour under seismic action (Roca, Cervera, Gariup, & Pela', 2010). In general, two different methods are used. These are the Finite Element Method (FEM) and Discrete Element Method (DEM) (Roca, Cervera, Gariup, & Pela', 2010; Smoljanović, Živaljić, & Nikolić, 2013). FEM is used very successfully to simulate pre failure situations and the global behaviour of large buildings (Mistler, Butenweg, &Meskouris, 2006) but it cannot accurately simulate post cracking scenarios. DEM's main feature is that it can simulate the separation between each masonry block without knowing the failure mechanism of the building (Giordano, Mele, & De Luca, 2002).

Another important aspect in Numerical modelling is the element size. The size of the element depends on the level of detail of the building being simulated. In studies performed on masonry buildings (Lemos, 2007; Dimitri, De Lorenzis, &Zavarise, 2011; Casolo, Milani, Uva, &Alessandri, 2013); DeJong&Vibert, 2012; Ulrich, Gehl, Negulescu, &Foerster, 2012), it can be concluded that if the element size was the same as the masonry unit, and placed on each other as actual, and using DEM, the failure mechanism of the building can be modelled satisfactorily.

AEM (Meguro &Tagel-Din, Applied Element Method for Structural Analysis: Theory and Application for Linear Materials, 2000), a numerical mathematical model which forms part of the DEM family (Lemos, 2007) was chosen because of its ability to simulate the behaviour of the masonry heritage building from initial loading to total collapse (Meguro &Tagel-Din, Applied Element Method Used for Large Displacement Structural Analysis, 2002). This is achieved in AEM by modelling the masonry building by rigid elements, connected together with matrix springs (Normal and Shear springs) (vide Figure 1), which can simulate both the material stresses and deformations in the elements (Meguro &Tagel-Din, Applied Element Method for Structural Analysis: Theory and Application for Linear Materials, 2000). An additional feature when compared to DEM is that contact between two detached elements is simulated by contact springs (Normal and Shear springs) (Tagel-Din, 2009, pp. 7-23).
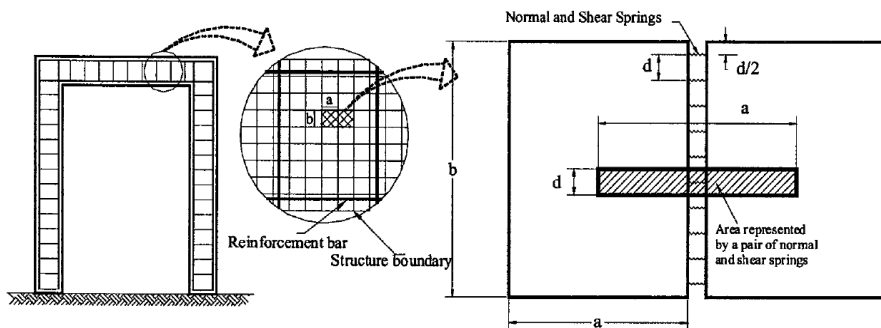
(a) Element generation in AEM (b) Spring distribution and area of influence

Figure 1. Modelling of the structure in the AEM (Souce: (Meguro &Tagel-Din, Applied Element Method Used for Large Displacement Structural Analysis, 2002))

Seismic analysis of a simple Masonry Heritage building typology

Three aspects that form the key part of the study are selecting the simple masonry heritage building typology, the simulation of the building in AEM and the ground motion adopted. Since AEM was never used to simulate masonry heritage buildings in Malta, the building selection involves identifying a building typology with simple masonry technology in order to limit as many variables as possible.

The simulation of the simple masonry heritage building involves the rationalisation of the actual building without eliminating main building irregularities. This can be grouped by regularising the masonry unit sizes, selecting common masonry and mortar properties and selection of ground-building conditions.

No past seismic record of earthquakes that have damaged masonry heritage buildings exists (Galea, 2007). Thus the ground motion that is adopted for the study is to reflect the maximum earthquake intensity that the masonry heritage building can sustain, since the earthquake intensity is one of the main parameters that influence the seismic vulnerability of the building (Tomaževič, 1999)
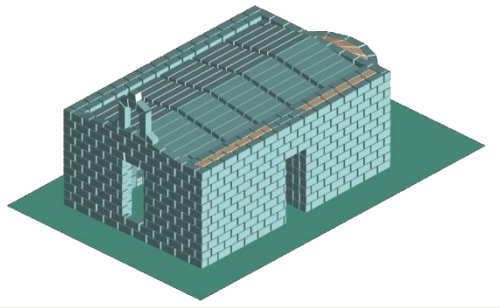
Figure 2. A simple masonry heritage building modeled on AEM.

Conclusion

The study offers more understanding on the seismic vulnerability on heritage buildings, starting from observing the seismic behaviour of simple masonry heritage building typology. Since no seismic record of damaging tremors in Malta exists, any historical record of buildings damaged due to past tremors was collected to understand the past seismic vulnerability of heritage buildings. Then different numerical structural modelling used for heritage buildings were studied from which AEM was chosen. From the seismic analysis by AEM the seismic vulnerability of Heritage buildings was better understood. One factor that greatly influences the seismic vulnerability which cannot always be mimicked with AEM is the quality of workmanship including lack of maintenance of the building which increases the seismic vulnerability of masonry heritage buildings in general, a reason which was also noted in previous earthquakes.

Acknowledgements

References

Abela, M. (1969).Earthquakes in Malta.Unpublished undergraduate dissertation, University of Malta.

Casolo, S., Milani, G., Uva, G., &Alessandri, C. (2013).Comparative seismic vulnerability analysis on ten masonry towers in the coastal Po Valley in Italy.Engineering Structures, 49, 465-490.

DeJong, M. J., &Vibert, C. (2012). Seismic response of stone masonry spires: Computational and experimental modeling. Engineering Structures, 40, 566–574.

Dimitri, R., De Lorenzis, L., &Zavarise, G. (2011).Numerical study on the dynamic behavior of masonry columns and arches on buttresses with the discrete element method. Engineering Structures, 33(12), 3172–3188.

METHODOLOGY TO ESTIMATE THE DAMAGE AND EARTHQUAKE LOSSES IN URBAN AREAS, NORTH-EASTERN ALGERIA

Hamidatou, M.

Research CentreinAstronomyAstrophysics and Geophysics (CRAAG), BP 75 Ain Smara 25000 Constantine Algeria, m.hamidatou@craag.dz

In its history, many destructive earthquakes have hit Algeria. Among the more recent earthquakes, we can cite those of 10th October 1980 in El Asnam (Mw = 7.3), of 25th October 1985 in Constantine (Ms = 6.0), and 21st May 2003 Boumerdes (Mw = 6.8). The seismic events that have generated disastrous results showed the vulnerability of Algeria to seismic risk due to the presence of dense population and of industry in the northern regions. To minimize the disastrous effects of a future earthquake that will strike the region again, this paper presents the scenario of seismic risk of Constantine City, which lies in north-east Algeria. A specific study of the seismic vulnerability assessment has been performed for the historic square that includes Coudia, Bellvue-Ciloc, and Old Town. This scenario allows us to assess the maximum acceleration of ground motion in rock using empirical attenuation laws using a reference earthquake (the Constantine earthquake of 1985), the effects on sites depending on the geology of the region, damage to buildings, and seismic vulnerability. To realize and visualize this scenario, a Geographic Information System (GIS) has been used.

PERIOD-HEIGHT RELATIONSHIPSFOR EXISTING BUILDINGS IN SE SICILY

Panzera F.[1], Lombardo G.[1], Longo E.[1], Torrisi A.[2]

[1]Dipartimento di Scienze Biologiche, Geologiche e ambientali,Università di Catania– Italy,fpanzera@unict.it

[2] Dipartimento della Protezione Civile, Servizio Regionale di Protezione Civile – Catania, Italy

Introduction

The dynamic properties of a building are usually described through its natural frequency (or period T) and the damping ratio ($\square$). Their knowledge is therefore particularly important for estimating the seismic base shear force F in designing earthquake resistant structures. Following the Eurocode8 (2003), F can be expressed as:

$$F = Sa\,(T;\xi)\cdot m\cdot\lambda \quad (1)$$

where $Sa\,(T;\xi)$ is the ordinate of the target spectrum at period T and damping ξ, m is the total mass of the building above the foundation (or above the top of a rigid basement) and λ is a correction factor. The $Sa\,(T;\xi)$ is evaluated considering the local geological features, which influence the site response in term of amplification of the ground motion, as the seismic input travels from the bedrock to the overlying soil deposits. The engineering practice usually derives the dynamic behaviour of buildings through numerical or experimental methods, achieving empirical relationships that estimate building resonant periods as a function of either the height or the number of floors (Satake et al. 2003; Gallipoli et al. 2009; Panzera et al. 2013). In the present study we evaluated the buildings dynamic response in the city of Catania, Siracusa, Lentini, Carlentini e Lampedusa through experimental measurements based on ambient noise recordings.

Methodology

Generally the dynamic properties of a building are evaluated through the vibration mode shapes obtained by the records of two or more sensors monitoring the motion at different locations in the building. Undoubtedly, the best approach would be to adopt earthquake records as exciting source. However, due to the need of a long observation time and to the high cost, this method can only be used in a small number of buildings. Alternatively, ambient noise measurements are used and the subsequent estimate of the fundamental frequency is obtained through spectral ratio techniques. This methodology, originally adopted as a quick estimate of the seismic site response (Nakamura 1989), has shown to be in good agreement with results obtained from both numerical modelling and other experimental techniques, in estimating the dynamic properties of buildings (e.g. Oliveira & Navarro 2009).

The fundamental period of the building is obtained by computing the ratio between the amplitudes of the Fourier spectrum of horizontal components of

motion, recorded on both the top and the ground floor. This method is also known as standard noise spectral ratio (SNSR) technique. During data acquisition the seismometer is usually placed at the geometrical center of the top floor in the stairwell, assuming that this point coincides with the center of mass of the floor and as close as possible to the RC frame to minimize vertical modes of beams or floors.
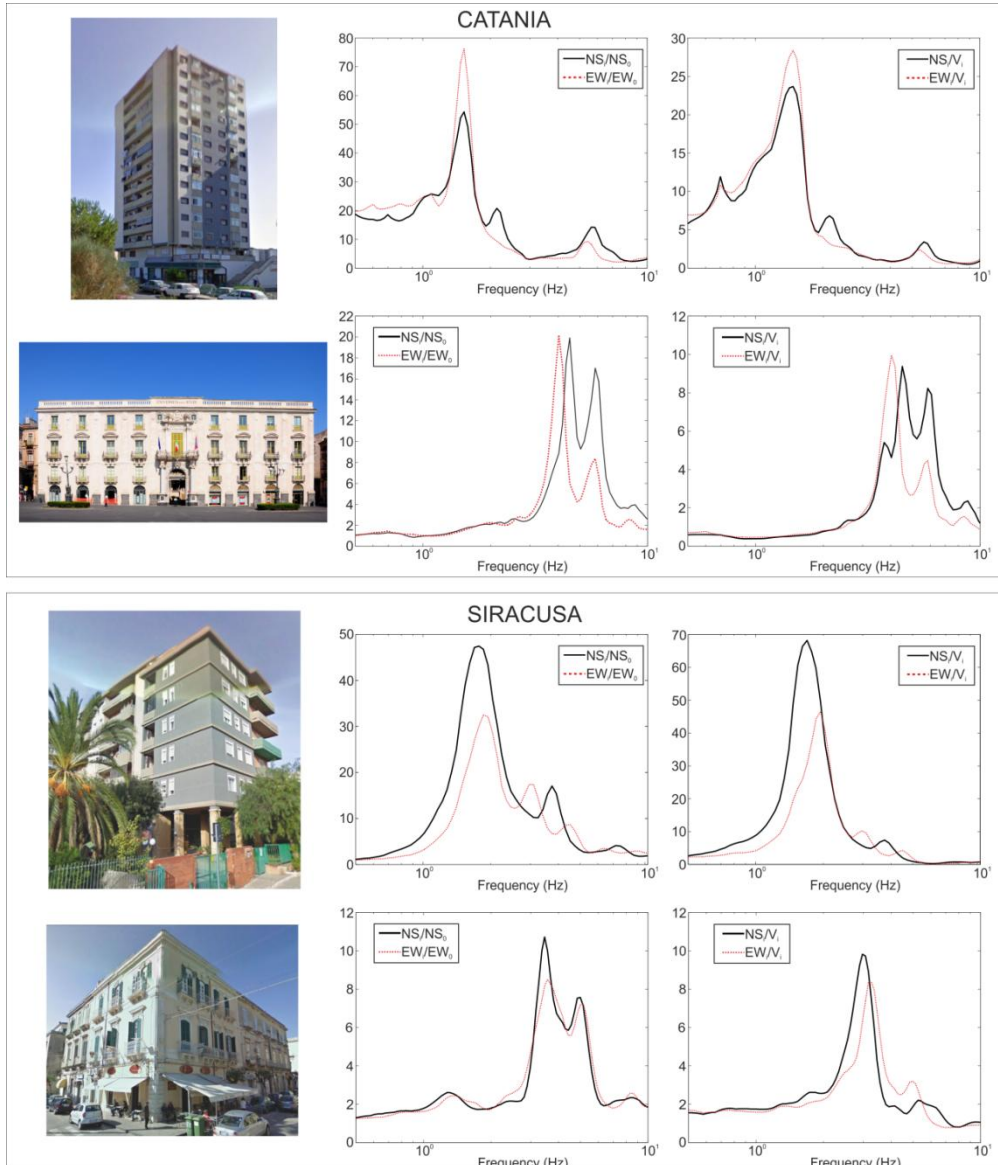

Figure 1. Examples of HVNR and SNSR for typical RC and MA buildings in Catania and Siracusa. The y-axis specifies the amplitude ratio.

To observe the influence of the geometry, the two main axes of sensors are oriented as coincident with the main directions of the building (NS ≡ T ≡ transverse ≡ minor axis; EW ≡ L ≡ longitudinal ≡ major axis) in order to better highlight their respective contribution. In the present study, both the horizontal to vertical noise ratio (HVNR) and the standard noise spectral ratio (SNSR) techniques were used to identify the building's fundamental frequencies (see examples shown in Fig. 1).

Measurements were performed in 106buildings distinguished according to their construction typologyinto 44 masonry buildings (MA) and 62 reinforced concrete (RC) buildings. As fundamental period for each building we considered the peak with the higher amplitude in both HVNR and SNSR, evaluating for each curve the related average ±1σ confidence interval. Ambient noise was recorded using a three-component velocimeter (Tromino) sampling the signal at a frequency of 128 Hz. In each building, 10 minutes length of ambient noise were recorded both at the top and at the ground floor. According to the guidelines suggested by the European project Site EffectS assessment using AMbient Excitations (SESAME 2004), time windows of 10 s were considered, selecting the most stationary part and not including transients associated to very close sources. Fourier spectra were calculated in the frequency band 0.5–15 Hz and smoothed using a triangular average on frequency intervals of ± 5% of the central frequency. Figure 1shows few examples for typical MA and RC buildings in the area. Finally, a preliminary test was performed in Lampedusa island in order to set up a computer approach aiming to automate the evaluation of the building heights in an urbanized area. The used method allow us to extract, through aGeographic Information System (GIS), the building tallness as the difference in the heights mapped through a DSM (Digital Surface Model)anda DTM(Digital Terrain Model). Since the DSM plots the earth surface including objects on it whereas, DTM draws into a map the earth surface only without any objects, the difference between the two elevation models gives back the building heights. Such procedure, together with the experimentally obtained period-height relationships could be adopted as a method to perform a quick survey aiming to characterize the dynamic properties of buildings in a urbanized area.

Description of results and concluding remarks

The inspected buildings exhibit clearly different characteristics both in the plan shape and in elevation with *T* values ranging between 0.09 s and 0.80 s.The fundamental periods obtained through the HVNR technique show values quite similar to the ones obtained through the SNSR method.

Another important aspect that was highlighted, through measurements in our tested buildings, concerns the observed difference between periods evaluated for the longitudinal (L) and the transverse (T) directions. This difference, that ranges between -0.09 s to 0.25 s, can be interpreted as different rigidity of the building which is also dependent on its geometry. Indeed, the results show that in most of the examined buildings a larger deformation is observed in the transverse direction

rather than in the longitudinal one. Such effect is testified by the lower frequencies which are predominant in the direction parallel to the transverse (shorter) side of the structure.

Figures 2(left panel) shows the experimental fundamental periods as a function of height for the considered cities, whereas in Figures 2 (right panel) period vs height, discriminatingRC and MA building, are reported. We also derived a functional form for the fundamental period regressing the observed data and taking into account both HVNR and SNSR periods for both vibration directions.

It is worth noting that significant differences are observed between fundamental periods of buildings in RC and MA which are mostly located in the historical part of each considered city. These differences are likely due to the role played by the stiff masonry infills on the fundamental period of edifices. This aspect has been widely discussed by several authors (Masi &Vona 2009 and references therein) that have pointed out as the existence of infill walls has the effect of increasing the mass and lateral stiffness of the system. Moreover, it was observed that in the evaluation of fundamental periods, the influence due to the presence of connected adjacent buildings has to be taken into account. Contiguous structures add indeed their own eigenfrequency to the one of the studied structure, and this as observed by Boutin &Hans (2009), can affect the vibration mode of the studied building, decreasing its original value by about 10%.
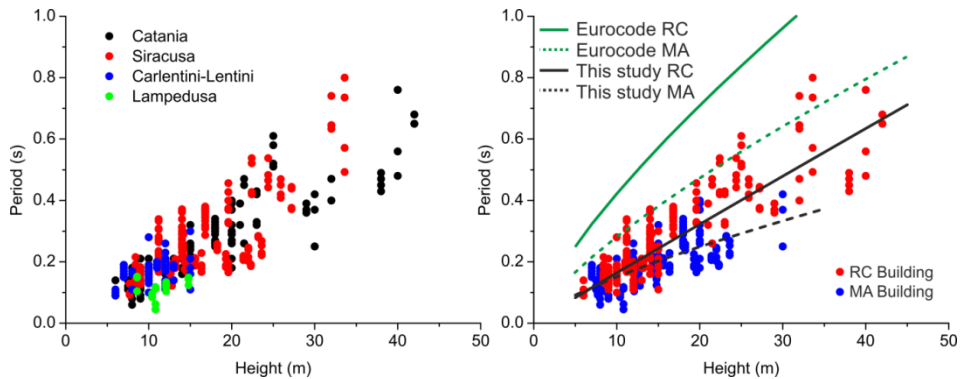

Figure 2. Period-Height values from experimental values observed in the investigated towns (left panel) and comparison with relationships obtained by Eurocode8, 2003 (right panel).

The period-height relationships obtained from the present research are also compared with the fundamental period–height relationships (Fig. 2 right panel) provided by the Eurocode8 (2003; EC8 – RC; EC8 – MA). In general, the equations provided by the Eurocode8 (2003) both for RC and MA building show important differences with the curves obtained in this study. A possible explanation for this disagreement may be found in the use of ambient noise that it is a low energy input source. Hong &Hwang (2000) and Trifunac *et al.*(2010) observe also

that the fundamental period of buildings, designed according to the seismic code, usually shows a period much lower than the value expected during earthquakes. However, we believe that the level of shaking cannot be considered as the only issue responsible for the observed discrepancy between experimental and Eurocode8 (2003) height-period relationships. We rather think that the most likely explanation has to be found in the contribution linked to the presence of infill walls. They induce a pronounced stiffness increase that implies a decrease of the fundamental period of the building and consequently a change of its seismic response (Cinitha *et al.* 2012). Through measurements performed on a frame, before and after the implementation of infills, Mucciarelli & Gallipoli (2007) observed indeed a frequency increase of 1.5 times due to the role of the stiffness of masonry infills. Modern codes do not consider the contribution of the infills, trying to obtain a diffuse damage on a RC frame that is designed with adequate ductility resources whereas, existing buildings may show a completely different behavior.

Acknowledgements

References

Boutin, C., andS. Hans (2009). How far ambient noise measurement may help to assess building vulnerability? In: Increasing Seismic Safety by Combining Engineering Technologies and Seismological Data NATO Science for Peace and Security Series C: Environmental Security, 151-180.

Cinitha, A., Umesha, PK., R.I. Nagesh (2012). A Rational Approach for Fundamental Period of Low and Medium Rise Steel Building Frames, International Journal of Modern Engineering Research 2(5) 3340-3346.

Eurocode8 (2003). Design of structures for earthquake resistance. Part1: general rules, seismic actions and rules for buildings. CEN European Committee for standardization, Brussels.

Hong, L.L., and W.L. Hwang (2000).Empirical formula for fundamental vibration periods of reinforced concrete buildings in Taiwan,Earthq Eng Struct Dyn 29 327-337.

Gallipoli, M.R., Mucciarelli, M., Šket-Motnikar, B., Zupančić, P., Gosar, A., Prevolnik, S., Herak, M., Stipčević, J., Herak, D., Milutinović, Z., T. Olumćeva (2009). Empirical estimates of dynamic parameters on a large set of European buildings. Bull.Earthq. Eng. 8(3) 593-607.

Masi, A., M. Vona (2009). Experimental and numerical evaluation of the fundamental period of undamaged and damaged RC buildings. Bull. Earthq. Eng. doi: 10.1007/s10518-009-9136-3.

Mucciarelli, M., M.R. Gallipoli (2007).Damping estimate for simple buildings through non-parametric analysis of a single ambient vibration recording, Ann. Geophys. 50 259–266.

Nakamura, Y. (1989). A method for dynamic characteristics estimation of subsurface using microtremor on the ground surface,Quarterly Report Railway Technical Research Institute 3025–33.

Oliveira, C.S., and M Navarro (2009). Fundamental periods of vibration of RC buildings in Portugal from in-situ experimental and numerical techniques, Bull. Earthq. Eng. 8(3) 609-642.

Panzera, F., Lombardo, G., I. Muzzetta (2013).Evaluation of buildings dynamical properties through in-situ experimental techniques and 1D modelling: the example of Catania, Italy, Phys. Chem. Earth. doi: 10.1016/j.pce.2013.04.008.

Satake, N., Suda, K., Arakawa, T., Sasaki, A., Y. Tamura (2003).Damping evaluation using full-scale data of buildings in Japan, J. Struct. Eng-ASCE 129 470-477.

SESAME (2004). Guidelines for the implementation of the H/V spectral ratio technique on ambient vibrations: Measurements, processing and interpretation, SESAME European Research Project WP12, deliverable D23.12, 2004,http://sesame-fp5.obs.ujf-grenoble.fr/Deliverables 2004.

Trifunac, M.D., Todorovska, M.I., Manić, M.I., and B.D. Bulajić (2010). Variability of the fixedbase and soil-structure system frequencies of a building – the case of Borik-2 building, Struct. Control. Health. Monit. 17 120-151. doi: 10.1002/stc.277.

RESONANCE FREQUENCY CHARACTERISTICS OF BUILDINGS IN MALTA AND GOZO USING AMBIENT VIBRATIONS

Galea, P., Micallef, T., Muscat, R., D'Amico,S.
Department of Geosciences, University of Malta, Msida MSD2080, Malta,
pauline.galea@um.edu.mt

Introduction

The Maltese islands, lying in the Sicily Channel between Sicily and Tunisia, cover a total area of around 317 km2 and have a present population of around 452,000, which inflates in the summer season by the arrival of over 1 million tourists. The population density of 1,346 km-2 is one of the highest in Europe. A large proportion of residential buildings in the Maltese islands are traditionally constructed of loadbearing unreinforced masonry blocks, utilising local Globigerina limestone blocks, having roofs and diaphragms of reinforced concrete. Older buildings having stone slab roofs are still found in town and village cores, sometimes more than 5 floors in height. Other building stock, in particular taller buildings, are a mix of reinforced concrete frames and masonry construction. The last earthquake to produce some building damage on the islands occurred almost 100 years ago in 1923 (Galea, 2007), while in historical times, the earthquake known to have produced the maximum local intensity of VII – VIII (EMS98) was in 1693. This event was a magnitude 7.4 earthquake along the east coast of Sicily that caused more than 50,000 casualties on that island.

Over the past 50 years, construction in the Maltese islands has mushroomed, with most towns and villages growing steadily outwards along their peripheries. The Northern and Southern Harbour districts, around the Valletta Grand Harbour, have developed into one large conurbation housing almost half the whole population of the islands. The western half of Malta and the smaller island of Gozo are more rural and still relatively sparsely populated, although pockets of urbanisation, especially in coastal areas, are growing rapidly to cater for tourism. The exposure of the islands to earthquake risk has thus increased significantly, while the public perception of earthquake hazard is still low.

The islands are composed entirely of an Oligo-Miocene layer-cake sequence of marine carbonates and clays, heavily disrupted by mainly normal faulting, with a patchy cover of Quaternary deposits and soils of terrestrial origin. The main formations in order of deposition are the Lower Coralline Limestone (LCL), the Globigerina Limestone (GL), the Blue Clay (BC) and the Upper Coralline Limestone (UCL). In the eastern half of Malta, which is the more populated and industrialised, the two youngest layers of the sequence are absent, and the GL outcrops over most of the area. In the western half of Malta, and on most of Gozo, however, the full sequence is present, so that a number of urban centres are constructed on the UCL which is underlain by the soft, and easily weathered BC layer, which can reach thicknesses of up to more than 50 m.

262

The behaviour of local constructions under dynamic earthquake loading is a problem that has begun to draw attention in recent years. Moreover the effect of the thick buried layer of clay on the dynamic seismic response is also being investigated. In this paper, we report on preliminary measurements of ambient vibrations in a set of buildings to yield information on fundamental resonance frequencies and period-height relationships. Although it is expected that building resonance frequencies would depend on a number of factors, such as construction typology, connectedness with other buildings, plan shape, etc. this study does not attempt to investigate such factors, but only the effect of building height, and the transfer of the site response to the building in the case of underlying clay. Nonetheless, most buildings studied are either of unreinforced masonry, or mixed masonry/reinforced concrete structures.

Methodology

An extensive, free-field ambient noise study carried out in 2010 (Vella et al, 2013) as well as other, denser surveys in various areas (Pace et al, 2011; Panzera et al, 2012; Galea et al, 2014) mapped the site seismic resonance frequency over all the geological outcrop lithologies in the whole archipelago. The method used was the Horizontal-to-Vertical Noise Spectral Ratio technique (HVSR) (Nakamura,1989) which is a fast and cost-effective method that reliably reveals the resonance frequency, if any, of the stratigraphic column. The study showed very clearly that the GL/UCL can be regarded as the bedrock of the local stratigraphic sequence, in that the HVSR curves on these outcrops are always relatively flat. On the other hand, free-field sites on UCL outcrop are consistently and ubiquitously characterised by a significant peak in the HVSR at a frequency between 1.0 and 2.0 Hz, which is attributed to the BC layer. Sites lying directly on the BC outcrop show higher resonance frequencies, varying between 2.0 and 10.0 Hz, depending on the thickness of the BC remaining after erosion. The same ambient noise methodology was applied in the present study to investigate the resonance of buildings. Such measurements have been widely used in a number of countries and settings (e.g. Michel et al, 2008, Gallipoli et al, 2010; Gosar et al, 2010; Oliveira and Navarro, 2010; Chiauzzi et al, 2012)

Two main surveys were carried out, in 2013 and 2014 respectively, targeting different building characteristics. In the first survey, carried out in Malta, 21 buildings were selected, that stood on Globigerina limestone outcrop, so that there was no "free-field" response, and which were relatively isolated. This geological foundation represents the majority of buildings on the islands. The second survey was carried out on 19 buildings in Gozo, targeting buildings constructed on UCL (Nadur and Victoria plateaux) or BC (Victoria) outcrops. The instruments used were of the type Micromed Tromino (www.tromino.eu) , a lightweight, portable, battery-operated, 3-component tromograph that can easily be placed at any location inside or outside a building with minimum disturbance.

Measured buildings in Malta ranged in height between 1 and 22 floors, while those in Gozo ranged between 1 and 7 floors. One seismometer was placed

on the ground floor, or basement level if available, while another was placed at roof level. When possible, measurements were carried out also on intermediate floor levels. The N axis of the Tromino was always aligned with the long plan dimension of the building (longitudinal direction) so that the E component corresponds to the transverse direction. Ambient noise time series of 15 – 30 minutes were recorded, and analysed for spectral ratio by the software Grilla ™. In the case of the Gozo buildings lying on UCL and BC, free-field measurements were also taken close to the buildings in order to evaluate the stratigraphic response of the site.

Results and Discussion

Figure 1 shows three examples of results of ambient vibration measurements in buildings constructed on UCL, BC and GL (bedrock). The left-hand panels show the HVSR on each measured floor, while the right-hand panels show the Floor Spectral Ratio (FSR) in the transverse direction on each floor. The FSR represents the ratio of the horizontal component spectrum at the ith floor, H_i, to that at the basement level H_o, and may be thought of as the transfer function of the building. Since the response at basement level is generally identical to that in the free-field, the ratio H_i/H_o essentially deconvolves the stratigraphic site response from the building response, and distinguishes the site resonance frequency from the building's fundamental resonance frequency. In buildings lying on bedrock (Figure 1 (e), (f)), the HVSR on all floors and the FSR yield approximately the same values for the fundamental frequency. Thus, for a rapid survey of a large number of buildings, it would be enough to perform a single HVSR measurement on the roof of the building. In buildings lying on the UCL it can be clearly observed in Figure 1(a) that the site response peak at 1.5 Hz on UCL is transferred upwards through the floors of the building, without any appreciable increase in amplitude, as opposed to the building oscillation at 5.5 Hz which increases in amplitude nearer the top. The building's natural frequency is given by the FSR which eliminates completely the free-field response (Figure 1(b)). The FSR in this example also shows a second resonance peak at around 8.0 Hz. It is highly unlikely that this corresponds to some higher mode of vibration, and is most likely due to coupling with the adjacent building, which is of a different height. In buildings on the BC in Gozo, the total building response appears more complex and furthermore varies greatly from one building to another. It should be said that building directly on Blue Clay outcrop may involve a number of different methodologies, such as concrete platform construction and different types of piling. Such methods, although expected to influence the building behaviour, are not directly investigated in this study, and will be more rigorously examined in further work.   In the example given (Figure 1(c)) the site response (observed separately in the free-field at close to 3 Hz, typically of BC outcrops) appears to mask the building resonance in the HVSR curves, with the lower floors exhibiting a higher overall HVSR ratio than the upper floors. The FSR, on the other hand, reveals a building natural frequency of 5.5 Hz.
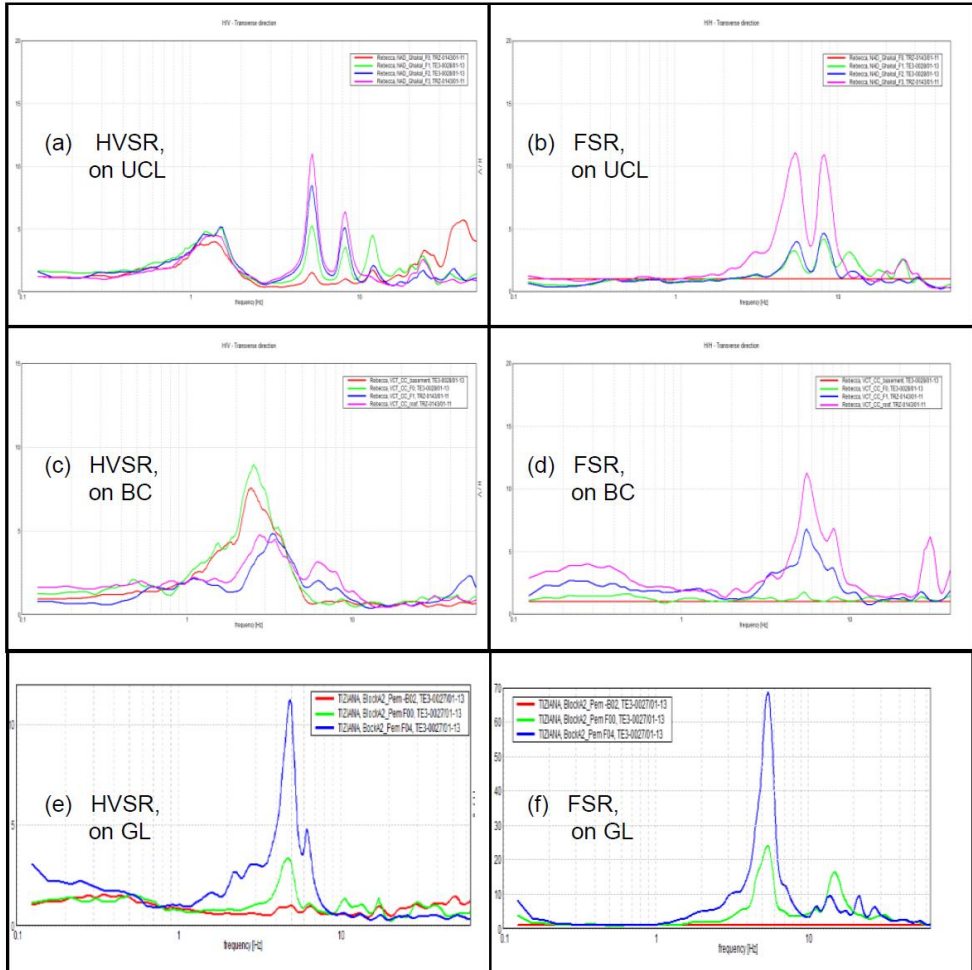
Figure 1. Horizontal-to-Vertical Spectral Ratios (HVSR) and Floor Spectral Ratios (FSR) for: (a), (b)   a 5-storey building on UCL outcrop; (c), (d)   a 4-storey building on BC outcrop; (e), (f) a 4-storey building on GL outcrop (bedrock).

Figure 2 shows the relationship between the fundamental resonance period (T, in seconds) measured from the FSR in the transverse direction as a function of the height of the building (in number of floors, N). The buildings in Malta and Gozo are shown in different symbols. Although the sampled number of buildings in Gozo is too small to be statistically reliable, there appears to be an appreciable difference between the two, the buildings in Gozo having higher fundamental frequencies than their Maltese counterparts. This is true for buildings lying on bedrock as well on UCL/BC. It is not yet clear what the reason for this difference is, however, it is likely due to the fact that buildings sampled in Gozo were not isolated, as in the case of most of the sampled buildings in Malta, and generally

265

consisted of more intricate plan shapes. In any case, a much wider sample of buildings needs to be measured in order to derive a suitable relationship. The linear regression for the buildings in Malta yields the relationship $T= 0.051N$ for the fundamental frequency in the transverse direction, for buildings up to 12 floors high (taller buildings, including the 22-floor Portomaso Tower in St. Julian's, have been left out of this relationship because they involve very different construction typologies, although their behaviour merits a separate study). This is very similar to relationships derived for the Catania area (Italy) by Panzera *et al* (2013) and for Slovenia (Mucciarelli and Gallipoli, 2007), although in general it predicts much higher frequencies than the commonly quoted Goel and Chopra (1997) as well as the EC8 guidelines (CEN, 2004).
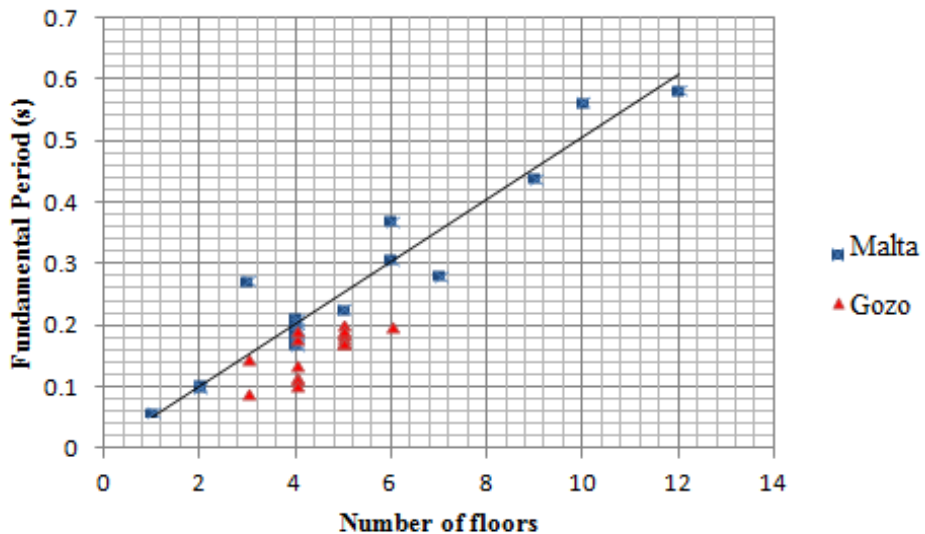
Figure 2. Period – Height relationships for fundamental, transverse oscillations of the sampled buildings in Malta and Gozo

Conclusion

This study represents a first, preliminary attempt at characterising Maltese buildings in terms of their fundamental resonance frequency. Such information is important when assessing the performance of buildings subjected to earthquake shaking, and will eventually contribute towards a national seismic risk evaluation. The danger of building collapse or heavy damage during an earthquake is intensified if the resonance frequency of the underlying soil is close to that of the building – a phenomenon known as double resonance. The probability of strong earthquake shaking on the islands is small but not negligible, and may be larger in areas where the geology includes a thick clay layer. In the case of buildings in Malta and Gozo, the large majority of buildings are constructed on bedrock (mostly GL), so that the phenomenon does not occur. Double resonance may occur in

buildings constructed directly on Blue Clay outcrop (a situation encountered in a few areas in Gozo and Malta), since the resonance frequency related to the surface clay layer (2 – 10Hz) falls in the same range as that of short - to - medium height buildings. It could also occur in buildings in the approximate height range of 10 - 15 floors that are built on UCL outcrops since these will have a building resonance frequency in the range of that measured on such outcrops (between 1.0 and 2.0 Hz). Although such buildings are not at present found in the western half of the archipelago, where this lithology exists, it is important to keep such considerations in mind when planning future development. Further studies will attempt to derive more specific relationships based on construction typology and geometrical parameters.

Acknowledgements

References

CEN (2004) Eurocode 8: Design of Structures for Earthquake Resistance – Part I: General rules, Seismic Actions and Rules for Buildings, *Committee for Standardization,* Brussels

Chiauzzi, L., Masi, A., Mucciarelli, M., Cassidy, J. F., Kutyn, K., Traber, J., ... & Yao, F. Estimate of fundamental period of reinforced concrete buildings: code provisions vs. experimental measures in Victoria and Vancouver (BC, Canada). In *Proceedings of the 15th World*
Conference on Earthquake Engineering, Paper Reference (Vol. 3033)

Galea, P. (2007). Seismic history of the Maltese islands and considerations on seismic risk. A*nnals of Geophysics*, **50** no. 6, 725 – 740

Galea, P, D'Amico, S. and Farrugia, D. (2014) Dynamic characteristics of an active coastal spreading area using ambient noise measurements – Anchor Bay, Malta. *Geophysical Journal International*. **199** (2): 1166-1175 doi: 10.1093/gji/ggu318

Gallipoli, M. R., Marco Mucciarelli, B. Šket-Motnikar, P. Zupanćić, Andrej Gosar, Snježan Prevolnik, Marijan Herak et al. Empirical estimates of dynamic parameters on a large set of European buildings. *Bulletin of earthquake engineering* 8, no. 3 (2010): 593-607

Goel, R. K., & Chopra, A. K. (1997). Period formulas for moment-resisting frame buildings. *Journal of Structural Engineering*, *123*(11), 1454-1461

Gosar, A., Rošer, J., Motnikar, B. Š., & Zupančič, P. (2010). Microtremor study of site effects and soil-structure resonance in the city of Ljubljana (central Slovenia). *Bulletin of earthquake engineering*, *8*(3), 571-592

Michel, C., Guéguen, P., & Bard, P. Y. (2008). Dynamic parameters of structures extracted from ambient vibration measurements: An aid for the seismic vulnerability assessment of existing buildings in moderate seismic hazard regions. *Soil Dynamics and Earthquake Engineering*, *28*(8), 593-604

Mucciarelli, M., & Gallipoli, M. R. (2007). Non-parametric analysis of a single seismometric recording to obtain building dynamic parameters. *Annals of Geophysics*, **50**, 259 - 266

Nakamura, Y. (1989). A Method for Dynamic Characteristics Estimation of Subsurface using Microtremor on the Ground Surface, *Quarterly Report of Railway Technical Research Institute , **30 (1)***, 25-33

Oliveira, C. S., & Navarro, M. (2010). Fundamental periods of vibration of RC buildings in Portugal from in-situ experimental and numerical techniques. *Bulletin of Earthquake Engineering*, *8*(3), 609-642

Pace, S., Panzera,F., D'Amico,S., Galea, P., Lombardo,G. (2011) Modelling of ambient noise HVSR in a complex geological area - case study of the Xemxija Bay area, Malta. In*Proceedings of the 30th congress of the Gruppo Nazionale di Geofisica della Terra Solida,* Trieste, November 2011

Panzera F., D'Amico, S., Lotteri A., Galea P., Lombardo G., 2012. Seismic site response of unstable steep slope using noise measurements: the case study of Xemxija bay area, Malta. *Natural Hazard and Earth Science System,* 12, 3421-3431, doi:10.5194/nhess-12-3421-201

Panzera, F., Lombardo, G., & Muzzetta, I. (2013). Evaluation of building dynamic properties through in situ experimental techniques and 1D modeling: The example of Catania, Italy. *Physics and Chemistry of the Earth, Parts A/B/C*, *63*, 136-146

Vella, A., Galea, P., D'Amico, S. (2013) Site frequency response characterization of the Maltese islands based on ambient noise H/V ratios, *Engineering Geology* **163**, 89 – 100

ADVANCES IN EVALUATING TSUNAMI FORCES ON COASTAL STRUCTURES

Rossetto, T.[1], Eames, I[.2], Lloyd, T.O.[3]

[1]EPICentre, CEGE Department, University College London, Gower Street, London, WC1E 6BT, UK,t.rossetto@ucl.ac.uk
[2]Departmentof Mechanical Engineering, University College London, UK,i.eames@ucl.ac.uk
[3]AIR Worldwide Ltd. London, UK,tlloyd@air-worldwide.com

Introduction

At source, tsunami waves have relatively small wave heights (typically 0.5-2m), but very long wavelengths. As these waves approache the shoreline and enter the shallower waters, their wavelength reduces and their wave height increases dramatically. The resulting waves can cause violent impacts on infrastructure and structures, and the long wavelengths lead to extensive inundation inland causing destruction over large areas of coast as seen recently in Japan (2011). Clearly there is a need for a systematic analysis of the physics of tsunami flows in and around buildings and the forces and pressures they produce on structures as a function of time. The first steps towards such a study are presented.This paper presents preliminary observations obtained from sets of unique physical experiments designed to study the impact of tsunami-like waves on coastal structures towards the development of tsunami design/assessment guidance.

The UCL-HR Wallingford Experiments

Through a UCL-HR Wallingford collaboration an innovative method for generating tsunami in the laboratory was developed that uses a pneumatic, rather than a paddle system. Tests carried out using the new tsunami generator demonstrate that it is the only facility worldwide currently able to produce wavelengths long enough to represent tsunami and generate stable trough-led waves (see Rossetto et al. 2011). The maximum wavelength generated to date corresponding to the Mercator recording (2004 tsunami) with wavelength of 23km reproduced at scale 1/50.The original aim of this study was to model accurately the propagation of earthquake-generated tsunami through the surf zone and to the inundation of buildings behind the shoreline. New tsunami runup equations have been produced, following a better understanding of the tsunami evolution onshore (Charvet et al. 2013). A better understanding of the evolution of forces and pressures over time is also arising from the results of a limited number of experiments carried out on structures in the flume using the tsunami generator and a number of small scale tests carried out at UCL (see Figure 1) to better characterise steady flows around rectangular cylinders (Lloyd, 2014 and Qi et al. 2014). In particular, the latter show that for a single configuration and blockage ratio, that once a critical Froude Number is surpassed the flow regime around the square cylinder passes from being sub-critical (where drag forces dominate) to choked (where hydrostatic forces dominate). In recognition of the fact that the

majority of numerical models cannot represent buildings explicitly in their simulations, Qi et al (2014) propose a set of equations for describing the forces on the rectangular cylinder from only knowledge of the flow velocity, depth and Froude number in front of the cylinder and the ratio of the cylinder width to that of the flume. When these steady state equations are applied to the unsteady case of the rectangular buildings tested under tsunami,
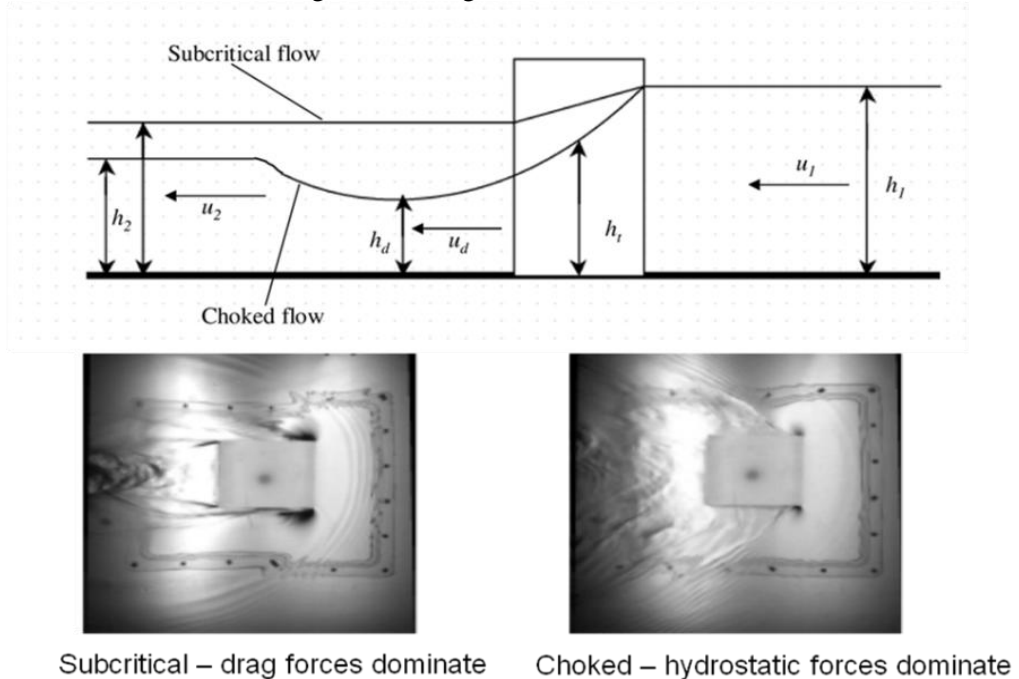

Figure 1. Schematic diagram and photos of the steady flow tests at UCL showing the identified Choked and Subcritical flow regimes (adapted from Lloyd 2014 and Qi et al. 2014).

Figure 2 results; i.e. the measured force time-histories seem to agree well with those predicted by the steady flow equations. These results suggest that a steady flow assumption may be applied to the unsteady case of tsunami onshore flow. However, it is recognised that the UCL-HRW tests for forces on a rectangular body subjected to tsunami onshore flow are few (13 waves repeated 3 times each) and pertain to a single structural configuration.

Conclusions and Next Steps

This paper presents research on tsunami forces that is very much a work in progress. The author was successful in obtaining an ERC Starting Grant called "URBAN WAVES" for the continued experimental and numerical modelling of tsunami flows around buildings but also for the study of tsunami impact on coastal defences. This project sees an improved version of the pneumatic tsunami generator built and placed in a 100m x 1.8m flume located at HR Wallingford.

Using the new facility, three phases of experiments will be carried out during the 5 years of the grant and will be accompanied by extensive numerical analysis.
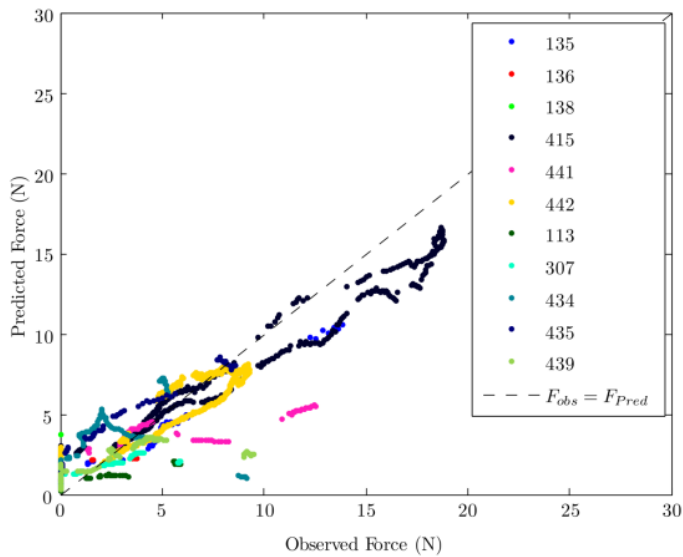
Acknowledgements

Figure 2. UCL-HRW tests of forces on a rectangular body subjected to 13 different tsunami-like waves: Observed forces versus those predicted by the Qi et al. (2014) equations.

References

Charvet, I., Rossetto, T., Eames, I. (2013). New Tsunami Runup Relationships Based on Long Wave Experiments. *Ocean Modelling.*69: 79-92.

Lloyd, T. (2014).*PhD Thesis*.Submitted.

Qi, Z.X., Eames, I., Johnson, E.R. (2014), Forces acting on a square cylinder fixed in a free-surface channel flow. *Journal of Fluid Mechanics*, 756:716-727.

Rossetto, T., Allsop, W., Charvet, I., Robinson, D. I. (2011).Physical modelling of tsunami using a new pneumatic wave generator.*Coastal Engineering* 58(6), 517-527.

THE DEVELOPMENT OF A RAPID EMPIRICAL SEISMIC VULNERABILITY ASSESSMENT METHODOLOGY FOR CONTEMPORARY LOAD-BEARING MASONRY BUILDINGS IN THE MALTESEISLANDS

Torpiano, A.[1], Bonello, M.A.[1], Borg, R.P.[2], Sapiano, P.[1], Ellul, A.E.[1]

[1]*Departmentof Civil and Structural Engineering, Faculty for the Built Environment, University of Malta, Tal-Qroqq, Msida MSD 2080,MALTA*
alex.torpiano@um.edu.mt

[1]*Departmentof Civil and Structural Engineering, Faculty for the Built Environment, University of Malta, Tal-Qroqq, Msida MSD 2080, MALTAmarc.bonello@um.edu.mt*

[2]*Departmentof Construction and Property Management, Faculty for the Built Environment, University of Malta, Tal-Qroqq, Msida MSD 2080, MALTAruben.p.borg@um.edu.mt*

[1]*Departmentof Civil and Structural Engineering, Faculty for the Built Environment, University of Malta, Tal-Qroqq, Msida MSD 2080, MALTApetra.sapiano@um.edu.mt*

[1]*Departmentof Civil and Structural Engineering, Faculty for the Built Environment, University of Malta, Tal-Qroqq, Msida MSD 2080, MALTAann.m.ellul@um.edu.mt*

According to historical records, the last major earthquake reported to have caused extensive damage in the MalteseIslands dates back to 1693. It is not possible to assess the vulnerability of masonry structures to seismic action through post-earthquake damage assessments. Considering a return period of 475 years, the probability of occurrence of a major seismic event is quite high. This study is an attempt at addressing the issue of the seismic response of the building stock in Malta. It focuses on the typical contemporary load-bearing masonry building typology. This typology mainly consists of blocks of apartments including a semi-basement with no internal walls and, in most cases, roofed over by hollow core precast prestressed planks, and with around 4 overlying residential floors in addition to a penthouse level.

The methodology developed draws on other methodologies employed within other countries and on the experiences of regions with a high incidence of earthquakes, where such methodologies have been well-calibrated. In particular, reference is made to a number of first and second level pre- and post-earthquake assessmentmanuals and their corresponding forms, which have been developed in Italy over the past 40 years, not only with respect to the actual parameters listed but also with respect to the background principles affecting the seismic vulnerability of buildings as outlined in the manuals to these forms. These include the 'Analisi della Condizione Limite per l'Emergenza (CLE) dell' insediamento urbano', the

'Agibilita' e Danno nell' Emergenza Sismica (AeDES)' and 'Edifici in muratura in zona sismica. Rilevamento delle carenze strutturali – Manuale per la compilazione della scheda delle carenze'. A number of GNDT manuals also provide an important background to this study. These include the 'Scheda per la valutazione qualitativa dei possibili effetti locali nei siti di ubicazione di edifici strategici e monumentali', and the manuals and corresponding forms of the GNDT first and second level vulnerability assessment methods. Following the verification of the applicability of these assessment methods to the local contemporary load-bearing building typologies present in Malta and Gozoit is clear that the methods employed in other countries cannot be directly transposed to the local building stock due to inherent variations in local construction methods and materials and the presence of particular building characteristics. In addition the soft storey effect, could have a negative effect upon the seismic vulnerability of the building typology being considered and is, therefore, considered in more detail in the proposed method. The need for the development of a new seismic vulnerability assessment method for the seismic vulnerability assessment of individual buildings in the MalteseIslands is, therefore, evident. The newly-developed Form is based on the existing seismic vulnerability assessment forms, but is further adapted to cater for the specific construction methods and materials and building characteristics present in the contemporary load-bearing masonry building typology present in Malta and Gozo.

The method was used in a Pilot study in Msida (Malta) and this allowed for the refinement of the Form prior to its use in the Test Sites, namely Xemxija (Malta) and Nadur (Gozo), where the seismic vulnerability assessment of a total of 183 individual buildings was carried out. The extensive field surveys of the buildings present in the Test Sites and in the Pilot Study, together with the extraction of parameters related to the internal layouts of buildings from the Malta Environment and Planning Authority (MEPA) Development Permit Drawings, allowed for the completion of an exhaustive and detailed database.

The method is based upon ten main areas and therefore the Form is likewise divided into ten sections including: general building identification, general characteristics, vertical and horizontal structural systems (general and seismic vulnerability characteristics), the pre- and post-earthquake condition of the building, ground characteristics, building information and use, accuracy of assessment, post-earthquake assessment outcome, and a final section with the degree of seismic vulnerability.

The last section of the Form summarizes the seismic vulnerability rating resulting from the relevant sections of the new assessment form, in order to establish a final rating following a qualitative assessment of the ratings concluded for these previous sections of the form which is based on the characteristics of the individual building under evaluation. By reference to FEMA 154, the study identifies 4 main parameters of the vertical structural system which are considered to have a greater bearing on the seismic vulnerability rating, thereby allowing for the formulation of a more refined rating for this section of the Form.

The study includes a FEMA 154 assessment and a GNDT Level II seismic vulnerability evaluation for all the 183 buildings assessed in the Test Sites. A refinement of the GNDT Level II ranges corresponding to the Low, Medium-Low, Medium and Medium-High seismic vulnerability ratings was carried out, in order to make it more applicable to the scenario of the MalteseIslands. A comparison of the results obtained using the different methods, was carried out. This was intended to assess the differences between the methods when these are applied to the typology analysed and also to assess the merits of the proposed new method developed for the MalteseIslands.

Acknowledgements

References

AeDES, Scheda di 1° livello di rilevamento danno, pronto intervento e agibilità per edifici ordinari nell' emergenza post-sismica, Dipartimento della Protezione Civile (AeDES 05/2000).

Commissione Tecnica per la Microzonazione Sismica (2013), Analisi della Condizione Limite per l' Emergenza (CLE) dell' insediamento urbano,Version 2.0.

FEMA (2002), Rapid visual screening of buildings for potential seismic hazards: A handbook, FEMA 154. 2nd Edition.

FEMA (2005), Rapid visual screening of buildings for potential seismic hazards: Student Manual, FEMA 154 -SM. 2nd Edition.

GNDT(INGV) / DIS (Politecnico di Milano) (2001),Scheda per la valutazione qualitativa dei possibili effetti locali nei siti di ubicazione di edifce strategici e monumentali.

GNDT/CNR (2003),Regione Toscana: Rilevamento della vulnerabilita' sismica degli edifici in muratura. Manuale per la complilazione della scheda GNDT/CNR di II livello. Versione modificata Regione Toscana.

GNDT/CNR (2007) Regione Abruzzo: Manuale per il rilevamento della vulnerabilita' sismica degli edifici – Istruzione per la compilazione della scheda di I livello.

Regione Molise (2008) 3H- Analisi dei costi di intervento e riduzione della vulnerabilita' sismica degli edifice residenziali. Modello di analisi.

Regione Toscana (2004),Edifici in muratura in zona sismica. Rilevamento delle carenze strutturali – Manuale per la compilazione della scheda delle carenze.

UPDATE ON THE MALTA SEISMIC NETWORK

Agius, M.R., Galea P., D'Amico S.
Seismic Monitoring and Research Unit, Department of Geosciences, Faculty of Science, University of Malta, Msida, Malta.

Introduction

The Central Mediterranean is one of the most seismically active and tectonically dynamic regions in the Mediterranean characterised by a system of extension in the north (Appenines), a slab rollback in the centre (Calabria) and a rift zone in the south (Sicily Channel), all within a general convergent setting between the African and European plates. Unlike the northern regions of the Central Mediterranean (and others such as along the Hellenic subduction zone), earthquake monitoring within the Sicily Channel has, so far, been inadequate. During the last two years the Seismic Monitoring and Research Unit (University of Malta) has been upgrading its earthquake monitoring capabilities, with the addition of new broadband seismic stations and state-of-the-art real-time monitoring. The new setup will not only help to investigate better the regional seismicity within the Sicily Channel, but will also facilitate early warning of potentially felt earthquakes originating hundreds of kilometres away from Malta. This investment is part of the project SIMIT (B1-2.19/11) funded by the Italia-Malta Operational Programme 2007–2013.

Seismic network and instrumentation

A seismic network code for Malta (ML) has been registered with the International Federation of Digital Seismograph Networks (FDSN). The new network will consist of 3 permanent, broadband seismographs: the current station WDD (Agius et al., 2014), which is located in the south of Malta and part of the MEDNET (MN) program (Boschi and Morelli, 1994), and 2 new stations: one located on the island of Gozo and one located in the centre of the island of Malta. The new stations will help to improve the detection and location of local and regional earthquakes in general, and in particular earthquakes occurring close to the Maltese islands. The new seismographs consists of a Trillium 120 PA broadband seismometer and a Centaur-3 digital seismic acquisition system, both manufactured by Nanometrics. Real-time data will be transmitted to SMRU using the SeedLink protocol and redistributed to international data centres. The TCP connections will be managed through the SeisComP software. Another broadband seismometer, a Trillium Compact 120 s, is also available as a portable station. This roving station, which can be powered by solar energy or a car battery, will be used for site effect studies and local geophysical investigations.

Site selection

Various sites have been considered for the permanent selection to house the seismographs. Each site underwent an initial H/V spectral ratio analysis. This

gives an indication of the suitability of the site in terms of the underlying geology. Other considerations were the permanent housing permits and reliable electrical power and internet connections. A number of sites have been selected for a prolonged investigation on the seismic data quality. The data from each temporary deployment was used to study recorded earthquake seismograms and to analyse the seismic ambient noise levels of the site. These were then compared with the data of the current permanent seismic station WDD. One of the preferred sites is at the University of Malta, Msida Campus (MSDA). A vault has been constructed to house the seismic station on top of Lower Globigerina Limestone. Figure 1 shows examples of recorded earthquakes at the site of MSDA, power spectral analysis to assess the noise levels, and a picture of the vault.
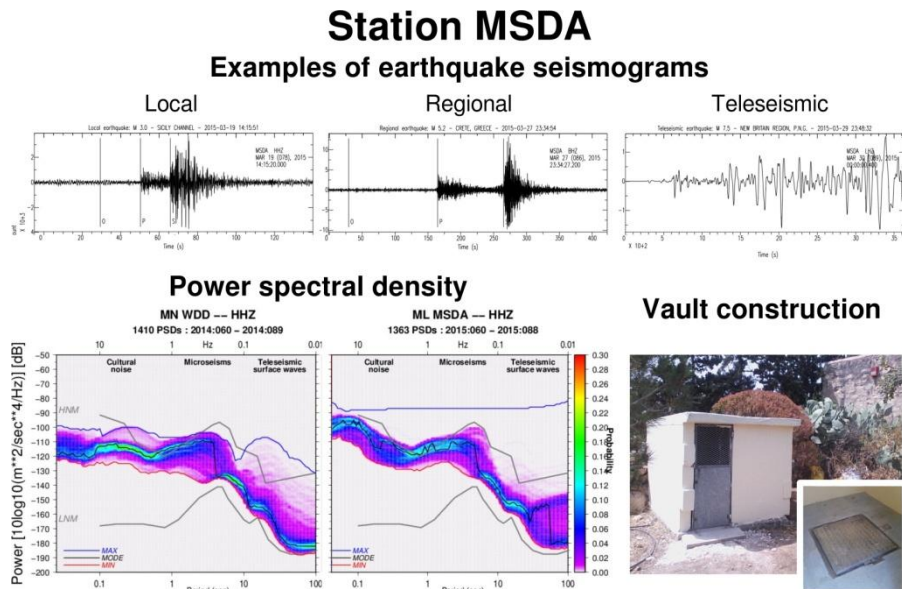

Figure 1. Earthquake seismograms, spectral analysis and vault construction of seismic station MSDA. Top: Examples of earthquakes recorded at MSDA that are typically registered at other nearby stations in the Central Mediterranean: local (≤100 km): Sicily Channel; regional (≤1000 km): Crete, Greece; and, teleseismic (>1000 km): Papua New Guinea. The streams HH (100 sps), BH (20 sps), and LH (1 sps) of the vertical component (Z) are shown, respectively, to better show the dominant frequency content of each earthquake. Bottom left: Noise-level analysis of MSDA and WDD (the current permanent station). Seismic spectral analysis for the month of March based on the calculation of Power Spectral Density (PSD) distribution using a Probability Density Function (PDF) (McNamara and Boaz, 2006). Grey curves: low noise model (LNM) and high noise model (HNM) (Peterson, 1993). Blue and red curves: maximum and minimum PSD for the data, respectively. Black curve: the highest probability mode. Note: MSDA data is from the temporary deployment and not from the final setting inside the vault. Bottom right: The external and internal view of the vault to house station MSDA.

Real-time monitoring

The SMRU is running SeisComP3 software, configured to acquire seismic data in real time from various networks such as MN, IV, TT, GE, G. The station coverage is distributed to reflect seismically active areas that pose a greater hazard to the Maltese islands, such as the eastern coast of Sicily (Fig. 2) and the Hellenic arc. SeisComP is also used as an earthquake alert system. Earthquakes originating in Greece take at least 2 minutes for the primary wave to reach Malta. With the current configuration SeisComP issues an automatic e-mail and SMS alert within, typically, less than 2 minutes. Following manual verification of an earthquake, and, in the case that the earthquake is of interest to the local authorities, a report is generated and sent to the Civil Protection Department via e-mail.

Figure 2. Screen shot of SeisComP3 graphic user interface showing the location of an earthquake (red circle on map) and the corresponding seismograms (right). Each trace is from a station shown as a coloured diamonds on the map, connected with a fine white line to the epicentre.

References

Agius, M.R., D'Amico, S., Galea, P., & Panzera, F. (2014). Performance evaluation of Wied Dalam (WDD) seismic station in Malta. Xjenza, 2(1), 78-86.

Boschi E., Morelli A. (1994). The MEDNET program. Annali di Geosica, 37(5).

McNamara D. E., Boaz R. (2006). Seismic noise analysis system using power spectral density probability density functions: A stand-alone software package. U.S. Geological Survey.

Peterson, J. (1993), Observations and modeling of seismic background noise, U.S. Geological Survey Open File Report, 93-322.

CTBT INTERNATIONAL MONITORING SYSTEM AND ITS CONTRIBUTION TO DISASTER EARLY WARNING AND TO ASSESSMENT OF SEISMIC AND TSUNAMI HAZARDS

Kalinowski M.
CTBTO -Scientific Methods Unit

The Comprehensive Nuclear-Test-Ban Treaty Organization (CTBTO) builds and maintains the International Monitoring System (IMS) primarily for the use of treaty-related verification tasks. In addition, the IMS data and related products of the International Data Centre (IDC) have the potential of saving lives in disaster mitigation and emergency response as well as for scientific studies on the geosphere, atmosphere and the oceans. Many National Data Centres are located at national seismic observatories and integrate the processing of data from IMS stations with their national network. Following the 2004 Sumatra earthquake which resulted in a devastating tsunami, an agreement between the CTBTO and the United Nations Educational, Scientific and Cultural Organization (UNESCO) was signed to provide for the supply of IMS data to recognized Tsunami Warning Centres. As of mid-2015, 14 centres in 13 countries including three in the Mediterranean (France, Greece and Turkey) have initiated such data forwarding arrangements with the CTBTO. This presentation provides an overview of the present situation regarding the use of IMS data for tsunami warning and other applications related to seismic and tsunami hazards.

FROM PREPARATION TO OPERATIONAL MANAGEMENT OF SEISMIC CRISIS: SUPPORTING TOOLS FOR CIVIL-PROTECTION SERVICES

Auclair, S., Monfort, D., Colas, B., Bertil, D., Rey, J., Winter, T., Langer, T.
BRGM (French geological survey), 3 avenue C. Guillemin, Orleans, France.s.auclair@brgm.fr

Introduction

Experience of past earthquakes underlines the need for crisis managers to have at their disposal rapid-response tools able to assess consequences caused by earthquakes, even for moderate events. BRGM and its partners have developed tools to meet these operational needs, in order to automatically and quickly produce maps of seismic ground-motions, as well as sectored assessments of damages. To go further in taking account operational requirements related to the management of seismic crisis, work is being done in order to provide the authorities with a quick assessment of the human tolls that may control their actions, structured within reports dedicated to civil-protection teams. Exploratory tracks are also being considered in order to enrich the information feedback from the field by using techniques of "crowd-sourcing", thanks to the use of distributed "citizen" sensors or of social-networks. So as to guarantee a proper adoption of these innovative tools by crisis-managers as well as for training civil-protection services, BRGM also actively contributes to the organization and animation of "earthquake" civil-protection's exercises, together with French authorities. Whenever an earthquake occurs, authorities in charge of crisis-management need to act rapidly, effectively, and in coordination on the basis of incomplete knowledge of the situation in the field, with the dual objective of reacting to the emergency in the short-term, while also encouraging a return to normality as promptly as possible. In this way, Emergency Operational Centers (EOCs) have to achieve situational awareness through consolidation of an evolving Common Operational Picture (COP): firstly by synthesizing feedback data that are patchy, qualitative, emotionally biased, and often contradictory, then, as time passes, taking into account qualitative assessments obtained through reconnaissance missions in the field. This generally comes down to preliminary general, rough assessments, which are subsequently refined over time. As return-periods of damaging earthquakes are relatively long in most of Mediterranean countries and thus limit experience of relevant civil-protection services, it is therefore necessary to train EOCs' members to these problematics. In addition, ad-hoc "rapid response tools" have to be developed so as to allow them to take the measure of the crisis by estimating trends about the extent of damages / losses / dysfunctions.

To date, two projects carried out in the pilot area of Pyrenees (border area between France and Spain) allowed BRGM and its partners to develop scientific demonstrators for rapid and automatic assessment and diffusion (few minutes after

the first tremors) of damages (project ISARD) and ground-motion amplitudes (project SISPyr).

These tools are based on a continuous analysis of real-time seismic records, using a zonation of geological site-effects as well as a sectored assessment of physical vulnerability of buildings. Tested during seismic crisis exercises, these tools have proven to be valuable to guide EOCs during the acute phase of the first hours of the crisis. The operational deployment of these tools, however, requires the pursuit of developments on the basis of a dialogue between designers from the scientific community and crisis-managers, as well as regular testing of these tools under realistic conditions through crisis-exercises.

Ability to quickly assess strength of shaking intensity

Seismic risk being the combination between seismic hazard and exposed vulnerable assets, the first necessary step to estimate potential damages induced by an earthquake concerns the spatial assessment of the shaking intensity. However, this intensity results from multiple and complex phenomenon which, added to each other, may induce high spatial variability. Among the main determinants phenomenon, particular mention should be done to "source-effects" that can result in preferential direction for wave propagation, as well as to "site-effects" that can locally modify amplitude of ground-motions because of resonance of seismic waves produced by topography or soft-soils. Therefore, empirical ground-motion prediction equations (GMPEs) simulating isotropic attenuation of the amplitude of seismic-waves with epicentral-distance are insufficient in themselves to produce reliable-enough assessments useful for crisis-managers. Thus, it is necessary to cross different types of data in a spatial analysis integrating at the same time:

- Permanent regional data coming from pre-analysis:
- Regional models of attenuation;
- Spatial information-layer characterizing mean seismic amplification due to site-effects.
- Event-related data collected in real-time after occurrence of an earthquake:
- Rapid assessment of the event's magnitude and location;
- Real-time seismic records coming from seismological stations;
- Rapid assessment of macroseismic intensity from testimonies collected thanks to web-questionnaires.

These analyzes are carried out in a fully automatic way using the ground-motion and shaking intensity calculation code ShakeMap (Wald et al., 1999) that has been recently implemented and adapted to the whole Pyrenean massif (Bertil et al., 2012). Resulting maps are automatically posted on the www.sispyr.eu website, with regular updating depending on the availability of new data. This tool has still aroused the interest of the French and Spain civil protection authorities as a potential help for seismic crisis management.

Providing authorities with reliable and sectored trends about human and material losses

Although rapid and spatial assessment of seismic intensity provided by ShakeMaps is useful to draw up a first "crisis landscape" and has still aroused the interest of the French and Spain civil protection authorities, experience shows that problems of interpretation remain for non-seismologists. Furthermore, so as to assist authorities in dimensioning their operational response, it is necessary to go further and to assess trends on potential losses associated with this seismic aggression. Two approaches are possible in order to tackle this issue:

Damages modeling: the ISARD tool

When working on areas for which seismic vulnerability of buildings has been globally characterized, it is then possible to cross intensity-maps (cf. previous chapter) with a spatial information-layer characterizing vulnerability of each "homogeneous building area" thanks to a vulnerability function. This approach allows to precisely modelingphysical damages to buildings and then to deduce rough human tolls in terms of number of fatalities, slightly/severely injured and homeless people (see Sedan et al., 2013).

The "Rapid Response System" (RRS) called "ISARD" (Goula et al., 2008) that covers the eastern part of the Pyrenees is based on such a method for an automatic and rapid calculation and dissemination of loss assessments. Using real-time seismic data recorded in the area, the ISARD RRS thus produces in minutes after the occurrence of an earthquake cross border informative notes that are currently used by civil protection authorities of the Spanish autonomous region of Catalonia for crisis management purposes.

Direct loss assessment

For areas that are not covered by vulnerability studies, USGS has developed a "PAGER" simplified methodology for estimating losses resulting from earthquakes (Wald et al., 2008). Principle of the PAGER approach is to assess the extent of losses thanks to the crossing of an intensity ShakeMap with a map of the residential population considered as a spatial proxy of vulnerable assets in presence. The logic is thus different form the one used for modeling damages, the latter explicitly taking into account physical vulnerability of considered assets.

In practice, PAGER generates estimates of the ranges of potential fatalities and economic losses using empirical relationships calibrated on a database listing observed losses from past earthquakes. In order to complete the Pyrenean ISARD/SISPyr tools, BRGM is carrying out the declination of the PAGER method for the whole territory of mainland France. The French transposition of the PAGER tool aims to provide rapid estimates of the number of fatalities and homeless people, which are the main determinant parameters for sizing the civil-protection operational response. One of the data sources used for this is the population geo-database provided by the French Institute of Statistics with a mesh size of 200 m, which allows high-resolution loss estimates.The next ongoing step of development

of the tool aims at automating the process so as to quickly and autonomously generate bulletins that could be sent to authorities to enlarge their situational awareness, and doing so to optimize their first actions.
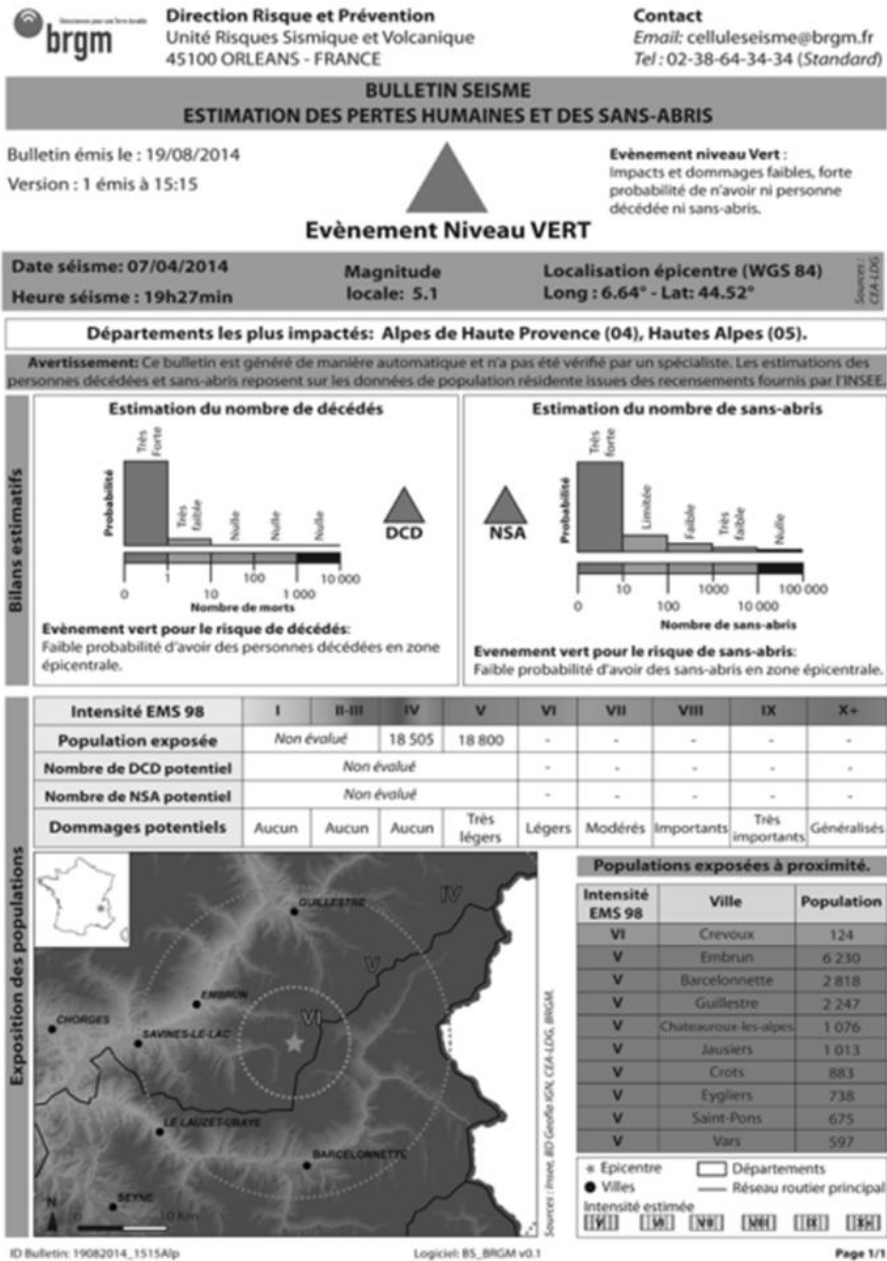

Figure 1.Example of a PAGER-like bulletin adapted for France by BRGM: here the case of the Barcelonnette earthquake of April 7th, 2014.

Toward the inclusion of citizen-based data to enlarge the situational awareness

While most of existing seismic-RRS lies on real-time seismological data only, possibility provided by the USGS ShakeMap software to integrate macroseismic citizen-based data for the analysis is particularly interesting. Nevertheless, these data are collected through an active crowd-sourcing approach thanks to online questionnaires available on institutional websites, and thus often remain insufficient for covering quickly and homogeneously enough the affected area. Two emerging crowd-sourcing strategies seem particularly promising today for tackling this issue. The first one is to encourage the development and to take advantage of citizen seismic networks (e.g. the Community Seismic Network - CSN - csn.caltech.edu, or the Quake-Catcher Network – QCN - Cochran et al., 2009) using microelectronic accelerometricsensors (MEMS). With a very low cost, they are widely embedded in smartphones, gaming consoles and other laptops, and can also be USB-connected to personal computers. Thanks to a continuous improvement of their performances, some MEMS are now considered as reliable enough for seismological purposes (Evans et al., 2014) and can usefully complement traditional measures achieving better calibrate ShakeMaps (e.g. Lawrence et al., 2014).

In addition, social-networks are also a real-time source of very interesting information. Very popular worldwide and disposing of an increasing number of users, Twitter microblogging network has notably demonstrated its ability to broadcast very quickly information after earthquakes. In particular, the flow of earthquakes-related posts is an excellent indicator for automatically detecting earthquakes when they are sufficiently felt by the population, and can lead to early-detections faster than the ones from seismological-services (Sakaki et al., 2010; Earle et al., 2011). As some tweets are "geotagged" (i.e. are associated with GPS coordinates) – and geographic information can be extracted from textual messages - it is then also possible to automatically extract geographical indicators. In France, such analyses have been successfully investigated following the occurrence of the Barcelonnette earthquake in April 2014 (Marcot et al., 2014), allowing a prompt detection and assessment of the area of perception. Alike the USGS' TED (Tweet Earthquake Dispatch) system (Earle et al., 2011), BRGM has just worked-out a "robot" allowing a passive crowd-listening of Twitter earthquake-related posts (French language), with the final objective to better calibrate ShakeMaps and – in turn – rapid loss assessments.

Exercises: essential step for training of crisis-managers and testing of innovative tools

New modes of information gathering, processing and dissemination such as described in previous chapters need to be adopted by the players in order to facilitate deployment in a crisis situation. At the same time, one of the main levers for improving decision-support assistance in a crisis situation is to make sure that

all individuals have the opportunity to train with the systems and tools that they will be expected to operate in the event of the emergency, and to exercise their know-how and thinking abilities (Fredholm, 1999). An analysis of lessons learned from a certain number of emergency situations shows, moreover, that independently of the origin of the crisis or how competent the persons involved may be, and despite the fact that certain procedures already exist to prevent or manage accidents or disasters, it is mainly elements involved in perception (mental representations that are often unshared), cooperation, and communication among players that determine the reactions and the strategic decisions that are made. Thus it is evident that experience gained on a daily basis is often not enough to constitute a means of learning that is continual, effective and sufficient, owing to the rare occurrence of catastrophic events (Borodzicz et al., 2002). In this context, training exercises in crisis management are indispensable. Besides allowing the players involved to hone their skills in team management, communication, and modes of strategic reasoning, these exercises also guarantee proper adoption of tools that are useful in crisis management. Initiated in 2007 as part of a national plan for prevention of seismic risk, the French civil-protection runs yearly departmental seismic crisis exercises with the scientific support of BRGM. Called "RICHTER", these exercises enable the training of crisis-managers from many services (prefectures, firefighters, police, army, municipalities, etc.) as well as a strong awareness of the stakeholders, and in particular of local communities

Figure 2.EOC members during a RICHTER exercise ©BRGM

Definition of objectives is the basis for RICHTER exercises: besides general objectives that truly set boundaries of the exercise, specific objectives of each participant are also very important as they enrich the scenario and enable testing of

multiple crisis-management key-procedures. These targets may cover all or part of the four main phases of a crisis:

1. Assessment of the scale of the crisis and of its impacts;
2. Emergency management;
3. Long-term crisis-management;
4. Post-event management.

Depending on the objectives of each exercise, the challenge is then to build a credible scenario - both scientifically and societally speaking. For each exercise, BRGM therefore proceeds in the realization of a crisis "atlas" resulting in a spatial quantification of losses (both damages to residential buildings and victims), and based upon a fine modelling of a scenario-earthquake and its related consequences owing to the actual vulnerability of buildings. This atlas guarantees the credibility of the scenario and enables participants to become aware of the reality of seismic-risk and of tangible consequences that can result.Last but not least, experience feedback from these exercises is a very important issue. Under the program RICHTER, this feedback goes beyond identification of items with good or bad and should define the scope for future exercises. Dominos effects that can be seen after major earthquakes demonstrate in particular that it is impossible to test everything under one single crisis-exercise. It is therefore necessary to evaluate previous exercises with a great attention so as to test a different panel of events in each exercise. The experience feedback also impulses significant inflections on the planning of the crisis-management.

Acknowledgements

References

Bertil D., Roviro J., Jara J.A., Susagna T., Nus E., Goula X., Colas B., Dumont G., Cabanas L., Anton R., Calvet M. (2012). ShakeMap implementation for Pyrenees in France-Spain border: regional adaptation and earthquake rapid response process. Proc. of the 15[th]World Conference on Earthquake Engineering, paper n° 2078.

Borodzicz E.P. and Van Haperen K. (2002). Individual and group learning in crisis simulations, Journal of contingencies and crisis management 10(3): 139-147.

Cochran, E.S., Lawrence, J.F., Christensen, C., Jakka, R. (2009). The Quake-Catcher Network: Citizen science expanding seismic horizons, *Seismological Research Letters*, 80, 26-30.

Earle, P. S. and Bowden, D. C., and Guy M. (2011) Twitter earthquake detection: earthquakemonitoring in a social world. Annals of Geophysics, 54 (6), 708-715.

Evans, J.R., Allen, R.M., Chung, A.I., Cochran, E.S., Guy, R., Hellweg, M., Lawrence, J.F. (2014).Performance of Several Low-Cost Accelerometers.*Seismological Research Letters*, 85, 147-158.

Fredholm L. (1999). Emergency management as coordinated cognitive modeling on different time-scale, Lundstekniskahögskola.

Goula, X., Dominique, P., Colas, B., Jara, J.A., Roca, A. and Winter, T. (2008). Seismic rapid response system in the Eastern Pyrenees.XIV World Conference on Earthquake Engineering, October 12-17, Beijing, China.

Lawrence, J.F., Cochran, E.S., Chung, A., Kaiser, A., Christensen, C.M., Allen, R., Baker, J.W., Fry, B., Heaton, T., Kilb, D., Kohler, M.D., Taufer, M. (2014).Rapid Earthquake Characterization Using MEMS Accelerometers and Volunteer Hosts Following the M 7.2 Darfield, New Zealand, Earthquake.*Bulletin of the Seismological Society of America*, Vol. 104, No. 1, pp. 184–192.

Marçot N., Verrhiest-Leblanc G., Auclair S., Fontaine M., De Michele M., Raucoules D., Fissier L., Genois J-L. (2014). Séisme de l'Ubaye du 7 avril 2014 - Rapport de retour d'expérience. Rapport BRGM/RP-63789-FR.

Sakaki, T., Okazaki, M. and Matsuo, Y. (2010) Earthquake shakes Twitter users: real-time event detectionby social sensors, *Proceedings of WWW*.

Sedan O., Negulescu C., Terrier M., Roullé A., Winter T. and Bertil D. (2013).Armagedom – A Tool for Seismic Risk Assessment Illustrated with Applications. Journal of Earthquake Engineering 17(2):253-281.

Wald, D. J., P. S. Earle, T. I. Allen, K. Jaiswal, K. Porter, and M. Hearne (2008).Development of the U.S. Geological Survey's PAGER system (Prompt Assessment of Global Earthquakes for Response).Proc. 14th World Conf. Earthq.Eng., Beijing, China, 8 pp.

Wald, D.J., Quitoriano, V., Heaton, T.H., Kanamori, H., Scrivner, C.W., and Worden, B.C., 1999, TriNet "ShakeMaps": Rapid generation of peak ground-motion and intensity maps for earthquakes in southern California: *Earthquake Spectra*, v. 15, no. 3, p. 537-556.Gutenberg, B. (1959). Physics of the Earth's Interior, Academic Press, New York, 111-113.

A FRAMEWORK FOR EMERGENCYMANAGEMENT INFRASTRUCTURE SUPPORTED BY GEOGRAPHIC INFORMATION SYSTEMS. THE CASE OF MALTA.

Canas, C.,[1], Attard, M.,[2]

[1]*Institute for Climate Change and Sustainable Development. University of Malta, carlos.canas@um.edu.mt*
[2]*Institute for Climate Change and Sustainable Development. University of Malta, maria.attard@um.edu.mt*

Introduction

When a disaster strikes the key factors that save lives, resources and critical infrastructure are identified through these questions: where and how has the damage occurred; what and who has been affected; how to reach them; and what do they need and who can provide it? All the information about places, people and resourcestied to a location are known as geospatial information (Folger, 2009).

Easy access to current and reliable geospatial information is crucial to managing disasters in any emergency situation. However, when a disaster strikes the participants involved usually need to face inaccurate, out of date and defragmented data from different sources and formats. They also have to face lack of data that seriously impede them in making appropriate decisions under time pressure (Gibbs, et al., 2005). The ability to make effective timely decisions to combat emergencies and disasters is clearly linked with the availability, integration and interoperability of high quality geospatial data at all levels of governance and this can be achieved through Geographic Information System (GIS) solutions (Cutter, 2003).

Developing a GIS Infrastructure provides the capability of compiling, managing, updating, sharing and showing geospatial databases through common interactive platforms amongst all the participants involved in the emergency management process (Emrich, at el., 2009). Dynamic and interactive maps give an entirely new perspective to data analysis and visualization that cannot be seen in a table or list format. GIS facilitates not only the integration of quality spatial data but also creates an environment of informed decision making (Tanasescu, et al.2006).

This paper aims to establish the framework for Emergency Management (EM) supported by a GIS infrastructure. In addition, the paper explains how GIS can be a reliable and useful tool for emergency planning and management necessities for the actions taken before, during and after disaster events. Finally, attention is focussed on the challenges and possible solutions about data quality and interoperability for the particular case of the Malta.

Method

An important step in examining the role of GIS in Emergency Management is selecting a conceptual framework to help organise existing research and development activities. One such framework that appears widely in the emergency management literature is the "comprehensive emergency management" (CEM) (Drabek and Hoetmer, 1991). This relies on the temporal dimension of disasters to organise the emergency management process into a cycle of four, often overlapping, phases: mitigation, preparedness, response and recovery.

In the first case, mitigation activities eliminate or reduce the probability of disaster occurrence, or reduce the effects of unavoidable disasters. Secondly, the goal of preparedness programs is to achieve a satisfactory level of readiness to respond to any emergency situation. Thirdly, the aim of response is to provide immediate assistance to maintain life, improve health and support the affected population. And finally, the recovery phase strives to return life to normal or improved circumstances (Cova,1999).

Once the emergency methodology has been established and the specialised human resources have been trained, it is mandatory to provide the system with the data, tools and interoperability infrastructure to achieve the best decision making for each stage. Given this need, GIS represents a significant tool to decision makers at all levels, not only because GIS supports the effective creation and management of geospatial data, but also because analytical and modelling tools support the generation of new information. This permits the integration of data from multiple sources, leading to collaborative knowledge generation on EM by all the involved participants.

For this reason, some governments are currently providing authoritative guidance (e.g. MacFarlane, 2005)on the application of GIS to managers and end-users operating in the multi-agency civil protection environment in order to:

(a) Maximise the potential benefits of GIS to the process of planning for and managing emergencies and disasters, thereby enhancing environment national resilience to such events;

(b) Establish a wide base of understanding of common applications, methods and terminology as the first step towards improving interoperability between different participants and civil protection;

(c) Assist users in making sound decisions within the process of scoping, specifying, acquiring, updating and maintaining GIS data;

(d) Stimulate wider understanding and debate within the user community to guide research and development of applications and interoperability solutions.

A CEM framework implemented through GIS is shown in Figure 1.The effectiveness of the GIS infrastructure is based on the integration of geospatial data. Any information with a spatial key (address, coordinates, parcel/area, etc.) could be integrated within GIS, irrespective of the origin. (Meaden and Aguilar-Manjarrez, 2003).In order to implement the GIS infrastructure within the CEM it is necessary to supply emergency services personnel with GIS hardware, software

and specific training. There is a wide variety of GIS hardware and software, both proprietary and open source, as well as a vast range of tutorials and bibliography for GIS training. This paper focuses on the potential of GIS infrastructures to assist
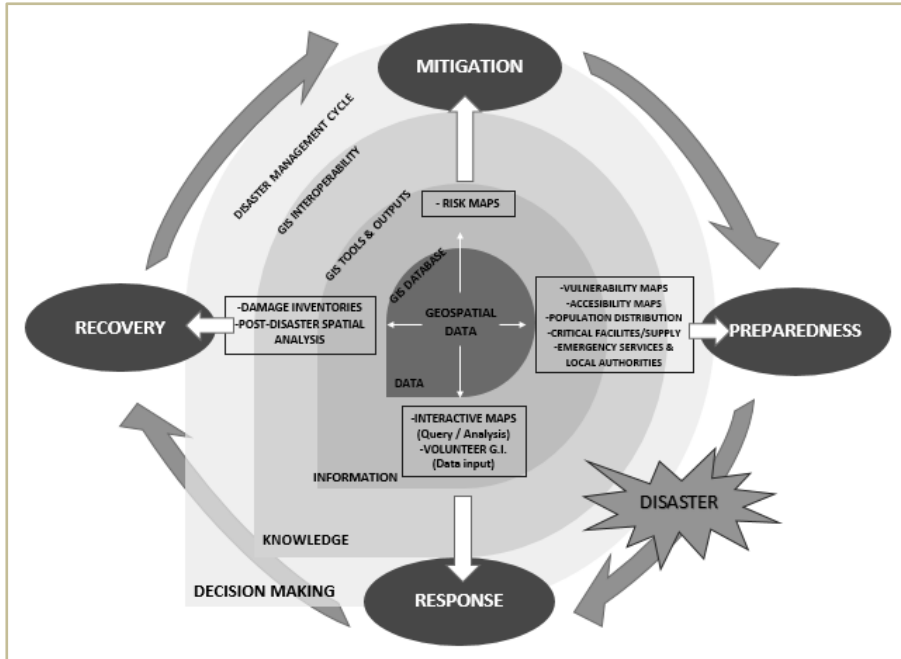
CEM.
Figure 1. Comprehensive emergency management supported by GIS infrastructure (adapted from Godschalk, 1991).

Quality spatial data is the foundation of any GIS infrastructure and poor quality data is detrimental to the whole CEM cycle. Established components of data quality (accuracy, precision, consistency and completeness) have to be implemented in order to describe phenomena with spatial, temporal and attribute components (Berry, 1964; Sinton, 1978). Anotherquality criteria is availability. However there is no single, universally applicable quality standard for geospatial data. Instead, the concept of "fitness for use" is widely adopted. Any database for CEM must find a balance between relevant, accurate and timely data for each specific context.

For the specific purpose of GIS infrastructure supporting CEM, it is necessary to define the type of data collected. This depends on the objectives of the emergency and management plan. Risk maps, accessibility maps and post-disaster inventory maps could be part of the same emergency management cycle and wouldrequire some common data. However their use is generally dictated by specific data (ESRI, 2008).Although different emergency scenarios need specific data to support decision making, there are key data groups relevant to emergency planning. This entails the managementof data attributes about potential hazards, the

community, the built environment, the natural environment, infrastructures and human-related resources (Cutter, et al., 1997).

Once the database is completed and the spatial, temporal and thematic data has been reviewed, one of the key strengths of GIS is the ability to transform data into information. Through different GIS tools and procedures "raw data" is processed, summarised, analysed spatially and selectedfor the purposesof interpretation. For the mitigation stage risk maps are very useful. All the risk factors associated with one specific hazard (i.e. floods, landslide, fires, etc.) highlight zones which are more likely to be affected. These risk maps are very useful for decision support when locations for new facilitiesand infrastructures need to be identified (Evans, et al., 2007).

A wide variety of GIS tools are used for preparedness depending on the necessities of the emergency activities. Vulnerability maps highlight the specific facilities, infrastructure and population that might be more vulnerable in case of an emergency, such as unstable constructions and so on (van Westen, et al., 2002).Accessibility maps show the attributes and connectivity of the transport network, they give high value information in case of time pressure actions such as fastest routes and closest facilities (Huang and Pan, 2007). Whilst population distribution maps show where the population is potentially located when a disaster occurs (i.e. schools, worship centres, commercial areas). This information helps to prioritise emergency response. Maps showing critical facilities and supplies locate places and infrastructures that could potentially worsen the emergency situation or develop new emergency scenarios (e.g. firework factories, fuel storage tanks) and also locate the facilities that in case of incapacity or destruction could impact on security, the economy, public health or safety (e.g. water, electricity, fuel and telecommunications supply) (Anjum, et al., 2011).

In the case of response, interactive maps not only enable participants to visualise and share all the geospatial information created during the preparedness stage, but also to create added value thanks to the GIS capabilities in spatial analysis. One very powerful and relatively innovativemovement has been the creation and provision of Volunteered Geographic Information (VGI), where citizens act like "human sensors" and send information related to the emergency situation they are experiencing at that moment (Mioc, et al. 2008). With regard to recovery, damage inventory maps and post-disaster spatial analysis help to determine the severity of the damage and quantify the people and facilities affected. They are effective tools to calculate the cost of the recovery and to prioritise the necessary actions. All these GIS tools transform the dataset into information and then knowledge to support decision making in every emergency management stage.

A GIS Infrastructure for CEM for Malta.

The development of a GIS Infrastructure to support CEM in Malta was partially funded by the project SIMIT (Integrated System for Transboundary Italo-Maltese

Table 1. SIMIT GIS database (compiled by authors)

DATA	SOURCE	AVAILABILITY	SPATIAL ACCURACY	TEMPORAL ACCURACY	ATTRIBUTE ACCURACY	COMPLETENESS	COVERAGE
Geology	Faculty of Science, Physics Department, University	Open data	Medium (georeferenced polygon	High (2014)	Medium high	100%	100%
Hydrology	Faculty of Science, Physics Department, University	Open data	Medium (georeferenced polyline	High (2014)	Medium high	100%	100%
Digital Elevation Model	Faculty of Science, Physics Department, University	Open data	Medium (raster data, 10m resoluti	High (2014)	High	100%	100%
HVSR	Faculty of Science, Physics Department, University	Open data	High (coordinates)	High (2014)	High	100%	100%
Police	Malta Police Force	Open data	Medium high (address)	High (2014)	High	90%	100%
Civil Protection	Civil Protection Department Malta	Open data	Medium (incomplete address)	High (2014)	Medium (missing attributes: contact details, human/mate	90%	100%
Emergency Fire & Rescue Unit	Emergency Fire & Rescue Unit Malta	Open data	Medium (incomplete address)	High (2014)	Medium (missing attributes: contact details, human/mate	90%	100%
Volunteer Associations	Red Cross Malta	Open data	Medium high (address)	High (2014)	High	100%	100%
Local Councils	Government of Malta	Open data	Medium (incomplete address)	High (2014)	High	100%	100%
Hospitals & Health centres	Government of Malta, Ministry for Energy and Health	Open data	Medium high (address)	High (2014)	Medium high (missing attributes: capacity, some contact	100%	100%
Schools	Government of Malta, Ministry for Education and Empl	Open data	Medium (incomplete address)	High (2014)	Medium low (missing attributes: capacity, some contact c	80%	100%
Sport Centres	Institute for Climate Change and Sustainable Develo	Open data	High (coordinates)	High (2014)	Medium low (missing attributes: capacity, contact details	90%	100%
Places of worship	Institute for Climate Change and Sustainable Develo	Open data	High (coordinates)	High (2014)	Medium low (missing attributes: capacity, contact details	90%	100%
Industrial States	Government of Malta, Ministry for the Economy, Invest	Open data	Medium high (approximate coord	High (2014)	Medium low (missing attributes: capacity, contact details	90%	100%
Firework factories	Institute for Climate Change and Sustainable Develo	Open data	High (coordinates)	High (2014)	Medium low (missing attributes: contact details)	90%	100%
Power stations	Government of Malta, Ministry for the Economy, Invest	Open data	High (coordinates)	High (2014)	Medium low (missing attributes: contact details)	100%	100%
Commercial areas	Planning Authority Malta	Open data	Medium (georeferenced parcels	Low (1997)	Low (missing attributes: capacity, contact details)	100%	100%
Tourist attractions	Government of Malta, Ministry for Tourism	Open data	High (coordinates)	High (2014)	Low (missing attributes: capacity, contact details)	70%	100%
Land Use	CORINE Land Cover	Open data	Medium low (raster data, 100m, re	Medium (2006)	Medium	100%	100%
Protected areas	European Environmental Agency, Malta Environmen	Open data	High (Georeferenced Parcels)	High (2014)	High	100%	100%
Population distribution	National Statistic Office, Malta	Open data	Medium low (data by local counc	edium high (20	Low (missing attributes: demographic data)	100%	100%
Transport network	Institute for Climate Change and Sustainable Develo	Open data	High (georeferenced polylines)	edium high (20	Medium (missing attributes: connectivity, drive time)	90%	100%
Transport nodes	Institute for Climate Change and Sustainable Develo	Open data	High (coordinates)	High (2014)	Medium high (missing attributes: capacity, contact detail	100%	100%
Dwellings Vulnerability	Faculty of Built Environment, University of Malta	Open data	High (data by building)	High (2014)	High	<5%	<5%
Electricity distribution centres	EneMalta plc	Confidential data.	-	-	-	-	-
Electricity supply network	EneMalta plc	Confidential data.	-	-	-	-	-
Reservoirs	Water Services Corporation, Malta	Confidential data.	-	-	-	-	-
Water tratment plants	Water Services Corporation, Malta	Confidential data.	-	-	-	-	-
Desalinization plants	Water Services Corporation, Malta	Confidential data.	-	-	-	-	-
Water supply network	Water Services Corporation, Malta	Confidential data.	-	-	-	-	-
Fuel storage	EneMalta plc	Confidential data.	-	-	-	-	-
Petrol service stations	Malta Resouces Authority	Confidential data.	-	-	-	-	-
Fuel supply network	EneMalta plc	Confidential data.	-	-	-	-	-
Repeater stations	Melita	Confidential data.	-	-	-	-	-
Telecommunication supply ne	Melita	Confidential data.	-	-	-	-	-

Civil Protection). This project aimed at developing an integrated civil protection network between Sicilian and Maltese authorities involved in the risk forecast, prevention and mitigation processes, and moreover in the planning and management of emergencies. The partners involved in the project are the University of Malta, the University of Catania, the University of Palermo, the Civil Protection Department of Malta and the Civil Protection Department of Sicily.

For the first time in Malta, the Institute for Climate Change and Sustainable Development (ICCSD) is creating, collecting, improving the spatial, temporal and attribute components, standardising and integrating geospatial information into a GIS infrastructure to support Emergency Management in case following potential seismic activity in Malta. In this case the common thematic data proposed include:

- Natural environment: terrain, geology and hydrology;
- Emergency operational centres: civil protection, police, heath centresand local councils;
- Critical facilities: hospitals, schools, factories, industrial areas;
- Transport: transport networks and nodes.
- Utilities supply: electricity, water, fuel and telecommunication utilities;
- Population distribution: residential, commercial, touristic and recreation areas.

Although new spatial data can be generated using GIS technologies, it is costly and time consuming. For this reason, the first step in the project looked at the compilation of existing data, the sources of such data and its availability. Upon compilation a quality assurance procedure identifies the spatial, temporal and attribute components relevant for the specific emergency management aims and circumstances. Table 1 shows the SIMIT database including source, availability, completeness and coverage.In order to complete the GIS database a number of online sources were reviewed, as well as individual meetings were held to obtain a reasonable level of quality and information. Professional networks in this case played a very important role

In the case where data was freely available, the issue of data quality was identified as a major weakness. Data quality depends on the purpose of the data itself, with most of the institutions producing data for other purposes and not emergency management. For this reason, most of the data compiled did not have display the required balance between spatial, temporal and attribute information quality. For example, the location of geospatial data was mainly provided through the address, although in some cases the address was incomplete. Whilst this information could be accurate enough for the purposes of the individual institutions, for the specific case of a GIS Infrastructure to support CEM, the specific coordinates must be identified. In the cases where the coordinates were not provided, the Institute had to create newpoint locations based on address information. Once all the data was georeferenced using the same spatial framework, it was possible to spatially interconnect the data within the project.

The temporal component was another area of concern. As mostgeographic data is very dynamic, its update in necessary to provide reliability within the GIS infrastructure. Some of the data identified for the SIMIT project was dated which of course could lead to errors that could potentially affect effective management in the case of disaster.

Similar to the spatial and temporal components of data, attribute information related to geographic features play an important role in CEM. Relevant information about the number and type of people using a facility is critical when assessing risk and managing disaster. Other key attributes include up to date information for communication and response. In most cases this information was not forthcoming, thus jeopardising the effective management of disaster during deployment, routing and response.

Finally the completeness and coverage of spatial data are essential. In the case of the SIMIT project both completeness and coverage are high, with the exception of building vulnerability, which is still undergoing as part of the project. Case studies on a small number of buildings in Xemxija, Malta and Nadur, Gozo, are currently being undertaken by the Faculty of the Built Environment at the University of Malta.

When the GIS database is completed,different GIS tools and outputs can be developed totransform data into knowledge.In the case of the SIMIT project, risk and vulnerability maps related to seismic activity will be identified, but notin a national scale due primarily to limitations in the availability and quality of data.

Conclusion

In the case of emergency, GIS has the potential to create a 'shared operational picture' that is crucial for making informed decisions under time pressure. The technological revolution of mobile devices and the worldwide network connectivity through internet have extended the use of GIS to different locationsall around the world, demonstrating very positive impacts in the emergency management. Some well-known examples are the Indian Ocean Tsunami (2004), the earthquake in Haiti (2010), the forest fires in USA (2012), the draught in East Africa (2012) or the very recent earthquake in Nepal (2015) with initiatives like Mapping for Change or MapAction (http://www.mapaction.org/map-catalogue/mapdetail/2426.html) Malta and the central Mediterranean are not immune to natural and anthropogenic disasters. For this reason the implementation of a national GIS infrastructure to support CEM is a very importantpriority. The first step, undertaken within the SIMIT project, looked at the identification of a framework for GIS in CEM, the compilation of stakeholder data for CEM and a review of spatial data quality for emergency management and response. This study has found that substantial amounts of spatial data are not available and the quality of the data is not conducive to support CEM. Some of the tools within GIS have been used to visualise seismic activity and risk, however the data is not good enough to support emergency management in preparedness, response and recovery activities at a high level of exigency. Beyond

the data issues, it is also necessary that all the stakeholders involved in emergency management are familiar with GIS and ensure interoperability between systems.In view of the results of this project a strong investment in human, material and technical resources is being recommended to support effective emergency management.

References

Anjum, M., Rana, M., Ivanova, J. and Abdalla, R. (2011) GIS based emergency management scenario for urban petroleum storage tanks. International Workshop on Multi-Platform/Multi- Sensor Remote Sensing and Mapping, M2RSM2011, January, pp.1–5, IEEE, Xiamen.

Berry, B.(1964) Approaches to regional analysis: a synthesis. Annals of the Association of American GeographersVol. 54(2): 11

Cova, T.J. (1999) GIS in emergency management. In: Geographical Information Systems: Principles, Techniques, Applications, and Management P.A. Longley, M.F. Goodchild, D.J. Maguire, D.W. Rhind (eds.), John Wiley & Sons, New York, pp. 845-858.

Cutter, S. (2003) GI Science, Disasters, and Emergency Management. Transactions in GIS Vol. 7(4): 439-445. Available at http://webra.cas.sc.edu/hvri/pubs/2003_GIScienceDisastersAndEM.pdf.

Cutter, S.L., Mitchell, J.T., Scott, M.S. (1997)Handbook for conducting a GIS-based hazards assessment at the county level. South Carolina Emergency Preparedness Division. Office of the Adjutant General. Available at http://webra.cas.sc.edu/hvri/docs/handbook.pdf. Accessed 25 May 2015.

Drabek, T.E., Hoetmer, G.J. (eds.) (1991)Emergency Management: Principles and Practice for Local Government. Washington, D.C.: International City Management Association.

Emrich, C.T., Cutter, S., Weschler, P.J. (2009) GIS and Emergency Management. The Sage Handbook of GIS and Society. Available at https://www.google.com/url?sa=t&rct=j&q=&esrc=s&source=web&cd=1&ved=0C B4QFjAA&url=https%3A%2F%2Fopenisdm.iis.sinica.edu.tw%2Findex.php%3Fop tion%3Dcom_docman%26task%3Ddoc_download%26gid%3D65%26Itemid%3D1 06&ei=Kd9iVa-EGMSSsAGLpoHoCQ&usg=AFQjCNHwHxNvlgZriCYxn4xYPuRy-WuiBQ&sig2=4PrAk0qFE2DiMEhutuL4qA&bvm=bv.93990622,d.bGg. Accessed 25 May 2015.

ESRI (2008) Geographic Information Systems: Providing the Platform for Comprehensive Emergency Management. An ESRI White Paper. October. Available at https://www.esri.com/library/whitepapers/pdfs/gis-platform-emergency-management.pdf. Accessed 25 May 2015.

Evans, S.Y., Gunn, N., Williams, D. (2007) Use of GIS in Flood Risk Mapping. National Hydrology Seminar GIS (Geographic Information Systems) in Hydrology Applications – Modelling – Data Issues (Tullamore, Ireland), pp. 1-12.

Folger, P. (2009) Geospatial Information and Geographic Information Systems (GIS): Current Issues and Future Challenges. Congressional Research Service 7-5700. Available at https://ggim.un.org/3rd%20Prep%20Meeting/Geospatial%20Information%20and%2 0GIS-Report-for-Congress.pdf. Accessed 25 May 2015.

Gibbs, M.R., Shanks, G., Lederman, R. (2005) Data Quality, Database Fragmentation and Information Privacy. Surveillance and Society Vol. 3(1): 45-58. Available at http://www.surveillance-and-society.org/Articles3(1)/data.pdf. Accessed 25 May 2015.

Godschalk, D.R. (1991). Disaster Mitigation and Hazard Management. In Emergency Management: Principles and Practice for Local Government, T.E. Drabek, G.J. Hoetmer (eds.),International City Management Association, Washington, DC, pp. 131-60.

Huang, B., Pan, X. (2007) GIS coupled with traffic simulation and optimization for incident response. Computers, Environment and Urban Systems. Vol. 31: 116-132.

MacFarlane, R. (2005)A Guide to GIS Applications in Integrated Emergency Management, Emergency Planning College, Cabinet Office. Available at https://www.gov.uk/government/uploads/system/uploads/attachment_data/file/6120 3/gis_guide_acro6.pdf. Accessed 25 May 2015.

Meaden, G.J. Aguilar-Manjarrez, J. (eds.) (2013) Advances in geographic information systems and remote sensing for fisheries and aquaculture. FAO. Available at http://www.fao.org/docrep/017/i3102e/i3102e00.htm. Accessed 25 May 2015.

Mioc, D., Nickerson,B., MacGillivray,E., Morton, A., Anton,F., Fraser,D., Tang,P., Liang, G. (2008) Early warning and mapping for flood disasters.The International Archives of the Photogrammetry, Remote Sensing and Spatial Information Sciences. Vol. XXXVII. Part B4. Beijing 2008. Available at http://www.isprs.org/proceedings/XXXVII/congress/4_pdf/263.pdf. Accessed 25 May 2015.

Sinton, D.F.(1978) The inherent structure of information as a constraint in analysis. In G. Dutton (ed.) Harvard papers on geographic information systems. Addison-Wesley, Reading (USA).

Tanasescu, V., Gugliotta, A., Dominguel, J., Gutiérrez Villarías, L., Davies, R., Rowlatt, M., Richardson, M. (2006) A Semantic Web GIS based Emergency Management System. Available at http://projects.kmi.open.ac.uk/dip/resources/ESWC06-SemGov/ESWC06-SemGov.pdf. Accessed 25 May 2015.

van Westen, C.J., Montoya, A.L., Boerboom, L.G.J. and Badilla Coto, E. (2002) Multi - hazard risk assessment using GIS in urban areas : a case study for the city of Turrialba, Costa Rica. In: Proceedings of the regional workshop on best practices in disaster mitigation : lessons learned from the Asian urban disaster mitigation program and other initiatives 24-26 September 2002, Bali, Indonesia. pp. 120-136.

LANDSLIDE SPATIAL RISK ASSESSMENT ALONG THE HIGHWAY IN CALABRIA (SOUTHERN ITALY)

Conforti, M.[1], Rago, V.[2], Muto, F.[2], Versace, P.[3]

[1]*CNR – Istituto per Sistemi Agricoli e Forestali del Mediterraneo (ISAFOM), Rende, Italy, massimo.conforti@isafom.cnr.it*

[2] *Dipartimento di Biologia, Ecologia e Scienze della Terra (DiBEST), Universita` della Calabria, Arcavacata di Rende, Italy, valeria.rago@unical.it, francesco.muto@unical.it*

[3] *Dipartimento di Ingegneria Informatica, Modellistica, Elettronica e Sistemistica (DIMES), Università della Calabria, Arcavacata di Rende, Italy, linoversace@unical.it*

Introduction

Landslides represent a serious hazard in many areas of the Mediterranean belt, because of its social and economic impacts; landslides are responsible both for direct and indirect damages, may cause loss of life and property, damages of natural resources and hamper infrastructure projects such as roads, bridges and communication lines. In particular, in Calabria region (south Italy) many areas are affected by mass movements (Conforti et al., 2012; 2014a, 2014b); their presence and distribution is influenced mainly by geological, morphological, and climatic conditions of the region and very often by unsustainable land management. Therefore, landslide risk evaluation in these areas is important to get mitigation measures and for planning of the territory.

In landslide risk assessment, risk is often viewed as product between hazard, vulnerability and elements at risk. Due to the high conceptual complexity, there are many points of view, with some overlapping between hazard and risk or with understanding of exposure either as element of hazard or as part of vulnerability (Margarint et al., 2013). In this context, the study proposes an assessment of land¬slide spatial risk performed on the basis of landslide susceptibility and exposed elements maps, with¬out considering the temporal variability of landslides or the economic or functional dimension of vulnerability.

This methodology was applied along a section of highway (about 28 km) "A3, Salerno-Reggio Calabria", between Cosenza Sud and Altilia (northern Calabria). The study is included in a wider research project, named: PON01-01503, Landslides Early Warning - "Integrated Systems for Hydrogeological Risk Monitoring, Early Warning and Mitigation Along the Main Lifelines" - aimed at the hydrogeological risk mitigation and at the early warning along the highways.

Study area

The study area is characterized by very rough morphology and landslide-prone outcrops (Figure 1). From a geological point of view, the study area is characterized by a sequence of nearly flat-lying nappes including Paleozoic

methamorphic and plutonic rocks, and Mesozoic to Paleogene ophiolitic, metasedimentary and sedimentary rocks. These rocks are unconformably covered by Miocene to Quaternary deposits. The main thrust fault crops out in the upper portion of the study area, where gneiss tectonically overlies the schist and the phyllite. Neogene normal and strike-slip faults abruptly increased tectonic uplift, and changed the orientations of drainage channels.

Geology and tectonics have strongly controlled the geomorphology, which is dominated by a landscape characterized by steep slopes, more than 30° in average, and a high local relief due to the rapid uplift of the Coastal Range deeply dissected by V-shaped valleys, which are locally fault controlled. Most morphotectonic features indicate recent tectonic activity. Also, tectonic control on geomorphology of the drainage basin is recognizable in the almost rectangular drainage pattern, in the presence of fault scarps and, principally, in the reversal of the drainage direction. Where phyllitic schists predominate, the ridges show a sharp crests and the slopes are affected by widespread slope instability (Le Pera and Sorriso-Valvo, 2000). Therefore, in the study area the dominant slope processes are related to landslides and running-water processes that essentially control the present-day morphological evolution of the reliefs and are responsible for serious damage to property and infrastructure.

The climate is sub-humid, with average annual precipitation of 1100 mm, distributed over 105 rainy days, and average temperature of 16 °C. Rainfall peaks occur in the period October–March, during which mass wasting and severe water erosion processes are triggered (Formetta et al., 2014).
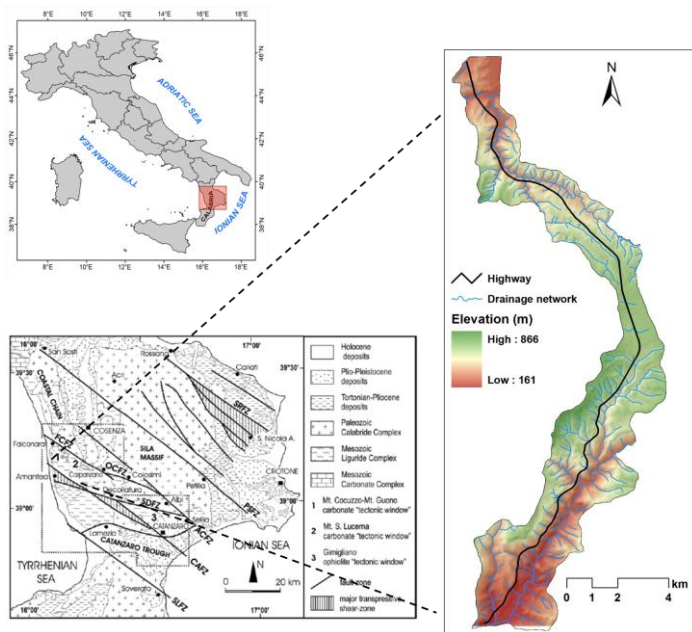
Figure 1. Location of the study area.

Methodology

The risk evaluation started with geological and geomorphological analysis, based on air-photo interpretation and systematic field survey, followed by processing and management of collected data through a Geographic Information System (GIS). Consequently geological, geomorphological and landslide inventory maps were prepared.

The landslide susceptibility was performed on the basis of 'Conditional Analysis' statistical method applied to a subdivision of the territory into Unique Condition Units (Carrara et al., 1995). Therefore landslide susceptibility is expressed as landslide density in correspondence with different combinations of predisposing factor classes (Clerici et al., 2006).
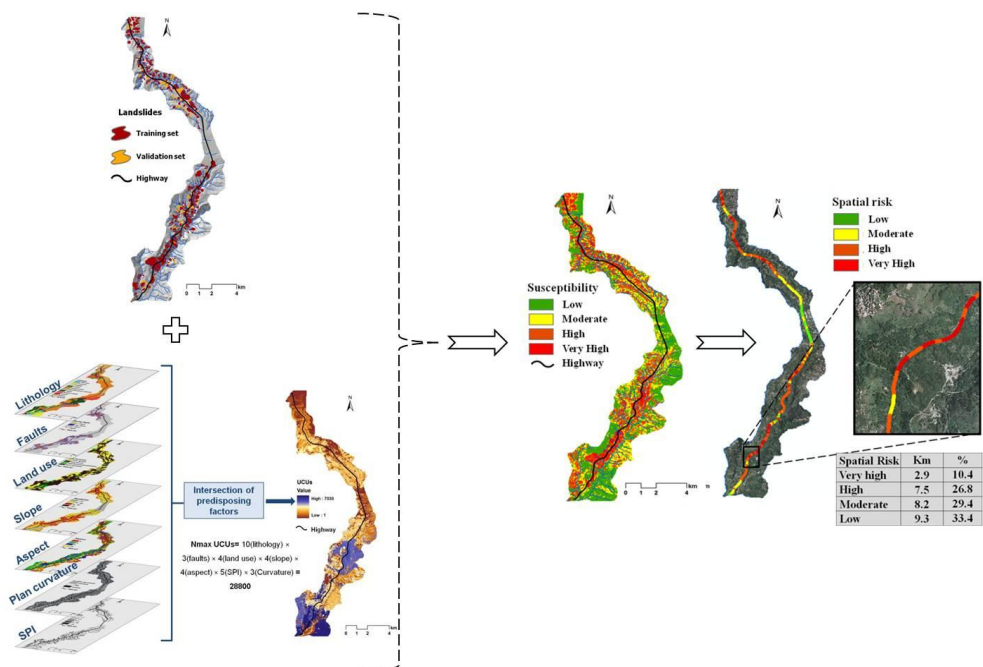
Figure 2. Steps for the evaluation of landslide susceptibility and spatial risk in the study area.

The geo-environmental features of an area have different effect on the occurrence of landslides, and can be utilized as predisposing factors in the prediction of future landslides (VanWesten et al., 2008). In this study, the predisposing factors were selected among the most commonly used in literature and in according with the geological and geomorphological settings of the study area. Lithology, distance from faults, land use, slope, aspect, stream power index (SPI) and plan curvature were assumed as predisposing factors (PF). Lithologies and faults were derived from the geological map. The land use was classified through air-photo interpretation and *Corine Land Cover* project maps. Slope, aspect and slope

curvature were automatically derived from DEM with a resolution of 20 x 20 m pixel size.

In order to estimate and validate landslide susceptibility map, the landslide inventory was randomly divided in two groups. One group (LS-training set) was used to prepare susceptibility map and the second group (LS-validation set) to validate the susceptibility map (Figure 2).

The thematic layers of predisposing factors were crossed in order to obtain all the possible combinations present in the study area of the various classes. Each specific combination represents a Unique Condition Unit (UCU) (Figure 2). Their number and size depend on the criteria used in classifying the input factors. Subsequently, the landslide presence, represented by the landslide area, is determined within each UCU and the landslide density is computed. Assuming the principle that slope failure in the future is more likely to occur under those conditions which led to slope-failure in the past, the computed landslide density is equivalent to the future landslide probability (Carrara et al., 1995). The conditional probability was calculated using the following equation: P(L|UCU) = landslide area / UCU area where the probability of landslide occurrence (L), in an unique combination of factors (UCU), is given by the landslide density in that specific UCU. Landslide density, which represent the susceptibility values, in each UCU was computed and the susceptibility map was obtained (Figure 2).

The validation of the susceptibility map, built with the landslides of the training set, was carried out through the validation set (not used in the training phase). Therefore to quantify the accuracy of the statistical method and evaluate its predictive capability, the receiver operating characteristic (ROC) curve was developed and the area under curve (AUC) was calculated (Beguería, 2006). For the assessment of the spatial risk, the section of highway studied, which represents the only vulnerable element taken into consideration in this work, was digitized from the orthophotos at 1:10000 scale and overlapped on the landslide susceptibility map.

Results and conclusion

Detailed landslide inventory map at the 1:10000 scale was carried and a total of 835 landslides were mapped and the type of movement are represented mainly by slides and complex and subordinately flow (according to Cruden and Varnes, 1996). Furthermore, most of the observed slope movements are active; as for the evolutionary trend of slope movements in the area, retrogressive evolution generally prevails. The UCU's map, derived by the combination of the predisposing factors in GIS environment, shows that of all the 28800 possible combinations, only 7030 are present in the study area (Figure 2). The landslide susceptibility, obtained by the overlay between UCU's map and LS-training set, was classified into four class: low, moderate, high and very high (Figure 2). The results showed that the 33% of the study area is characterized by a high to very high values of susceptibility.

Susceptibility map was validated crossing the group of the landslide of LS-validation set with the susceptibility map. The results showed that over 75% of the landslides of the LS-validation set were correctly classified, falling in high and very high susceptibility classes. Also, the ROC curve had shown an AUC value of 0.79 which demonstrates a good reliability of the adopted statistic method and of the selected predisposing factors.

The overlapping of the section of highway, acquired in vector format, with the landslide susceptibility map, had lead to the zonation of spatial risk which allowed a qualitative evaluation of the involvement of the highway in the different susceptibility areas (Figure 2). The results showed that 37.2% of the highway studied (10.4 km) falls in high to very high susceptibility classes. Finally, the analysis showed that this susceptibility method is successful at identifying landslide-prone areas whereas for the spatial risk assessment. In particular, the susceptibility map and the exposed elements can serve to decision makers for a sustainable territory planning. This approach must be continued and completed at a much higher detail level, including with the estimation of the potential socio-economic and environmental costs.

Acknowledgements

References

Beguería, S. (2006). Validation and evaluation of predictive models in hazard assessment and risk management, Natural Hazards 37, 315–329.

Carrara, A., Cardinali, M., Guzzetti, F., and Reichenbach, P. (1995). GIS technology in mapping landslide hazard. In: Carrara, A., Guzzetti, F. (Eds.), Geographical Information Systems in Assessing Natural Hazards. Kluwer Academic Publisher, Dordrecht, pp. 135–175.

Clerici, A., Perego, S., Tellini, C., and Vescovi P. (2006). A GIS-based automated procedure for landslide susceptibility mapping by the Conditional Analysis method: the Baganza valley case study (Italian Northern Apennines), Env. Geol., 50, 941-961.

Conforti, M., Robustelli, G., Muto, F., and Critelli, S. (2012). Application and validation of bivariate GIS-based landslide susceptibility assessment for the Vitravo river catchment (Calabria, south Italy), Natural Hazards 61, 127–141.

Conforti, M., Muto, F., Rago, V., and Critelli, S (2014a). Landslide inventory map of north-eastern Calabria (South Italy), Journal of Maps,10(1):90-102.

Conforti, M., Pascale, S., Robustelli, G., and Sdao, F. (2014b). Evaluation of prediction capability of the artificial neural networks for mapping landslide susceptibility in the Turbolo River catchment (northern Calabria, Italy). Catena, 113, 236-250.

Cruden, D.M. and Varnes, D.J. (1996). Landslide types and processes, In A.K. Turner & R.L. Schuster (Eds.), Landslides, investigation and mitigation (pp. 36–75). Washington, DC: National Academy Press.

Formetta, G., Rago, V., Capparelli G., Rigon, R., Muto, F., and Versace, P. (2014). Integrated Physically based system for modeling landslide susceptibility, Procedia Earth and Planetary Science 9, 74 – 82.

Le Pera, E., and Sorriso-Valvo, M. (2000). Weathering, erosion and sediment composition in a high-gradient river, Calabria, Italy, Earth Surface Processes and landforms, 25: 277-292.

Margarint, M.C., Juravle, D.T., Grozavu, A., Patriche, C.V., Pohrib, M., and Stângă, I.C. (2013). Large landslide risk assessment in hilly areas. A case study of Huşi town region (North-East of Romania), Italian Journal of Engineering Geology and Environment, 6:275-286.

VanWesten, C.J., Castellanos Abella, E.A., and Sekhar, L.K. (2008). Spatial data for landslide susceptibility, hazards and vulnerability assessment: an overview, Engineering Geology 102, 112–131.

IDENTIFICATION OF SOIL REDISTRIBUTION USING ^{137}CS FOR CHARACTERIZING LANDSLIDE-PRONE AREAS: A CASE STUDY IN SARNO-QUINDICI, ITALY

De Lauro, E., De Martino S., Falanga M.

Dipartimento di Ingegneria dell'Informazione e Elettrica e Matematica Applicata, Università di Salerno, Via Giovanni Paolo II, 84084 Fisciano (SA), ITALY

Introduction

The fallout radionuclide caesium-137 has been increasinglyused in recent years as a suitable approach to estimate rates soil redistributionboth on cultivated and not cultivated areas. Actually, the measurement of the 137Cs as tracer for soil movements is a wellestablished tool in evaluating soil erosion balance. Obviously, the successfulapplication of this approach depends heavily on the availability of reliableconversion models to estimates soil redistribution rates. This paper illustrates the results of a measurement programme aimed tovalidate the study of ^{137}Cs concentration to monitor soil redistribution ratesin basins that are subjected to recurrent instability phenomena. In particular,this work examines an area interested to the events, occurred on 5-6May, 1998, when 150 landslides along the slopes of the Pizzod'Alvano relief,(Campanian Apennines, Italy) were triggered by intense and prolongedrainfall. These landslides affected the pyroclastic deposits that cover extensivelythe carbonatic mountains and killed more than 150 people in downstreamtowns. The area chosen for this investigation, located near Sarno town,is potentially subject to debris flows, i.e. a particular morphological concavity, known as zero-order basin.

On 5-6 May 1998, several days of heavy and continuous rainfall (100-180mm) triggerednumerous landslides in a 70km^2 mountain area of the Campania region (southern Italy).The basins of the Pizzod'Alvano massif (about 1000m a.s.l.) and consequently thefour towns (Bracigliano, Quindici, Sarno and Siano) located at the foot of this relief (see Fig. 1) were subjected to several landslides episodes that killed about 150 people. The major damages as well as substantial changes in the landscape morphology haveaffected the town of Sarno (located 18km to the east of the Somma-Vesuvius volcanicedifice). The landslides canbe classified as soil slip-debris flows.To understand the failure mechanisms and influencing factors of the landslides, comprehensive studies were carried out which involve: examinations of the characteristics of the landslides, field and laboratory investigations of the geological and hydrological properties of rocks and soils (Zhou et al. 2013; Yang et al. 2012), detailed evaluations of representative unstable slope profiles (Zhuang et al. 2013) and how the occurrence of earthquakes (Wu et al. 2012), volcanic eruption (De Lauro et al., 2012), heavy or prolonged rainfall and snowmelt greatly increase landslide occurrence. Several methods are suggested for evaluating where landslides are prone to be initiated and hence for early warning (Yeh et al. 2013;

Zhuang et al. 2013). The aim of the present work is to verify the use of 137Cs radionuclide for identifying potential areas of triggering landslides with respect to areas that are more stable.
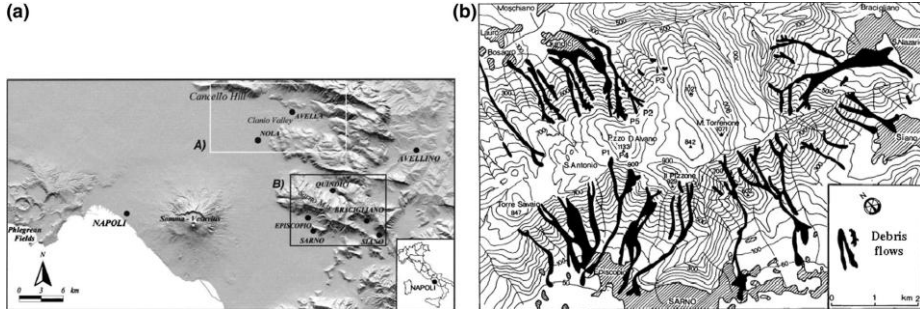

Figure 1. a)Location map of the towns (Bracigliano, Quindici, Sarno and Siano) affected by the 1998 events, Campania region, Southern Italy;b)Pizzod'Alvano massif: plan view of debris flows occurred in May 1998.

Since 40 years, the[137]Cs technique has been successfully used to investigate rates andpatterns of soil redistribution (soil loss and deposition) in a wide range of environmentsand in many different areas of the world. The basis of the technique is well establishedand extensively documented, for example, in Owen and Walling (1996). We extend thistechniques to the case of major landslides and describingthe condition in a starting area (sediment budgeting).

The sites chosen for this investigation is an area potentially subject to debris flows, i.e.a particular morphological concavity are the zero-order basins (zobs) definedas an unchannelized hollow with convergent contour lines(Takashi et al. 2002). The study area chosen to monitor the rates and thepatterns of soil redistribution is ''Vallone del Tuostolo''basin (40 5002900N, 14 3603900E) of the Pizzod'Alvanorelief. It lies N–W of the town of Sarno that it has beenaffected by the 1998 debris flows (Fig. 2). In particular, inthis area we have considered two zobs, named 1 and 2,which are adjacent and characterized by a pyroclasticcover. Zob 1 has not experienced scouring by debris flowand it has never been cultivated, whereas zob 2 wasinfluenced by the 1998 event..The unperturbed area selected as reference site is thePiano di Prato polje situated in Eastern part of thePizzod'Alvano massif.

Method and Results

The ^{137}Cs radionuclide technique is suitable for investigating rates and patterns of soil redistribution because it strongly adheres to soil particles and therefore can be used as a tracer in soil movement studies. Its subsequent redistribution, both vertically and laterally, reflects the erosion, transport, translocation, and deposition of soil. The key requirement of ^{137}Cs technique is the determination of a reference inventory that reflects the fallout input at a local stable site where neither significant erosion nor deposition has occurred. The basic principle of this technique is that the actual point inventory of ^{137}Cs, for a generic

sample of soil collected from the study area, can be directly compared with the reference inventory at the time of sampling. A ^{137}Cs inventory that is less than the reference value is assumed to be indicative of erosion, whereas an inventory greater than the reference value provides evidence of deposition.
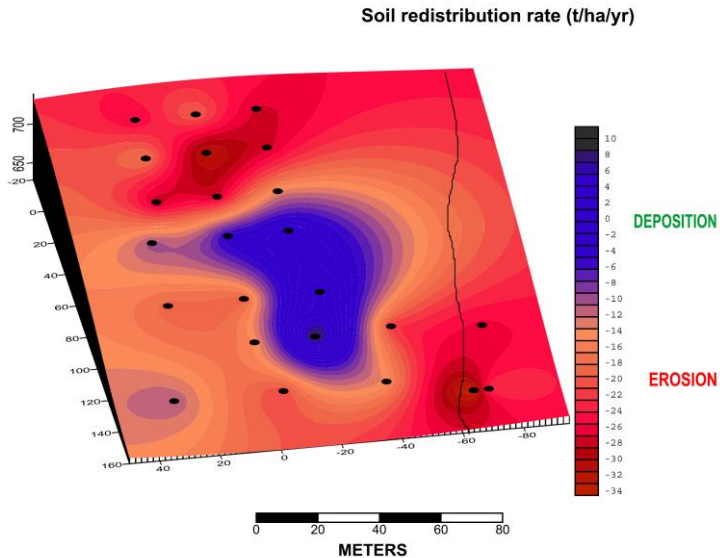

Figure 2. Spatial pattern of soilredistribution rate at zob.

The ^{137}Cs-derived erosion rates estimated for the zob 1 vary from 2 ± 0.5 to 34 ± 1 t ha-1 year-1; the deposition rates range from 0.5 ± 0.1 to 10 ± 2 t ha^{-1} year^{-1} (Buccheri et al., 2014). It is important to observe that these results are consistent with other studies of gully erosion (Zhang et al. 1994). With respect to zob 2 that experiences principally accumulation, the ^{137}Cs-derived deposition rates estimated vary from 5.0 ± 0.05 to 26.0 ± 0.03 t ha^{-1} year^{-1}). For evaluatingerosion/deposition, we checked that the measured ^{137}Csis within a 94 % confidence interval of the mean referencesite inventory constructed with the standard error of themean and t student distribution.As an example Fig.2 shows the spatial pattern of soil redistribution rates at zob 1.

There clearly is not a mass balance in zob 1:gully erosion is greater than deposition implying that somematerial has been lost out of the plot (or has been blownaway on the wind). On the contrary, zob 2 is an areacharacterized by a sedimentation process, which occursfaster and more intense than the accumulation in zob 1.Indeed, the soil accumulation rate with respect to the referenceunperturbed site is about one order of magnitudegreater than that of the central part of zob1, despite that areasuffered a strong erosion process caused by the events of1998. The obtained results are in agreement with the factthat Pizzod'Alvano massif is an area widely covered bypyroclastics soils, whose pedogenetic processes havechanged their original mineralogy forming soils. As aconsequence, extremely variable configurations can beobserved all over the massif when referring, for example,

305

tothe thickness of the pyroclastic deposits. Indeed, along theslopes, the hydrogeological features of the pyroclasticdeposits are mainly related to the arrangement and continuityof ashy and pumice soil layers that affect the rainfallinfiltration process. The light ash soilare easily redistributed on the steep upper slopes of themassif by local mass wasting processes, and evidentlyaccumulated in hollows at the heads of gullies where debrisflows are prone to be initiated. This appears to be relevant,particularly because the rate of hollow filling could becorrelated with the magnitude and/or frequency of debrisflow occurrence. This approach, therefore, allows to highlightthe existence of a hot spot, i.e. an accumulation area inthe middle of a larger area of erosion. This information canbe very useful in the landslide prediction since it could beused for preventive actions, i.e. by mechanically removingthe accumulated soil and, therefore, the trigger points.

References

Buccheri, G., E. De Lauro, S. De Martino, M. Esposito, M. Falanga, and C. Fontanella (2014). Identification of soil redistribution using ^{137}Cs for characterizing landslide-prone areas: a case study in Sarno-Quindici, Italy, Environ Earth Sci.72(6) 2129-2140.

De Lauro, E., M. Falanga,and S.Petrosino (2012). Study on the Long-Period source mechanism at CampiFlegrei (Italy) by a multi-parametric analysis. Phys. Earth. Planet. Int. 206–20716–30.

Owens, P.N., and D.E. Walling (1996). Spatial variability of Cesium-137inventories at reference sites: an example from two contrastingsites in England and Zimbabwe. Appl. Rad.Iso. 47699–707.

Takashi, G., R.C. Sidle, and J.S. Richardson (2002). Understanding processesand downstream linkages of headwater systems. Bioscience52905–916.

Wu, S.R., J.S.Shi, and H.B.Wang (2012). Analysis of activity intensity forlandslides triggered by the Wenchuan earthquake, SichuanProvince, China. Environ. Earth. Sci. 65(4)1021–1028.

Yang, Y.G., H.L.Xiao, S.B.Zou, L.J.Zhao, M.X.Zhou, L.G.Hou, and F.Wang (2012).Hydrochemical and hydrological processes in the differentlandscape zones of alpine cold region in China. Environ.Earth. Sci. 65(3)609–620.

Yeh, H.F., C.H. Lee (2013). Soil water balance model forprecipitation-induced shallow landslides. Environ. Earth. Sci.702691–2701.

Zhang, X., D.E.Walling, T.A.Quine, and Z.Li (1994). Application of theCaesium-137 technique in a study of soil erosion on gully slopesin a yuan area of the Loess Plateau near Xifeng, Gansu Province,China. Geogr. Ann. 76103–120.

Zhou, B.B, Y. Li, Q.J. Wang, Y.L.Jiang, and S. Li (2013). Preferential waterand solute transport through sandy soil containing artificialmacropores. Environ. Earth. Sci. 702371–2379.

Zhuang, J.Q., P. Cui, J.B.Peng , K.H. Hu, andJ. Iqbal (2013). Initiation processof debris flows on different slopes due to surface flow andtrigger-specific strategies for mitigating post-earthquake in oldBeichuan County, China. Environ. Earth. Sci. 68(5)1391–1403.

GEOETHICS AND HAZARD EDUCATION IN ANTHROPOCENIC POSTMODERN SOCIETY

De Pascale, F.[1], Bernardo, M.[1], Muto, F.[2]

[1]*Departmentof Languages and Educational Sciences, University of Calabria, Cosenza, Italy,francesco.depascale@unical.it, bernardo@unical.it*
[2]*Departmentof Biology, Ecology and Earth Sciences, University of Calabria, Cosenza, Italy, francesco.muto@unical.it*

Geoethics and Geography in harmony to save the planet

Geoethics(Peppoloni and Di Capua, 2012) deals with the ethical, social and cultural implications of research and of geological and geographical practice, representing a meeting point of Geosciences, Geography, History, Philosophy and Sociology. Through the identification of principles that should support our actions towards the Geosphere (Peppoloni and Di Capua, 2015), Geoethics may provide an opportunity for scientists to become more aware of their social responsibilities and can become a tool to inform the society about the issues related to the defense against natural hazards, the sustainable use of resources and environmental protection. Geoethics can contribute to the construction of a proper social knowledge, strengthening the connection with the territory, as a common heritage to share. Geoethics can promote a cultural renewal in the way we relate to the planet and a growing awareness of the defense of life and richness of system Earth in all its forms (Peppoloni andPievani, 2013). Specifically, it is demanded of the ethics to provide useful information to address the problems related to major changes that results of scientific research and technological innovation have produced in today's society, particularly in the relationship between man and territory. This has led to a development of the debates about the so-called "environmental ethics". In the third millennium, scientists therefore claim their right to intervene in an area previously considered the exclusive competence of philosophers and religious individuals: the one of values. In this context, science plays a role of social responsibility that is greater than that commonly assigned to it. This new ethic considers the good and the bad, not so much with regard to man, the typical anthropocentric view, but in respect of the territory, ecocentric vision, seen as an entity that has its intrinsic value, regardless of the use it is made of it. The territory, in fact, as an expression of a given culture, of a given history, of a special relationship between man and nature, is a documentary evidence that can be considered full-fledged as cultural heritage: from this derives its priority right to exist and to be protected and appraised (Piacente, 2013). The analysis of the issues dealt by the Geoethics leads to some considerations. First of all, in order to establish selection criteria of appropriate behaviors, it would be necessary to identify the values upon which to base those behaviors. In addition, it would be appropriate to question the issue of the responsibility of those working in the Geosciences fields, focusing the ethical issues on the subject, as expert of the area and of all its dangers, both operating in the research field and in the public and

institutional one, carrying out professional activities or engaged in teaching and in scientific divulgation (Peppoloni, 2011). In this context, environmental sciences are a traditional means of gathering material for geographic information systems. Through GIS (Geographic Information System) it is possible to study atmospheric phenomena, ocean ones, the morphology of the planet and its geological composition; it is possible to observe the nature and distribution of organic forms, the life and death of plants, animals and human beings, and the way in which man organizes, damages or improves the world in which he lives. Every dynamic within the environment and between the environment and humans may be represented at different scales in its complexity. The opportunities for scientific reflection are now widely extended through even more sophisticated systems. They are now operating in the global network, beyond the traditional concept of geodatabase in a stand-alone configuration. If until a few years ago, researchers, professionals and ordinary people interested in environmental issues, depended on a limited range of resources, mostly of institutional or commercial kind, the advent of open source, webgis or, more generally speaking, of distributed implementation and documentation, has greatly improved the ability to access data and technologies (Casagrande, 2010). It is necessary, therefore, to take advantage of new technologies in order to have a greater «geoethical control» of the most significant environmental emergencies: pollution and waste problems, the greenhouse effect and climate change, the critical analysis related to the use of natural resources, accurate information about the dangers and the risks of the territory, the development of environmentally friendly technologies.

Geography, should serve as a «channel» between social and physical-biological sciences, interacting between knowledge that allows quantitative measurements and knowledge that instead mainly relies on qualitative considerations. Such possibility of interactions, both for their educational values and for methodological possibilities they open up, should be valued at their best in educational environment, as they can mark a significant step toward educational-methodological settings capable to let acquire skills and competencies of immediate expendability, as, for example, the importance of acquiring the capability to «know how to translate quantitative elements in qualitative and vice-versa» (Bissanti, 1991).

A questionnaire on seismic risk perception in Calabria and Basilicata, southern Italy

The research foresaw the distribution of a questionnaire to primary and middle-school students from some of Calabria and Basilicata villages. The aim of this was to discover the effective knowledge the students had with regard the correct behaviour to adopt in the event of an earthquake, their reactions during and after an earthquake, the way the students' perceptions of seismic risk varied according to age, experience and place of residence and, finally, to have them reproduce on paper their mental representation of the earthquake. The students' questionnaire was made up of 35 questions, 33 of which were multiple choice,

while another, which asked students to describe their own first-hand earthquake experiences, was open (De Pascale et al., 2015). The finalquestion asked the students to design a ''mental map''regarding what to do should an earthquake occur while theyare in the classroom with classmates and the teacher (De Pascale et al., 2014). A mental map is an internal representation, the mental image an individual has of his environment ("the world in one's head"), "a person's organised representation of some part of the spatial environment" (Downs andStea, 1977). Mental maps are related to spatial and visual capacities of thought, limited to environmental knowledge (Axia, 1986). This means that, because it is a product of "cognitive mapping", it simply refers to visual-spatial aspects of that knowledge. Cognitive mapping is the set of mental processes which set in motion all of the cognitive abilities that allow a person to acquire information from his surroundings and to transform it into a mental image (Lovigi, 2013).

The therapeutic function of mental maps

Children who have experienced traumatic stress often require an individual approach in order to help him to revisit the traumatic event and to give proper meaning to the experience. It is recommended, therefore, a specific therapeutic procedure to enable the child to describe in detail the traumatic experience and to understand the significance of their reactions (Stanulovic, 2005, p. 126). Pynoos and Eth (1986) have described in detail what they call «therapeutic interview» or «talk therapy». The interview is a therapeutic intervention that is performed in a single session and can last up to 90 minutes. It is based on the use of methods of expression and aims to allow the child to express themselves more easily through drawings, manipulation of clay, etc. so that the therapist can grasp the meaning which has had the traumatic experience for the child and, consequently, its reactions and its behavior. The phase of trauma consists of six therapeutic steps: revisit the experience; reconstruct the extreme event; refer the child to the expression of sensory experiences; outline the details that have been particularlytraumatic during experience; describe the most terrifying and unpleasant moments; process the violence and the physical loss inherent traumatic event and integrate the traumatic experience (Stanulovic, 2005, p. 127). The design, the game and handling are a key to access the mental representation of the traumatic event that the child has formed. They are also used as indicators of the child experience and how he solves the traumatic elements of the event.(Pynoos and Nader, 1993).

In this research, Basilicata and Calabria students have designeda large number of maps that represent the men under the desks, sometimes accompanied by men under the lintels of a door. Some maps are simple and rough, other maps are complete and correct. We can identify, in fact, different stages of cognitive mapping (Downs andStea, 1973) which evolve according to the level of environmental spatial knowledge of the student. So, there are maps that represent a limited space of the class, the men under the desk and the teacher who invites pupils to remain calm (Fig. 2). The most significant objects in the class are

represented in advanced maps; there are other complete maps that represent the actions to be taken in order, on the occasion of an earthquake occurrence. The most advanced maps were created by students from the fifth primary and secondary school. It was thus confirmed that the cognitive mapping is a stadialprocess that evolves over the years.

Particular mental maps were designed by students of Tortorasecondary school: in fact, the objects in the classroom, as the clock, the map, books, pens, crucifix, calendar etc. are also represented in maps of "fourth and fifth grade" (Fig. 1). In some maps, the students were adept to represent the moment of typical chaos of an earthquake, bringing even the cries of help and panic (Fig. 1). In other maps, we can see even the clock to pieces as a symbol of the time that is "broken", which stopped during the shock. A strong shock, in fact, blocks the knowledge of space and time in that moment and stores it in the man's memory (Mazzoleni, 2005, p. 147).

Figure 1. Advanced mental map designed by students of Tortora secondary school,inserted in a CIGIS project (Community Integrated GIS), section "Perception of earthquakes".

The pupils' mental representations in neogeographical technologies

The children through the use of new technologies could become the true voluntary of geographic information (Goodchild, 2007), pointing out their perceptions, their emotions directly on the web. In fact, with the advent of Web 2.0, experience based on mass collaboration, it has become from "Wikinomics" to "Socialnomics", where citizens are voluntary sensors. Over the past few decades, the main issu for GIS applications has been the availability of a sound spatial information. Today, the wide diffusion of electronic devices that provide geo-referenced information have resulted in the production of a great amount of territorial information. This trend has led to a "wikification GIS", where mass collaboration plays a key role in the context of territorial informations (hardware, software, data and people).

Figure 2. Simple mental map in which Calabria pupils represented men under the desks during an earthquake, inserted in a CIGIS project, section "Perception of earthquakes".

Neogeography, term appeared for the first time in the English-speaking world in 1922 and used in France by the philosopher François Dagognet (1977) plays an fundamental role in providing new challenges to scholars and territorial planners to address territorial issues and a new asset of updated data, usually created by people who are interested in geographically related phenomena. The attention is devoted to the creation and display of geographic contents, in this case, by children who become the real key players and producers of data and informations, enriching any eventual maps with their feelings and perceptions. This is an original educational experiment that first of all provides the opportunity for youngest people to become aware of earthquake's risk, using in addition to icon-cartographic representations (including "mental maps"), also the most effective and oldest in the world media communication: the word (Consoli *et al.*, 2008), through the use of GPS and positioning devices (mobile phones, PDAs, browsers). This mechanism is a kind of collective mental map and a valuable tool for spatial studies which uses the techniques of participatory cartography; in addition, it can also be converted into a participatory democracy instrument or, rather, of active citizenship, or even in participatory science. In fact, this tool could also be useful for the earthquakes perception and to know the reactions of young people and adults when a seismic event happens. The confirmation that the so-called "participatory science" is an important low-cost tool and complementary to research, comes from a study conducted by the U.S. Geological Survey (USGS). At global level, the sensors for earthquakes detection are a few, in proportion to the territory, and this means that communication signals can take about twenty minutes before they can be processed by the research center. The new instruments, according to the study, have the ability to raise awareness into population and gain valuable information very quickly. In fact, the seismic monitoring stations app for

311

smartphones such as "Did you feel it?" in the U.S. or the Italian "Hai sentitoilterremoto?" or "Did you feel it?" of Seismic Monitoring & Research Unit in Physics Department of University of Malta (http://seismic.research.um.edu.mt/questionnaire.php), allow citizens to give notice of any earthquakes.

The report of the earthquake through the mobile phone or Internet becomes also a tool of psychological support for the child, who strives to identify some positive aspects to serve as consolation, thus enhancing the resilience, which mainly find its purpose for what concerns the scope of his ability to effectively manage stress and daily difficulties, and in this case a possibly traumatic event, an earthquake. Therefore, in the context of risk education, improving communication, awareness of the complexity of the risk and the level of preparation would increase the resilience of the territory and allow a more effective management and planning (De Pascale *et al.*, 2014).

Conclusions: the fundamental role of resilience and risk education

The increased risk resulting from a catastrophic event, in addition to increase in the occurrence of natural disasters, would seem, also, be more due to the increasing loss of ecological safety and the resulting increase in sensitivity of the human ecosystem towards these events, thus making some areas more vulnerable to the risk (Tecco, 2011); if we refer, for example, the number of people killed or affected by natural disasters, the greater vulnerability of the Asian and African continents is evident. It is significant to mention the recent earthquake in Nepal occurred at 11:56 NST on 25 April 2015. In this context, the sensitivity would be made then of a higher level of vulnerability due to factors, often anthropogenic, that would mean that in some areas of the planet, the boundary conditions, whether of human, physical, territorial, economic or educational nature, would increase the probability that the natural event will become a disaster. In fact, the Kathmandu Valley, with 1.5 million inhabitants, located near a river, is one of the most densely populated regions in the world, but the regulations are not respected and buildings, constructed with the latest anti-seismic technologies, are almost absent. Therefore, the study of resilience is crucial, since it is able to incorporate within it both a physical and environmental dimension, and a social dimension that refers to social and economic aspects, connecting the local scale with the larger scale of system. A disaster happens when human societies are not able to "absorb" an extreme event and collapse. Nepal earthquake is an important case in which the failure of dynamic equilibrium among population, environment and resources was the cause of the outbreak of the catastrophe.

Geography has always been concerned with the study of the phenomena induced as modifying agent, conscious or unconscious, of the earth's surface (Palagiano andPesaresi, 2011, p. 85). This reinforces even more the perception of Paul Crutzen and other scientists that we are in Anthropocene geological era (Crutzen and Stoermer, 2000; Monastersky, 2015). It is essential that awareness makes us better understand what is happening to our planet, or "a geological

revolution of human origin" (Bonneuil andFressoz, 2013). In this reality, Geoethics, emerging discipline, is born by the need to reconsider the relationship between the man and the land, the man and the planet. Geoethics stands as an effective tool to raise awareness of the scientific community and even the society as a whole with respect to issues such as risk. Gabriella Arena showed that "there is a situation that no creature has never seemed to be able to settle: the risk" (Arena, 2011, p. 91). We must consider, in fact, not only the chains existing between risk and risk of disease, or between risk and diseases induced by the elements that generate the risk situation, but also the effects on the physical state of man derived from the awareness of living in an environment subjected to risk, in which the occurrence of a catastrophe becomes a probable fact (Arena, 2011, p. 76). Geoethics can find the right solutions for the preservation of the Earth system and the health of its inhabitants. Any failure of the natural environment also produces untold damage to human health (Palagiano andPesaresi, 2011, p. 86). In fact, there is the urgent need to provide adequate knowledge, so that people understand and respect the natural processes that control the life of our planet. This is crucial to guide the choices that must be made at the time and in the future on the part of individuals, society and politicians (Matteucci*et al.*, 2012, p. 368). The risk education, while not the most effective in the immediate time, is certainly influential in the long term, and above allows to get a lasting effect over time (Peppoloni, 2014, p. 131). Therefore, the challenge of effective transfer of information and proper education to new generations must be won, and geographers and geologists, together with the whole scientific community, have an ethical obligation to be at the forefront in this context.

References

Arena, G. (1992),*Convivere con ilrischiosismico. Assuefazioneallo stress?*, in C. Palagiano, G. De Santis, and M.G. Scifoni (Eds.), *Atti del Quarto SeminarioInternazionale di GeografiaMedica(Roma, 4-6 dicembre 1991)*, Ed. Rux, Perugia, 75-94.

Axia, G. (1986), *La mente ecologica*, Giunti Barbera,Firenze.

Bissanti, A. (1991), *Puglia. Geografiaattiva.Perché e come*, Adda, Bari.

Bonneuil, C., J. Fressoz (2013), *L'événementanthropocène. La Terre, l'histoireet nous*, Éditions du Seuil,Paris.

Casagrande, G. (2010), *I GIS nellescienzeambientali*, in S. Bozzato (Ed.), *GIS tranatura e tecnologia. Strumento per la didattica e la diffusionedellaculturascientifica*,Carocci, Roma, 2010, 151-171.

Consoli, A. *et al.*, *La prassididattica*, in A. Ciaschi (Ed.), *La montagna a scuola: cartografia, vocabolario, web,* Carocci, Roma, 2008, 97-120.

Crutzen, P. J., and E.F. Stoermer(2000),*The "Anthropocene"*,Global Change Newsletter, 41: 17-18.

Dagognet, F., *Une Epistemologie de I'espaceconcret: Neo-geographie*, Vrin, Paris, 1977.

De Pascale, F., M. Bernardo, F. Muto, and V. Tripodi (2015), *Geoethics and seismic risk perception: the case of the Pollino area, Calabria, southern Italy and comparison with communities of the past*, Geological Society, London, Special Publications, 419, first published on March 20, 2015, doi:10.1144/SP419.16.

De Pascale, F., M. Bernardo, and F. Muto (2014), *Hazardscape, Territorial and Individual Resilience in an interdisciplinary study: the Case of Pollino, Southern Italy*, in G. Lollino *et al.* (Eds.), *Engineering Geology for Society and Territory*, Vol. 7,DOI: 10.1007/978-3-319-09303-1_21,Springer International Publishing Switzerland, 2014, 109-113.

De Pascale, F., A. Ruffolo, and M. Bernardo (2014), *Educating people about the mountains and risk reduction through new technologies and neogeography: A geoethical interdisciplinary approach*, in *Proceedings International Network of Philosophers of Education, Biennial Conference,* Cosenza, 20-23 August 2014, 392-395.

Downs, R. M., and D. Stea (1973), *Cognitive Maps and Spatial Behavior: Process and Products*, in R.M. Downs and D. Stea (Eds.), *Image and Environments*, Aldine, Chicago, 8-26.

Goodchild, M. (2007), *Citizens as sensors: The world of volunteered geography*, GeoJournal, 69, 211–221.

Lovigi, S. (2013),*Immagini di Padova. Analisi delle percezioni della città e dei suoi quartieri in alunni di classi terza e quinta della scuola primaria*. Cleup,Padova.

Matteucci, R., G. Gosso, S. Peppoloni, S. Piacente, and J. Wasowski, *AHippocratic Oath for geologists?*,*Annals of Geophysics*, 2012, 55 (3), pp. 365-369; doi:10.4401/ag-5650.

Mazzoleni, D., A. Verderosa, and E. Colaci (2005), *Identitàambientale e terremotodel 1980 nellapercezionesoggettiva: ilcaso di Lioni*, in D. Mazzoleni and M. Sepe (Eds.), *Rischiosismico, paesaggio, architettura: l'Irpinia, contributi per un progetto*, CRdC, AMRA, Napoli, 130-157.

Monastersky, R. (2015), *Anthropocene: The human age*, Nature 519, 144–147 (12 March 2015) doi:10.1038/519144a.

Palagiano, C., and C. Pesaresi (2011), *La salute nelmondo.Geografiamedica e qualitàdella vita*, Carocci, Roma.

Peppoloni, S., and G. Di Capua (2015), Chapter 1 – Themeaning of geoethics. In: M. Wyss and S. Peppoloni, (Eds.), *Geoethics: Ethical Challenges and Case Studies in Earth Sciences*, Elsevier, Amsterdam, 3–14,http://dx.doi.org/10.1016/B978-0-12-799935-7.00001-0.

Peppoloni, S. (2014)*, Convivere con irischinaturali. Conoscerli per difendersi*, Il Mulino, Bologna.

Peppoloni, S., and T. Pievani (2013), *Le Scienzedella Terra e illorocontributo al rinnovamentoculturaledellasocietà*, Contributo al Festival dellaScienza, Genova, 23 ottobre - 3 novembre 2013.

Peppoloni, S. (2011), *Checosasignifica "Geoetica"?Dentro le parole, ilsensodell'attività del geologo*, Geoitalia (FederazioneItaliana di Scienzedella Terra), vol. 34, 12-13.

Piacente S. (2013), *Contributo per la tavolarotonda, Geoetica: ilvalore del territoriotrascienza, politica e informazione*, in IX edizione del Forum Italiano di Scienzedella Terra, "Le Geoscienze per la Società", Pisa, 15-18 settembre 2013.

Pynoos, R.S., S. Eth (1986), *Witness to violence: The child interview*, Journal of the American Academy of Child Psychiatry, 25 (3), 306-319.

Pynoos, R.S., K. Nader (1993), *Issues in the treatment of post-traumatic stress in children and adolescents*, in J. Wilson and B. Raphael (Eds.), *International Handbook of Traumatic Stress Syndromes*, Plenum Press, NYC, 535-549.

Stanulovic, N.K. (2005), *Psicologiadell'emergenza. L'intervento con i bambini e gli adolescenti*, Carocci, Roma.

Tecco, N. (2011),*Educazione geografica, resilienza e catastrofi naturali*,in C. Giorda, and M. Puttilli (Eds.), *Educare al territorio, educare il territorio. Geografia per la formazione*. Carocci, Roma, 308–320.

http://seismic.research.um.edu.mt/questionnaire.php.

PUBLIC PERCEPTIONS ON COASTAL EROSION IN THE MALTESE ISLANDS: A CASE STUDY OF ST GEORGE'S BAY (ST JULIANS) AND PRETTY BAY (BIRŻEBBUĠA)

Farrugia, M. T.

ANU College of Engineering and Computer Science, The Australian National University, RSISE Building 115, North Road, Acton, ACT, 2601, Australia,
maria.farrugia@anu.edu.au

Introduction

This paper focuses on two nourished beaches within the Maltese Islands, St George's Bay (St Julians) and Pretty Bay (Birżebbuġa), both of which have undergone extensive sand augmentation during the past decades and looks at the extent of how coastal erosion and beach replenishment may have influenced public perception. Through a triangulation of interviews, it seeks to understand the views of beach users, researchers, representatives, and beach managers. It presents divergences in ideas on St George's Bay and Pretty Bay and illustrates that public perception tends to reflect the type of urban area surrounding each replenished beach. Recommendations and suggestions are also presented to promote awareness towards coastal processes and their impacts and to provide management techniques for limiting the effects of coastal erosion on the urban environment.

Coastal erosion can be regarded as one of the natural processes creating the coastal dynamic system, which is influenced by the erosion, transportation and deposition of sediment. Although coastal erosion is mostly evident in conditions of poor sediment availability, where sediment is available in large quantities shoreline retreat and coastal erosion do still occur (Horn, 2002). This research looks at the perception of people towards coastal erosion and beach quality at two bays in Malta highlighting the differences between the two. St George's Bay and Pretty Bay are two sandy beaches situated both in an urban setting and have undergone extensive sand augmentation (henceforth referred to as 'beach nourishment') during the past decade. Given the popularity of these beaches by users especially in the summer months, the extent of how such interventions may have influenced public perception is being studied using recent survey techniques applied in other Mediterranean settings such as Costa Brava in Spain, the Slovenian coast and the Ligurian coast (Dursi et al,2009; Kontic, Kross and Peterlin,2005; Roca and Villares, 2007).

The scope of the research is being substantiated through a triangulation of interviews, whereby beach users have been interviewed quantitatively by means of a structured interview, and two types of stakeholders were interviewed qualitatively using unstructured interviews. The stakeholders consisted of representatives from a number of organisations including Nature Trust, whose technical knowledge of the two beaches in question outlines the extent and nature

of the two beaches' coastal erosion, and beach managers from a top-level grade, who were in charge of the actual beach management.

Case Studies Investigations

Since the Maltese Islands have around 270km of coast and a land area of only 315km2 taking in consideration the coastal environment when carrying out urban and spatial planning is important for these islands. However, the need for effective planning and use of coastal zones depends on a solid understanding of the natural processes and systems affecting these dynamic areas (Planning Authority, 2002). Focusing on the two case study areas one notes that St George's Bay is located on the northwestern coast of Malta, as seen in Figure 1. Morphologically the bay is composed of a promontory and a headland surrounding a sandy beach which has been the result of beach nourishment. Contrasting to St George's Bay, Pretty Bay is located on the south-eastern part of the Maltese Islands. Morphologically the bay is composed of a headland containing a rocky shoreline which is located on one side of the bay and a beach which has been augmented throughout the years.

Whilst the area surrounding St George's Bay is focused on recreation and tourism, the augmented beach of Pretty Bay is enclosed within an industrial shield, containing important industrial activities such as the Malta Freeport and even a fuel depot. The geology is also different at the two bays. Pretty Bay consists mostly of Lower Globigerina Limestone whilst the coastal shore of St George's Bay is dominated by Lower Coralline Limestone. This indicates that Pretty Bay may be more susceptible to erosion than its counterpart in St Julians. In addition to this, the fined small-sized beach sediment at Pretty Bay may be easier to be carried away by winds in contrast to the coarse grain sized sediment at St George's Bay.

Both case study areas have undergone beach nourishment by means of an increase in sediment which was the result of direct government intervention in order to boost tourism (Ebejer, 2004; Caruana, 2005; World Bank, 2003). This increase in sediment led to more people using the bays and to an increase in economic activities (Caruana, 2005; Chetcuti, 1999; Ebejer, 2004; Guillaumier 2005; World Bank, 2003). The embellishment of the beaches provided users also with greater aesthetic and amenity values.

Materials and methods

The techniques used at both St George's Bay and Pretty Bay are similar to those carried out in other Mediterranean beaches including the North-eastern coast of Spain, the Slovenian coast and the Ligurian coast where both the opinion of beach users and that of relevant stakeholders such as beach managers and local authorities were considered. Truly, seeking an understanding of how individuals perceive beaches is highly useful for beach managers engaged in integrated beach management. In addition all the techniques mentioned above were based in the Mediterranean coastal region, where similarly to the local scenario; tourism is considered an important sector of the economy.

In this study, public perception was identified through beach user questionnaires which were divided into a number of sections dealing with beach use, beach quality, coastal erosion and people's perception about it, and also beach management. To determine the number of distributed surveys, the average number of persons visiting the bays was identified.
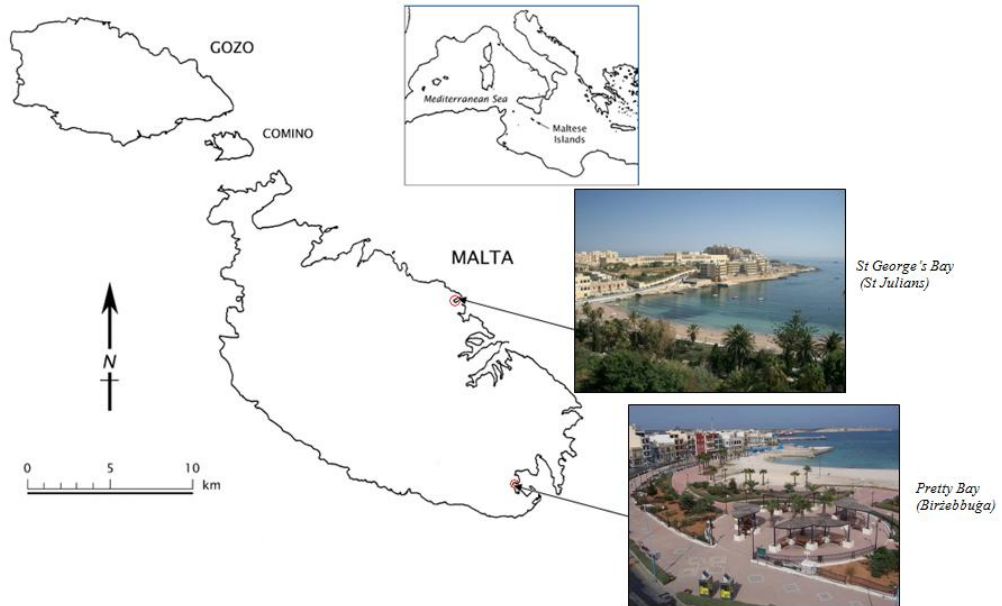

Figure 1: Location of case study areas (Modified from: Guérout ,2004).

In addition to public perception questionnaires, a number of unstructured interviews were held with beach managers and researchers within a number of organisations. These included the Malta Tourism Authority (MTA), the International Ocean Institute (IOI) - Malta Operational Centre, Euro-Mediterranean Centre on Insular Coastal Dynamics (ICOD), Nature Trust, the Birżebbuġa Environment Action Group, Adi Associates and Ecoserv. Since the representatives in the above organisations were not specialised on all the relevant aspects of the case study areas but on only certain themes related to the geography of the bays, the questions that were asked had to be tailored accordingly.

The results from the above surveys were then compared to identify whether different stakeholders held different perceptions of the two case study areas. Some of the most important points taken in consideration included whether the stakeholders think that St George's Bay (St Julians) and Pretty Bay (Birżebbuġa) are susceptible to significant coastal erosion; if beach nourishment had an impact on the beaches and its users; whether the beaches should be enhanced further and if beach users should pay for using the beaches.

Discussions of achieved results

Results emerging from the above mentioned methodologiesare various and quite interesting for this research. A comparison between of St George's Bay (St Julians) and Pretty Bay (Birżebbuġa) indicates that different types of people visit these two bays. Whilst the dominant people at Pretty Bay are local visitors coming from nearby towns and villages, at St George's Bay, the dominant visitors are tourists.

A difference has also arisen regarding whether people visiting the two bays know about coastal erosion processes in both beaches. At St George's Bay this may be attributed to the fact that most of the people recreating at this case study area are tourists who lack knowledge about any shoreline changes in the area and are only interested at the recreational uses of the bay. On the contrary, at Pretty Bay most of the people questioned were actually residents or visitors from nearby towns and villages who were aware of coastal erosion at the bay. Stakeholders involved on this bay seem not to be aware of this, although they mention that only people living in the surrounding areas used to visit the beaches prior to beach nourishment.

Moreover, the fact that both beaches had undergone beach nourishment may have influenced the way how people actually see the bays. Not noting any decrease in beach material over the years they would deduce that there are no problems arising from coastal erosion at the bays. Yet, people at Pretty Bay actually said that the beach structure and shape tends to change seasonally. This was mentioned also by the stakeholders involved on this bay. Even stakeholders at St George's Bay noted that the beach is heavily influenced by seasonal changes.

Also beach protection was deemed as being equally important at the two bays. This indicates that even though people may not be aware of the natural processes at the coastal zone, they still consider their importance and the need for protection against their effects. However, when looking at how much people would pay to protect beaches on a daily basis, it is evident that there are also differences at the two bays. Whilst most of the people at Pretty Bay claim that they should not pay, the users at St George's Bay do not know and some of them also indicate that a small fee could be paid daily for beach use. Yet stakeholders at this bay state that access to the beach should be free and only services should be paid for.

Results at both bays also indicate that interviewees are unsure about who should pay for beach protection against coastal erosion. At St George's Bay the interviewees commented that residents, tourist and local visitors could contribute some of these funds. At Pretty Bay, beach managers were also included giving beach protection a more holistic approach where all stakeholders could be involved.

Thus one may determine that beach nourishment at St George's Bay and Pretty Bay has influenced public perception. Through the surveys it seems evident that an increase in sand at a beach could be to a further reason why people visit such beach. Also beach nourishment works tend to change the way how people see beaches and bays as such areas are commonly considered not prone to the problems of coastal erosion. Only residents and local visitors who visit such

beaches frequently seem to see the results emanating from the coastal erosion process. Other people such as tourists may be unaware of this and usually see beach nourishment works as a positive solution to loss of sediment by coastal erosion.

Regarding the stakeholders involved in the management of the bays, it is noted that whilst for Pretty Bay the stakeholders seem to have similar opinions, for St George's Bay these opinions differ. It seems also that organisations seem to contradict each other on whether beach enhancement should be carried out and whether awareness on coastal erosion shall be carried out. Also from the interviews carried out, one notes that different representatives have different ideas towards beach protection. For example whilst the tourism authority and its environmental consultants consider the removal of dry Posedonia oceanica banks from the beach as positive, other consultants like Dr. Alan Deidun from IOI considers this as impacting negatively the presence of sand at the beach (Deidun, 2010).

Conclusions and recommendations

Overall, from this paper it seems evident that coastal erosion processes not only shapes, moulds and sculpts the shorelines of the Maltese Islands but they also influence public perceptions. Bearing in mind that Malta has around 270 km of coast and a land area of only 315 km2, one should thus give priority to coastal processes such as coastal erosion. Recommendations should be made towards the identification of these processes and eventually towards the protection of the urban areas which surround the coastal zones. Yet, one has to consider the protection of the shoreline itself, as actions should be attempted at minimizing the rates of erosion and not at maximizing them.

Taking the example of both Pretty Bay and St George's Bay, it is evident that the interference of stakeholders with fragile coastal zoneshas led to beach engineering works specifically beach nourishment. These works as indicated at both bays can increase the popularity of the beach itself as more people will visit it. This popularity may also affect the economic development surrounding the beach as more activities will start taking place in the area.

Also one should consider the involvement of people in trying to manage the relationship between coastal erosion and urban development. As shown in this study, stakeholders should be made more aware of the considerations and opinions of beach users and of other persons involved in beach management. The considerations and opinions of stakeholders and those of beach users should be made accessible to every person involved in beach management.

Therefore more public-private consultations would be suitable as these decrease differences that exist between beach users' opinions and those of people and entities that are responsible for the beaches. Public consultations would indicate whether the development proposed in a coastal zone is approved by residents and whether they see it as a need or not.

Yet public consultations should be used in conjunction with environmental impact assessments that need to be created to ensure that beach engineering

approaches like beach nourishment works are satisfactory. Monitoring is also important as it identifies coastal movements and their relationship with the urban environment over a period of time. Though it is important highlighting that people, living in coastal areas or even in nearby towns and villages, usually identify the latter movements and relationships better than those people who visit the beach temporarily for recreational purposes. This has been the case of both Pretty Bay and St George's Bay.

Moreover, one should consider carrying studies on both short term and long term basis. The long term approach is more ideal for identifying and analysing coastal changes as these changes are usually identifiable through historical analysis. The use of mapping programs like ArcGIS is important to discover long term changes and a good knowledge of such mapping programs needs to be considered when looking at long term approaches. Yet, shorter time spans are important as these could be used to delineate the main processes acting on the coast.

Overall one can maintain that actions and recommendations need to be taken mostly on persuading stakeholders in seeing the coast as an area to be safeguarded rather than exploited. For such reason positive coastal protection measures need to be coupled with monitoring and eventually public participation measures as the coastal zone is one of the most important venues for tourism purposes and one of the most important areas with regard to biodiversity.

Acknowledgements

References

Caruana, C. (2005). An economic valuation of a beach on the island of Malta: Pretty Bay, B'Bugia. Unpublished M.A. dissertation, University of Malta, Msida, Malta.

Chetcuti, N. (1999). A land-cover appraisal of the St. George's Bay Area : with emphasis on the impact of development on the habitats and biota. Unpublished Diploma dissertation, University of Malta, Msida, Malta.

Deidun, A. (2010, January 11). Consultant, Physical Oceanography Unit, IOI- Malta Operational Centre, Personal Communication.

Dursi, R., Fabiano, M., Ivaldi, R., Marin, V., and Palmisani, F. (2009). Users' perception analysis for sustainable beach management in Italy. Ocean & Coastal Management, (52), 268–277.

Ebejer, J. Creating a Sandy Beach in St. George's Bay: A new Experience for Malta. In A. Micallef, A. Vassallo, & M. Cassar (Eds.), Proceedings of the First International Conference on the Management of Coastal Recreational Resources - Beaches, Yachting and Coastal Ecotourism - 20-23 Oct 2004, Malta (pp. 161 – 167). Valletta, Malta: Euro-Mediterranean Centre on Insular Coastal Dynamics; Foundation for International Studies.

Guérout, M. (2004). Carte de Malte [Map]. Retrieved September 15, 2009, from http://www.archeonavale.org/Malte_2004/carte.php

Guillaumier, A. (2005). Bliet u Rhula Maltin: Enciklopedija ta' Taghrif dwar kull Belt u Rahal (5th ed., Vol. 2). Valletta, Malta: Klabb Kotba Maltin.

Horn, P. D. (2002). Beach Groundwater Dynamics. Geomorphology, (48), 121-146.

Information Division (1983). Reports on the Working of Governmental Departments for the Year 1982. Valletta, Malta: Governmental Press.

Kontic, B., Kross, B. C., and Peterlin, M. (2005). Public perception of environmental pressures within the Slovene coastal zone. *Ocean & Coastal Management*, (48),189–204.

Planning Authority (2002). Coastal Strategy Topic Paper. Floriana, Malta: Planning Authority Services.

Roca, E. and Villares, M. (2007). Analysis of beach users' perception in tourist coastal areas: A case study in the Costa Brava, Spain. In E. Ozhan (Ed.) Proceedings of the 8th International Conference on the Mediterranean Coastal Environment, Medcoast '07 (pp. 295-304). Ankara, Turkey: Middle East Technical University.

World Bank (2003). Port reform toolkit: effective decision support for policymakers. Washington D.C, USA: World Bank Publications.

INFRARISK: NOVEL INDICATORS FOR IDENTIFYING CRITICAL INFRASTRUCTURE AT RISK FROM NATURAL HAZARDS

Jimenez, MJ.[1], O'Brien, E.[2], and INFRARISK Consortium (O'Connor, A., Tucker, M., Ni Choine, M., Adey, B., Hack, J., Heitzler, Iosifescu, I., Segarra, M., Salceda T., Gavin, K., Martinovic, K., Van Gelder, P., Garcia-Fernandez, M., D'Ayala, D., Cheng, T., Ghel, P., Taalab, K., Medda, F., Prak, P., Roman, D., Berre, A., Richtey, T., Sabeur, Z., Meachan, M.)

[1]Institute of Geosciences, CSIC, UCM, Spain, mj.jimenez@csic.es
[2]ROD, Dublin, Ireland, eugene.obrien@rod.ie

Extreme, low probability, natural hazard events can have a devastating impact on critical infrastructure (CI) systems in Europe and the Mediterranean. The EU project INFRARISK (Novel Indicators for identifying critical INFRAstructure at RISK from natural hazards) aims to develop reliable stress tests to establish the resilience of European CIs to rare low frequency extreme events and to aid decision making in the long term regarding robust infrastructure development and protection of existing infrastructure. The core objective of the INFRARISK project is to develop a stress test framework to tackle the coupled impacts of natural hazards on interdependent infrastructure networks through identifying rare low-frequency natural hazard events, which have the potential to have extreme impacts on critical infrastructure.

A stress test structure is been developed for specific natural hazards on CI networks and a framework for linear infrastructure systems with wider extents and many nodal points (roads, highways and rail roads) further applicable across a variety of networks (e.g. telecom, energy). An integrated approach to hazard assessment considering the interdependencies of infrastructure networks, the correlated nature of natural hazards, cascading hazards and cascading effects, and spatial and temporal vulnerability is established and implemented through the development of GIS based and web based stress test algorithms for complex infrastructure networks.

The developed framework will be tested through simulation of complex case studies. The methodological core of the project is based on the establishment of an "overarching methodology" to evaluate the risks associated with multiple infrastructure networks for various hazards with spatial and temporal correlation. This is the basis for the development of stress tests for multi-risk scenarios which defines the general framework, providing a tool for decision making based on the outcome of the stress test.

The overarching methodology captures and incorporates, into a GIS platform, the outputs from an extensive profiling of natural hazards and infrastructure, and analysis of single event risk for multiple hazards and space-time variability of a CI network. An INFRARISK strategic decision support tool is being developed to ensure network models and stress test procedures are integrated

323

and used under specific process work flows and modules. The application on selected case studies in Italy and Croatia will verify the modelling techniques and procedures developed in INFRARISK.

A COMPARISON OF GIS-BASED LANDSLIDE SUSCEPTIBILITY METHODS IN AMENDOLARA TOWN (SOUTHERN ITALY)

Rago, V.[1], Muto, F.[1], Armaş, I.[2], Conforti, M.[3], Gheorghe, D.[2]

[1]*Dipartimento di Biologia, Ecologia e Scienze della Terra (DiBEST), Universita` della Calabria, Arcavacata di Rende, Italy, valeria.rago@unical.it, francesco.muto@unical.it*

[2] *Department of Geomorphology, Faculty of Geography, University of Bucharest, Bucharest, Romania, iuliaarmas@yahoo.com*

[3]*CNR – Istituto per Sistemi Agricoli e Forestali del Mediterraneo (ISAFOM), Rende, Italy, massimo.conforti@isafom.cnr.it*

Introduction

Landslides represent one of the most widespread natural hazards in Italy and have always posed serious threats to settlements and structures that support transportation and natural resources (Guzzetti, 2000). Large areas of the Calabria region (southern Italy), have been affected historically by mass movements (Carrara and Merenda, 1976; Calcaterra and Parise; Iovine et al., 2010; Conforti et al., 2014a), due to its peculiar geological, geomorphological, seismic and climatic features and frequently to regionally unsustainable land management (Conforti et al., 2014b). Therefore, to identify the spatial distribution of potentially unstable slopes based on a study of predisposing factors is an important starting point for landslide risk management. Landslide susceptibility, in its mathematical form, is just the probability of the spatial occurrence of known slope failures given a set of geo-environmental conditions (Guzzetti et al., 2005). Landslide susceptibility maps provide valuable information for government agencies, planners, decision makers, and local landowners to make emergency plans to reduce the negative effects on infrastructure, superstructure, and human life (Kavzoglu et al., 2013).

The process of creating these maps involves several qualitative or quantitative approaches. Qualitative methods depend on expert opinions, whereas quantitative methods are based on numerical expressions of the relationship between controlling factors and landslides. All these methods can be grouped in: geomorphological hazard mapping, analysis of landslide inventories, heuristic, statistical and geotechnical methods (Guzzetti et al., 1999). Statistical and geotechnical models have been widely used, but recently, also geographical information system-based multi-criteria decision analysis was used to carry out landslide susceptibility assessment (Armaş, 2011; Pourghasemi et al., 2012).

The aim of this study was to create landslide susceptibility maps in the territory surrounding Amendolara town (Calabria region, southern Italy), using three different methods and then to analyze and compare the results of each model. The models applied have been statistical Hazard Index (HI) (van Westen, 1997; Conforti et al., 2012), Weight of Evidence (WOE) (van Westen et al. 2003,

Barbieri and Cambuli, 2009, Armaş, 2012), and Spatial Multi-Criteria method (SMC) (Komac, 2006; Castellanos Abella and Van Westen, 2007).

Study area

The study area is located in the north-eastern sector of Calabria region (Figure 1). This sector of the region is known as one of the most landslide prone areas of Calabria because of its geological and climatic characters (Conforti et al., 2014a).

From a geological point of view, the study area is located on the border between the Southern Apennine and Calabrian Arc (Monaco et al., 1995). In the Amendolara territory, the main rock types present are Tertiary age marine and continental sedimentary deposits. In particular in the study area outcrops late pliocenic gray-blue silty clay, with poorly cemented, yellow sand at the top of the Tertiary sequence. These deposits are covered by Pleistocene polygenic conglomerates. Holocene alluvial deposits are present along valley floors.

The geomorphological setting of the study area is strongly controlled by geological and structural features, where rocks erodibility is higher, the landscape is characterized by hilly morphology with undulating topography, gentle slopes and wide, slightly incised valleys. The hillslopes are often deeply gullied as a result of erosion caused by ephemeral streams.

The Amendolara town is located on a marine terrace, dissected by narrow V-shape valleys. with steep slopes, as a consequence of the Quaternary tectonic activity and sea level changes (Ferranti et al., 2009), along which often trigger landslides.

The landscape of the study area is mainly dominated by gravitational landforms even if, in many places, landforms related to running water were observed (Conforti et al., 2014a). Along slopes carved into clay deposits, was observed "calanchi" landforms which producing a typical stream dissected morphology, with very steep gullies separated by narrow ridges. The geomorphological survey inside the badland areas put in evidence that, within the main gullies, small mass movements and dissecting processes work together to give blunted ridges. On the contrary, vertical dissection processes prevail in secondary channels, thus forming narrower and knife-edge ridges, finally, debris flow cones are often accumulated at the mouth of various order drainage channels.

Methodology

The study was characterized by four main steps: (1) data collection and construction of a spatial database of landslides and predisposing factors, (2) landslide susceptibility assessment by means the methods that were chosen for the analyses, (3) validation of the results, and (4) comparison of the results.

The construction of the spatial database was based on three different tasks: digitizing and editing of previous cartographic information, air-photo interpretation and field surveys. GIS database includes the landslide predisposing factors that were chosen in according with the geological and geomorphological settings of the

study area (lithology, land use, distance from drainage network, distance from roads, and morphometric parameters, namely slope and aspect) and the landslides inventory map.

Landslide susceptibility evaluation was performed using GIS-based HI, WOE and SMC methods and the same predisposing factors were used. For the analyses only landslide scarps were used and these were divided in two group: training set, to construct the models, and validation set, to validate the landslide susceptibility maps.
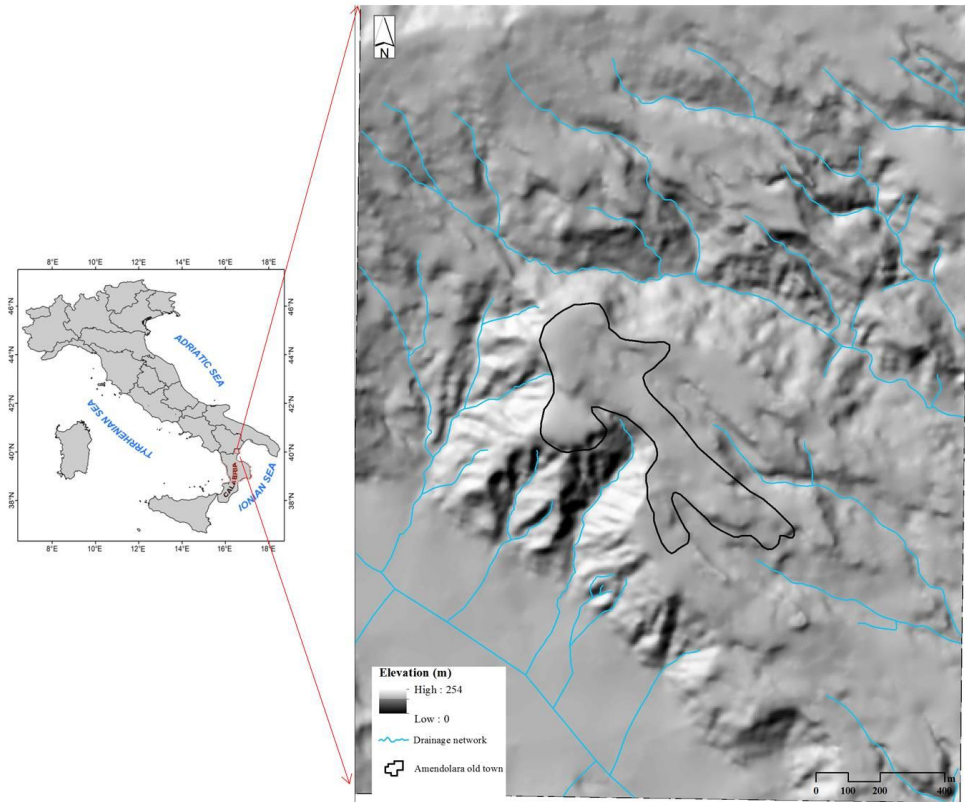
Figure 1. Location of study area.

All data layers were transformed in raster format with pixel size of 10x10 meters. The GIS software ILWIS (3.4) was used to perform the susceptibility analyses (ILWIS 2001). The bi-variate statistical HI method is based upon the formula (van Westen, 1997):

$$Wi = ln\left(\frac{Densclas}{Densmap}\right) = ln\left(\frac{\frac{Area\,(Si)}{Area\,(Ni)}}{\frac{\sum Area\,(Si)}{\sum Area\,(Ni)}}\right)$$

Where Wi is the weight given to a certain parameter class (e.g. a rock type, or a slope class), Densclas is the landslide density within the parameter class, Densmap is the landslide density within the entire map, Area(Si) is the area which contain landslides in a certain parameter class, and Area(Ni) is the total area in a certain parameter class. The method is based on map crossing of a landslide map with a certain parameter map. The map crossing results in a cross table, which can be used to calculate the density of landslides per parameter class. A standardization of these density values can be obtained by relating them to the overall density in the entire area, for this landslide density per class is divided by the landslide density in the entire map. The natural logarithm is used to give negative weights when the landslide density is lower than normal, and positive when it is higher than normal. By combining the maps of weight-values a susceptibility map can be created.

WOE method is an approach based on Bayes rule for combining data to predict occurrence of events. The simple form of Bayes' theorem applied uses the binary map method. This method has two states (e.g., presence/absence of the event within a pixel) and is based on the decision of which state is more likely to occur grounded on the available data (Armaş, 2012). Applied to the landslide susceptibility approach, the technique of log-likelihood ratios aims to identify the degree of influence, expressed as ''weight'' that each variable has on the development of a landslide event (Barbieri and Cambuli, 2009). Weights are calculated based on the spatial development of landslides in the thematic maps used as evidence.

For each predisposing factor is calculated a positive weight (W+), when the event occurs, and a negative weight (W-), when the event does not occur. The weights are measures of correlation between evidence (predisposing factors) and event, facts that make them easy to interpret in relation to empirical observation. The calculations are density functions:

$$W+= ln\frac{P\,(F|Af)}{P(F|\bar{A}f)} = ln\left[\frac{\frac{Landslide\ area\ in\ the\ considered\ class}{Total\ landslide\ area}}{\frac{Stable\ area\ in\ the\ considered\ class}{Total\ stable\ area}}\right]$$

$$W-= ln\frac{P\,(\bar{F}|Af)}{P(\bar{F}|\overline{Af})} = ln\left[\frac{\frac{Total\ landslide\ area\ in\ other\ class}{Total\ landslide\ area}}{\frac{Total\ stable\ area\ in\ other\ classes}{Total\ stable\ area}}\right]$$

The difference between the W+ and W- weights is known as the weights contrast, C (C =W$^+$ + W$^-$), where C reflects the overall spatial association between a predictable variable and landslide occurrence. A contrast value equal to zero indicates that the considered class of causal factors is not significant to the analysis. C calculated individually for all the predisposing factors are added to produce the

susceptibility map. SMC is a process that transforms and combines geographical data and value judgments to obtain information for decision making (Malczewski, 1999) with respect to a particular goal (in this case a susceptibility assessment). It is an ideal tool for transparent group decision making, using spatial criteria, which are combined and weighted with respect to the overall goal. The theoretical background for the multicriteria evaluation is based on the Analytical Hierarchical Process (AHP) developed by Saaty (1980). In the analysis a number of steps were followed. First the problem was structured into a main goal and a number of sub-goals. For each of these sub-goals a number of criteria were defined, which measure their performance. Once this was defined, a criteria tree was created, which represents the hierarchy of the main goal, sub-goals, and criteria. For each of the criteria a link was made with the relevant spatial and attribute information. As the criteria were in different formats (nominal, ordinal, interval etc.) they were normalized to a range of 0-1. The criteria classes were weighted against each other, then the criteria belonging to the same sub-goal and eventually also the sub-goals themselves were weighted, using either pair wise comparison, or rank ordering methods. Once the standardization and weighting was done, a composite index map was calculated for each sub-goal, and the landslide susceptibility map was produced, and classified into a number of classes (Castellanos and Van Westen 2007).

The major pitfall of this method is represented by the fact that the outcome depends significantly on the expertise of the researcher and the accuracy of the primary data (Armaş, 2011).

Results and conclusion

HI, WOE and SMC methods provided three landslide susceptibility maps, which values were reclassified into five classes using the natural breaks classification scheme: no or very low, low, moderate, high and very high susceptibility (Figure 2). In the landslide susceptibility map produced with the HI method the 54.3% of the total area is covered by high and very high susceptibility classes. In this map, no or very low, low and moderate landslide susceptibility zones comprised 13.7%, 12.2%, and 19.7% of the total area, respectively. The landslide susceptibility map obtained from the WOE method contained 37.5% of the total area in the high and very high susceptibility class. Its very low, low and moderate landslide susceptibility zones constituted 21.2%, 8.5%, and 32.8% of the total area, respectively. The landslide susceptibility map obtained from the SMC method contained 22.3% of the total area like high and very high classes. Its very low, low and moderate landslide susceptibility zones constituted 18.2%, 5.3% and 7.7% of the total area, respectively (Figure 2).

The accuracy of each model was evaluated by comparing the maps with known landslide locations (Ozdemir and Altural, 2013). The 17 training landslide scarps (4780 pixels), 16 validation landslide scarps (1299 pixels) and 33 landslide scarps (6079 pixels), were overlaid onto the landslide susceptibility maps, and then

the percentages of the existing landslide pixels within the different landslide occurrence potential classes were determined (Figure 2).

The results obtained from overlaying the landslide susceptibility map produced by the HI method with the training, validation, and all landslides indicated that 94.7%, 75.9% and 89% of the observed landslides were concentrated in the high and very high landslide susceptibility class, respectively. These percentages were 89.6%, 68.5%, and 83.3% for the WOE method and 41,4%, 36.6% and 41.5% for the SMC method, respectively. These results suggest that HI and WOE methods appears to be reliable, because they correspond most closely to the prediction of landslide susceptibility in the study area, since these two maps correctly classified that most landslide scarps of the validation set fall into the most susceptible classes.

Finally, these landslide susceptibility maps for the study area show the areas prone to landslides and represent a good informative map that can be used for land use and infrastructure planning process. Moreover, the accurate mapping of landslides susceptibility provides the baseline information for further evaluations of landslide hazards and related risks.
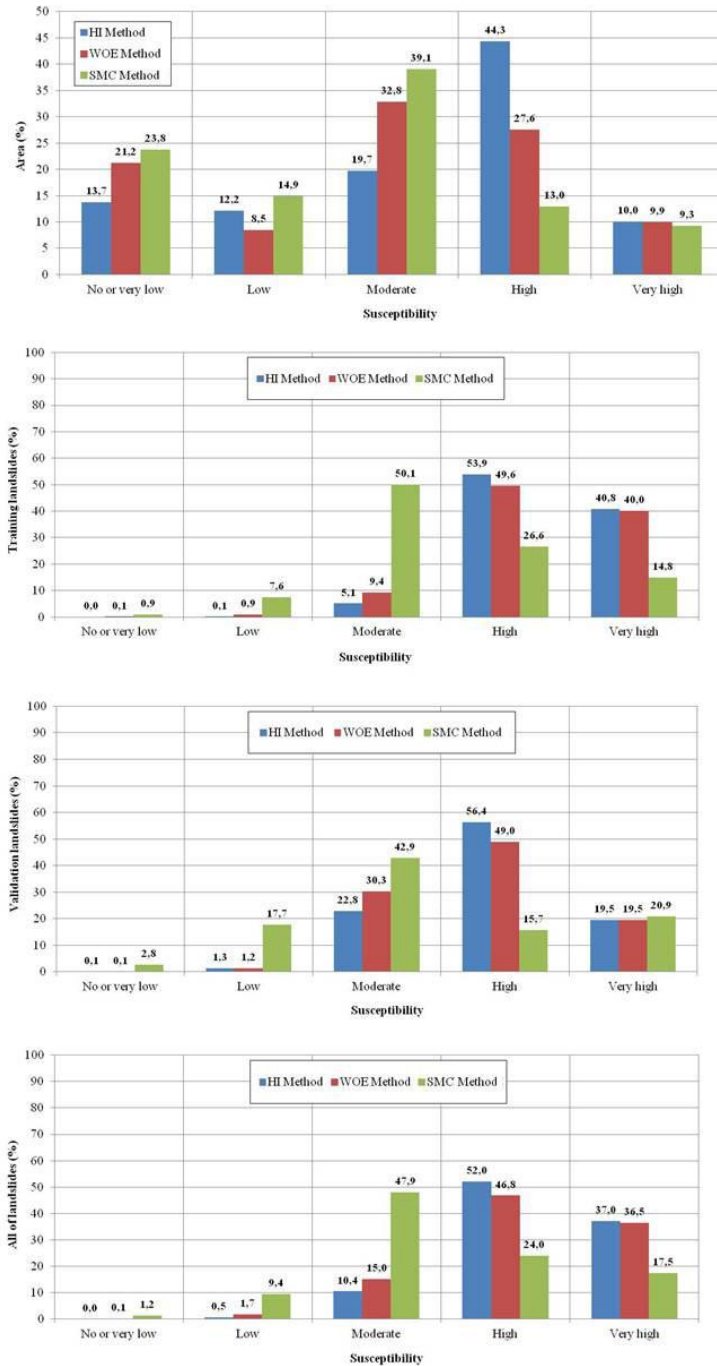
Figure 2. Distribution of: training, validation, and all landslides falling in each susceptibility class and susceptibility distribution . Percentage of the susceptibility classes for each model.

References

Armaş, I. (2011). An analytic multicriteria hierarchical approach to assess landslide vulnerability. Case study: Cornu village, Subcarpathian Prahova Valley/Romania, Z Geomorphol 55(2):209–229.

Armaş, I. (2012). Weights of evidence method for landslide susceptibility mapping. Prahova Subcarpathians, Romania, Nat Hazards, 60:937–950.

Barbieri, G. and Cambuli, P. (2009). The weight of evidence statistical method in landslide susceptibility mapping of the Rio Pardu Valley (Sardinia, Italy), 18th world IMACS/MODSIM congress, Cairns, Australia. http://www.mssanz.org.au/modsim09, 13–17 July 2009.

Calcaterra, D., and Parise, M. (2010). Weathering in the crystalline rocks of Calabria, Italy, and relationships to landslides. In: Calcaterra, D., Parise, M. (Eds.), Weathering as predisposing factor to slope movements. Geological Society of London, Engineering Geology Series, Special Publication, 23, pp. 105–130.

Carrara, A., and Merenda, L. (1976). Landslide inventory in Northern Calabria, Southern Italy, Geological Society of America Bulletin 87, 1153–1162.

Castellanos Abella, E.A., and Van Westen, C.J. (2007). Generation of a landslide risk index map for Cuba using spatial multi-criteria evaluation, Landslides 4(4):311–325.

Conforti, M., Muto, F., Rago, V., and Critelli S. (2014a). Landslide inventory map of north-eastern Calabria (South Italy). Journal of Maps, 10, 90-102.

Conforti, M., Pascale, S., Robustelli, G., and Sdao, F. (2014b). Evaluation of prediction capability of the artificial neural networks for mapping landslide susceptibility in the Turbolo River catchment (northern Calabria, Italy). Catena, 113, 236-250.

Conforti, M., Robustelli, G., Muto, F., and Critelli, S. (2012). Application and validation of bivariate GIS-based landslide susceptibility assessment for the Vitravo river catchment (Calabria, south Italy), Natural Hazards 61:127–141.

Ferranti, L., Santoro, E., Mazzella, M. E., Monaco, C., and Morelli, D. (2009). Active transpression in the northern Calabria Apennines, southern Italy. Tectonophysics, 476, 226–251.

Guzzetti, F. (2000). Landslides fatalities and the evaluation of landslide risk in Italy, Engineering Geology 58, 89–107.

Guzzetti, F., Carrara, A., Cardinali, M., and Reichenbach, P. (1999). Landslide hazard evaluation: a review of current techniques and their application in a multi-scale study, Central Italy, Geomorphology 31(1–4):181–216

Guzzetti, F., Reichenbach, P., Cardinali, M., Galli, M., and Ardizzone, F. (2005). Landslide hazard assessment in the Staffora basin, Northern Italian Apennines, Geomorphology 72, 272–299.

Iovine, G.G.R., Lollino, P., Gariano, S.L., and Terranova, O.G. (2010). Coupling limit equilibrium analyses and real-time monitoring to refine a landslide surveillance system in Calabria (southern Italy). Natural Hazards and Earth System Sciences 10, 2341–2354.

Kavzoglu, T., Kutlug Sahin, E., and Colkesen, I. (2013). Landslide susceptibility mapping using GIS-based multi-criteria decision analysis, support vector machines, and logistic regression, Landslides, DOI 10.1007/s10346-013-0391-7.

Komac, M. (2006). A landslide susceptibility model using the analytical hierarchy process method and multivariate statistics in perialpine Slovenia, Geomorphology 74(1–4):17–28.

Malczewski, J. (1999). GIS and multicriteria decision analysis, John Wiley and Sons, Toronto.

Monaco, C., Tortorici, L., Morten, L., Critelli, S., and Tansi, C. (1995). Geologia del versante nord-orientale del Massiccio del Pollino (confine calabro-lucano): Nota illustrativa sintetica della carta geologica alla scala 1:50.000. Bollettino della Società Geologica Italiana, 114, 277–291.

Ozdemir, A. and Altural, T. (2013). A comparative study of frequency ratio, weights of evidence and logistic regression methods for landslide susceptibility mapping: Sultan Mountains, SW Turkey, Journal of Asian Earth Sciences, http://dx.doi.org/10.1016/j.jseaes.2012.12.014.

Pourghasemi H. R., Pradhan B., Gokceoglu C., and Deylami Moezzi, K. (2012). Landslide Susceptibility Mapping Using a Spatial Multi Criteria Evaluation Model at Haraz Watershed, Iran, in: B. Pradhan and M. Buchroithner (eds.), Terrigenous Mass Movements, DOI: 10.1007/978-3-642-25495-6_2, Springer-Verlag Berlin Heidelberg.

Saaty, T. (1980). The analytical hierarchy Process, McGraw-Hill, New York.

TC I (2001) ILWIS 3.0 academic—user's guide. ITC, Enschede.

van Westen, C., Rengers, N., and Soeters, R. (2003). Use of geomorphological information in indirect landslide susceptibility assessment, Nat Hazards 30:399–419.

van Westen, C.J. (1997). Statistical landslide hazard analysis, ILWIS 2.1 for Windows application guide, ITC Publication, Enschede, pp 73–84.

ENHANCEMENTS OF SEAFLOOR OBSERVATORIES AND APPLICATIONS FOR NATURAL HAZARD ASSESSMENT AND ENVIRONMENTAL MONITORING

Italiano F.[1, 4, 5], Agius M. R.[2], Caruso C.[1], Corbo A.[1], D'Amico S.[2], D'Anca F.[3], Galea P.[2], Hicklin W.[2], Lazzaro G.[1], Nigrelli A.[1], Zora M.[6] , Zammit-Mangion L.[7], Favali P.[4,8]

[1]*Istituto Nazionale di Geofisica e Vulcanologia (INGV), Palermo, Italy*
[2]*University of Malta, Department of Geosciences, Malta*
[3]*CNR-IBF, Palermo, Italy*
[4]*EMSO Interime Office, c/o INGV, Roma, Italy*
[5]*Consiglio Nazionale delle Ricerche-Istituto Ambiente Marino Costiero (CNR-IAMC), Spianata San Ranieri, Messina, Italy*
[6]*DAIMAR srl, Mazara, Italy*
[2]*University of Malta, Department of Physics, Malta*
[8]*Istituto Nazionale di Geofisica e Vulcanologia (INGV), , Roma2, Italy*

The final target of the MONSOON project (MONitoraggio SOttOmariNo for environmental and energetic purposes) is to build up a prototype of a new generation of seafloor observatory for which specific technological developments in terms of power consumption reduction, new data logger and new sensors have been planned. The project is carried out in the main frame of the wide range of scientific and technological activities developed by EMSO Research Infrastructure (European Multidisciplinary Seafloor and water-column Observatory, www.emso-eu.org).

The new seafloor observatory is planned to operate either in stand-alone and real-time modes. The latter is possible with the connection to a surface buoy able to 1) provide (via modem) an internet connection to the sea-floor system and 2) communicate with the sea-floor observatory. The observatory is planned to be deployed down to a water depth of 2000m, even in an extreme marine environment, with the presence of hydrothermal vents.

All the newly developed components of the observatory have been planned and laboratory-tested. In cooperation with the University of Malta a special activity is carried out to find out technical solutions for the detection of body and surface seismic waves and for the integration of specific seismic sensors into the multidisciplinary seafloor observatory. The purpose of that activity is the integration of a seismic sensor (either a short period or a broad band seismometer) in the same data acquisition system that manages the whole observatory in order to make the observatory able to be used in studies and monitoring activities in the georisks field. After a successful laboratory testing activity, experiments in a selected, real environment are planned.

The choosen test site is located at the Aeolian islands where the management of natural risks (seismic and volcanic) required a special attention in the period 2002-2003 when a low-energy submarine explosion occurred at shallow depths off the coasts of Panarea island (Caracausi et al., 2005). The degassing activity induced by the explosion was followed by a huge landslide and a tsunami wave originated at the nearby island of Stromboli. A few weeks later a large eruption started from the flank of Stromboli. The sudden unrest of submarine volcanic activity that occurred off the island of Panarea (November 2002) opened a "crater" of 20 by 10 meters wide and 7 meters deep. That event dramatically changed the geochemical features and the degassing rate of the submarine hydrothermal vents of the area and pushed the scientists to develop new methods to monitor the sea-floor venting activity. During the unrest period, the huge degassing activity increased the CO_2 flow rate by some orders of magnitude. Apart from the former venting areas, degassing occurred from many new fractures opened at the seafloor along a N40°E trend and from the crater.

Besides the periodical sampling activity (gases and hot waters collection by diving activity, Figure 1), a continuous monitoring had been carried out by a small sea-floor observatory developed to provide data from a sensors to measure the temperature of vented thermal waters, the pressure of the water column and the noise of the vented gases. The changes observed in the temperature besides the data of the acoustic probe (hydrophone), working in a frequency range of 0.5-3 kHz, gave useful information for a tight link between the submarine volcanic activity of Panarea Island and the crater explosions of the volcanic island of Stromboli. (Heincke et al., 2009)

Figure 1: Fluids sampling activity during the 2002-2004 unrest of the submarine volcanic activity at Panarea island.

Figure 2:The sea-floor observatory deployed off the island Panarea at shallow depth. The picture shows two observatories contemporary working and connected to same cable. The black vessel contains the electronic devices that will feed the seafloor observatory developed in MONSOON project. There are three probes connected: the dissolved CO_2 (white probe, digital output), a hydrophone and the very sensitive temperature probe from Sea-Bird (bronze probe, analog output). The geophone will be connected to the same electronic cards. (bottom panel) Schematics of the sea-floor observatory and the geophone integrated in a vessel able to work at a depth of 2000m. The heavy platform is necessary to couple the geophone with the sea-floor. The geophone is equipped with an electronic compass and an system to check the tilt

As that approach allowed us: 1) to gain a deeper insight for the management of such an unrest of the submarine volcanic activity results and 2) to recognize that the observed changes in the fluids geochemistry were caused by a magmatic input showing that the nearby active volcanic system of Stromboli Island is somewhat involved in feeding magmatic fluids to Panarea, we decided to enhance the capabilities of the multidisciplinary observatory which is now able to measure either geochemical (e.g. dissolved CO_2 content in sea-water, dissolved oxygen, pH, dissolved CH_4) and geophysical parameters (hydrophones and geophones).

The test site is located in a shallow hydrothermal system off and after the end of the 2002-2004 volcanic crisis, it allows an easy access to an extreme submarine environment with temperatures up to 140°C, pH less than 3 and electrical conductivity higher of the normal sea-water. In that hostile environment we tested all the materials planned to be used to manufacture the different parts of the observatory (Figure 2), as well as all the sensors including those off-the-shelf and those planned within the MONSOON project: probes for acoustic signals, dissolved CO_2 data as well as a short period seismic sensor. Special attention will be paid to the correct coupling of the geophone with the seafloor using a heavy plate that avoids seismic frequencies cuts and losses. The coupling will be manually arranged. All the probes are connected to the observatory by submarine cables and connectors to a vessel hosting the electronics made of new low-power cards for data collection, electrical power management, sensor driving and control, network communication and data storage. The power is provided by high capacity Lithium-polymer batteries. The tests are carried out using a permanent INGV infrastructure made of a buoy cabled to a seafloor station operating at a depth of 23 metres two miles to the East of the Panarea island. This infrastructure allowed to perform the communication tests and to check the status of all the probes by near-real time communication.

The developed technologies greatly enhanced the capabilities of the seafloor observatory planned for environmental applications (target of MONSOON project) making possible to use the same observatory for natural hazards monitoring and assessment purposes (Figure 2). The activities support the EMSO scientific infrastructure, and make available new technologies for seafloor continuous monitoring of a wide range of scientific parameters including oceanographic, chemical, seismic and physical sensors.

Acknowledgements

References

Caracausi A., Ditta M., Italiano F., Longo M., Nuccio P.M., Paonita A. (2005) Massive submarine gas output during the volcanic unrest off Panarea Island (Aeolian arc, Italy): inferences for explosive conditions. Geochemical Journal, 39, 5, 449-467

Heinicke J., Italiano F., Maugeri R., Merkel B., Pohl T., Schipeck M. (2009) Evidence of tectonic control on active arc volcanism: The Panarea-Stromboli tectonic link inferred by submarine hydrothermal vents monitoring (Aeolian arc, Italy), Geophys. Res. Lett., 36, L04301, doi:10.1029/2008GL036664

Italiano F. (2013) Importance of multi-parameter seafloor monitoring for earthquake and volcanic hazards. Invited talk at EMSO Meeting, ROMA, November 13-15th, 2013

Italiano F. (2014) EMSO - European Multidisciplinary Seafloor and Water-Column Observatory, Southern Italy-Sicily Region case study. Workshop on the use of Structural Funds for the construction of distributed e-infrastructures supporting ESFRI-ENV initiatives, Bruxelles, May 12, 2014

Italiano F., Maugeri R, Mastrolia A, Heinicke J (2011) SMM, a new seafloor monitoring module for real-time data transmission: an application to shallow hydrothermal vents. Procedia Earth and Planetary Science 4 (2011) 93 – 98

Authors Index

Part of the SIMIT project:
Integrated civil protection system for the Italo-Maltese cross-border area.

The conference was supported by:

www.visitMALTA.com

AMBASCIATA D'ITALIA MALTA

Istituto Italiano di Cultura
LA VALLETTA

JCR
IMPORTS LIMITED

TERRACORE
INDEPENDENT CREDIBLE RELIABLE

solidbase
LABORATORY LTD.